

A Thesis Submitted for the Degree of PhD at the University of Warwick

Permanent WRAP URL:

<http://wrap.warwick.ac.uk/99840/>

Copyright and reuse:

This thesis is made available online and is protected by original copyright.

Please scroll down to view the document itself.

Please refer to the repository record for this item for information to help you to cite it.

Our policy information is available from the repository home page.

For more information, please contact the WRAP Team at: wrap@warwick.ac.uk

Enhancing the conductivity of PEDOT:PSS

on

Bulk Substrates

by

B. T. A. H. Thompson

A thesis submitted in partial fulfilment of the requirements for the degree

of

Doctor of Philosophy (PhD)

University of Warwick

WMG

June 2017

Abstract

PEDOT:PSS was investigated, using the dopants TWEEN 80 and MEK. The mixture was applied as a thin film on a PET substrate using three techniques, spincoating, dipcoating and spraycoating, with an aim to produce a bulk manufacturing conductive material. The dopants also improved the film forming of PEDOT:PSS.

There was a problem with adhesion and durability of the film to the substrate. Several different materials were investigated to solve this problem. The adhesion problem was solved by adding a layer of methyl cellulose between the substrate and the PEDOT:PSS layers which acted as an adhesion promotor.

One of the aims of this project was to determine a bulk manufacturing method which is viable for PEDOT:PSS. Three manufacturing techniques were investigated to see how this affected the film quality, film conductivity, thickness, orientation, and durability. Spincoating gave thinner films with a final thickness of 1- 2 μm and was more conductive than films manufactured using dipcoating or spraycoating.

Spincoated films made using the dopants enhanced the bulk conductivity of the starting material by two orders of magnitude from 1494 Ωcm for the 100 % PEDOT:PSS dispersion used as a starting material, to 25 Ωcm for the doped 97.22 % PEDOT:PSS. The dipcoated and spraycoated samples were enhanced by three orders of magnitude, although, overall the spincoated samples were the most conductive.

The enhanced 95 % to 98 % PEDOT:PSS dispersion with additives TWEEN 80 and MEK samples, remained more conductive than the starting material even after 62 weeks of storage under air. It was found that storage under air caused an increase in resistivity over the stored time period in doped PEDOT:PSS and 100% PEDOT:PSS films. High voltage studies up to 50V proved the material withstands repeated high voltage application over a period of 62 weeks.

The mechanism of charge transport in the 97 % and 98 % PEDOT:PSS samples was found, using UV, to be due to the formation of polarons. Polaron charge carriers were formed when the polymer became ionised, lost an electron, and formed a positive charge on the polymer chain. In order to stabilise this the PEDOT molecule changes shape from the aromatic to the quinoid conformation. The most conductive films were found to be predominantly in the quinoid form whereas the less conductive films were mainly aromatic.

Acknowledgements

There are simply too many people, who have given up their time to help and advise me during my research to name everyone, but without the constant encouragement and support of my colleagues, friends and family the work that makes up this thesis may never have been completed.

I especially want to thank my supervisor, Dr Vannessa Goodship, for her support and very valuable advice throughout the course of my PhD.

Thanks, to Dr Bethany Middleton, Dr Eleni Fiamegkou, Professor Gordon Smith, everyone in the PAWS team for all their help, advice and support.

Thanks to Dr Kylash Makenji for his advice and help in my first year, Dr Darren Hughes, for his help using the Synchrotron, Dr Paul Milne for his valuable advice using IR, Dr Nessa Fereshteh Saniee for her help using the DSC.

Thanks for all the friendship, help, advice and support from my fellow students: Jai Gupta, Michael Wood, Lucasz Ofrecht, Jianwang Liang, and Ruth Cherrington.

Also, thanks to Helen Gough for taking the trouble to help me so many times with library access problems.

Most of all, thank you to my partner, Mick Kimberley, for always believing in me and encouraging me to follow my own pathway.

Contents

Abstract		i
Table of Figures		viii
Table of Tables		xv
Abbreviations		xviii
Declaration		xx
1.0	Introduction	1
1.1	The Research Problem	1
1.2	The aims and objectives of the PhD research	2
2.0	Literature Review	4
2.1	Introduction	4
2.2	Polythiophenes	4
2.3	PEDOT and PEDOT-Derivatives	6
2.4	PEDOT:PSS	11
2.4.1	Particle size	12
2.4.2	Thickness	13
2.4.3	Agglomeration	16
2.5	PEDOT as a Semiconductor	17
2.5.1	Resonance structures and energy levels	18
2.5.2	Charge transport	21
2.6	Tracking the changes in the shape and conductivity of the PEDOT molecule	26
2.6.1	The mechanism of charge transport in PEDOT:PSS	29
2.7	Doping of PEDOT:PSS	32
2.7.1	Acids	32
2.7.1.1	pKa	33
2.7.2	Water	33
2.7.3	Alcohols and high boiling point solvents	34
2.7.4	Ionic liquids	40
2.7.5	Surfactants	41

2.7.5.1	Aggregation/agglomeration and surfactant	45
2.8	Film forming and Adhesion	46
2.8.1	Humidity	47
2.8.2	Temperature	49
2.8.3	Morphology	50
2.8.4	Crystalization of PEDOT:PSS	51
2.8.5	Aging	54
2.8.6	Thermal analysis	54
2.8.7	Summary	55
2.9	TWEEN 80	56
2.10	MEK	58
2.11	Hypothesis for using MEK and TWEEN 80 as dopants	58
2.12	Conclusions	59
3.0	Methodology	62
3.1	Introduction	62
3.2	Materials	64
3.2.1	Polymers	64
3.2.2	Solvents	65
3.2.3	Additives	66
3.2.3.1	Surfactant	68
3.2.4	Substrates	70
3.2.5	Optimisation of the solution preparation	71
3.3	Manufacturing methods	75
3.3.1	Cleaning of the substrate	75
3.3.2	Scoping experiments	76
3.3.2.1	Solid Cast 100 % PEDOT:PSS	76
3.3.2.2	Pipetting	77
3.3.2.3	Annealing temperature	78
3.3.3	Optimising the manufacturing	78
3.3.3.1	Spraycoating	78

3.3.3.2	Dipcoating	79
3.3.3.4	Spincoating	79
3.3.4	Adhesion	80
3.3.4.1	Chemical modification	80
3.3.4.2	Mechanical abrasion	81
3.3.4.3	Methyl cellulose roughness	82
3.4	Characterisation	82
3.4.1	pH measurements	83
3.4.2	Viscosity measurements	84
3.4.3	Differential scanning calorimetry (DSC)	85
3.4.4	Surface energy of the substrate	86
3.4.5	Electrical conductivity testing	90
3.4.5.1	Bulk resistivity	91
3.4.5.2	Sheet resistance	91
3.4.5.3	Four-point-probe	92
3.4.5.4	Two-point-probe	95
3.4.6	Optical Microscopy	97
3.4.7	Scanning Electron Microscopy (SEM)	97
3.4.8	Profilometer	98
3.4.9	Spectroscopy	99
3.4.9.1	Ultra Violet-Visible spectrophotometer (UV-Vis)	100
3.4.9.2	Fourier Transform Infra Red (IR)	102
3.3.9.3	Raman Spectroscopy	104
3.4.10	Synchrotron Small Angle Xray Scattering (SAXS) and Wide Angle Xray Scattering (WAXS)	105
3.4.11	Nuclear Magnetic Resonance (NMR)	108
3.5	Conclusions	108
4.0	Results	109
4.1	Introduction	109
4.2	Scoping	110
4.2.1	Conductive polymers	110

4.2.2	Solid cast 100 % PEDOT:PSS samples	111
4.2.3	Substrate selection	112
4.2.4	Surface energy	113
4.2.5	Manufacturing techniques	113
4.2.6	Pipetting	113
4.2.7	Spraycoating and Dipcoating	114
4.2.8	Conductivity of the 100 % PEDOT:PSS	115
4.2.9	TWEEN 80 surfactant and MEK	116
4.2.10	Adhesion	118
4.2.11	Conclusions from scoping	119
4.3	Optimisation of the films	120
4.3.1	pH	120
4.3.2	Viscosity measurements	121
4.3.3	Spraycoating	122
4.3.4	Dipcoating	130
4.3.5	Electrical measurements	139
4.3.5.1	Four Point Probe - dipcoated	140
4.3.5.2	Four Point Probe - spraycoated	142
4.3.5.3	Four Point Probe - spincoated	143
4.3.6	Film Thickness using Optical microscopy	144
4.3.6.1	Spraycoated film thickness	144
4.3.6.2	Dipcoated film thickness	145
4.3.7	Spincoating	146
4.3.7.1	Spincoated film thickness	146
4.3.7.2	Resistivity of spincoated samples	147
4.4	Adhesion studies	150
4.4.1	Chemical Modification	150
4.4.2	Four-point-probe measurements of the chemically modified substrate, spincoated sample sets	153
4.4.3	Two-point probe resistivity of the chemically modified substrate, spincoated sample sets	154

4.4.4	Methyl cellulose studies with water	157
4.4.5	Mechanical Abrasion	159
4.4.6	Roughness studies of non-abraded samples	159
4.4.7	Roughness of the PET	160
4.5	Electrical resistivity measurements of adhesion modified samples	161
4.5.1	Four-point probe measurements of abraded spincoated samples	161
4.5.2	Two-point probe measurements of the abraded spincoated samples	163
4.5.3	Film thickness of the abraded samples	165
4.5.4	Film thickness of the chemically modified samples	167
4.6	Spectroscopy	171
4.6.1	Ultra Violet (UV) Spectroscopy	171
4.6.2	Infra red (IR)	173
4.6.3	Raman	176
4.6.3.1	The 785 nm laser	177
4.6.3.2	The 633 nm laser	178
4.6.4	Nuclear Magnetic Resonance (NMR)	179
4.6.5	Synchrotron	179
4.7	Thermal analysis using Differential Scanning Calorimetry (DSC)	180
4.8	Conclusions	182
5.0	Analysis	183
5.1	Introduction	183
5.2	Solutions	185
5.2.1	pH and viscosity	185
5.3	Film Properties	186
5.3.1	Bulk and surface resistivity	186
5.3.1.1	Sheet resistance	187
5.3.1.2	Bulk resistivity	190
5.3.1.3	High Voltage Testing	192

5.4	Manufacturing Routes	200
5.4.1	Sheet resistance of the modified samples	202
5.4.2	Bulk resistivity of the modified samples	205
5.4.3	High voltage of the modified samples	207
5.5	Spectroscopy	209
5.5.1	Ultra Violet (UV) spectroscopy and Charge carriers	210
5.5.1.1	PSS identification	217
5.5.2	Vibrational spectroscopy	217
5.5.2.1	Infra red	217
5.5.2.2	Aromatic and aliphatic CH groups.	219
5.5.2.3	Carbonyl (C=O) peak	224
5.5.2.4	C-O-C groups	229
5.5.2.5	Aromatic-quinoid transition	233
5.5.2.6	Sulphur groups and the fingerprint region	235
5.5.3	Raman	237
5.6	Thermal analysis	244
5.6.1	Thermal analysis using Differential Scanning Calorimetry (DSC)	245
5.7	Conclusions	246
6.0	Shelf-life / Degradation studies	251
6.1	Sample life of the dipcoated samples	251
7.0	Conclusions	259
7.1	Contribution to knowledge	263
7.2	Further research opportunities	264
REFERENCES		268

Table of Figures

Figure 2.1:	The structure of polythiophene	4
Figure 2.2:	Polythiophene showing stable aromatic and the charged quinoid resonance structures	5
Figure 2.3:	The structure of PEDOT	7
Figure 2.4:	The Structure of PEDOT:PSS (Ouyang, 2013b)	11
Figure 2.5:	Aromatic and quinoid resonance forms of polythiophene (Rasmussen, 2011)	18
Figure 2.6:	Representation of the charge carriers generated and being raised from the HOMO level to the LUMO level in semi-conductors	20
Figure 2.7:	Adapted from: Generation of polarons and bipolarons in polythiophene, PEDOT and related polymers (Kroon, Mengistie <i>et al.</i> , 2016)	24
Figure 2.8:	Structure of sorbitol (Anon (a))	39
Figure 2.9:	Structure of mono-ethylene glycol (Anon (b))	40
Figure 2.10:	The structure of TWEEN 80 surfactant	57
Figure 3.1:	Sequence of experiments	63
Figure 3.2:	The SCS 6800 Spincoater	80
Figure 3.3:	The pH meter used to measure the pH of the solutions	83
Figure 3.4:	Brookfield Viscometer used for all viscosity measurements	84
Figure 3.5:	Attension Optical Tensiometer	87
Figure 3.6:	The surface energy of the substrate affects how a liquid will spread	88
Figure 3.7:	The measurement of surface energy using Sessile Drop Analysis	89
Figure 3.8:	The Jandel RM3000 four-point-probe	93
Figure 3.9:	Measurement of sheet resistivity using a four-point-probe (University of Toledo, 2011)	94
Figure 3.10:	The Keithley 6517b high resistivity meter	96
Figure 3.11:	Microscopy samples were mounted in resin and polished	97
Figure 3.12:	Alicona profilometer	98
Figure 3.13:	Alicona calculation of Rz	99
Figure 3.14:	The Cary 60 UV-Vis spectrophotometer	101
Figure 3.15:	The Bruker Tensor 27 FTIR	102
Figure 3.16:	The ATR crystal inside the FTIR	103

Figure 3.17: The Renishaw RE04 in Via Raman	105
Figure 3.18: Diamond Synchrotron showing Pilatus WAXS and SAXS	106
Figure 3.19: Diamond Synchrotron showing (a) Linkham DSC and (b) shows the location of the windows which allow the beam to pass through the sample	107
Figure 3.20: Sample preparation for the Synchrotron	107
Figure 4.1: (Left) the paper cased samples, (Right) Silicon cake case sample of 100 % PEDOT:PSS after annealing	112
Figure 4.2: Benchtop SEM of the sample showing what appears to be bubbles on the surface of the PEDOT/TWEEN 80/MEK film	113
Figure 4.3: 100 % annealed PEDOT:PSS sprayed onto PET film does not wet well.	114
Figure 4.4: The spraycoated PEDOT:PSS solution on PET showing better wetting with addition of surfactant	118
Figure 4.5: Measured pH showing the concentration of PEDOT:PSS in each solution	121
Figure 4.6: Viscosities for the PEDOT:PSS/TWEEN 80/MEK solutions at 21 °C	122
Figure 4.7: Spraycoated 99 % PEDOT:PSS (bottom) and 100 % PEDOT:PSS (top)	123
Figure 4.8: Spraycoated Set 1 resistivity at various voltages using Keithley 6517b	124
Figure 4.9: Spraycoated Set 2 resistivity at various voltages using Keithley 6517b	124
Figure 4.10: Spraycoated Set 3 resistivity at various voltages using Keithley 6517b	125
Figure 4.11: Spraycoated Set 4 resistivity at various voltages using Keithley 6517b	125
Figure 4.12: Spraycoated Set 5 resistivity at various voltages using Keithley 6517b	126
Figure 4.13: Average resistivity values for sets 1-5 for the 97 % PEDOT:PSS , 99 % PEDOT:PSS and 100 % film samples at 1 V – Spraycoated	127
Figure 4.14: Average resistivity values for sets 1-5 for the 97 % PEDOT:PSS, 99 % PEDOT:PSS and 100 % film samples at 2 V - Spraycoated	127
Figure 4.15: Average resistivity values for sets 1-5 for the 97 % PEDOT:PSS, 99 % PEDOT:PSS and 100 % samples at 5 V - Spraycoated	128
Figure 4.16: Average resistivity values for sets 1-5 for: 97 % PEDOT:PSS, 99 % PEDOT:PSS and 100 % film samples at 10 V - Spraycoated	128

Figure 4.17: Average resistivity values for sets 1-5 for the 97 % PEDOT:PSS, 99 % PEDOT:PSS and 100 % film samples at 20 V – Spraycoated	129
Figure 4.18: Average resistivity values for sets 1-5 for the 97 % PEDOT:PSS,, 99 % PEDOT:PSS and 100 % film samples at 30 V – Spraycoated	129
Figure 4.19: Average resistivity values for sets 1-5 for the 97 % PEDOT:PSS, 99 % PEDOT:PSS and 100 % film samples at 40 V – Spraycoated	130
Figure 4.20: Average resistivity values for sets 1-5 for the 97 % PEDOT:PSS, 99 % PEDOT:PSS and 100 % film samples at 50 V – Spraycoated	130
Figure 4.21: The dip-coated samples on PET, Left (1) 97 % PEDOT:PSS, 99 % PEDOT:PSS centre (2), right (3) 100 % films of PEDOT:PSS	131
Figure 4.22: Dipcoated Set 1 resistivity at various voltages using Keithley 6517b	132
Figure 4.23: Dipcoated Set 2 resistivity at various voltages using Keithley 6517b	132
Figure 4.24: Dipcoated Set 3 resistivity at various voltages using Keithley 6517b	133
Figure 4.25: Dipcoated Set 4 resistivity at various voltages using Keithley 6517b	133
Figure 4.26: Dipcoated Set 5 resistivity at various voltages using Keithley 6517b	134
Figure 4.27: The average for the 97 % PEDOT:PSS, 99 % PEDOT:PSS and 100 % PEDOT:PSS resistivity at 1 V using Keithley 6517b	134
Figure 4.28: The average for the 97 % PEDOT:PSS 99% PEDOT:PSS and 100 % PEDOT:PSS resistivity at 2 V using Keithley 6517b	135
Figure 4.29: The average for the 97 % PEDOT:PSS, 99 % PEDOT:PSS and 100 % PEDOT:PSS at 5 V for dipcoated sets 1-5 using Keithley 6517b	135
Figure 4.30: The average for the 97 % PEDOT:PSS, 99 % PEDOT:PSS and 100 % PEDOT:PSS dipcoated sets 1-5 at 10 V	136
Figure 4.31: The average for the 97 % PEDOT:PSS, 99 % PEDOT:PSS and 100 % PEDOT:PSS dipcoated samples at 20 V	136
Figure 4.32: The average for the 97 % PEDOT:PSS, 99 % PEDOT:PSS and 100 % PEDOT:PSS for dipcoated sets 1-5 at 30 V	137
Figure 4.33: The average for the 97 % PEDOT:PSS, 99 % PEDOT:PSS and 100% PEDOT:PSS dipcoated sets 1-5 at 40 V	137
Figure 4.34: The average for the 97 % PEDOT:PSS, 99 % PEDOT:PSS and 100 % PEDOT:PSS dipcoated sets 2-5 at 50 V	138
Figure 4.35: Measured resistivity vs applied voltage for the 97 % PEDOT:PSS, dipcoated PEDOT:PSS film samples	138
Figure 4.36: Measured resistivity vs applied voltage for 99 % PEDOT:PSS dipcoated PEDOT:PSS film samples	139
Figure 4.37: Measured resistivity vs applied voltage for the 100 % dipcoated PEDOT:PSS samples	139

Figure 4.38: Sheet resistance of dipcoated sample showing mean, minimum and maximum results obtained using a four-point probe at 10 nA	141
Figure 4.39: Bulk resistivity of the dipcoated samples using a four-point probe at 10 nA	142
Figure 4.40: Sheet resistance of the spraycoated samples	142
Figure 4.41: Bulk resistivity of spraycoated samples	143
Figure 4.42: Sheet resistance of the spincoated samples	143
Figure 4.43: Bulk resistance of the spincoated samples	144
Figure 4.44: The range of film thickness for the electrically tested spraycoated samples	145
Figure 4.45: Measured film thickness of the dipcoated samples	146
Figure 4.46: Film thickness measurement of the 100 % PEDOT:PSS spincoated sample	146
Figure 4.47: The film thickness measurements of 97 % and 99 % unmodified, spincoated samples	147
Figure 4.48: Resistivity of spincoated set 1 with no surface modification	148
Figure 4.49: Resistivity of spincoated set 2 with no surface modification	148
Figure 4.50: Resistivity of spincoated set 3 with no surface modification	149
Figure 4.51: Resistivity of spincoated set 4 with no surface modification	149
Figure 4.52: Resistivity of spincoated set 5 with no surface modification	150
Figure 4.53: The 3 % Additives, 97 % PEDOT:PSS (1:30) ratio sample after chemical modification using methyl cellulose.	151
Figure 4.54: Sheet resistance of the chemically modified samples	153
Figure 4.55: The bulk resistivity of the chemically modified sample	153
Figure 4.56: Resistivity of the chemically modified substrate sample set 1	154
Figure 4.57: Resistivity of the chemically modified substrate sample set 2	155
Figure 4.58: Resistivity of the chemically modified substrate sample set 3	155
Figure 4.59: Resistivity of the chemically modified substrate sample set 4	156
Figure 4.60: Resistivity of the chemically modified substrate sample set 5	156
Figure 4.61: The surface of chemical modification using methyl cellulose on a PET substrate x 20 magnification – No water immersion	157
Figure 4.62: Chemical modification with methyl cellulose showing the edge where the chemical modification ends x 20- before water immersion	158
Figure 4.63: The edge of the cellulose after immersion in water on PET substrate x 20 magnification	159

Figure 4.64: The 400 cycles spincoated 97 % PEDOT:PSS film sample showing visible scarring from the abrasion	160
Figure 4.65: Sheet resistance of the mechanically abraded samples	162
Figure 4.66: Bulk resistivity of the mechanically abraded samples	162
Figure 4.67: Abraded samples set 1 Keithley results	163
Figure 4.68: Abraded samples set 2 Keithley results	164
Figure 4.69: Abraded samples set 3 Keithley results	164
Figure 4.70: Abraded samples set 4 Keithley results	165
Figure 4.71: Abraded samples set 5 Keithley results	165
Figure 4.72: The mounted 100 % PEDOT:PSS spincoated film was immersed in epoxy and the film was measured using optical microscopy	167
Figure 4.73: Spincoated 97 % PEDOT:PSS film samples on methyl cellulose showing how the method was improved to give good films.	168
Figure 4.74: Alicona measurement (x 20) of the 97 % PEDOT:PSS film sample	169
Figure 4.75: UV spectra of all ratios of PEDOT:PSS/TWEEN 80/MEK and 100 % PEDOT:PSS	171
Figure 4.76: UV spectrum of 100 % PEDOT:PSS	172
Figure 4.77: UV spectrum of TWEEN 80 + MEK solution	172
Figure 4.78: UV of 100 % TWEEN 80	173
Figure 4.79: 100 % PEDOT:PSS solid annealed film as a KBr Disc showing full scanning range	174
Figure 4.80: IR of the annealed films from 4000 to 500 cm^{-1}	175
Figure 4.81: IR of the PET film used as substrate	175
Figure 4.82: IR of 100 % PEDOT:PSS film through hole in insulating PET film in order to do electrical testing	176
Figure 4.83: The full Raman spectra for all samples	177
Figure 4.84: Raman spectra showing changes in peak height at 413 cm^{-1}	177
Figure 4.85: Raman of the 98 % PEDOT:PSS film sample at 785 nm	178
Figure 4.86: Raman spectra of all conductive samples using the 633 nm laser	178
Figure 4.87: DSC pan cut in half to see if there was any PEDOT:PSS left inside after synchrotron/DSC analysis. There is a black residue which must be the remains of the PEDOT:PSS	180
Figure 4.88: The Glass Transition temperature of the 100 % PEDOT:PSS film sample and of the 97 % PEDOT:PSS film sample	181

Figure 5.1:	Sheet resistance of the PEDOT:PSS samples using a four-point probe at 10 nA	188
Figure 5.2:	Bulk resistivity of PEDOT:PSS using a four-point probe at 10 nA	191
Figure 5.3:	A typical profile of the samples using a Keithley 6517b at different applied potential differences with the surface measurements from the Jandel four-point-probe	193
Figure 5.4:	Resistivity of the 97 %, 99 % and 100 % dipcoated samples with unmodified substrates at different applied potentials using Keithley 6517b	198
Figure 5.5:	Resistivity of the 97 %, 99 % and 100 % dipcoated samples at 5 V	199
Figure 5.6:	Resistivity of the 97 %, 99 % and 100 % spraycoated samples at 5 V	199
Figure 5.7:	The rise in resistivity with increasing applied Voltage for the 97 % dipcoated samples	200
Figure 5.8:	The sheet resistance of the dipcoated samples	203
Figure 5.9:	The sheet resistance of the spraycoated samples	203
Figure 5.10:	Comparison of sheet resistance the spincoated samples	204
Figure 5.11:	Bulk resistivity of the unmodified spincoated samples	206
Figure 5.12:	Comparison of bulk resistivity of the chemically and physically modified spincoated samples	206
Figure 5.13	Resistivity of the chemically modified spincoated samples using Keithley 6517b	208
Figure 5.14	Chemically modified spincoated samples at 5 V	208
Figure 5.15	Abrasion modified spincoated samples at 5 V	209
Figure 5.16:	UV Spectra showing all solutions at 700-800 nm	211
Figure 5.17:	UV spectra of 97 % PEDOT:PSS sample and: 98 % PEDOT:PSS sample	212
Figure 5.18:	KBr discs of the PEDOT /TWEEN 80/MEK annealed films from 4000 to 500 cm^{-1}	218
Figure 5.19:	The difference between COC and COROC	221
Figure 5.20:	IR of the 100 % PEDOT:PSS	222
Figure 5.21:	The samples in the conductive region (The 98 %, 97 % and 96 % PEDOT:PSS samples) from 1900 to 500 cm^{-1}	225
Figure 5.22:	IR showing carbonyls are not present in these Zone 3 samples	226
Figure 5.23:	IR of the Zone 3 samples showing a possible OH peak	228
Figure 5.24:	The IR spectra of 94 %, 96 %, 97 % and 98 % PEDOT:PSS samples in the most conductive region	230

Figure 5.25: IR spectra between 1700 and 400 cm^{-1} for 99 %, 98 %, 97 % and 96 % PEDOT:PSS	231
Figure 5.26: The full spectra of 96 % PEDOT:PSS, 97 % PEDOT:PSS, and 98 % PEDOT:PSS samples	232
Figure 5.27: IR of the C=C aromatic peaks in the 99 % PEDOT:PSS zone 3 sample at 1540 and 1575 cm^{-1}	233
Figure 5.28: IR of 100 % PEDOT:PSS showing the the quinoid group peaks	234
Figure 5.29: IR of the 97 % sample possibly showing C-S peaks and SO_3	236
Figure 5.30: Raman of the 98 % PEDOT:PSS sample using 785 nm laser	239
Figure 5.31: Raman spectra using 633 nm laser of the 97 % PEDOT:PSS, zone 2 sample	240
Figure 5.32: Raman scan at 633 nm on the 97 % PEDOT:PSS sample	242
Figure 5.33: Raman of the 94 % PEDOT:PSS sample	243
Figure 6.1: Average sheet resistance of the dipcoated samples over 16 weeks of storage	252
Figure 6.2: Sheet resistance (Ωsq) of samples over 62 weeks	253
Figure 6.3: Keithley resistivity of samples measured at 40 V over 62 weeks	254
Figure 6.4: Bulk resistivity of the dipcoated shelf-life samples after 16 weeks of storage	255
Figure 6.5: Bulk resistivity (Ωcm) of samples over 62 weeks	255
Figure 6.6: Heat generated (J) from the applied potential difference	257

Table of Tables

Table 2.1:	Examples of the many polythiophene derivatives	6
Table 2.2:	Commercially available PEDOT analogues (http://www.sigmaaldrich.com)	8
Table 2.3:	The different conductivity of PEDOT analogues tested by Zotti (a) denotes electrochemically prepared and (b) denotes chemically prepared	9
Table 2.4:	Table of film thickness	14
Table 2.5:	Surfactant effects on PEDOT, adapted from Nasybulin (Nasybulin <i>et al.</i> , 2012)	45
Table 3.1:	Conductive polymers sourced for scoping experiments	64
Table 3.2:	Experiments for PEDOT made for spraycoating on substrates	65
Table 3.3:	Solvents used for scoping experiments	66
Table 3.4:	Chemicals used for doping experiments	67
Table 3.5:	Experiments for different PEDOT analogues with Ethanol as solvent on a PET substrate	68
Table 3.6:	Solutions of TWEEN 80 non-ionic surfactant as made up to mix with PEDOT:PSS	69
Table 3.7:	Solutions of TWEEN 80 and MEK were mixed with PEDOT:PSS	69
Table 3.8:	Literature surface energy of plastics	70
Table 3.9:	Manufacturers tolerances for equipment used for measuring solutions	71
Table 3.10:	The proportions of dopant additives made from TWEEN 80 and MEK (A1)	71
Table 3.11:	PEDOT:PSS, TWEEN 80 and MEK solutions	72
Table 3.12:	Solution A1 concentrations with PEDOT:PSS showing actual concentration of PEDOT in each solution	74
Table 3.13:	Pipetting experiments with different PEDOTs and different solvents	77
Table 3.14:	Table of different chemicals used for substrate modification to prevent delamination	81
Table 3.15:	The mechanical abrader cycles	81
Table 3.16:	Setting used for the viscosity measurements	85
Table 3.17:	Surface energies of polymer substrates	89
Table 4.1:	Designations used for analysis of films and solutions	109

Table 4.2:	Average sheet resistance results of 10 readings taken over 1 minute using the Jandel four point probe at 10nA for the 100 % sample	115
Table 4.3:	Average resistivity results of 5 samples using the Keithley 6517b for the 100 % sample at different applied potential differences	116
Table 4.4:	An example of the sheet resistance results from measuring with the Jandel four-point-probe	140
Table 4.5:	An example of the results for bulk resistivity obtained from the Jandel four-point-probe	141
Table 4.6:	Chemical modification of PET showing the Keithley resistivity results and bending of samples	152
Table 4.7:	Results of mechanical abrasion with uncoated sample	161
Table 4.8:	Spincoated samples with mechanical Abrasion modification to the substrate. Note there are no results for some samples due to total delamination	166
Table 4.9:	Average thickness of 5 samples using spincoated samples with chemical modification	170
Table 4.10:	Table of identification names for samples	174
Table 4.11:	Measured Glass Transition using DSC	181
Table 5.1:	Designations used for analysis of films and solutions	184
Table 5.2:	Zones of conductivity	187
Table 5.3:	An example of the current measured using the Keithley two point probe at 1 - 10 ⁵ Volts.	195
Table 5.4:	An example of the current measured using the Keithley two point probe at 10 - 30 Volts	196
Table 5.5:	An example of the current measured using the Keithley two point probe at 40 - 50 Volts	197
Table 5.6:	Film thicknesses of different manufacturing techniques	201
Table 5.7:	Table of symbols	213
Table 5.8:	Table of band gaps for the samples in Figure 5.17	214
Table 5.9:	Table of functional group analysis by IR using different literary reports	220
Table 5.10:	Functional groups found in 100 % PEDOT:PSS annealed film	223
Table 5.11:	Table of IR absorptions of ammonia	227
Table 5.12:	Raman peaks found in spectra of PEDOT:PSS (Kalagi and Patil, 2016)	239

Table 5.13:	Raman analysis of the 97 % PEDOT:PSS sample:	241
Table 5.14:	Raman spectrum using 633 nm laser and the 94 % PEDOT:PSS sample	244
Table 5.15:	The glass transition of different samples using DSC:	245
Table 5.16:	Charge carriers in Zone 2 samples	249
Table 6.1:	Heat energy generated (J) from the applied potential difference	258
Table 7.1:	Bulk resistivity enhancement of the samples measured using a four-point-probe	259
Table 7.2:	Conductivity enhancement of the samples from four-point-probe measurements	262

Abbreviations

Alkyl ester polythiophenes	PPET
Alkyl ester polythiophenes	PHET
Alkyl ester polythiophenes	PDET
Alkyl ester polythiophenes	PMBET
Aqueous	(aq)
Attenuated Total Reflection	ATR
Atomic-force microscopy	AFM
A type of PEDOT:PSS	Clevios PH1000
Band gap	E_g
Bis(2-ethylhexyl) sulfosuccinate Sodium salt	AOT
Carbon atom – sulphur atom	C-S
Carbon nanotubes	CNTs
Carboxymethylcellulose	CMC
Cetyl trimethylammonium bromide	CTAB
Conduction band	CB
Deuterated water	D ₂ O
Differential scanning calorimetry	DSC
Dimethylformamide	DMF
Dimethyl sulphoxide	DMSO
Double bonds (π)	π
Dynamic mechanical analysis	DMA
Electrode specific capacitance	$C_E, F\ cm^{-2}$
Electron spin resonance	ESR
Ethylenedioxythiophene	EDOT
Ethylenedithiathiophene	EDTT
Ethylene glycol	EG
Ethylmethyl ketone	MEK
1-ethyl-3-methylimidazolium Tetrafluoroborate	EMIMBF ₄
Ethyleneoxythiophene	EOTT
Glass transition temperature	T _g
Grazing incident small angle Xray Spectroscopy	GISAXS.
Grazing incident wide angle Xray spectroscopy	GIWAXS.
Helium gas	He
Hexadecyl (2-Hydroxyethyl) dimethylammonium dihydrogen phosphate	HDHEDMA
Hexadecyltrimethylammonium p-toluenesulfonate or Cetyltrimethylammonium Bromide	HDTMA
Highest occupied molecular orbital	HOMO
Hydrochloric acid	HCl
Hydrogen bonding	H-bonding
Hydroxyl group	OH
Hydrogen ion	(H) and H ⁺
Ionization constant (K _a) of an acid	pK _a
Isopropyl alcohol	IPA
Lowest unoccupied molecular orbital	LUMO
2-Mercaptoethylamine	2-MEA
Microfibrillated cellulose	MFC
Nanofibrillated cellulose	NFC
Nitrogen gas	N ₂
N-methyl pyrrolidinone	NMP
Nuclear Magnetic Resonance	NMR

Ohms squared – sheet Resistance	Ωsq
Organic light emitting diodes	OLEDs
Oxygen gas	O_2
Photoelectron spectroscopy	XPS
Polycarbonate	PC
Poly-(9,9-dioctylfluorene)	PFO
Poly 3,4-ethylenedioxythiophene	PEDOT
Poly(3,4-ethylenedioxythiophene), bis-poly(ethyleneglycol), lauryl terminated	PEDOT:PEG
Poly(3,4-ethylenedioxythiophene)-poly(styrenesulfonate)	PEDOT:PSS
Poly(3,4-ethylenedioxythiophene), Tetramethacrylate end-capped solution	PEDOT:Tosylate
	PEDOT:OTs
	PEDOT:Tos
Polyethylene glycol sorbitan monooleate solution or Polysorbate 80 or Polyethylene sorbitol ester	TWEEN 80
Polyethyleneimine	PEI
Polyethylene terephthalate	PET
Polymer light emitting diodes	PLEDs
Polypropylene	PP
Polypyrrole	PPy
Polystyrene sulphonate	PSS
Polyvinyl alcohol	PVA
Polyvinylpyrrolidone	PVP
Potassium Bromide	KBr
Propylenedioxythiophenes	ProDOT
Saturated carbon atoms	C-C
Scanning Electron Microscopy	SEM
Seimans per centimeter	S cm^{-1}
Sigma, single bonds	σ
Silicon dioxide	SiO_2
Small angle Xray scattering	SAXS
Sodium ion	(Na) Na^+
Sodium dodecyl sulfonate	SDS
Sodium p-toluene sulfonate	TsONa
Sulphate groups	SO_2/SO_3
Sulphated plant polysaccharide	K-Carrageenan
Sulfuric acid	H_2SO_4
Tetrahydrofuran	THF
4-(1,1,3,3-tetramethylbutyl)phenyl-Polyethylene glycol	TritonX-100
2,5,8,11-tetramethyl-6-dodecyne-5,8-diol ether	PEG-TmDD
Unsaturated carbon atoms	C=C
Ultra Violet- Visible – Near Infra red	UV-Vis-NIR
Valance band	VB
Vinylenedioxythiophene	VDOT
	Polybenzo-EDOT
Water	H_2O
Wide angle Xray scattering	WAXS
Xray diffraction	XRD

Declaration

This thesis is submitted in partial fulfilment of the requirements for the degree of Doctor of Philosophy at the University of Warwick. The research was carried out at WMG, University of Warwick from October 2013 to June 2017. The research described here is my own and not the product of collaboration. No part of this thesis has been submitted to any other university, or as part of any other submission to the University of Warwick.

Bracken Tracy Anne Heather Thompson

WMG

University of Warwick

June 2017

1.0 Introduction

1.1 The Research Problem

Electroactive polymer engineering, is growing as an area of interest for manufacturers and research institutes. Plastic electronics has the potential for device manufacture in a low cost, mass-produced way with an aim to reduce energy consumption and costs for the individual householder or business. In order to bulk manufacture components such as sensors, thin film electrodes, solar cells, batteries, organic light emitting diodes (OLEDs) and other devices, new manufacturing techniques and new bulk materials are needed. Candidates for manufacturing include techniques such as inkjet printing, screen-printing, spraycoating and injection moulding, which will make these devices more accessible, and affordable, for ordinary people.

Poly(3,4-ethylene dioxythiophene) (PEDOT) is a commercially available electrically conducting polymer which is a good candidate material for use in mass-produced electronic systems for such devices when made into thin films. However, despite already being electrically conductive, the conductivity of commercially available PEDOT is really quite low, when compared to that of metals (Elschner, Kirchmeyer *et al.*, 2011). Sigma Aldrich (<https://www.sigmaaldrich.com>) give a stated manufacturer's sheet resistivity of, <100 Ω/sq for PEDOT:PSS and 1-10 M Ω/sq for [PEDOT:OTs]N. The literature reports a conductivity of between 1 and 450 Scm^{-1} for electrodeposited analogues of PEDOT (Zotti *et al.*, 2003) and PEDOT:PSS is reported to have a range of starting conductivities of 0.2-1 S cm^{-1} by Kim *et al* (Kim, Sachse *et al.*, 2011).

The conductivity can be enhanced by doping with additives. Some variants of PEDOT whilst having virtually identical properties to begin with have very different conductivities after doping (Ouyang, 2013a). The mechanism of the charge carrier generation of the electrically conducting films of PEDOT is also not well understood.

In order to manufacture devices which work efficiently, more background information on the different mechanisms of charge transfer occurring in PEDOT needs to be investigated. There is a huge gap in previous knowledge with respect to high voltage applications using PEDOT. Despite the many articles in the literature, applying a potential difference above 1.5 V, so the behaviour of PEDOT at high voltages can be investigated, has so far been completely ignored by the academic community due to previous research stating that high voltage applications were impossible. There is also a commercial interest in this research since it is of interest to know how PEDOT reacts to higher applied potential difference in order to understand what would happen in, for example, an environment where an electrical surge occurs since this will widen potential applications.

1.2 The aims and objectives of the PhD research

After considering the knowledge gaps identified in the literature search, the aims and objectives of this PhD were identified. The aims were:

- To identify the most viable analogue of commercially available PEDOT for future bulk applications
- To enhance the electrical conductivity of PEDOT with a view to eventually having a bulk application polymer for use in mass production.
- To investigate different methods of manufacture which could be scaled up to bulk applications.

The objectives therefore were:

- To investigate and identify the mechanism of charge transfer occurring in PEDOT.
- To investigate the effects of higher applied potential difference on PEDOT and evaluate the effects of applying voltages from 1-50 V

- To analyse and characterise the doped PEDOT films.
- To dope PEDOT to produce more electrically conducting films.
- To consider aging of doped PEDOT films

2.0 Literature Review

2.1 Introduction

The aim of this chapter is to define PEDOT and to explain how PEDOT can be electrically conductive, and what mechanism this conductivity takes. It will also discuss relevant state of the art in PEDOT. However, this chapter begins with polythiophenes which is the family of materials to which PEDOT belongs.

2.2 Polythiophenes

Polythiophenes are polymers made from thiophene. The structure of polythiophene is shown in Figure 2.1.

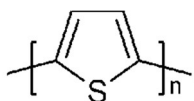


Figure 2.1: The structure of polythiophene

In general, polythiophenes are some of the most environmentally and thermally stable polymer materials. In addition, polythiophenes have high conductivity when doped. Doping is when electrons are either added or removed from the π -orbitals (discussed later in this section), using an additive, which oxidises or reduces the polymer and leaves a charge on the atoms in the ring structure. Various reagents have been used to dope polythiophene, the most successful being iodine and bromine which both give highly conductive polymeric materials. Horowitz (Horowitz and Delannoy, 1999) defines three states in which the material is found. There is the neutral undoped state where polythiophene is a semi-conductor. In the doped state the material becomes

conducting. There is also a third state where the material can be reversibly doped and undoped with an electrochemically reversible redox reaction.

The conductivity of doped polythiophenes is due to them being aromatic molecules with delocalised electrons. As aromatic molecules, polythiophenes, are conjugated. This means they contain double (π) bonds in an alternating sequence with single bonds. When polythiophene is doped, two or more theoretical structures are possible. In the case of polythiophene Figure 2.2 shows the structure for the doped and undoped molecule.

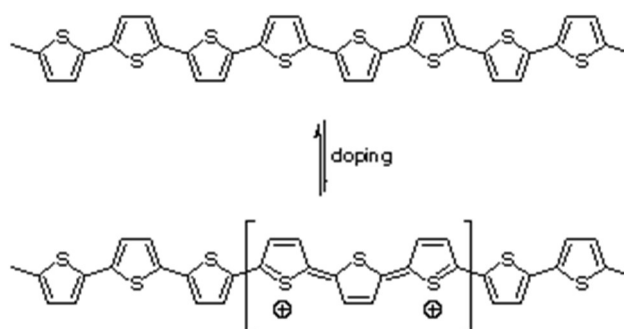


Figure 2.2: Polythiophene showing stable aromatic and the charged quinoid resonance structures.

The alternating double and single bonds have what is known as resonance where they can exist in more than one structure due to the electrons being delocalised. This allows the electrons to move along several units of the polymer chain and makes the polymer conductive. The only differences between the theoretical structures is the location of the double and single bonds. In the case of polythiophene, the two resonance structures that are possible are known as the aromatic and quinoid structures. Both structures are shown in Figure 2.2. The quinoid structure is more likely to form as a result of the polymer being doped. Note that the double bonds are in different locations on the doped structure in Figure 2.2. The removal of electrons due to doping leads to ionisation and the delocalisation of the electrons, which after ionisation, become mobile and able to move along the polymer chain. In turn the

quinoid structure forms to stabilise the polymer and allows the formation of delocalised mobile charge carriers. Polythiophene, and its derivatives, like most aromatic compounds, are usually insoluble due to having a rigid backbone. However, when substituted at the 3 and 4 positions it becomes more soluble in organic solvents. Table 2.1 shows a small number of the polythiophenes derivatives currently being investigated and there are more being discovered all the time.

Table 2.1: Examples of the many polythiophene derivatives

Polymer	Abbreviation	Reference
Alkyl ester polythiophenes	PPET PHET PDET PMBET	(Kang, Kim <i>et al.</i> , 1995)
Propylenedioxythiophenes	ProDOT	(Cirpan, Argun <i>et al.</i> , 2003, (Elschner, Kirchmeyer <i>et al.</i> , 2011)
Vinylendioxythiophene	VDOT Polybenzo-EDOT	(Elschner, Kirchmeyer <i>et al.</i> , 2011)
Ethyleneoxythiophene	EOTT	(Elschner, Kirchmeyer <i>et al.</i> , 2011)
Ethylenedithiathiophene	EDTT	(Elschner, Kirchmeyer <i>et al.</i> , 2011)
Poly 3,4-ethylenedioxythiophene	PEDOT	(Elschner, Kirchmeyer <i>et al.</i> , 2011)

2.3 PEDOT and PEDOT-Derivatives

The PEDOT family are known as intrinsically conducting polymers (ICPs) and have transparency and environmental stability (Elschner, Kirchmeyer *et al.*, 2011). PEDOT

has been used as the active material in flexible organic electronics such as polymer LEDs, antistatic coatings, sensors, batteries, solar cells, electrodes,

RFID transistors (Elschner, Kirchmeyer *et al.*, 2011), Kossmehl and Engelmann, 1999).

PEDOT is substituted in the 3 and 4 positions and is electrically conducting. PEDOT has a heterocyclic structure with more than one ring structure which adds to its potential to become delocalised with resonance forms. The two oxygens in PEDOT's second ring structure attach to the polythiophene ring as shown in Figure 2.3. This has unpaired electrons, which can donate into the polythiophene ring and stabilise the PEDOT polymer. When doped with a suitable additive the conductivity can be increased considerably. The amount of conductivity increase depends on what the dopant is, the level of dopant, and the method of doping. Generally, PEDOT is found with a counterion which allows it to become a dispersion in a liquid. This helps with processing of the PEDOT into thin film devices for electronic applications. Commercially available PEDOT has several different counterions. A few of the common variants are listed in Table 2.2.

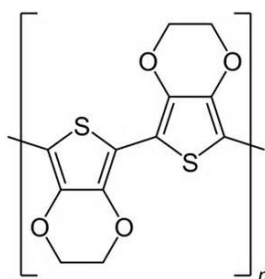


Figure 2.3: The structure of PEDOT

Table 2.2: Commercially available PEDOT analogues ([http:// www.sigmaaldrich.com](http://www.sigmaaldrich.com))

	Abbreviation	Weight % of PEDOT	Solvent	Dopant	Synonym	Resistance (typical surface resistance of film)	Conductivity ($S\ cm^{-1}$) (bulk)
Poly(3,4-ethylenedioxythiophene), tetramethacrylate end-capped solution	PEDOT: OTs	0.5 wt. %	propylene carbonate, 89.5 wt. %	p-toluenesulfonate	Oligotronics TM (tetramethacrylate end-capped)	1-10 M Ω /sq	0.1-0.5
Poly(3,4-ethylenedioxythiophene), tetramethacrylate end-capped solution	PEDOT: OTs	0.5%	nitromethane, 83.4 wt. %, isopropanol, 0.3 wt. %, ethanol, 5.8 wt. %	p-toluenesulfonate as dopant	Oligotronics TM tetramethacrylate	1-10 M Ω /sq (surface resistance of film)	0.1-0.5 S cm^{-1} (bulk)
Poly(3,4-ethylenedioxythiophene), bis-poly(ethylene glycol), lauryl terminated	PEDOT: PEG	0.2-0.7 wt. %	Nitromethane, 90-95 wt. %, Acetonitrile, 4-8 wt. %, propylene glycol, 0.0-0.3 wt. %, proprietary processing additive, 0.1-0.7 wt. %	perchlorate as dopant	Aldotronics TM , C3 polymer	600-3000 Ω /sq	10-60 S cm^{-1}
Poly(3,4-ethylenedioxythiophene), bis-poly(ethylene glycol), lauryl terminated	PEDOT: PEG	0.3-0.8 wt. %	1,2-Dichlorobenzene, 80-95 wt. %, ethanol, 4-8 wt. %, isopropanol, 0.2-0.8 wt. %, processing additive, 0.1-0.4 wt. %	p-toluenesulfonate as dopant	Aldotronics TM TM-P3 polymer	?	0.01-0.05 S cm^{-1} (bulk)
Poly(3,4-ethylenedioxythiophene), bis-poly(ethylene glycol), lauryl terminated	PEDOT: PEG	0.8-1.2 wt. %	nitromethane, 90-95 wt. %, isopropanol, 0.2-0.8 wt. %, ethanol, 4-8 wt. %	p-toluenesulfonate as dopant	Aldotronics TM TM-P3 polymer	?	10-2-10-4 S cm^{-1} (bulk)
Poly(3,4-ethylenedioxythiophene), bis-poly(ethylene glycol), lauryl terminated	PEDOT: PEG	0.2-0.9 wt. %	propylene carbonate, 90-95 wt. %, acetonitrile, 4-8 wt. %, propylene glycol, 0.0-0.3 wt. %	C12-PEG-block-PEDOT-block-PEG-C12, PEDOT: PEG	Aldotronics TM TM-C3 polymer	?	10-45 S cm^{-1} (bulk)
Poly(3,4-ethylenedioxythiophene)-poly(styrenesulfonate)	PEDOT: PSS	1.1%	Water	polystyrene sulfonate	Capacitor	<100 Ω /sq	?

The type of counterion, and the method of polymerisations were studied by Zotti (Zotti, Zecchin *et al.*, 2003). The first thing of note is that the synthesis of the polymer was strongly affected by which counterion was used. Zotti investigated PEDOT:Tos (also written as PEDOT:OTs), PEDOT:Tos(H), PEDOT:Tos(Na), PEDOT:PSS(Na) and PEDOT:PSS(H) films. Using, cyclic voltammetry Zotti notes that the back and forward redox behaviour was identical in all analogues of PEDOT tested. According to Zotti's analysis, this indicates that the PEDOT backbone was identical in all cases. The only difference was found to be in the reduction peak for PEDOT:PSS which, at the same film thickness, was higher than was found for the rest of the polymers. Zotti believed this was due to the electrolyte motion slowing during the charging and discharging. Zotti also discovered large conductivity differences between the different PEDOT analogues tested that had been prepared by different methods.

Table 2.3: The different conductivity of PEDOT analogues tested by Zotti. (a) denotes electrochemically prepared and (b) denotes chemically prepared. Adapted from (Zotti *et al.*, 2003)

POLYMER	Conductivity ($S\ cm^{-1}$)
PEDOT:PSS (Na) a	1
PEDOT:PSS(H) a	80
PEDOT:PSS b	0.03
PEDOT:PSS(H)(aq) a	50
PEDOT:Tos(Na) a	400
PEDOT:Tos(H) a	450

From Table 2.3 it can be seen that the chemically prepared analogue of PEDOT:PSS is of much lower conductivity than the electrochemically prepared analogues. Zotti believed this was due to the chemically prepared PEDOT:PSS having an excess of PSS which was probably due to the monomers causing micelles within the emulsion. Zotti added that if NMP (N-methyl pyrrolidinone) was used to dope the PEDOT:PSS the conductivity increased by 10 times and believed this to be due to the organic

solvent causing a segregation between the PEDOT:PSS and the free PSS in the mixture, which then allowed a better conductive pathway. The conclusion was that when PEDOT:PSS is electropolymerised, the PEDOT takes up the minimum PSS to attain charge neutralisation, but when chemically prepared there is a large excess of PSS. Zotti further concludes that the reason for the large range in conductivity of different analogues of PEDOT is down to the number of sulphate groups present, which are not involved in the doping process, since they lead to an increased hopping distance and this results in the huge range of conductivities. It is also of interest to note that the stated conductivity of Zotti's analogues of PEDOT, in Table 2.3, exceeds in all cases the conductivity of those commercially available PEDOTs detailed in Table 2.2.

Kim *et al* (Kim, Kim *et al.*, 2006) also reported that the type of solvent used to synthesise PEDOT greatly affects the amount of conductivity that results. They state that the solvent causes the polymer to swell and this gives rise to a change in order which affects interchain hopping.

There is some disagreement on the crystalline structure of PEDOT. Elschner (Elschner, Kirchmeyer *et al.*, 2011) describes how PEDOT:Tosylate has a paracrystalline structure and although it can be identified using X-ray analysis, the material has only short and medium range ordering in the "lattice", which is more similar to the liquid crystal phase and lacks the long-range ordering of a real crystal structure, at least in one direction. So if the atoms were measured from a specific point in the "lattice" then the distances between them would vary. With a truly crystalline structure this would not be the case. However, PEDOT:PSS is not crystalline and instead PEDOT:PSS is described as paracrystalline (Elschner, Kirchmeyer *et al.*, 2011) having disordered conjugated chains which allow for easy charge transfer due to the fact that there is no sharp boundary between the insulating

PSS chains and the PEDOT groups so allowing the electrons to flow from one region of the PEDOT to the other relatively easily. This is contrary to what Bubnova (Bubnova, Khan *et al.*, 2014) has discovered. Bubnova suggests that in the solid state PEDOT has self-organised into crystalline domains. However, Bubnova is in this case referring to PEDOT:Tosylate.

2.4 PEDOT:PSS

PEDOT:PSS or poly(3,4-ethylenedioxythiophene): poly(styrene sulfonic acid) is commercially available in various different analogues, usually as a colloidal dispersion in solvent. The structure of PEDOT:PSS is shown in Figure 2.4. Often the solvent is water although sometimes this can be an organic solvent. The number of PEDOT groups to PSS groups varies depending upon the method of synthesis. Different methods of synthesis give very different properties to the polymer as is shown in Table 2.3.

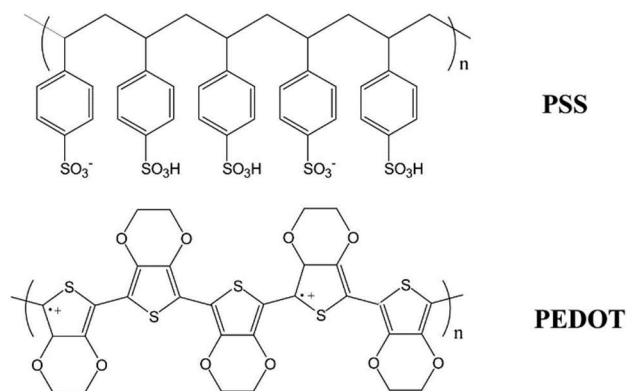


Figure 2.4: The Structure of PEDOT:PSS (Ouyang, 2013b)

PEDOT, when alone, is insoluble but when combined with insulating PSS it becomes soluble in water which has obvious environmental and processing advantages. The PSS molecule is not part of the conductive entity (Kim, Sachse *et al.*, 2011) but is in fact an insulator and is present in the mixture to allow the PEDOT molecule to dissolve into common solvents such as water. When mixed with PSS, PEDOT becomes water-

soluble. When PSS is removed Kim (Kim, Sachse *et al.*, 2011) found the conductivity greatly increases. Friedel (Friedel, Brenner *et al.*, 2011) though contrary to most authors, reports that up to a certain level the PSS group enhances conductivity. However, generally PEDOT:PSS is characterized by low conductivity with respect to other analogues of PEDOT such as PEDOT:PEG and PEDOT:OTs. This is related to both particle size and agglomeration which will be explained in the next section.

2.4.1 Particle size

Some variants of PEDOT:PSS, whilst having virtually identical properties to begin with, have very different conductivities after secondary doping. Ouyang (Ouyang, 2013a) reports on variants of the Clevios group of PEDOTs (made by Heraeus Holding GmbH, Hanau, Germany) which have the same conductivity of between $0.2 - 1 \text{ S cm}^{-1}$ when manufactured, but when doped with the same concentration of ethylene glycol, the conductivity of the resultant PEDOTs varies from 200 S cm^{-1} - 700 S cm^{-1} . Ouyang believed this is due to the particle size distribution. Other reagents used to dope the PEDOT to enhance conductivity include various solvents such as DMSO, DMF, THF and even water (DeLongchamp, Vogt *et al.*, 2005, Kim, Jung *et al.*, 2002).

The optimum size for PEDOT particles is however in some dispute. Friedel (Friedel, Brenner *et al.*, 2011) found that smaller particle sizes of 40 nm gave a better conductivity to PEDOT:PSS than particle sizes of 230 nm. Zhu (Zhu, Liu *et al.*, 2015) found conductivity of PEDOT increased when treated by DES solvents which removed the insulating PSS molecules and enlarged the particle size of PEDOT due to swelling, so in this case the bigger the particle the more conductive PEDOT was found to become. However, Zhu compared particle size using AFM images of roughness rather than measuring actual particle size so it is impossible to draw a definite conclusion from these authors. Lang (Lang, Müller *et al.*, 2009) investigated

the morphology of PEDOT:PSS and found the PEDOT grains vary in size in diameter from 50-80 nm (depending on manufacturer) and are between 5-10 nm thick with a PEDOT core and a PSS shell. In conclusion, the optimum particle size for PEDOT is very debatable and probably depends on the dopant used and the intended application.

2.4.2 Thickness

Film thickness, has been mentioned by many investigators as directly linked to conductivity, with the majority of research groups aiming for thinner films believing this to give enhanced conductivity. There are a few researchers who have found thicker films to give better results. For example, Li (Li, Qin *et al.*, 2015) as explained in 2.7.3 and Xia (Xia, Sun *et al.*, 2012a) in 2.7.1 found enhanced conductivity with some of the thicker films manufactured. Many authors (Fan, Mei *et al.*, 2008, Kim and Brédas, 2008, Zotti, Zecchin *et al.*, 2003, Zykwiniska, Domagala *et al.*, 2003), whilst stating they have enhanced conductivity fail to include the thicknesses of the film they created. This is a problem when analysing their work since the film thickness is important to conductivity with thinner films being more conductive according to many authors. Film thicknesses found by various research groups are listed in Table 2.4.

Table 2.4: Table of film thickness

Experimenter	Film thickness of PEDOT:PSS	Section number
Chang (Chang, Liao <i>et al.</i> , 2007)	15 nm, 25 nm and 50 nm	2.4.2
Alemu (Alemu, Wei <i>et al.</i> , 2012)	50-60 nm	2.4.2, 2.7.3, 3.3.2
Shaheen (Shaheen, Radspinner <i>et al.</i> , 2001)	100 nm	2.4.2
Krebs (Krebs, 2009, Krebs, Jørgensen <i>et al.</i> , 2009)	250 nm	2.4.2,
Snook (Snook, Peng <i>et al.</i> , 2007)	0.5-1.6 mm	2.4.2,
Xia (Xia, Sun <i>et al.</i> , 2012a)	66-109 nm	2.4.2, 2.7.1, 2.7.3
Jönsson (Jönsson, Birgersson <i>et al.</i> , 2003)	70 nm 110 nm	2.4.2, 2.8.3, 2.9
Kang (Kang, Lee <i>et al.</i> , 2005)	500 nm	2.2, 2.4.2, 2.8.1, 2.8.6, 3.3.1
Friedel (Friedel, Keivanidis <i>et al.</i> , 2009)	25-160 nm, 70 nm was the optimum	2.2, 2.4, 2.4.1, 2.4.2, 2.4.3, 2.8.6, 2.13
Li (Li, Qin <i>et al.</i> , 2015)	Dipped films: 113 nm pristine, 106 nm EG treated, 57 nm acid treated. PEI +2- MEA treated: 130 nm pristine, 124 nm EG treated, 61 nm acid treated	2.4.2, 2.7.3, 2.7.5, 2.8.6

Some authors do state the film thickness they obtained. For example in the experiments done by Chang (Chang, Liao *et al.*, 2007) for PLEDs, the film thickness was 15 nm, 25 nm and 50 nm. Chang found the thinner 15 nm film conducted by more than two orders of magnitude than the thicker 50 nm film did. However, Chang measured current density to obtain these results. Chang believed the injection hole barrier decreased with decreasing thickness of PEDOT:PSS and that this was due to migration of PSS into the poly-(9,9-dioctylfluorene) (PFO film) substrate. This was causing p-doping of the substrate and consequently a lowering of the PEDOT hole injection barrier. Chang used spincoating to achieve these thicknesses. Similarly, Alemu (Alemu, Wei *et al.*, 2012) used spincoating to achieve thicknesses when spin coating of 50-60 nm with PEDOT films made using ethanol or methanol. Shaheen

(Shaheen, Radspinner *et al.*, 2001) used screen printing to fabricate films of 100 nm and Krebs (Krebs, 2009, Krebs, Jørgensen *et al.*, 2009) used a combination of screen-printed or slot-die-coated PEDOT:PSS to produce a 250 nm PEDOT:PSS layer. Snook (Snook, Peng *et al.*, 2007) used cyclic voltammetry to deposit a 0.5 mm to 1.6 mm thick film of PEDOT:PSS onto the substrate in order to investigate the electrode specific capacitance (C_E , $F\text{ cm}^{-2}$) against the mass of the PEDOT:PSS. Snook was investigating supercapacitor materials and determined that PEDOT:PSS at these thicknesses, and made in this way, was higher than the electrode specific capacitance of both polypyrrole and polyaniline despite them both having a higher specific mass. Snook compared the results of the thick films made by using cyclic voltammetry and electrochemical impedance spectrometry. PEDOT films were found to have linear values for electrode specific capacitance (C_E , $F\text{ cm}^{-2}$) that increased with the film deposition charge. According to Snook in 2007, this is “currently the highest amongst all reported materials”.

Xia (Xia, Sun *et al.*, 2012a) made films with thicknesses between 66 and 109 nm and Xia found the thicker films had lower resistivity as described in Section 2.7.1. Jönsson (Jönsson, Birgersson *et al.*, 2003) states the film thickness achieved for pristine PEDOT:PSS was 700 Angstrom (or 70 nm) but for the solvent enhanced film made from sorbitol, NMP and isopropanol mixed with PEDOT:PSS was 1100 Angstroms (or 110 nm) in thickness. Both films were made by spincoating. Kang (Kang, Lee *et al.*, 2005) gives the thickness of the film produced as 500 nm. The variation in film thicknesses even when made using the same methods is huge which makes it very difficult to give a decent and reliable analysis of findings with respect to film thickness and conductivity effects. In most cases, it would seem that thicker films conduct less. This is not the case across the board with a few exceptions such as Li in Section 2.7.3 and Xia Section 2.7.1 finding the thicker films conduct more. This seems to come down to certain reagent combinations, for example Xia (Xia, Sun *et al.*, 2012a) used

PEI along with common dopants such as sulphuric acid and EG which gave a thicker film with higher conductivity than the thin films. The method of manufacture also seems to make a difference. For example electro-deposited films seem to generally have higher conductivity than those made from commercially obtained dispersions as found by Zotti in Section 2.3 (Zotti, Zecchin *et al.*, 2003). However, in most cases there is little or no indication of the film quality and thickness of film achieved by different manufacturing methods and the electrical conductivity testing regimes are also different making it very difficult to make comparisons.

2.4.3 Agglomeration

Agglomeration due to removal of PSS is believed to occur due to increased Van der Waals forces because the negatively charged PSS molecules have been removed. PEDOT:PSS also agglomerates when stored (Choi, Cho *et al.*, 2010). Friedel (Friedel, Keivanidis *et al.*, 2009) found particles of PEDOT:PSS that had been sonicated agglomerated over a period of time. This means the older the solution the more it will have agglomerated. Friedel does not believe agglomeration to be a problem for PEDOT:PSS solutions used immediately. When Snaith (Snaith, Kenrick *et al.*, 2005) used glycerol as a dopant, it was found that after heat treatment to cure the films, no glycerol was present in the dried film. Snaith believed the increased conductivity was due to the swelling and aggregation of the PEDOT particles. Choi (Choi, Cho *et al.*, 2010), however, found agglomeration to be a huge problem even in newly made solutions. Friedel (Friedel, Keivanidis *et al.*, 2009) found agglomeration to occur during the film forming process and used filtration to try to combat this. Despite filtering, agglomeration increased with time and after 30 minutes large agglomerates had been found to form in the solution. Although agglomeration does occur with solutions of PEDOT this can be dealt with relatively easily by incorporating filtration or sonication into the scheme of work. It is also possible that when conductivity is increased after adding a dopant the agglomeration of the particles

could be, as Snaith (Snaith, Kenrick *et al.*, 2005) believed, the reason why conductivity increases.

2.5 PEDOT as a Semiconductor

PEDOT:PSS and similar electrically conducting polymers are usually classified in the materials category as semiconductors. Their electrical conductivity is related to the band gap (E_g) where the energy gap between the highest occupied molecular orbital (HOMO) and the lowest unoccupied molecular orbital (LUMO) is small (Rasmussen, 2011). The material's conjugation, and delocalisation, is directly related to the band gap and therefore to the energy difference between the filled and unfilled molecular orbitals. The E_g is a forbidden band which cannot be populated. This energy gap determines a materials lowest energy absorbance and also, any emission energy. The bond length of the material is also important and is considered to have a large effect on the E_g of any material. The more conjugation that is present within a molecule the larger the E_g is expected to be. In an aromatic structure, the aromatic form is considered to be the most stable form which is therefore the lowest in energy level, whereas the quinoid form is of higher energy.

In the case of substituted polythiophenes such as PEDOT the polymer backbone also contributes to how conductive the material will be. If there is a loss of planarity due to steric hindrance where larger side groups have been added to the structure this can inhibit the conductivity by disrupting the conjugation and stopping the macromolecules from coming into contact in such a way as to allow a conductive pathway.

2.5.1 Resonance structures and Energy levels

In the seminal paper by Bredas (Bredas, Themans *et al.*, 1984) the reason why the structure must be quinoid rather than benzoid is discussed. Figure 2.5 shows the quinoid and aromatic conformations of polythiophene.

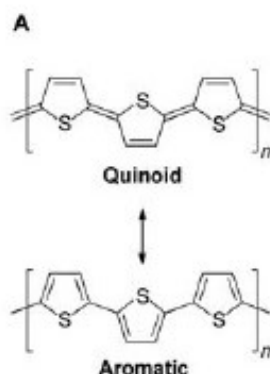


Figure 2.5: Aromatic and quinoid resonance forms of polythiophene (Rasmussen, 2011)

Although Bredas's work is dated 1984 it has been quoted by most investigators of charge carriers in polythiophene and PEDOT. Bredas explains that the quinoid form of polythiophenes has an envisaged resonance structure between the benzoid form, which is aromatic, where low energy aromatic rings are joined by one single sigma-bond, but the higher energy quinoid form is the resonance structure where the two thiophenes are joined by double pi-bonds between the thiophene molecules. The quinoid structure, was found to have a lower ionisation potential and a higher electron affinity, which would result in a smaller band gap than the conductive trans-polyaniline structure with which it was compared. What this means is it is easier to remove an electron when it is in the quinoid form and the same quinoid structure will also attract electrons or negative charges more easily than the aromatic structure. When doped the aromatic structure relaxes into the quinoid form and causes formation of a charged defect in the structure. This lowers the ionisation energy of the structure. The quinoid part of the chain in polythiophene molecules changes from pi (π) to sigma (σ)

bonds in order to compensate for the energy needed to produce the quinoid and to create the charged defect.

It is of interest to note that at low doping levels Bredas found that the polaron charge carrier forms, and this is associated with the quinoid structure. This probably extends over 4-5 segments of the polythiophene ring (or it is reasonable to assume over the PEDOT) rings. Bredas suggests that formation of the polaron produces both a bonding state which is predicted to be slightly above the valence band (VB) edge and an antibonding state which is predicted to be slightly below the conduction band (CB) edge. The valence band equates to the HOMO and the conduction band equates to the LUMO. Bredas also calculated that when there are two polarons adjacent to one another, they become unstable due to pairing of their spins and they go on to form a bipolaron which has no spin. In contrast to conductive polymers such as trans-polyaniline which conducts via a sigma to pi-bond interchange which amounts to a soliton mechanism rather than a polaron-bipolaron mechanism, the charges in the polythiophene family of molecules must form polarons and bipolarons in order to move and therefore to produce an electrically conductive polymer. Therefore the bipolaron is probably the mechanism of conductivity in PEDOT:PSS and similar systems. Figure 2.6 shows a representation of the charge carriers generated and being raised from the HOMO level to the LUMO level in semi-conductors such as PEDOT:PSS.

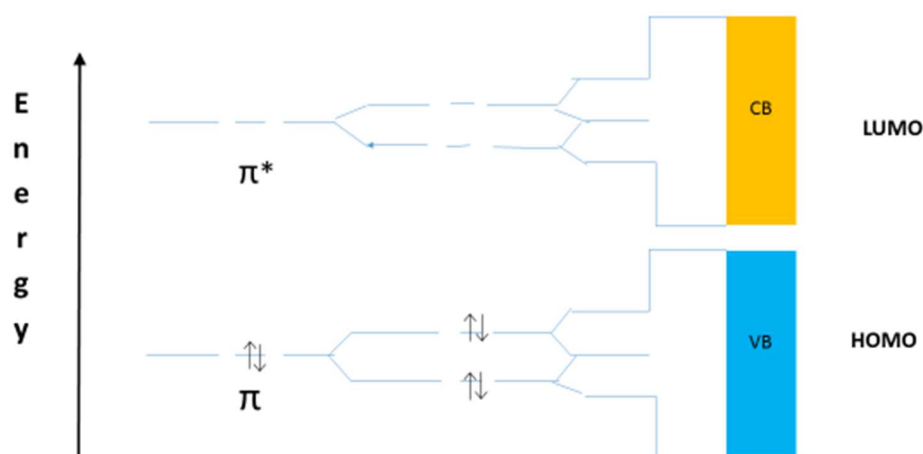


Figure 2.6: Representation of the charge carriers generated and being raised from the HOMO level to the LUMO level in semi-conductors

In 2003, Geskin (Geskin and Brédas, 2003) did a theoretical study regarding polaron – bipolaron interactions in polythiophene chains. Note that the study did not take into account solvent effects. Geskin was interested in whether a polaron on a polythiophene chain was intrinsically stable or relatively stable. If intrinsically stable then it is stable without the presence of counterions. If relatively stable it must rely on a second polaron, or in other words be part of a bipolaron.

To check which structure was predominant Geskin used bond length calculations. The aromatic benzoid structure has different bond lengths to the quinoid structure, and also the bond lengths between the C-S are different in each structure. The calculations lead to the prediction that the charge carrier is a bipolaron when the chain is long because, according to the studied bond lengths, the charge is in the centre of the chain. On a shorter chain, the charges, are predicted to be separated at each end of the chain so a short chain must contain two separate dissociated polarons.

Gao (Gao, Liu *et al.*, 2002) disagrees with this theory, and believes that as the chain increases in length, there is a change from the polaron to bipolaron forms. The small chained polymers with oligomers up to 6 units have charge carriers that are bipolarons but above this chain length Gao believes the charge carriers become two-polaron structures which is the opposite of Geskin's view. This means the bipolaron pair can exist in short oligomers and the separate polarons become the most prevalent in longer chained polymers. Gao also believed that there is a transition state between the bipolaron structure and the two separate polarons since this would be energetically preferred.

However, both of these results are obtained from data for polythiophenes with a variety of oligomer sizes. Actual data was from experiments using oligothiophenes rather than polythiophenes, however it is reasonable to expect that PEDOT would, being a polythiophene molecule, have similar conductivity mechanisms to these oligomers. Massonet (Massonet, Carella *et al.*, 2014) also believed the formation of the polaron to bipolaron mechanism depends upon the quinoid structure. Massonet found that post treatment using ethylene glycol did not modify the oxidation state of the PEDOT or enhance conductivity and the Seebeck effect was enhanced as expected. Generally, as the conductivity of PEDOT:PSS decreases the Seebeck effect is found to increase (Kroon, Mengistie *et al.*, 2016).

2.5.2 Charge transport

Harima (Harima, Eguchi *et al.*, 1999) did an in situ measurement on poly(3-methylthiophene) which is part of the polythiophene family of conductive polymers. They used electron spin resonance (ESR) to probe the charge transport of polarons and bipolarons and concluded that below a doping range of 0.1 % only polarons carry charge but when the doping level is increased up to 1 % it is diamagnetic bipolarons

that are the charge carriers and this enhances the conductivity. Harima also believed that doping levels above 1 % gave the polymer a metallic charge transport character.

This is an interesting conclusion, but it must be stressed that this result was for a different member of the polythiophene family of intrinsically conducting polymers. Although many experimenters have agreed that PEDOT:PSS generates polarons and bipolarons, most researchers do not think that PEDOT:PSS, or any other variant of the PEDOT family, actually gain metallic character. Elschner describes PEDOT as having a paracrystalline structure and there seems to be no conclusive evidence that PEDOT in any of the analogues has a truly metallic character.

However, it was found by Palumbiny (Palumbiny, Heller *et al.*, 2014) that some forms of doping can cause crystallites to form amidst the amorphous chains which can be detected by GIWAXS. Also according to Rasmussen (Rasmussen, 2011), if a heteroatom has high electron affinity this will lower the E_g , since it will stop the potential of the material to change to the quinoid form by confining the π -electrons to the aromatic ring structure. Since PEDOT contains both sulphur and two oxygen atoms, PEDOT contains several heteroatoms. If the E_g is lowered this will stop the delocalisation and so reduce conductivity. If these type of electrically conductive polymers are doped with some other kind of atoms this causes an increase in the number of charge carriers present and creates a charge carrier complex which contains delocalised radicals. The delocalised radicals can be radical, cationic or anionic depending on the nature of the added dopant. Kvarnstrom (Kvarnström, Neugebauer *et al.*, 1999) believes the low bandwidth of PEDOT is due to the electron donating effects of the two oxygen atoms on the dioxy-ring which attach at the 3 and 4 positions to the thiophene structure. Zykwinska *et al.* (Zykwinska, Domagala *et al.*, 2003) believed that polarons and bipolarons exist in PEDOT:PSS and that their numbers depend upon doping levels. They found that paramagnetic centres existed

in PEDOT. Zykwincka used electron spin resonance to identify polarons and bipolarons. A polaron can be detected due to having a spin resonance of $\frac{1}{2}$ which means it is a paramagnetic species whereas the bipolaron has no spin due to the electrons pairing. Zykwincka believed that polarons and bipolarons co-exist at intermediate doping levels. They also interact with each other so any response spectroscopically will potentially be due to the presence of both species, and also be influenced by any other paramagnetic charge carrier species that could be present in the polymer. Even at low potentials and after de-doping, the ESR spectra showed residual spins. Zykwincka believed this proved that a quinoid structure, not a benzoid structure existed in PEDOT. Analysis of the ESR lines showed the presence of radical cations or polarons appearing in the oxidised polymer. It was found that during the oxidation process a large increase in the concentration of spins was detected which later decreased in concentration which Zykwincka attributes to the polarons combining to form spinless bipolarons. Figure 2.7 shows how this may occur.

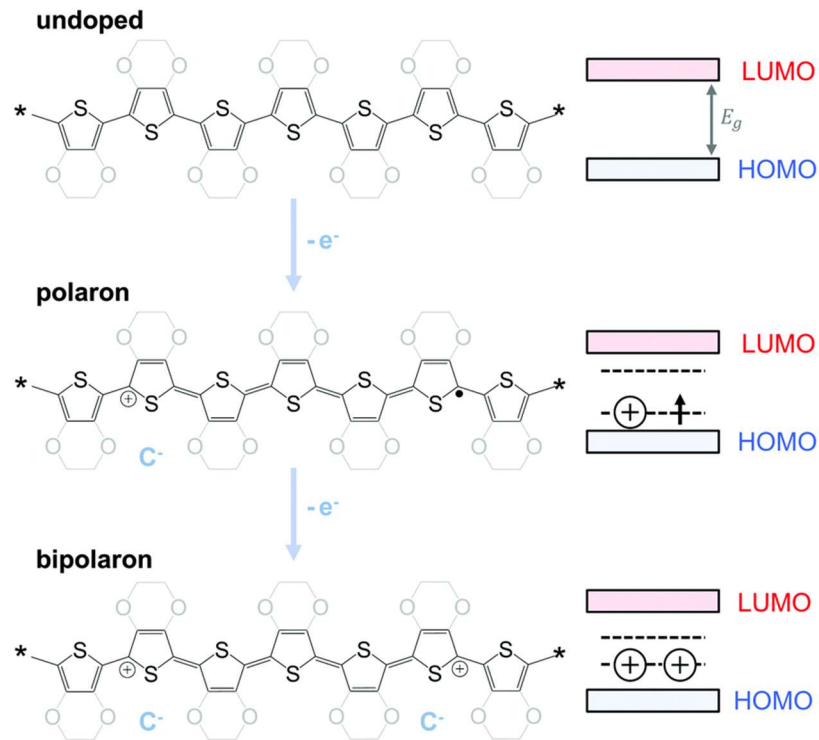


Figure 2.7: Adapted from: Generation of polarons and bipolarons in polythiophene, PEDOT and related polymers (Kroon, Mengistie *et al.*, 2016)

Elschner (Elschner, Kirchmeyer *et al.*, 2011) also describes the process where-by PEDOT:PSS forms a polaron and explains that it is due to a localised hole gaining energy due to coulombic attractions. This causes new energy levels to be created and electronic transitions to take place raising the charge carriers from i to i^* and from the VB to the CB bands.

Experiments by Park (Park, Park *et al.*, 2013) showed that the amount of oxidation of PEDOT is important. Park made PEDOT with a block co-polymer and a surfactant and controlled the level of oxidation in order to optimise the thermoelectric properties rather than the conductivity. Park believes that the level of oxidation is critical and they managed to enhance conductivity despite actually reducing the number of groups that are oxidised on the polymer chain. This suggests that there is a level of oxidation which is optimum. After this has been reached, although it is possible to oxidise PEDOT beyond this point, it is actually detrimental to conductivity to do so.

According to Bubnova in the article “semi-metallic polymers” (Bubnova, Khan *et al.*, 2014) controlling the oxidation levels of PEDOT allows optimisation of the thermoelectric properties. Bubnova postulates that removing the electrons from the top of the valence band in a single polymer chain may lead to two different defects both of which are positively charged. These positively charged radical cations are polarons. When formation of a di-cation occurs the two single cations join together to act as one unit charge which is a bipolaron. These charges are balanced by counterions in the polymer lattice. Bubnova postulates that the distortion of the lattice, due to formation of the defects will lead to alteration in the bond length around the location of the positive charge and this in turn “defines the extent of the wavefunction”. This is in agreement with Geskin (Geskin and Brédas, 2003). This means the bipolaron has a local distortion to the molecular structure which causes the in gap state to change from i to i^* . When a polaron is formed this means the level i is half filled but for a bipolaron it will be empty, as shown in Figure 2.7 which was adapted from Kroon (Kroon, Mengistie *et al.*, 2016). Similar to the experiments of Zykwska (Zykwska, Domagala *et al.*, 2003), Bubnova used ESR (Electron Spin Resonance) for detection of polarons and bipolarons. According to Bubnova, there is a localisation of polarons and bipolarons on a segment of the amorphous chains. At high levels of oxidation of the PEDOT molecule the results indicated that charge transport mechanisms in PEDOT:PSS and PEDOT:OTS is by both polarons and bipolarons at the same time as by hopping electrons.

Interestingly, when Mengistie (Mengistie, Chen *et al.*, 2014b) used dopants (ethylene glycol, polyethylene glycol, methanol, and formic acid) to enhance the electrical conductivity, the conductivity of PEDOT:PSS with formic acid was enhanced to a maximum of 1900 S cm^{-1} which gave the best enhancement. However, The Seebeck coefficient was hardly found to vary. It just plateaued out. Mengistie like Park (Park, Park *et al.*, 2013) believed this was due to the fact that although the secondary

dopants increase the conductivity, they do not change the level of oxidation. Denneulin *et al* (Denneulin, Bras *et al.*, 2011) found that an ink made from carbon nanotubes with carboxylic acid functionalisation gave better jettability when ink-jet printed using a PEDOT:PSS dispersion rather than an aqueous dispersion. It was discovered that PEDOT:PSS allowed the CNTs to orientate and to organise which gave better conductivity to the finished product. This suggests that the PEDOT chains may align and so cause the incorporated CNTs to line up as well. If PEDOT unravels and aligns in certain solvents that may explain the increase in conductivity when PEDOT has been doped since connectivity between the PEDOT chains would be enhanced. It would appear that the total number of charge carriers within a PEDOT chain is not increased by doping. This means doping, rather than increase the number of charge carriers, simply allows a better framework or lattice for the charges to travel within. Therefore, from these observations it seems to be likely there is no change to the number of charge carriers available regardless of what is used as a dopant and that there is a maximum oxidation level. Once this is reached it may be detrimental to conductivity to oxidise PEDOT any further.

2.6 Tracking the changes in the shape and conductivity of the PEDOT molecule

A number of researchers have used Ultra Violet-Visible-Near Infra red analysis (UV-Vis-NIR) in situ to show that PEDOT and PEDOT-analogues go through a three step redox cycle where the molecule converts, from the ground state, into polarons, then bipolarons and finally into a metallic state as described in Section 2.5.2. This system was illustrated in Figure 2.7. Chen (Chen and Inganäs, 1996) polymerised PEDOT electrochemically using cyclic voltammetry, With fast scanning Chen showed that PEDOT has three peaks which correspond to the three states in which it exists. Chen found three reduction peaks and two oxidation peaks which corresponded to the

transfer of electrons in polaron, bipolaron and metallic states. Using NIR, polarons and bipolarons can be detected and transition between different states observed. Nasybulin (Nasybulin, Wei *et al.*, 2012) states that in order to check the quality of the PEDOT:PSS it is sometimes possible to use UV-Vis-NIR spectroscopy since this is simple, powerful and should be able to show the polymer is in a conductive or oxidised state by studying the signature of the functional groups. UV can sometimes be used to find the conjugation bond lengths since it can detect the $\pi-\pi^*$ transition using a peak at 580 nm. In addition, because PEDOT is useful in solar applications and has a transparency in the visible spectrum at around 800 nm, this can sometimes be used to verify PEDOT is in the correct state to conduct. However, Ouyang (Ouyang, Xu *et al.*, 2004) found no differences between un-doped PEDOT:PSS and doped PEDOT:PSS when measured with UV. The UV absorbance spectrum of PEDOT:PSS shown in the paper written by Luo (Luo, Billep *et al.*, 2013) also shows no peak at 580 nm but rather a slow upwards inclination. It seems therefore that when measuring PEDOT and PEDOT:PSS by UV to show the $\pi-\pi^*$ transition, it may depend on the level of PEDOT, the manufacturer and the level of doping whether or not this peak is present. Nasybulin, found that cyclic voltammetry did not identify the transitions between the oxidised and reduced states of PEDOT. Nasybulin believed that UV-Vis-NIR was the better method for this purpose. Zotti (Zotti, Zecchin *et al.*, 2003) states that only the undoped PEDOT:PSS can be checked for conductivity using UV where it absorbs at 575 nm which is very close to the region stated by Nasybulin for the $\pi-\pi^*$ transition.

Palumbiny (Palumbiny, Heller *et al.*, 2014) manufactured the two types of doped PEDOT using spin-coating with glycerol mixed into the PEDOT:PSS solution but with EG being applied as a secondary dopant to the pre-made film afterwards. Palumbiny used a commercial solution of PEDOT:PSS and spin coated it onto glass slides. Palumbiny describes the conductivity mechanisms within the PEDOT polymer as

being higher along the backbone chain where delocalisation of the electrons is easiest due to conjugation in the molecules.

The mechanism of conductivity was described as being due to π - π stacking between the chains where the mechanism will be due to hopping transport. When Palumbiny doped PEDOT:PSS with glycerol and ethylene glycol, it was found that the shape of the molecules changed. Using Grazing Incident Wide Angle Xray Scattering (GIWAXS), the backbone as well as the π - π stacking became parallel to the substrate. This improved conductivity due to the now densely packed regions where the EG had removed PSS from the PEDOT chains. Removal of the PSS gave better charge transport. Addition of glycerol similarly changed the molecular shape. In the case of glycerol there was a slight increase in crystallinity. Interestingly this is the only report found where crystallinity slightly increases with the treated film to give larger crystallites and smaller amorphous areas between the chains. This would allow for better charge transport in the now crystalline regions. As previously stated Ouyang (Ouyang, Xu *et al.*, 2004) earlier reported this was not the case. Since Palumbiny's report is ten years later it must be concluded that recent developments have found PEDOT that has been treated with glycerol has been shown by one author to have crystalline regions within the material despite older research finding the opposite.

Kroon (Kroon, Mengistie *et al.*, 2016) believed that although PEDOT:PSS has not been found to be truly crystalline it conducts by two methods. Firstly, charge transport is more likely to occur due to intermolecular exchange in the direction of π -stacking of the polymer chains. This is in agreement with Palumbiny's edge-on orientation where larger crystallites were formed with respect to face-on arrangements within the PEDOT and this was attributed to ethylene glycol treatment. The edge-on arrangement was found to give increased conductivity from 0.2-1200 S cm⁻¹. Kroon states that since redox doping involves transfer of electrons this form of charge carrier

must form a donor-acceptor or ion pair. The other possible charge transfer method would be the transfer of an anion or cation to the polymer backbone. Kroon calls this acid-base doping. In order to maintain charge neutrality this method would need to have a counterion present. Following this method, in order to create polarons, either addition of or removal of an electron must occur or alternatively addition or removal of a cation or anion. The polaron will be negative if it is created using a radical anion or positive if created using a radical cation. When the levels of doping are high enough the polarons would convert to bipolarons which could then delocalise over several unconjugated π -bonded polymer segments. This would accompany formation of a quinoid resonance form of PEDOT as shown in Figure 2.2.

2.6.1 The mechanism of charge transport in PEDOT:PSS

The process of doping is a redox process between the polymer and the donors (which can also be called acceptors). This leads to an ionic complex of a positive (or negative) polymer with counterions of the opposite charge distributed along several repeating units. In PEDOT doping gives rise to p- or n- type semiconductors. The level of conductivity in theory can be controlled by the amount of doping and the type of the dopant. The alternating π -conjugation allows the electrons to become delocalised over all or part of the polymer chain depending on the chain length. Bubnova (Bubnova, Khan *et al.*, 2014), states that there is up to one charge carrier for up to three monomer units.

Conducting polymers can be divided into two types. Degenerate and non-degenerate. PEDOT is non-degenerate polymer. According to Furukawa (Furukawa and Tasumi, 1991), the tautomers of non-degenerate polymers have differing energies. A degenerate polymer exists when all possible tautomeric forms have identical structures and energy. A non-degenerate polymer has different tautomers with different structures and different energy. Degenerate applies in polymers such as

polyacetylene, where the energy of both possible tautomers is identical. Non-degenerate applies to polymers such as PEDOT and other polythiophenes. This is because PEDOT can have one or two charges (Elschner, Kirchmeyer *et al.*, 2011). In the case of PEDOT, no two molecules are identical in energy. Each tautomer has a different structure with different bond lengths between the atoms. The aromatic form of PEDOT is considered to be stable whereas the quinoid forms of PEDOT are less stable but higher in energy. This means the quinoid forms are able to allow conductive charge carriers to flow. When PEDOT conducts it is more likely to be ionised and therefore it will be in the quinoid structure, rather than the stable aromatic structure. Ionisation causes a positive or negative charge to occur on the polymer chain.

To gain the ionised structure, first an electron must be removed or added to the chain. When an electron is removed a radical cation is formed. This is a positive polaron. When a second electron is removed a dipolaron is formed. A positive dipolaron is a dication so has a (+2) charge, and the charge is delocalised over several repeating units of the chain. A polaron will delocalise over a longer chain than a dipolaron Furukawa (Furukawa and Tasumi, 1991).

The change from aromatic to quinoid means that the C=C and C-C bond lengths also change. This is due to the delocalisation of the electrons, which after ionisation, become mobile and able to move along the polymer chain. The electrons become mobile in order to attempt to neutralise the charge on the polymer chain and this causes a current to flow.

If an electron is added to the polymer chain an anion is formed and this equates to a negative polaron or anion. A dianion is a negative dipolaron and has gained two electrons, which will have delocalised over the repeating units in an identical way to the positive charges in order to attain equilibrium. A polaron has a spin of $\frac{1}{2}$ whereas a dipolaron has no spin due to the electrons pairing up. A soliton can be neutral,

positive or negative and equates to a neutral radical, a cation or an anion. The soliton mechanism is believed to cause the hopping mechanism.

Furukawa believed that a positive bipolaron or dication loses two electrons from the VB. One from the bonding orbital, one from the antibonding orbital. A negative dianion or dipolaron gains two electrons which are both added to the VB antibonding orbital. In both cases two transitions can be observed within the band gap (Furukawa and Tasumi, 1991). Several authors have stated that an extra band forms between the antibonding LUMO and bonding HOMO levels. Bredas, using polypyrrole (PPy) as the model, (Bredas and Street, 1985), cited in 2014 by Bubnova (Bubnova, Khan *et al.*, 2014), found that bipolarons are spinless charge carriers when observed with ESR. Bredas, believed that spinless bipolarons, when in highly doped concentrations, were screened from their counterions. This allows them to move freely within the polymer chain. In polypyrrole, Bredas used optical density versus eV measurements and observed that when the doping level was low there were three absorption peaks present which Bredas attributed to the presence of polarons or single charge carriers. The absorptions between the gap levels disappear as the doping level was raised and the absorptions change to one single larger peak. Bredas attributes this to the transition of the polaron to a bipolaron. Bredas experimented with several other conducting polymers including polythiophene and found very similar results. The only difference in the results was that at low doping levels there were two not three absorption peaks arising within the gap. Bredas attributes this to the fact the polythiophene is less disordered than PPy and therefore the polarons are more inclined to combine into bipolarons and only the bipolarons can be observed. Polythiophene, unlike polypyrrole, is believed to attain metal-like conductivity. Bredas believes this to be due to the merging of the upper and lower bipolaron bands in the VB and CB levels. When a p-type of doping is achieved this means the new level will

be formed in the VB and this will be empty. It must be remembered, however, that Bredas was measuring polythiophene and not the more stable PEDOT.

2.7 Doping of PEDOT:PSS

Many authors have concluded that PEDOT can be doped just like the parent polythiophene and that doping with certain reagents increases wettability as well as conductivity (Kim, Jung *et al.*, 2002, Ouyang, 2013b, Snaith, Kenrick *et al.*, 2005). The most common dopants include CNTs, Graphite, carbon, metal particles, ionic liquids, high boiling point organic acids and solvents, zwitterions, salts, co-solvents and inorganic acids and glycerol. (DeLongchamp, Vogt *et al.*, 2005 Greczynski, Kugler *et al.*, 2001, Greczynski, Kugler *et al.* 1999, Liu, Xu *et al.*, 2012, Luo, Billep *et al.*, 2013, Ouyang, 2013b, Ouyang, Xu *et al.*, 2004)

2.7.1 Acids

Greczynski (Greczynski, Kugler *et al.*, 2001, Greczynski, Kugler *et al.*, 1999) used X-ray photoelectron spectroscopy (XPS) to analyse the surface of PEDOT:PSS films. Greczynski found the PSS collects at the rough parts of the surface of the film and that the Na⁺ ions can be easily removed from the surface by rinsing with acid such as HCl. This would indicate that an acid based reagent may have the same effect on a PEDOT:PSS and might remove the PSS ions. Greczynski also found that the thickness of the film did not alter the ratio of PEDOT to PSS in the film. Using AFM to determine the structure of the film, Greczynski also determined that PEDOT:PSS must have a grain-like structure despite being a suspension and found the film surface was not homogeneous with respect to the PEDOT and PSS species within the grains. Xia (Xia, Sun *et al.*, 2012a) used sulfuric acid (H₂SO₄) to enhance a thin film of PEDOT:PSS from 0.3 S cm⁻¹ to 3065 S cm⁻¹. Xia applied several coats of thin films of PEDOT:PSS and reported a sheet resistance of 67 Ωsq when treating a three layered PEDOT:PSS film which had a reported thickness of 66 nm. A five layered film

was reported as having a sheet resistance of $39 \Omega\text{sq}$ with a thickness of 109 nm. This means Xia found the thicker film had lower resistivity which is an interesting result because it is the opposite of most researchers. Xia's result may have been due to there being five thinner layers making up a thick layer of PEDOT which gave an overall more homogeneous film which in turn enhanced conductivity.

2.7.1.1 pKa

Ouyang (Ouyang, 2013b) used organic acids which were added by post treating the cured PEDOT:PSS film. The conductivity was stated as increasing to around 3300 S cm^{-1} using this method. Ouyang explains the increase in conductivity as being attributed to a combination of the pKa of the acids used with methane sulfonic acid having a low pKa and acetic acid having a high pKa. The conductivity was found to be consistent with the pKa of each acid used so was assumed to be due to the concentration of the hydrogen ions and also to the shape of the individual acid molecules since although the pKa of malonic acid is higher than oxalic acid, malonic acid still gives the greater enhancement of electrical conductivity.

Acids seem to give thinner films which has been linked by several researchers to enhanced conductivity but whether it is best to mixture dope (or add the dopant into the mixture prior to annealing) or post dope the PEDOT seems very much to depend on the view of the individual research group.

2.7.2 Water

In 2005, DeLongchamp (DeLongchamp, Vogt *et al.*, 2005) used deionised water to rinse the PEDOT:PSS film which had been spin-cast and discovered that PSS was removed from the bulk polymer as a result. Ouyang (Ouyang, Xu *et al.*, 2004) also found that water can remove PSS. Since PSS is an insulator, removal or reduction of the concentration of PSS should allow a better connectivity of the conductive PEDOT

grains. Agarwal (Agarwal, Lvov *et al.*, 2006) used water as a solvent to produce an electrically conductive PEDOT:PSS coated paper.

2.7.3 Alcohols and High Boiling Point Solvents

Ouyang (Ouyang, Xu *et al.*, 2004) used cyclic voltammetry to test two films. The first film had ethylene glycol (EG) added into the PEDOT:PSS solution. The second film was where the films were treated after making the film. Both methods increased conductivity. The EG post treatment method increased conductivity from $0.4 - 200 \text{ S cm}^{-1}$. The method of movement of charge was believed to be due to charge hopping along and across the chains of PEDOT. Ouyang believed a dipole is formed between the organic solvent used and the PEDOT chains which leads to enhancement of the conductivity. The films were studied using cyclic voltammetry and UV and IR simultaneously from +0.7 up to -0.2 V and observed 40 % higher maximum at 600 nm using UV. Ouyang postulates that in the EG treated films, the polymer chains uncoil. With the untreated films they remain randomly coiled. This leads to the untreated film being only partly reduced but the EG treated film is completely reduced. Ouyang describes this as an “expanded-coil or linear structure”. Electron transfer between randomly coiled chains is more difficult than electron transfer between the expanded-coil structures. When Ouyang studied differences between the films using AFM he found that after the EG treatment there were large domains rather than smaller areas found with the untreated film. Contact angles with water also changed after EG treatment and the surface of the PEDOT had become more hydrophobic. Ouyang also notes that conductivity enhancement depends on what organic reagent is used. If EG, (which at room temperature is a liquid), is used, conductivity is always enhanced but some reagents can enhance conductivity only after having been annealed at high temperatures in an oven. Conductivity enhancement is very much dependent on the structure of the reagent. Having a polar

group such as acetonitrile, nitromethane, and methanol does not necessarily lead to conductivity enhancement and it appears that only when the reagent has several polar groups that the effect can be seen. There is likely therefore, to be some sort of dipole-dipole interaction between the reagents negatively charged functional groups and the positive charge on PEDOT. Ouyang also proposed the conductivity enhancement is due to the H-bonding of the reagent to the PSS molecule and the driving force for the conformational changes that occur when PEDOT:PSS is doped are due to dipole-dipole interactions between the reagent used for doping and the charges on the PEDOT chains. By bonding in this manner using multiple dipole-dipole interactions, the solvent can insert itself into the polymer structure and this causes an enhancement of conductivity. Interestingly the PEDOT was found to be amorphous after doping regardless of the dopant used despite being paracrystalline prior to doping (Elschner, Kirchmeyer *et al.*, 2011). According to Ouyang the structure of PEDOT is also changed from benzoid to quinoid. Bredas (Bredas, Themans *et al.*, 1984) had also determined that this must be the case for the polaron mechanism (see 2.6.1) and at low doping levels the polaron forms. This is due to the quinoid structure forming in the polythiophene molecules which changes from pi (π) to sigma (σ) bonds and this means it creates the charged defect.

Luo (Luo, Billep *et al.*, 2013) found similar results to Ouyang when studying the addition of a high boiling solvent to PEDOT:PSS. In this case DMSO, and post treatment with the high boiling solvent was compared after having made films of PEDOT:PSS. The post treatment method was better than in mixture treatment for enhancement of conductivity. Luo believed the conductivity was improved due to the PEDOT changing shape into an elongated network which allowed the electrons to move more easily. This also improved the Seebeck coefficient. See Section 2.7.5 for further information about Luo, Billep *et al.*'s research.

Li (Li, Qin *et al.*, 2015) used 2-MEA solvent to enhance the conductivity when spin casting PEI with PEDOT:PSS. The 2-MEA solvent itself is believed to enhance the electrical conductivity of PEDOT:PSS. When used alone Li found that 2-MEA enhanced conductivity of PEDOT:PSS to 744 S cm^{-1} when spin coated or to 687 S cm^{-1} when dip coating. Since the PEI alone was found to lower conductivity the increase when 2-MEA was present must be down to the solvent interactions and not to the PEI interactions. Li discovered that the film thickness of the EG treated PEDOT:PSS decreased and conductivity increased. Sulphuric acid treatment of PEDOT:PSS also thinned the film and again increased the conductivity. But when PEI was added the EG and sulphuric acid treated films decreased in conductivity whereas the pristine film had enhanced conductivity which was believed to be due to the 2-MEA solvent. Li also tested the effect of methanol and ethanol in post treatment by spin coating them on top of the PEDOT:PSS films and found they increased conductivity to 521 S cm^{-1} for methanol and 4 S cm^{-1} for ethanol. For film thicknesses see Section 2.4.2, Table 2.4. Snaith (Snaith, Kenrick *et al.*, 2005) used glycerol to enhance the conductivity of PEDOT:PSS and found the PEDOT particles appeared to swell and cause aggregation of the PEDOT molecules which enhanced conductivity. Kim (Kim, Kim *et al.*, 2006) found alcoholic solvents used during the polymerisation of PEDOT:OTs, including methanol, ethanol, hexanol and n-butanol enhanced the conductivity of PEDOT:OTs. In each case to achieve effective doping the solvent needed to be between 20 % and 23 % to enhance the conductivity. Most significant results were obtained with the use of hexanol which increased the conductivity by a factor of 200 compared with methanol which only increased conductivity by a factor of 5.3. However, all of the alcoholic solvents did increase conductivity by a measurable amount.

Kim (Kim, Jung *et al.*, 2002) found that the conductivity enhancement was due to the solvent being between the polymer main chains rather than through conformational

shape changes within the polymer chains. PEDOT:OTs was in particular found to change in conductivity in the presence of alcoholic solvents. In fact Kim (Kim, Kim *et al.*, 2006) found that the shorter chained alcohols enhanced the conductivity better than longer chained alcohols and the alcoholic series corresponded to the amount of enhancement caused; ie: methanol>ethanol>n-butanol>hexanol. Kim used the solvents as part of the synthesis reaction to make the PEDOT:OTs and did not post-dope the polymer to enhance the electrical conductivity. Kim, unlike other researchers, used alcoholic solvents with a single alcohol functional group but still found this enhanced conductivity. Kim also used DMSO, THF and DMF and found that DMSO enhanced the PEDOT conductivity by two orders of magnitude but that there was significantly less enhancement with both THF and DMF. Other polar organic solvents such as ethylene glycol, nitromethanol and glycerol have been used. To achieve enhancement, the high boiling point polar solvents must also have multiple hydroxyl groups. These have been found to enhance the conductivity to around 200 S cm^{-1} . Solids such as D-sorbitol have enhanced conductivity in a similar way. Clevios PH1000 has been reported to be enhanced to $600\text{-}700 \text{ S cm}^{-1}$ with the addition of EG or DMSO (Ouyang, 2013a, Xia, Sun *et al.*, 2012a). Alemu (Alemu, Wei *et al.*, 2012) used methanol applied in various different ways to enhance the conductivity of PEDOT from a starting point of 0.3 S cm^{-1} to a maximum of 1362 S cm^{-1} . Methods used included dropping onto films, mixing with the solution before the film was cast and a combination of both. Best results were obtained with post treatment. Alemu also experimented with propanol and ethanol but these were found to give inferior results. It was concluded the enhancement was due to removal of the PSS groups by the alcohol. This in turn caused conformational shape changes to the PEDOT chains. The starting material in this case was Clevios PH1000. Kim (Kim, Sachse *et al.*, 2011) created electrodes from PEDOT by adding the ethylene glycol (EG) to the PEDOT solution and optimising this until the best results were

achieved with an ethylene glycol concentration of 6 % which give a conductivity of 700 S cm^{-1} . Kim then post treated the film with ethylene glycol by immersing in a bath for several minutes before drying. The highest conductivity of 1418 S cm^{-1} was obtained by immersion times of 30 minutes. AFM showed there was a structural change where the film thickness was reduced and the PSS molecules removed. Kim also ascertained that the sheet resistance of the PEDOT increased with increasing exposure to air. However the PEDOT:PSS sheets tested with no solvent treatment had higher resistances than those that were post treated which was believed to be due to the hygroscopic and acidic, water attracting PSS groups. Kim found that the longer the film was immersed in solvent the better the conductivity, however post treatment was not infinite since the longer times of two hours immersion and above gave a result where the conductivity was reduced. Post treated films were also found to be rougher than un-treated films so post treating of PEDOT:PSS with ethylene glycol does several things. It increases conductivity up to a maximum, removes PSS groups and changes the film to a rougher surface. For optical applications where PEDOT transmission is of importance it was also found that there was no change in transmission regardless of the fact the film thickness was reduced after post treatment. Xia (Xia, Sun *et al.*, 2012b) reports that alcohols with two or more alcohol functional groups are required for conductivity enhancement and that alcohols that have only one OH group per molecule have virtually no effect on conductivity enhancement of PEDOT:PSS. This is in complete contrast to the enhancement reported by Kim (Kim, Kim *et al.*, 2006). Kim found ethanol and butanol to be the best enhancers of conductivity amongst alcohols tested. However, this research concentrated on PEDOT:OTs rather than PEDOTs containing polystyrenesulfonate counterions. This means the electrical differences within each molecule would be different due to the effects of the functional groups on the OTs and PSS molecules

and so the possibility of forming H-bonding to molecules such as alcohols, could also be different.

Pettersson (Pettersson, Ghosh *et al.*, 2002) reports that previously conductivity up to 500 S cm^{-1} was obtained by polymerising PEDOT with the OTs group into thin films, but PEDOT:PSS differed in that it is coated into a thin film from an aqueous dispersion. To the aqueous dispersion they added sorbitol prior to spin coating. Conductivity was around $0.1\text{-}10 \text{ S cm}^{-1}$ but when sorbitol, glycerol or other poly-ols were added to the solution before spin coating, and followed by annealing with heat the conductivity increased to around two orders of magnitude. It appears then that most researchers agree that a reagent with single alcoholic group makes little difference, but that multi-ols make considerable difference when enhancing conductivity is the objective. Furthermore, when the concentration of sorbitol (see Figure 2.8 for structure) was at 65 % by weight to the PEDOT:PSS solid electrical conductivity was achieved that was 56 S cm^{-1} which gave an increase in conductivity of around 60 times with respect to that of the starting material. Pettersson believed plasticisation of the material was taking place as the sorbitol was incorporated.

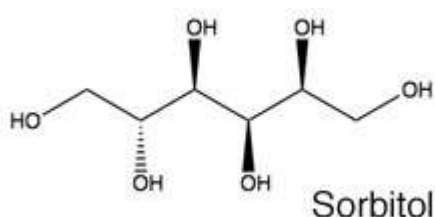


Figure 2.8: Structure of sorbitol (Anon (a))

This enabled the polymer chains to re-orientate allowing for more interchain interactions between the polymer chains which should in theory enhance conductivity due to the extra places where the different chains come into contact with each other, thus allowing a pathway for electron movement and therefore current flow. Ouyang

(Ouyang, 2013b) used ethylene glycol (EG) to cause enhancement up to 600-700 S cm⁻¹ for the PH1000(aq) form of Clevios PEDOT:PSS. This structure is shown in Figure 2.9.

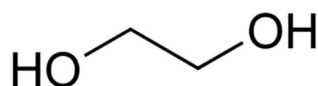


Figure 2.9: Structure of mono-ethylene glycol (Anon (b))

There is some disagreement between research groups as to whether single alcohols or multi-ols are best to enhance conductivity of PEDOT:PSS but it generally seems accepted that at least some alcohols do this. Possibly the effectiveness of alcohols and high boiling point solvents at doping PEDOT:PSS comes down to the method of application and any co-solvent effects.

2.7.4 Ionic liquids

Many different experimenters report using ionic liquids to aid conductivity in electroactive components. Ionic liquids have been used to help enhance conductivity of aqueous PEDOT:PSS films. Liu (Liu, Xu *et al.*, 2012) used ionic liquids to add to an aqueous PEDOT:PSS dispersion. Ionic liquids used were: 1-butyl-3-methylimidazolium tetrafluoroborate [bmim(BF₄)] and 1-butyl-3-methylimidazolium bromide [bmim(Br)]. After stirring together the ionic liquid and the aqueous PEDOT:PSS solutions, films were cast and then annealed in an oven. The maximum electrical conductivity obtained by Liu was 174 S cm⁻¹ which was more than one order of magnitude higher than the plain undoped PEDOT:PSS. The Seebeck coefficient was also improved by this method. There was no post doping. The substrate used was smooth and flexible PP. No detailed reference was made to how the conductivity study was measured other than saying the authors were using the four-probe method. They do not state what voltage was used for these tests. Zhu believed the conductivity

changes were due to interactions between the polyanionic PEDOT:PSS and the ionic liquids where the conductivity increased due to a polar interaction between the two. The interesting thing about this report is that both the conductivity and the Seebeck coefficient were found to increase. As previously stated, Luo (Luo, Billep *et al.*, 2013) also experimented with ionic liquids, using 1-ethyl-3-methylimidazolium tetrafluoroborate (EMIMBF₄) as a post treatment of the PEDOT:PSS film which caused a formation of a network of circular grains which enhanced the conductivity. Luo however stated that the Seebeck coefficient decreased as the conductivity increased. Kroon (Kroon, Mengistie *et al.*, 2016) was in agreement with Luo that the Seebeck effect works in such a way that as it decreases, electrical conductivity increases and vice versa.

2.7.5 Surfactants

Several authors including Fan (Fan, Mei *et al.*, 2008) report the increasing conductivity of PEDOT:PSS films when doped with surfactants. Surfactants used for this include cationic, anionic and also non-ionic. Fan *et al* used anionic surfactants such as sodium dodecyl sulfonate (SDS) and dodecylbenzenesulfonic acid to enhance the conductivity. Fan found the maximum conductivity of the PEDOT:PSS film made using sodium p-toluene sulfonate (TsONa) which was added to the aqueous PEDOT:PSS solution. It was then spin coated and annealed to give PEDOT:PSS (OTs), and produced a significant increase in conductivity. The starting conductivity was 0.16 S cm^{-1} but with addition of the TsONa solution the conductivity increased to 25.4 S cm^{-1} . The highest conductivity of PEDOT:PSS (OTs) film was found to be in the region of 37 S cm^{-1} when the molar ratio was 2.2 for the PEDOT:PSS and the tosylate ion. Similarly the addition of the SDS increased the conductivity to a value of 80 S cm^{-1} with a result that the sample had 500 times higher conductivity than the normal PEDOT:PSS. Fan postulates that there is a completely

different mechanism for the increased conductivity than for that proposed for the high boiling point solvents which are often used to enhance conductivity in PEDOT:PSS by changing the structure of the PEDOT:PSS molecules.

Ouyang, reporting on his own previous research states that a non-ionic surfactant used for improving wettability actually improved conductivity of PEDOT:PSS by a factor of about 20. However this was not reported in the original paper (Ouyang, Guo *et al.*, 2002). Ouyang used non-ionic surfactant polyoxyethylene (12) tridecyl ether (POE12) which was added into the solution of PEDOT:PSS. Ouyang believed the effect of surfactants on conductivity all depended on the chemical structure of individual surfactants. For example; with an anionic surfactant conductivity increase is reported as being enhanced by two orders of magnitude but the cationic surfactants hardly change conductivity.

Li (Li, Meng *et al.*, 2015) found a conductivity increase when using 2,5,8,11-tetramethyl-6-dodecyne-5,8-diol ether (PEG-TmDD), which is a non-ionic surfactant, as a wetting agent for PEDOT:PSS. Li also determined that the conductivity enhancement was dependent on how the annealing was achieved. This is not the case when doping with ethylene glycol (EG), however, so this was believed to be due to the PEG-TmDD decomposing during annealing into EG under acidic conditions. In this research the non-ionic surfactant was an additive used for wetting but also was found to improve conductivity to 526 S cm^{-1} . The type of PEDOT:PSS used was Ph1000, which was mixed with 4 % wt of PEG-TmDD. Li (Li, Qin *et al.*, 2015) found addition of PEI did nothing to aid in conductivity of two of the analogues of PEDOT (PH1000-SA AND PH1000-EG) since it actually caused a decrease, probably due to electron transfer taking place from the PEI to the PEDOT, but that the PH1000-p film was enhanced electrically by the PEI addition. Addition of sulphuric acid was found to enhance the conductivity of all three of the films. This was despite the fact that the PEI was used with a solvent which itself will enhance the conductivity of PEDOT to

744 S cm⁻¹. In this experiment Li used three grades of PEDOT:PSS, PH1000-p, PH1000-EG and PH1000-SA.

It is the view of Fan (Fan, Mei *et al.*, 2008), that the enhancement of conductivity with respect to the surfactants was to do with the anion involvement from the surfactant molecules rather than the cation. His argument is that since sodium chloride solution does not alter conductivity, and the counter cation for the surfactants is also sodium, then it has to be the anionic surfactant molecule that interacts and causes the conductivity increase. Normally the PEDOT chains will align in a region next to or near to the PSS chains. When the anionic surfactant is introduced, it replaces the PSS as a counter-ion to PEDOT, and this gives a conformational change in the orientation of the PEDOT molecules which results in higher electrical conductivity.

Nasybulin (Nasybulin, Wei *et al.*, 2012) also experimented with SDS but used surfactants as reagents for the electrodeposition of PEDOT rather than for adding to PEDOT at a later stage. Nasybulin also found enhanced conductivity with respect to films that had been deposited in the presence of SDS. Nasybulin was using electrochemistry to make the PEDOT films rather than depositing a pre-made commercial product into a thin film. It can be reasonably concluded then that SDS does enhance conductivity of PEDOT:PSS when it is made electrochemically despite originally being used as a solubilizing agent rather than as a dopant. Nasybulin used several other surfactants, amongst them TWEEN 80 (polysorbate 80 or polyethylene sorbitol ester). The main finding of Nasybulin, other than the influences of SDS on conductivity enhancement with surfactants, was that there is a delay before the initial polymerisation step begins. The length of this delay is dependent upon which surfactant is used. It was discovered that TWEEN 80 had the longest time of delay before polymerisation starts of the non-ionic surfactants investigated. Results from the cationic surfactants showed the longest time of delay. This gave the anionic surfactants as the best surfactant for electrodeposition of EDOT to produce PEDOT.

Nasybulin reports that TWEEN 80 has an oxidation potential with respect to being a solubiliser for EDOT of 0.85 V. Nasybulin was using cyclic voltammetry to polymerise the polymer rather than to test the already made polymer. The cyclic voltammetry was run from 0.00-1.0 V at a 100 mV/s scan rate. The polymerisation of EDOT was done using potentiostatic deposition and was run at 1.0 V by passing a charge of 6.25 mC/cm².

Like Fan (Fan, Mei *et al.*, 2008), Nasybulin believed the anionic surfactants gave better conductivity enhancement than cationic surfactants. However, nonionic surfactants seem to have given mixed results with Ouyang (Ouyang, 2013b) and Li (Li, Meng *et al.*, 2015) both stating conductivity was enhanced by a nonionic surfactant but Nasybulin finding a nonionic surfactant was slightly better than cationic but nowhere near as effective as an anionic surfactant. Of course the fact that each research group used slightly different parameters and different equipment must be taken into account when analysing which type of surfactant works the best in enhancing PEDOT. It could be that different parameters give completely different results with the same type of surfactant.

The conditions for each research group are completely different. However, nonionic surfactants do not start the initiation polymerisation process as fast as anionic surfactants. This does not mean the same nonionic surfactant will not enhance the conductivity of the sample, if the sample is post treated or if the surfactant has been added to the polymer solution before casting into film, rather than being used for the actual polymerisation reaction itself. Table 2.5 shows results from Nasybulin's research into surfactant effects on the properties of PEDOT.

Table 2.5: Surfactant effects on PEDOT, adapted from: Nasybulin (Nasybulin *et al.*, 2012)

Surfactant/solubiliser	Open circuit voltage	mA/cm ²
AOT	0.51	6.73
SDS	0.58	6.6
TWEEN 80	0.41	4.53
PSS	0.42	4.13
HDTMA	0.35	4.33
K-Carrageenan	0.36	4.13
TritonX-100	0.28	3.87
HDHEDMA	0.2	2.27

2.7.5.1 Aggregation/agglomeration and surfactant

Agglomeration or aggregation is a problem when trying to manufacture solid films of PEDOT from solution. Whether PEDOT has PSS or another copolymer makes no difference to the problem of agglomeration. Like many other experimenters Sukchol (Sukchol, Thongyai *et al.*, 2013) post doped with SDS surfactant. Sukchol also used SDS as a solubiliser to prevent agglomeration when investigating polymerisation of EDOT to PEDOT, as did Pham (Pham, Sohn *et al.*, 2012), who used a surfactant to disperse copper particles into PEDOT solution to make a PEDOT-copper composite. Pham mixed PVP and CTAB surfactant with PEDOT:PSS in order to both disperse the particles and to prevent the copper from oxidising. Very few references directly state using a surfactant to help prevent agglomeration, however many authors have doped with surfactants during polymerisation or during formulation prior to annealing the solution into a solid. Tkalya (Tkalya, Ghislandi *et al.*, 2012) reports on the use of TWEEN 80 surfactants with PEDOT:PSS and CNTs to form a dispersion. This suggests that surfactants may also help to stop the agglomeration of the PEDOT particles leading to a better film quality. As was stated by Wakizaka (Wakizaka, Fushimi *et al.*, 2004), the surface morphology of PEDOT films is not good regardless

of the technique used to manufacture them or the analogue of PEDOT used. In conclusion aggregation of PEDOT particles makes dispersion problematic and using surfactants seems to help with film forming as well as with doping of PEDOT:PSS.

2.8 Film forming and Adhesion

Cho (Cho, Hwang *et al.*, 2011) found delamination to be a problem although even when the PEDOT layer delaminated from the PET substrate it was still found to be conductive. Gerwig (Gerwig, Fuchsberger *et al.*, 2012) also had delamination problems when comparing electrodes made from CNTs and PEDOT:PSS with PEDOT:PSS where the PEDOT:PSS alone delaminated but the composite did not.

Several different authors have used chemicals to enhance the wettability or to modify the surface of a substrate in one way or another to enable adhesion of PEDOT to the substrate. For example, Vosgueritchian (Vosgueritchian, Lipomi *et al.*, 2012) used a fluoro-surfactant to achieve this. Dimic-Misic (Dimic-Misic, Gane *et al.*, 2013) experimented with coating printer paper with various concentrations of carboxymethylcellulose (CMC). In this case CMC was used to modify the surface of paper and the quality of print was then assessed along with print gloss. Although these experiments were performed for the printing industry the results can be applied to this project where the modification of the surface of plastics used as substrates is required. Morsy (Morsy, 2005) investigated the effects of soluble thickeners used as polymer coatings on paper treated with a base of clay, casein and oxidised starch. Polymers used were CMC with different degrees of substitution at pH 8.5. Morsy used gravure ink and reports an increase in the dielectric constant but with improved gloss and print quality. Dimic-Misic (Dimic-Misic, Gane *et al.*, 2013) did experiments with coating paper with various concentrations of microfibrillated cellulose (MFC), nanofibrillated cellulose (NFC) to assess using them instead of natural additives such as CMC. In this case CMC was used as a co-binder with either MFC or NFC as partial

replacement for some of the CMC that would usually be used for this purpose. It was found that incorporating some NFC into the CMC led to less water retention in the substrate. Encinas (Encinas, Abenojar *et al.*, 2012) had done experiments in altering the contact angle of a substrate which was in this case polypropylene. This was achieved by abrasion of the surface by sanding. Plasma treatment was also tried by Encinas to alter the wettability of the substrate.

Elschner (Elschner, Kirchmeyer *et al.*, 2011) reports on attempts to use various different additives to increase hardness and adhesion of PEDOT. It is interesting to note that several authors have made inorganic/organic composites to try and address the adhesion problems. More recently, Park (Soo Kim, Bin Oh *et al.*, 2010) reports on having made a silicon/PEDOT composite which incorporates a network of silicon onto the substrate so that PEDOT will adhere better. Park believed the PEDOT bound better to the substrate due to the surface covering of –OH groups which would allow for H-bonding of the PEDOT to the coating. This was believed to be due to a combination of interactions between both the Si-O-Si groups and the –OH groups on the surface of the glass which caused formation of a SiO₂ network. This made the PEDOT much harder and improved adhesion. Without the addition of the silicon the PEDOT delaminated very easily from the glass substrate. It seems an overall issue that PEDOT films delaminate and in order to gain adhesion it is necessary to somehow modify the substrate.

2.8.1 Humidity

It is important to mention that several authors have investigated the de-doping of PEDOT when water is present. Water whether from air or water molecules left in incompletely annealed film may cause de-doping of PEDOT which will decrease conductivity. Kang (Kang, Lee *et al.*, 2005) believed that de-doping occurs at high humidity (up to 50 %) and this caused the de-doping. Interestingly, removal of the

moisture from the samples caused a reversible re-doping to occur and the return to conductivity. However as pointed out by Elschner (Elschner, Kirchmeyer *et al.*, 2011) de-doping does not necessarily mean that PEDOT has actually been fully de-doped but instead that the number of ionised sites is reduced or altered. It would also seem that PEDOT:PSS thin films change in structure when absorbing water molecules since Huang (Huang, Miller *et al.*, 2005) states that “The hygroscopic PEDOT:PSS gel particles swell after water uptake. The films after thermal treatment have a PSS-rich component on the surface, which is especially hygroscopic and may cause H₂O molecules to form a thin layer above the PSS chains. The surface layer of H₂O molecules may suppress the influence of thermal and ambient gas on the morphology of the films”.

Huang goes on to state that PEDOT:PSS when made into films is hygroscopic to such a degree that it was possible to calculate that the amount of water absorbed corresponded to the number ratio of the PSS groups to those of PEDOT. Since the reason for the PSS being present at all is that it acts as a diluent to help to dissolve or disperse the PEDOT molecules into water this is a reasonable assumption to make. Huang however took this further and calculated that the ratio of PEDOT to PSS he was investigating was 1:6 and the amount of water absorbed corresponded to this with an estimated water content of 1:6 of PEDOT molecules. The PEDOT films which had been annealed in an oven were found to have a critical temperature (50 °C) when they begin to take in water molecules. As the temperature falls back to ambient so the PSS absorbs even more molecules of water. Furthermore, Huang found that O₂ annealed PEDOT films, even after absorbing water, were 13 times more conductive than the air annealed films. Films annealed under nitrogen were even more conductive. This suggests that annealing under a gas other than air may be beneficial for long-term conductivity despite Huang finding there was no obvious difference in conductivity of the PEDOT films immediately after manufacture. This could be

because cleavage of the polymer chains due to swelling may interfere with or stop conductivity. Mengistie (Mengistie, Chen *et al.*, 2014b) found that higher humidity caused PEDOT to become less brittle. Since brittleness is a problem this could be utilised to enhance flexibility and still be conductive. If a film is brittle it can fracture which will cause loss of conductivity due to breaking and delamination. Mengistie found the amount of humidity could be carefully controlled to give a less brittle but still electrically conductive sample. When Massonnet (Massonnet, Carella *et al.*, 2014) dipped layers of spin coated PEDOT:PSS into EG for 15 minutes the layer of PEDOT was separated from the substrate upon which it was made. After 20 minutes of immersing the PEDOT layer into EG the polymer had improved resistance to water. Massonnet believed the process was removing PSS from the PEDOT:PSS layer which would make the polymer more hydrophobic since PSS is the vehicle used to solvate the PEDOT into the water. Film thickness was from 80-100 nm. Other changes were improved electrical conductivity and improved mechanical resistance. Immersing the polymer for longer, Massonnet tried up to two weeks, was not found to give further improvements. Massonnet followed the immersions in EG with treatment with strong reducing agents in order increase the thermoelectric power of the films. To produce high conductivity samples annealing should really take place in an atmosphere that is free from water molecules. Despite this many investigators have reported reasonable results when they annealed in air.

2.8.2 Temperature

In order to extend shelf life it would be beneficial to store samples of PEDOT films at a minimum of 51 °C which is just above the temperature at which Huang (Huang, Miller *et al.*, 2005) in Section 2.8.2, determined was the critical temperature for stopping water molecules from binding to PEDOT:PSS. Huang (Huang, Miller *et al.*, 2005) discovered it is not just the choice of dopant that affects conductivity but also

annealing temperature and the gas under which the sample is annealed. At temperatures up to 250 °C annealing the films shows an increase in conductivity. However, Elschner (Elschner, Kirchmeyer *et al.*, 2011) states that PEDOT films are only stable up to 200 °C and that pristine PEDOT:PSS starts to degrade at 150 °C. After this the films lose conductivity.

2.8.3 Morphology

Jönsson (Jönsson, Birgersson *et al.*, 2003) investigated heating effects on dopants and how this affected the performance of the PEDOT films. Jönsson found that films doped with sorbitol lost dopant material when heated. Huang (Huang, Miller *et al.*, 2005) compared Jönsson's results with his own investigation and found that when films doped with glycerol were heated the dopant was lost which increased the ratio of the PEDOT to the PSS molecules when comparing with undoped PEDOT:PSS films. In Sections 2.7.3 and 2.7.4 it was discussed how Luo changed the morphology of PEDOT:PSS by doping with DMSO and an ionic liquid EMIMBF₄. Luo, who was trying to improve the Seebeck effect rather than the electrical conductivity of PEDOT:PSS, tried both addition of DMSO and post treatment of PEDOT:PSS using DMSO with EMIMBF₄ to see if it could affect the Seebeck effect, which it did, with post treatment being the better option. Luo believed the solvent gave a screening effect between the PEDOT chains and the PSS which allowed easier charge transport. Luo showed that there was a difference in the morphology of PEDOT:PSS when treated with different solvents since the treated grains of polymer became flatter which would allow better charge transport since the PEDOT molecules would touch more easily. However, this work also used an ionic liquid, 1-ethyl-3-methylimidazolium tetrafluoroborate (EMIMBF₄). It was believed that the post treatment of the film with EMIMBF₄ caused a formation of PEDOT film with a network of circular grains, which enhanced the conductivity. Luo discovered that post

treatment of PEDOT film with DMSO along with EMIMBF₄ caused a reduction in the thickness of the film correlating to the loss of PSS molecules by 40 %. Luo believed the post treated sample that was treated with DMSO had elongated PEDOT grains which were in the bipolaron state. However when the EMIMBF₄ was added in the post treatment this caused formation of a network of PEDOT with short circular grains. Luo believed these grains were the de-doped form of PEDOT and that a higher intensity type of polaron was formed which would account for the improvement of the Seebeck coefficient and the lowering of electrical conductivity.

It is necessary to achieve a balance when doping with different solvents since in order to enhance electrical conductivity the Seebeck effect does not need to be enhanced. If however the aim was to enhance the Seebeck effect, or the thermoelectric qualities of PEDOT a different choice of solvents would be needed. What Huang (Huang, Miller *et al.*, 2005) found was that the PEDOT molecules ended up being distributed more uniformly with respect to the untreated films. This would account for why doped films are more conductive since some of the PSS molecules are being removed, along with the volatile solvent, by the heat of annealing as part of the doping process. By removing some of the insulating PSS molecules Huang and other investigators are in effect concentrating the PEDOT so that the molecules touch more and provide a better conductive pathway for the charge carriers. The dopant was also partly removed by both investigators, which suggests, it is not actually the dopant that is the mechanism for the improvement of conductivity but actually the dopant is the mechanism for removal of the insulating PSS molecules. This, inadvertently, leads to improving the conductivity by concentrating the PEDOT and connecting the different PEDOT chains to provide a better pathway for the charge carriers to move.

2.8.4 Crystalization of PEDOT:PSS

Elschner describes (Elschner, Kirchmeyer *et al.*, 2011), PEDOT:PSS as having disordered conjugated chains which allow for easy charge transfer due to the fact that there is no sharp boundary between the insulating PSS chains and the PEDOT groups. This allows the electrons to flow from one region to the other relatively easily. Elschner also describes how PEDOT:OTs is paracrystalline and can be identified using X-ray analysis, but how PEDOT:PSS is not really crystalline and X-ray analysis is, therefore, of no use for analysis of PEDOT:PSS. For any polymer to conduct electrically the disorder in the system needs to be suppressed as much as possible so that high ion and electron mobility can be attained (Street, 2006). Since it is energetically favourable for the polymer chains to line up and to stack they then become less disordered and they are able to form two-dimensional crystallites. Kim (Kim, Kim *et al.*, 2006) used XRD to characterise his products and concludes that the solvent used during polymerisation of PEDOT changes how the molecules pack together which in turn affects how much electricity can be conducted. XRD showed the molecules pack more efficiently when using the shorter chain length alcohols as solvents and Kim suggests the solvents use hydrogen bonding to change the molecular ordering to enhance the interchain hopping of electrons which will give rise to better conductivity. Kim also found that when synthesizing the OTs analogue of PEDOT:PSS that methanol is the best solvent to use. Of course this could simply be down to the size of the molecule used as a solvent since methanol is also the smallest molecule of the solvents chosen by Kim for testing so would actually take up less room than a larger molecule would, when packed between the PEDOT chains. This then could simply be a steric effect and other than the simple fact of the dimensions of methanol being smallest there is no other reason for the solvent effect on enhancement of PEDOT:PSS. As described in Section 2.6 Palumbiny (Palumbiny, Heller *et al.*, 2014) doped PEDOT:PSS with glycerol and ethylene glycol was shown

by GIWAXS to change the shape of the molecules. The backbone of the PEDOT with its π - π stacking becomes parallel to the substrate. This improves conductivity due to the densely packed regions where the EG has removed PSS from the PEDOT molecules. Palumbiny also showed that glycerol changes the shape of PEDOT molecules and causes crystallites to form in pockets with smaller amorphous areas between the chains. Palumbiny showed that an edge-on orientation had larger crystallites formed than were found in face-on arrangements and this was attributed to ethylene glycol treatment. The edge-on arrangement was found to give increased conductivity from 0.2-1200 S cm⁻¹. If crystallites are formed within the edge-on doped structure of PEDOT as both Palumbiny and Kroon (Kroon, Mengistie *et al.*, 2016) believe, then this could explain the improved conductivity of doped as opposed to undoped PEDOT:PSS. Charge transport within crystallites would be more rapid and carriers more mobile due to the order allowing easy transport. Similarly in those regions where there are no crystallites it would be intra-chain charge hopping that would be the most likely mechanism. However, it is important to remember that despite the presence of crystallites the whole of the structure is a mixture of both crystallites and amorphous disordered regions. In order to ensure effective charge transport between the disordered amorphous area and the more ordered crystallite rich areas there are several other factors that should be noted. According to Kroon the way in which the disordered regions are arranged is of utmost importance. For efficient charge transport within these regions the polymer chains must be sufficiently long in order to be able to form bridges between the crystallite areas and disordered areas. These bridges would then allow for transport between crystallites far more efficiently. This would explain how a polymer such as PEDOT:PSS which is primarily disordered and amorphous can have conductivity at all. Street (Street, 2006) also states that when a polymer has ordered crystallites it will not have a high enough degree of order to give high mobility. This is because it may still contain randomly

orientated lamellae which will give inefficient charge transfer. If PEDOT does contain crystallites it would have to attain the kind of order where most of the conducting lamellae will lie in-plane. Kline (Kline, McGehee *et al.*, 2006) used XRD and found that the number of disordered crystallites depended on how hydrophobic the surface was. Kline proved that only a small amount of disorder will change the amount of charge transfer.

2.8.5 Aging

Experiments on aging of PEDOT:PSS were undertaken by Namkoong (Namkoong, Younes *et al.*, 2015) and as part of these the solvation of PEDOT:PSS was investigated. Results indicated that the best solvents to solvate the PEDOT molecules were those that are hydrophobic. In the case of isopropyl alcohol it was discovered that the solvent helped to make agglomerates in both pristine and old stored PEDOT:PSS smaller and better dispersed. This in turn enhanced the performance of spincoated active layers for PV solar cells. It is possible the carbon part of isopropanol which is hydrophobic is repelling absorbed water molecules. However, isopropanol contains both hydrophobic and hydrophilic groups. The repelled water molecules may then bind to the hydrophilic OH group. This will allow for a better dispersion of the PEDOT solution.

2.8.6 Thermal analysis

Friedel (Friedel, Keivanidis *et al.*, 2009) used thermal analysis to analyse PEDOT:PSS. Using thermal gravimetric analysis (TGA) of PEDOT:PSS Friedel found two weight loss results. These were believed to be caused by outgassing of SO_2/SO_3 from the PSS which occurred at 250 °C. For the type of PEDOT:PSS Friedel analysed the expected amount of weight loss amounted to 41 % of the starting material since there was a 1:16 ratio. There was also a third mass loss at 350 °C. This was attributed to the rupture of the polymer backbone. Using Differential scanning calorimetry (DSC)

and Dynamic mechanical analysis (DMA) there were found to be no phase transitions above 400 °C.

2.8.7 Summary

Processing issues with PEDOT include wettability, thickness of film, humidity and adhesion. Using various different methods of manufacturing, the PEDOT thin film can vary in thickness. This probably affects the conductivity. Most authors find the thinner films have better conductivity. For example Chang Chang (Chang, Liao *et al.*, 2007) found thinner, 15 nm, films were more conductive than 50 nm thick films. Friedel (Friedel, Keivanidis *et al.*, 2009), found the mid-range film the best with 70 nm thick films being the optimum in their research. Li (Li, Qin *et al.*, 2015) in Section 2.7.3 and Xia (Xia, Sun *et al.*, 2012b) in Section 2.7.1 found better conductivity with thicker films of 61-103 nm films and 109 nm respectively. Since different researchers have chosen films in completely different thickness ranges it becomes difficult to decide on optimum film thicknesses. However, it would be expected that film quality as well as thickness would make a difference to conductivity since any uneven sections or holes in the film would inhibit current flow. Different dopants and manufacturing techniques could also be a factor. In order to obtain a decent film at all on a substrate the PEDOT needs some help with wetting usually provided by surfactants or other additives. Obtaining a homogeneous film is reported to be a problem for most research groups. Whether it is a thick film or a thin film this seems to be an across the board issue. Several authors report needing to use a surfactant as an additive in order to produce a decent homogeneous film by increasing wetting. Possibly this may also help to inhibit agglomeration of the PEDOT particles which is an associated problem with film forming. Water content is a inhibits for conductivity of PEDOT as hygroscopic PEDOT:PSS particles swell after water uptake and Huang (Huang, Miller *et al.*, 2005) in Section 2.8.1 proved that films made under oxygen and nitrogen were far more

conductive than the air annealed films. This could be due to cleavage of the polymer chains from swelling which may interfere with conductivity. Water may also though be beneficial in controlled amounts as found by Mengistie (Mengistie, Chen *et al.*, 2014a) in 2.8.1 who proved films made in humid environments were less brittle due to water content than those with no water. This could be useful to prevent delamination due to flaking of very dry brittle films. To extend shelf life of stored samples they need to be stored above 51°C which Huang (Huang, Miller *et al.*, 2005) determined was the critical temperature to stop water being absorbed by PEDOT films in Section 2.8.1. Mengistie (Mengistie, Chen *et al.*, 2014a) found shelf life was affected by humidity. Adhesion to substrates, or rather lack of adhesion, is reported with many literature references stating the problems with PEDOT is mainly down to its delamination from most substrates. By using additives such as surfactants and aiding wettability some researchers have found improved substrate adhesion. Annealing temperature may also affect adhesion as may the gas under which the sample is annealed since annealing under nitrogen or oxygen rather than air may help to control the amount of humidity and therefore the amount of water absorbed (Huang, Miller *et al.*, 2005). De-doping due to absorption of water may be reversible as found by Kang (Kang, Lee *et al.*, 2005) in Section 2.8.1.

2.9 TWEEN 80

TWEEN 80 is a non-ionic surfactant with a similar structure to that of sorbitol which is shown in Figure 2.10. TWEEN 80 is also known as Polysorbate 80 or Polyethylene sorbitol ester. Surfactants are believed to give better film quality when used as a wetting agent as described in Sections 2.7 and 2.8. Sorbitol is believed to enhance the conductivity of PEDOT:PSS as described in Sections 2.7.3 and 2.8.3 (Jönsson, Birgersson *et al.*, 2003, Kim, Kim *et al.*, 2006, Pettersson, Ghosh *et al.*, 2002). The structure of TWEEN 80 is shown in Figure 2.10.

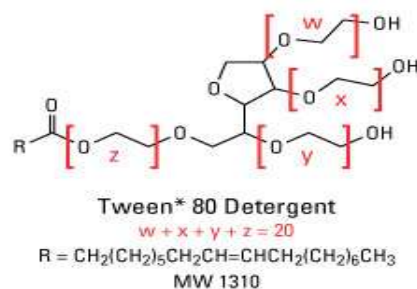


Figure 2.10: The structure of TWEEN 80 surfactant

A number of research groups have experimented with TWEEN 80 with PEDOT:PSS. Kopola (Kopola, Tuomikoski *et al.*, 2009) used Clevios PEDOT:PSS with TWEEN 80 surfactant to produce a polymer PLED¹ using gravure printing. The TWEEN 80 surfactant was incorporated into the solution to produce a homogeneous film. TWEEN 80 was used by Kopola to reduce the surface tension of PEDOT:PSS. Kopola (Kopola, Tuomikoski *et al.*, 2009) did not believe the TWEEN 80 had any influence on the conductivity of the PEDOT:PSS. Kopola used 1 % of TWEEN 80 in his formulation with isopropyl alcohol (IPA) as solvent. In a later paper Kopola (Kopola, Aernouts *et al.*, 2010) used PEDOT:PSS with 2-propanol to make four different formulations of ink and found the TWEEN 80 with PEDOT:PSS gave very different results when using different quantities of solvents. Other researchers who used TWEEN 80 with PEDOT:PSS include; Tkalya , Setti and Hrehorova (Tkalya, Ghislandi *et al.*, 2012) (Setti, Fraleoni-Morgera *et al.*, 2005), (Hrehorova, Pekarovicova *et al.*, 2006).

Nasybulin (Nasybulin, Wei *et al.*, 2012) experimented with TWEEN 80 and was the only investigator found who actually attempted to use this substance as a dopant for PEDOT:PSS. Typically it was used it as a dispersant or other kind of additive.

Nasybulin originally used TWEEN 80 as a solubilising agent and not as a dopant. Nasybulin ended up concentrating his research on a different surfactant instead as detailed in Section 2.7.5 which Nasybulin believed enhanced conductivity of PEDOT:PSS better.

2.10 MEK

The only reference found where MEK had been used as a solvent for PEDOT:PSS was the work of Middleton (Middleton, 2012) who did not use MEK as a dopant but did use it as a solvent when injection moulding OLEDs using PEDOT as the hole injection layer. Middleton found MEK was useful in diluting PEDOT:PSS for use in bulk manufacturing systems. Middleton used MEK to aid in spraycoating the PEDOT:PSS straight onto the injection moulding tool and then used the temperature and pressure gradients produced during the injection moulding process to anneal the PEDOT:PSS whilst producing a multi-layer device. No further references to using MEK with PEDOT were found.

2.11 Hypothesis for using MEK and TWEEN 80 as dopants

Several researchers have discovered that surfactants can be used for enhancing both wettability and the conductivity of PEDOT as explained in Section 2.7.5. Since film quality must also affect conductivity the combination of a solvent with TWEEN 80 surfactant could not only improve the quality of the thin film but may also enhance the conductivity. Although Middleton (Middleton, 2012) did not report any conductivity enhancement it is of interest to attempt to mix MEK with TWEEN 80 and use the resultant solution to improve the processing of PEDOT:PSS and see if this mixture may enhance the conductivity and improve the film quality.

2.12 Conclusions

Conclusions can be made as follows:

- 100 % PEDOT is paracrystalline and probably never achieves a metallic lattice structure.
- Doped forms of PEDOT have always been found to be amorphous, with the exception of Palumbiny (Palumbiny, Heller *et al.*, 2014), who used synchrotron GIWAXS and GISAXS experiments and found crystallite regions (rather than true crystallinity) mixed with amorphous regions when making a doped solution of PEDOT using glycerol. Addition of EG as secondary dopant removed these crystallites.
- The most highly conductive PEDOT is made in-situ using electrochemistry to deposit it as a film
- Chemically synthesised PEDOT is less conductive than electrochemically deposited PEDOT.
- Commercially available forms of PEDOT, which can be bought as a dispersion in solvents, are less conductive than electrochemically deposited PEDOT. This is probably due to the presence of excess PSS groups when the polymer is made chemically with an excess of PSS.
- When a solvent is added to PEDOT:PSS the PSS is liberated to give less crystallinity and to allow more connectivity between the PEDOT chains which enhances conductivity.
- There are a number of PEDOT derivatives that are more conductive than PEDOT:PSS but they are generally more difficult to process and tend to be available in less “Green” solvents. PEDOT:PSS is often available as an aqueous solution.

- Many authors do not state the thickness of the films they are measuring so no real comparisons of conductivity can be made with respect to film thickness. The range of film thicknesses is very hard to report accurately since some authors state their film thickness with respect to their conductivity but other authors only state conductivity and do not actually report what thickness the film they were measuring was. This means it is impossible to make any definitive conclusion as to how the thickness of the films really affects the conductivity. Some authors also make the point of mentioning that they have several orders of magnitude of differences in conductivity but never mention the starting conductivity of their samples.
- Adhesion problems are pretty common, with PEDOT that is applied as a dispersion.
- The range of PEDOT:PSS conductivities vary from starting conductivities of $0.2\text{--}1\text{ S cm}^{-1}$ to enhanced conductivities of 1418 S cm^{-1} (Kim, Sachse *et al.*, 2011), 200 S cm^{-1} - 700 S cm^{-1} (Ouyang, 2013a), 1200 S cm^{-1} (Palumbiny, Heller *et al.*, 2014), 25.4 S cm^{-1} - 80 S cm^{-1} (Fan, Mei *et al.*, 2008) 3300 S cm^{-1} (Ouyang, 2013b).
- Generally, as mentioned in 2.4, the particle size ranges from 40-230 nm depending on the manufacturer and techniques used to manufacture.
- Agglomeration of the PEDOT particles is a problem even in newly made up samples. It is possible that sonication, filtration and addition of surfactants may help to stop some of the agglomeration but inevitably agglomeration is going to occur. Samples in solution, which are stored have the worst agglomeration problems.
- The mechanism of conductivity is probably one where the band gap between the HOMO (VB) band and the LUMO (CB) band are highered and lowered

respectively. It is also possible that a new SOMO band similar to some semiconducting metals may be formed.

- Mechanisms of conductivity relative to the studies in the PhD are:
acid-base as described by Kroon in Section 2.6 or ionisation in which an electron is removed from the polymer backbone creating a charge in the form of a cation. PEDOT probably conducts by a mixture of hopping electrons, polarons and bipolarons. Polarons are believed to join together to form bipolarons and both probably exist together in some form of equilibrium. It is believed by most researchers that a bipolaron is the favoured charge carrier on longer chained molecules with two separate polarons being favoured on shorter polymers. The charge is probably dispersed over several segments of polymer chain and is accompanied by a balancing counterion. The formation of bipolarons may depend on doping levels but this is inconclusive. Polarons and bipolarons can probably be detected using spectroscopy. The aromatic form of PEDOT is the most stable and is believed to convert to the more energetic quinoid form when the polymer is ionised. It is believed the quinoid form is the form in which PEDOT conducts.

3.0 Methodology

3.1 Introduction

This chapter describes the materials and methods used during this PhD. The chapter begins by explaining how the materials were selected. This chapter continues by describing the scoping experiments (Section 3.3.2) which led to the manufacturing and characterisation procedures. Given the ambiguity in a number of PEDOT research areas, scoping experiments were performed to broadly understand the material, substrate and processing interactions. From the scoping experiments the materials were selected and further experiments were aimed at optimising the conductive films for PEDOT. The experiments from Section 3.3.3 onwards describe how the films were optimised. Section 3.3.4 details how the adhesion problems to the substrate were solved using chemical and physical modification of the substrate. Characterisation techniques are detailed in Section 3.4 onwards. Figure 3.1 shows the sequence of experiments in this chapter.

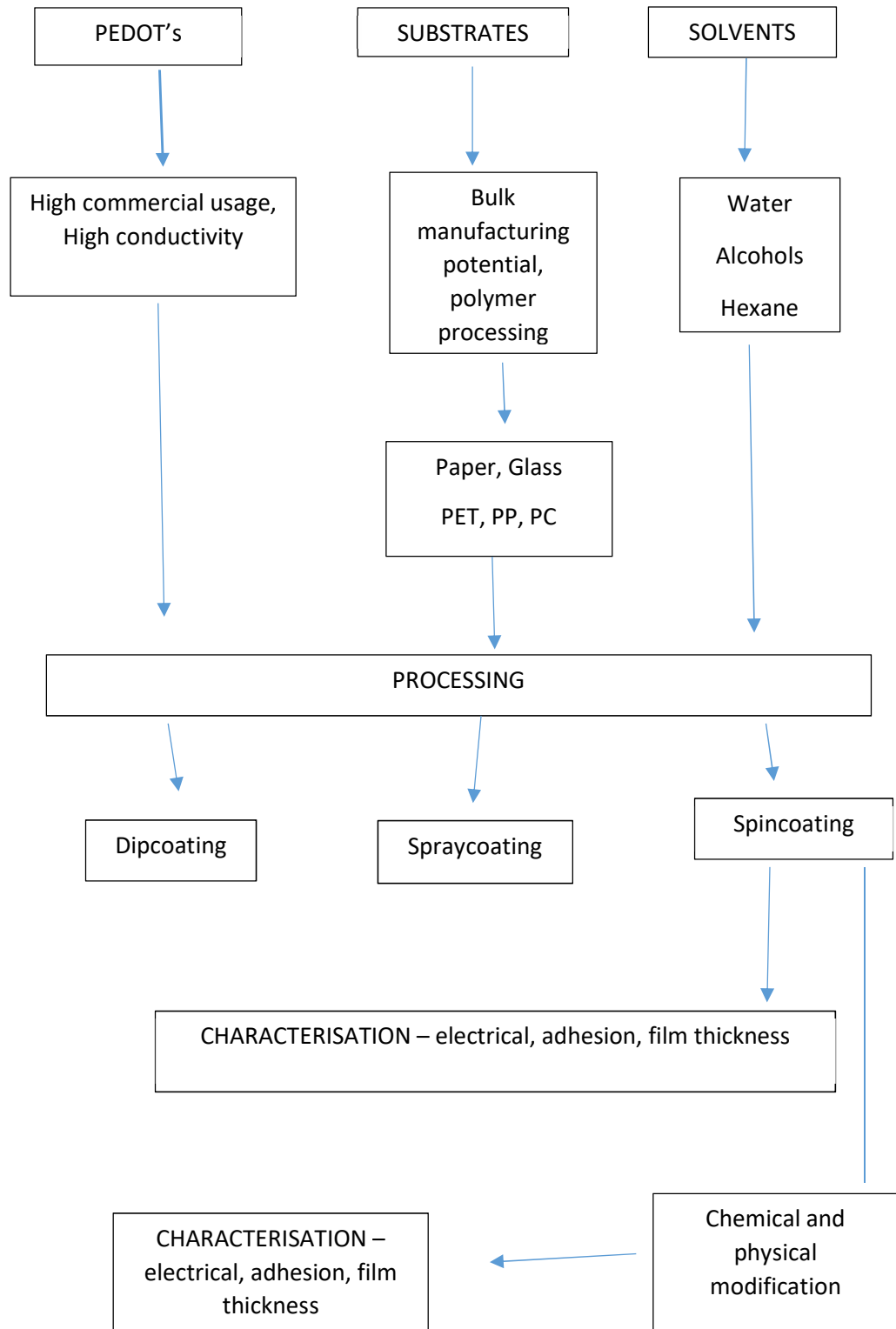


Figure 3.1: Sequence of experiments

3.2 Materials

This section is divided into Polymers, Solvents, Additives. Surfactants, Substrates,

3.2.1 Polymers

The Literature Review helped to identify possible candidates for this research. Conductive polymers selected were PEDOT:PSS, PEDOT:PEG, and two types of PEDOT:OTs as shown in Table 3.1 .

Table 3.1: Conductive polymers sourced for scoping experiments

Code	Name
PEDOT:PEG	Poly(3,4-ethylenedioxythiophene)-block-poly(ethylene glycol) solution [PEDOT:PEG]; from Sigma-Aldrich 649802
[PEDOT:OTs]PC	Poly(3,4-ethylenedioxythiophene), tetramethacrylate end-capped solution in 0.5 wt. % (dispersion in propylene carbonate), contains p-toluenesulfonate as dopant; from Sigma-Aldrich 649821
[PEDOT:OTs]N	Poly(3,4-ethylenedioxythiophene), tetramethacrylate end-capped solution in 0.5 wt. % (dispersion in nitromethane), contains p-toluenesulfonate as dopant; from Sigma-Aldrich 649813
PEDOT:PSS	Poly(3,4-ethylenedioxythiophene)-poly(styrenesulfonate) 1.1 % in H ₂ O, surfactant-free, high-conductivity grade [Synonym: Orgacon™ ICP 1050, PEDOT:PSS, Poly(2,3-dihydrothieno-1,4-dioxin)-poly(styrenesulfonate)] from Sigma-Aldrich 739332 Lot #STBF3722V

After cleaning the substrate as described in Section 3.3.1, each type of PEDOT was initially made up as an aqueous dispersion as a 100 % and a 1:1 mix with each solvent, to try and obtain a film which would homogeneously stick to the substrates. The intention was to attempt to spray this. To make the dispersion, an ultrasonic bath was filled to half-full with water and a few drops of detergent were added in order to improve cavitation and optimise the performance of the ultrasonic bath. The bath was then degassed for 15 minutes. The solutions were all sonicated, until what appeared to be a dispersion was achieved. This experiment was repeated using seven different

solvents (ethanol, butanol, propanol, butan-2-ol, hexane, water and MEK), in order to see if the change in solvent made a difference to wetting of substrate, film thickness or conductivity. The sample was annealed for 20 minutes in an oven at 120 °C under air. Further experiments were performed using different concentrations as shown in Table 3.2.

Table 3.2: Experiments for PEDOT made for spraycoating on substrates

PEDOT:PSS (ml)	MEK (ml)	PEDOT:PEG (ml)	MEK (ml)
2	1	2	1
2	2	2	2
2	4	2	4
1	4	1	4
1	6	1	6
10	1	10	1
1	10	1	10

3.2.2 Solvents

The literature review, (Chapter 2), indicated that certain solvents may enhance the electrical conductivity of PEDOT so this was investigated. Alcohols have also been used as dopants by several researchers as described in Section 2.7.3. From the Literature Review: several solvents, detailed in Table 3.3 and also deionised water were investigated as a solvent to disperse PEDOT:PSS.

Table 3.3: Solvents used for scoping experiments

Solvent	Source	Reference
Ethanol	University of Warwick Chemistry stores	Kim (Kim, Kim <i>et al.</i> , 2006)
Butanol	University of Warwick Chemistry stores	Kim (Kim, Kim <i>et al.</i> , 2006)
Butan-2-ol	University of Warwick Chemistry stores	Senghor (Senghor, Berson <i>et al.</i> , 2013)
Propanol	University of Warwick Chemistry stores	Alemu (Alemu, Wei <i>et al.</i> , 2012)
Ethyl methyl ketone (MEK)	University of Warwick Chemistry stores	Middleton (Middleton, 2012)
Hexane	University of Warwick Chemistry stores	Prieto (Prieto and Calvo, 2013)

Scoping experiments showed that Methylethylketone (MEK) was the most promising solvent to use for the system and this was sourced from the University of Warwick Chemistry stores and was stored in a solvent cabinet at room temperature. TWEEN 80 was selected after reading an unrelated paper (Prieto and Calvo, 2013) investigating the phase behaviour of the hexane/water formulations with TWEEN 80 and co-solvents such as butanol and ethanol. The intention was to formulate a mixture which would solvate the aqueous PEDOT:PSS dispersion in order to produce a homogeneous film.

3.2.3 Additives

The literature review had identified certain additives which when used as dopants may enhance the electrical conductivity of PEDOT. To investigate this, spraycoating experiments were conducted using carbon nanotubes (CNTs), carbon powder and activated charcoal, PVA (polyvinyl acetate) and CMC (carboxy methylcellulose), and metal particles and combinations of two or more of the additives. Chemicals used for the doping experiments are listed in Table 3.4 and were selected since they were

easily obtainable and had been used by other researchers to dope PEDOT as described in Sections 2.7 to 2.7.5.

Table 3.4: Chemicals used for doping experiments

Material	Source
Carbon, nanopowder, <50 nm particle size (TEM),	Sigma Aldrich
Carboxymethylcellulose sodium salt	Sigma Aldrich
Copper, powder (spheroidal), 10 μm , 99 %	Sigma Aldrich
Ethanol	Sigma Aldrich
Ethylmethyl ketone	Sigma Aldrich
Graphite, powder <20 μm , synthetic	Sigma Aldrich
TWEEN® 80, for molecular biology, syrup,	VWR
Zinc, dust, <10 μm , = 98 %	Sigma Aldrich
Propanol	University of Warwick Chemistry stores
Butan-1-ol	University of Warwick Chemistry stores
Butan-2-ol	University of Warwick Chemistry stores
Hexane	University of Warwick Chemistry stores
Polyvinyl acetate average M_n 5,000, PDI <1.2	Sigma Aldrich

Similar problems were found with film quality to the previous experiments and it was impossible to spray any of the solutions containing carbon, CNTs, graphite or combinations of these additives. These materials tended to agglomerate. Various sonication times and temperatures were trialled to solve agglomeration problems but even if sonicated they still agglomerated again during the spraying process. No improvement in conductivity was shown so no further experiments with these additives were undertaken.

Table 3.5 details an example of the experiments performed with different additives and analogues of PEDOT.

Table 3.5: Experiments for different PEDOT analogues with Ethanol as solvent on a PET substrate.

POLYMER	Weight of polymer (g)	CNT (g)	Graphite (g)	Carbon powder (g)	Result	Resistivity (Ω)
[PEDOT:PEG]	0.2449	0.1208			Very Tacky.	3.79×10^{-6}
[PEDOT:PEG]	0.2048			1.3517	Dried powdery and delaminates	Out of range
[PEDOT:PEG]	0.2597		0.8350		Sticky residue	9.49×10^{-7}
[PEDOT:PEG]	0.1958	0.0982		1.3643	Dried sticky and flakes off	Not measured
[PEDOT:PEG]	0.2194	0.0999	0.8709	1.2999	Powdery delaminates completely	Not measured
[PEDOT:OTs]PC	0.2453	0.1221			Yellowish sticky film	Not measured
[PEDOT:OTs]PC	0.2491			1.3011	Sticky yellow delaminates	Not measured
[PEDOT:OTs]PC	0.2541		0.8971		delaminates	Not measured
[PEDOT:OTs]PC	0.2499	0.0995		1.3111	delaminates	Not measured
[PEDOT:OTs]PC	0.2578	0.1051	0.8623	1.3102	delaminates	Not measured
[PEDOT:OTs]N	0.2449	0.1208			Tacky.	Not measured
[PEDOT:OTs]N	0.2048			1.3517	Tacky film	Not measured
[PEDOT:OTs]N	0.2597		0.8350		delaminates	Not measured
[PEDOT:OTs]N	0.1958	0.0982		1.3643	Dried but flakes off	Not measured
[PEDOT:OTs]N	0.2194	0.0999	0.8709	1.2999	delaminates completely	Not measured
PEDOT:PSS	0.2201	0.1001			delaminates	7.74×10^{-8}
PEDOT:PSS	0.2845			1.3192	delaminates	Out of range
PEDOT:PSS	0.2513		0.8666		delaminates	6.91×10^{-6}
PEDOT:PSS	0.2091	0.0992		1.2995	delaminates	3.89×10^{-7}
PEDOT:PSS	0.2153	0.1081	0.7998	1.3002	delaminates	Not measured

3.2.3.1 Surfactant

Polyethylene glycol sorbitan monooleate solution, also known as Polysorbate 80 or polyethylene sorbitol ester (TWEEN 80) was sourced from VWR International Ltd. (UK) and was stored at ambient temperature. The literature review had identified TWEEN 80 (Nasybulin, Wei *et al.*, 2012) as a candidate for increasing the wetting of PEDOT on the substrate and also as a possible additive for enhancing the conductivity. TWEEN 80 was obtained from VWR International. Three different concentrations of solutions of TWEEN 80 and different solvents were mixed with

PEDOT:PSS. Table 3.6 shows an example of the type of experiments trialled as wettability modifiers.

Table 3.6: Solutions of TWEEN 80 non-ionic surfactant as made up to mix with PEDOT:PSS

Solution ID	TWEEN 80 (ml)	MEK (ml)
A1	10	10
A2	10	20
A3	10	30
A4	10	40
A5	10	50
A6	10	60
A7	10	70
A8	10	80
A9	10	90

Each “A” solution was then mixed with PEDOT:PSS as a ratio as shown in Table 3.7.

Table 3.7: Solutions of TWEEN 80 and MEK were mixed with PEDOT:PSS

RATIO (v/v)	TWEEN 80 /MEK solutions (ml added)	PEDOT:PSS (ml)
1:1	1	1
1:2	1	2
1:5	1	5
1:10	1	10

Several methods were used to try to get the samples to dry completely.

Method 1: samples were left 12-18 hours at 120 °C in air.

Method 2: samples were left for up to 72 hours in a vacuum over at 50 °C.

Annealing at 120 °C in air for 20-30 minutes was found to give the most homogeneous film quality.

3.2.4 Substrates

In order to perform the experiments a substrate was required. Using previous literature (Chapter 2) as a starting point, the substrates were selected. These were: paper, polyethylene terephthalate (PET), polypropylene (PP), polycarbonate (PC) and glass.

Paper is cheap and widely available and a few researchers (Agarwal, Lvov *et al.*, 2006, Xuan, Sandberg *et al.*, 2012) have used paper in PEDOT research.

Glass has been widely used by many research groups and was therefore included. Glass is the literature research material of choice for many investigators which allows for an easy comparison with other researchers, and allows characterisation using various spectroscopic techniques.

Polypropylene (PP) was selected because it is a cheap, widely used commercial material. However, PP has a low surface energy making it harder to form a homogeneous film on the surface of PP. Polycarbonate (PC) was chosen because it has a higher surface energy than PP which should make it easier to coat with a thin film of PEDOT. PET was selected since it is a bulk plastic, has higher surface energy than PP and PC as shown in Table 3.8.

Table 3.8: Literature surface energy of plastics

Surface Energy (mNm). 20 °C at STP	Plastic	Reference
44.6	PET	(Ebnesajjad and Landrock, 2015)
30.1	PP	
34.2	PC	

3.2.5 Optimisation of the solution preparation

After completing the scoping experiments, the final analogue of PEDOT selected and used was PEDOT:PSS which was sourced from Sigma. The product number was 739332 Lot #STBF3722V, with the ratio of PEDOT to PSS to Sodium (Na) 1:2:5. The PEDOT:PSS dispersion was stored in a refrigerator as per the manufacturers recommendations.

After performing scoping experiments as described in Section 3.3.2, conductive solutions of PEDOT:PSS with MEK and TWEEN 80 surfactant were made using volume/volume (v/v) ratios. All glassware used for measuring when making up the solutions has a volumetric error. The manufacturer's tolerances for the glassware used are shown in Table 3.9.

Table 3.9: Manufacturers tolerances for equipment used for measuring solutions

PRODUCT USED	Manufacturer stated error
100 ml measuring cylinder	Tolerance: ± 0.5 ml
25 ml measuring cylinder	Tolerance: ± 0.5 ml
10 ml measuring cylinder	Tolerance: ± 0.1 ml
1 ml pipette	Tolerance: ± 0.125 ml

Several experiments were conducted using different concentrations of TWEEN 80 and MEK. In the end the solution as made in Table 3.10 was chosen since it seemed to produce samples with higher conductivity than the rest of the solutions. To make the A1 solution the TWEEN 80 was added to MEK as shown in Table 3.10. Using a magnetic stirrer, this was stirred for 30 minutes to thoroughly mix the components.

Table 3.10: The proportions of Dopant Additives made from TWEEN 80 and MEK (A1)

Solution	TWEEN 80	Equipment	Error from equipment	Total (ml)	MEK	Equipment	Error from equipment	Total (ml)	Grand total (ml)
A1	10 ml	10 ml measuring cylinder	± 0 ml	10.1 9.9	30 ml	100 ml measuring cylinder	Tolerance: ± 0.5 ml	30.5 25.5	35.4- 40.6

Then A1 solution was added to the polymer in a v/v quantity for example for a 1:10 ratio solution the experiment was performed using 1 ml of solution A1 to 10 ml of PEDOT:PSS solution giving a total of 11 ml in the final solution. Note that the original starting concentration of the PEDOT:PSS solution in all the experiments starts as a 1.1 % dispersion in water and not as a 100 % PEDOT:PSS solution. Table 3.11 shows the ratio of reagents and quantities used to make-up each solution.

Table 3.11: PEDOT:PSS, TWEEN 80 and MEK solutions

Solution A1 (ml)	PEDOT:PSS (ml)	Ratio	TWEEN 80 (%)	MEK (%)	TOTAL ADDITIVES (%)	PEDOT:PSS (%)
1	2	1:2	8.33 %	25%	33.33	66.67 %
1	6	1:6	3.57 %	10.71 %	14.28	85.71 %
1	10	1:10	2.27 %	6.82 %	9.09	90.91 %
1	15	1:15	1.56 %	4.69 %	6.25	93.75 %
1	20	1:20	1.19 %	3.57 %	4.76	95.24 %
1	25	1:25	0.96 %	2.88 %	3.85	96.15 %
1	30	1:30	0.81 %	2.42 %	3.23	96.77 %
1	35	1:35	0.69 %	2.08 %	2.78	97.22 %
1	40	1:40	0.61 %	1.83 %	2.44	97.56 %
1	50	1:50	0.49 %	1.47 %	1.96	98.04 %
1	70	1:70	0.35 %	1.06 %	1.41	98.59 %
1	90	1:90	0.27 %	0.82 %	1.01	98.90 %
0	100	100	0.00	0.00	0.00	100%

Each solution was sonicated for 15 minutes, using an ultrasonic bath, and immediately applied to the substrate using an airbrush to apply a spraycoating, or later using dipcoating or spincoating techniques. After coating the substrate, the sample was annealed flat in an oven under air at 120 °C for 20 minutes. When it was

completely annealed, it was a dark blue thin film coating the substrate. The solutions made are shown in Table 3.12 which gives a calculation of the volumetric errors and the actual concentration of PEDOT:PSS in each solution.

Table 3.12: Solution A1 concentrations with PEDOT:PSS showing actual concentration of PEDOT in each solution

RATIO (v/v)	A1 (ml)	Equipment	Error from equipment	Total Error (ml)	PEDOT:PSS (ml)	Equipment	Error from equipment	Total Error (ml)	Range of PEDOT:PSS (ml)	Total range PEDOT:PSS (%)	Real [PEDOT:PSS] (%)
1:10	1	pipette	Tolerance: ± 0.125 ml	0.875 - 1.125	10	10 ml measuring cylinder	Tolerance: ± 0.1 ml	9.9 - 10.1	10.78 - 11.23	91.5 - 91.8	0.010 - 0.010
1:15	1	pipette	Tolerance: ± 0.125 ml	0.875 - 1.125	15	25 ml measuring cylinder	Tolerance: ± 0.5 ml	14.5 - 20	15.38 - 21.13	93.9 - 95.5	0.010 - 0.011
1:20	1	pipette	Tolerance: ± 0.125 ml	0.875 - 1.125	20	25 ml measuring cylinder	Tolerance: ± 0.5 ml	19.5 - 20.5	20.38 - 21.63	95.3 - 95.6	0.010 - 0.011
1:25	1	pipette	Tolerance: ± 0.125 ml	0.875 - 1.125	25	25 ml measuring cylinder	Tolerance: ± 0.5 ml	20 - 30	20.88 - 31.13	95.4 - 96.9	0.010 - 0.011
1:30	0.5	pipette	Tolerance: ± 0.125 ml	0.375 - 0.625	15	25 ml measuring cylinder	Tolerance: ± 0.5 ml	14.5 - 15.5	14.88 - 16.13	96.7 - 97.0	0.011 - 0.011
1:35	1	pipette	Tolerance: ± 0.125 ml	0.875 - 1.125	35	100 ml measuring cylinder	Tolerance: ± 0.5 ml	30 - 40	30.88 - 41.13	96.9 - 97.6	0.011 - 0.011
1:40	0.5	pipette	Tolerance: ± 0.125 ml	0.375 - 0.625	20	25 ml measuring cylinder	Tolerance: ± 0.5 ml	15 - 25	15.38 - 25.63	96.8 - 98.1	0.011 - 0.011
1:50	1	pipette	Tolerance: ± 0.125 ml	0.875 - 1.125	25	25 ml measuring cylinder	Tolerance: ± 0.5 ml	20 - 30	20.88 - 31.13	95.4 - 96.9	0.010 - 0.011
1:70	0.5	pipette	Tolerance: ± 0.125 ml	0.375 - 0.625	35	100 ml measuring cylinder	Tolerance: ± 0.5 ml	30 - 40	30.34 - 40.63	98.4 - 98.8	0.011 - 0.011
1:90	0.5	pipette	Tolerance: ± 0.125 ml	0.375 - 0.625	45	100 ml measuring cylinder	Tolerance: ± 0.5 ml	40 - 50	40.34 - 50.63	98.8 - 99.0	0.011 - 0.011
100	0	n/a	n/a	n/a	100	n/a	n/a	n/a	n/a	100%	1.1

Human errors, which may have occurred when making up the solutions for coating the substrate include:

- Misreading the syringes used
- Misreading glassware used due to parallax
- Misreading instrumentation such as balances

It is impossible to calculate this error but it is estimated to be minimal. To try to reduce this as far as possible all solutions and all testing was repeated at least five times.

3.3 Manufacturing Methods

The first part of this chapter describes the scoping experiments which were used to decide on the final combination of materials to take forward and how, from the scoping experiments the solutions were manufactured into films. Different manufacturing techniques were trialled to identify the optimum method for producing a homogenous and conductive thin film. This section also describes how treatment and cleaning of the substrate aided adhesion of the film to the substrates, and how annealing temperature affected film quality. Finally, the enhancement of the adhesion of the polymer film to the substrate is detailed.

3.3.1 Cleaning of the substrates

At the beginning of the experiments, all substrates were cleaned by wiping with the same solvent as was being applied. The substrates were found to suffer from delamination of the annealed films. The degree of delamination varied depending upon the substrate used, solvent used and concentration of the PEDOT-mixture used. Addition of the TWEEN 80 surfactant was added as described in Section 3.2.3.1 and later in Section 3.2.5. This helped wetting but there was still a major issue with the PEDOT adhering to the substrate. Since literature sources (Kang, Kim *et al.*, 2008)

indicated that the problem could be due to insufficient cleaning of the substrate prior to PEDOT-solution application, to make the substrates compatible and to clean them, the substrates were cleaned using a mild surfactant in an ultrasonic bath. The ultrasonic bath was degassed for 10 minutes prior to using and the substrates were then immersed in it for 10 minutes. Then, they were thoroughly rinsed in deionised water and dried. After this, they were wiped with the same solvent used to make the dispersion. They were then dried in an oven prior to coating with the PEDOT-solutions.

3.3.2 Scoping experiments

Scoping experiments were undertaken on several different systems formulated with conductive polymers and potential additives and solvents. This was in order to determine which systems would best fit the needs of this project and to select the correct material combinations for this research and the best manufacturing method.

3.3.2.1 Solid cast 100 % PEDOT:PSS samples

In order to obtain a homogeneous film from the 100 % PEDOT:PSS, the solution was cast into paper cases and into a silicon mould and then dried to evaporate and anneal the solvent off in an oven under air.

The silicon mould was annealed for an hour initially at 60 °C for 45 minutes and then the oven temperature was raised to 100 °C for an hour. This process was repeated for the paper case sample.

The temperature was again raised to 120 °C for a further hour until a solid sample was achieved. The same experiment was repeated using a vacuum oven at 50 °C. No improvement was made using a vacuum oven instead of a normal oven.

3.3.2.2 Pipetting

Pipetting was used to apply the solutions. PET, PC and PP substrates were pre-treated and cleaned identically and experiments were performed for each solvent. The PEDOT samples were weighed and then mixed with 3 ml of solvent, sonicated for 15 minutes, (after degassing of the ultrasonic bath for 15 minutes), and then 0.5 ml of the solution was pipetted onto the substrate and dried in air for 30 minutes at 120 °C and 130 °C. Experiments were repeated using each substrate. Table 3.13 details the solutions made.

Table 3.13: Pipetting experiments with different PEDOTs and different solvents

PEDOT (g)	Ethanol (ml)	Hexane (ml)	MEK (ml)	Butal- 1-ol (ml)	Butal-2-ol (ml)	Water(ml)	Propanol (ml)
0.1039	20						
0.1037		20					
0.1384			20				
0.1511				20			
0.1168					20		
0.1128						20	
0.1039							20

The samples were left for up to 24 hours to become a solid film. Films were very uneven and where it was possible to measure resistivity results were unreliable due to the film quality achieved. Despite having sonicated the solution in order to degas and remove air when pipetting, the solution gained air bubbles which were annealed into the film. Pipetting was therefore not taken forward as a viable manufacturing method.

3.3.2.3 Annealing Temperature

From the Literature Review the temperature and time of annealing of thin films of PEDOT was found to vary dependent on the reporting group. To identify the annealing temperature which produced the most homogeneous quality films various temperatures were trialled. The samples as detailed in Section 3.3.2.2 were made in duplicate and then annealed in an oven at 100 °C, 120 °C, 140 °C, 160 °C. Identical experiments were repeated with all the analogues of PEDOT and each solvent. Eventually, after optimising the solutions as described in Section 3.2.5, the best film quality was obtained using an annealing temperature of 120 °C for 20 minutes.

3.3.3 Optimising the Manufacturing

Having identified the optimal system to use a manufacturing method was now required which could potentially be scaled up to a bulk manufacturing process. Several different techniques were identified and explored. This section details the different manufacturing methods trialled.

3.3.3.1 Spraycoating

A few scoping experiments had shown spraycoating may be a viable manufacturing method so this was explored further. The airbrush used had an attached mains powered compressor. The airbrush nozzle had an internal diameter of 0.30 mm which means any particles above this diameter will block it.

3.3.3.2 Dipcoating

For dipcoating, a copper tube was suspended between two retort stands and clamped in place, using bosses and clamps. Metal hooks made from wire were hung from this. The PET polymer film was cut into small rectangles and a hole made in one corner of each piece of film in order to hang up the dipped sample. The cleaned PET film as described in Section 3.3.1 was dipped into a petri-dish containing the 3 ml of the solution as made in Section 3.2.5 and fully coated. This was then hung from a hook suspended from the copper tube. Using gravity, the hanging sample was allowed to drip to produce an even thin film. After 45 minutes, this was transferred into an oven where it was hung from a shelf and was annealed for 20 minutes in an oven at 120 °C.

3.3.3.3 Spincoating

Spincoating was achieved using a SCS 6800 spincoater. To use the spincoater, the cavity inside was lined with foil to aid cleaning. The substrate was placed in the centre stand where a vacuum held it in position. A measured solution (1 ml) was pipetted onto the substrate. The spincoater lid was then replaced and the spincoater was turned on at 1000 rpm for 60 seconds. The solution was spread over the entire sample to give a very even film. Subsequently, the sample was annealed for twenty minutes in an oven at 120 °C. Figure 3.2 shows the spincoater used for experiments for this PhD.



Figure 3.2: The SCS 6800 spincoater

3.3.4 Adhesion

Throughout the scoping and subsequent experiments delamination of the thin films had been an issue. In order to try to improve the adhesion several strategies of altering the substrate surface were attempted.

3.3.4.1 Chemical modification

During the scoping experiments, the solution was modified using polyvinyl alcohol (PVA) and carboxymethyl cellulose (CMC). The same idea was investigated again later to improve adhesion. The chemicals used to modify the substrate surface were various analogues of cellulose and PVA. Table 3.14 shows the surface modifying agents trialled.

Table 3.14: Table of different chemicals used for substrate modification to prevent delamination

CAS number	Chemical	Water (g)	Modification chemical (g)	Concentration spray coated
9004-57-3	Ethyl cellulose	10.029	0.0574	0.6 %
9004-67-5	Methyl cellulose	10.021	0.0588	0.6 %
9004-32-4	Carboxymethylcellulose sodium salt	10.014	0.0548	0.5 %
9004-62-0	Hydroxyethyl cellulose	10.0355	0.0548	0.5 %
9002-89-5	PVA MW 89000-98000; 99 % hydrolysed	10.076	0.1022	1 %

To make up the solution the water was heated to boiling and then the adhesion promotor was added. The solution was stirred on a magnetic stirrer/hotplate until the solids dissolved. The solutions were then spincoated onto the substrates and allowed to dry in an oven. It was found that if the substrates were dried at 60 °C this gave a very homogeneous film. Freshly made PEDOT-mixtures were then spincoated onto the modified substrates and annealed.

3.3.4.2 Mechanical abrasion

For the mechanical modification of the substrate a Taber Rotary Abrader 5135 with Taber S11 refacing disc (catalogue number ST121102) was used. Different numbers of cycles were performed as shown in Table 3.15.

Table 3.15: The mechanical abrader cycles

SPEED (RPM)	NUMBER OF CYCLES
72	20
72	50
72	100
72	200
72	400
72	600
72	800
72	1000

After completion of the abrading, the samples were cleaned as described in Section 3.3.1 and coated with freshly made PEDOT-solution.

3.3.4.3 Methyl cellulose roughness

Water molecules that are present in air may eventually be absorbed by the cellulose as well as by the PEDOT. In order to discover how water would affect the cellulose coating used to modify the substrate several samples were immersed in water for one minute. The samples were allowed to dry in air over night. The samples were inspected using a profilometer before and after immersion. The results are shown in Section 4.4.4.

3.4 Characterisation

Characterisation of the materials was undertaken throughout the PhD. Initial characterisation was with respect to the raw materials used and included pH and viscosity measurements. Differential Scanning Calorimetry was performed on the films of pristine PEDOT:PSS as well as on some of the PEDOT-mixtures. After optimising the solutions with respect to wetting, conductivity and film quality, further testing was conducted on the solid films. Film thickness and quality measurements were performed using Optical Microscopy, Scanning Electron Microscopy and Profilometry.

Electrical testing was performed using a High Resistivity Meter and a Four-point-Probe. Spectroscopic techniques were devised to try to track charge carriers to see if the polaron or bipolaron activity could be detected using Ultra Violet Visible spectrophotometry. Infra Red and Raman were used to try and detect the presence of the quinoid groups and to distinguish between samples in the aromatic state and those in the quinoid state. NMR and Synchrotron Analysis were trialled but not found to give useful information.

3.4.1 pH measurements

The Literature Review had identified that pH could be connected to conductivity. Using a pH meter, as shown in Figure 3.3, with two buffers to calibrate the equipment the pH of the starting material and each final solution was measured 5 times. The results were then averaged and a standard deviation was calculated.



Figure 3.3: The pH meter used to measure the pH of the solutions

The pH of a solution is a measure of hydrogen ions in the solution where:

$$-\log_{10} H^+ = pH \quad [3.1]$$

pH is measured on a scale from 1-14 where 1 is acidic , 7 is considered neutral and 14 is alkaline.

In order to check calibration of the equipment two buffers were used. The buffers were pH 7.01 \pm 0.01 @ 25 °C and pH 4.01 \pm 0.01 @ 25 °C. The solutions were made up as previously described in Section 3.2.1. Sigma report the pH of the

PEDOT:PSS starting material is pH <2.5. In order to check this the original pH was tested and this was compared with the rest of the solutions.

3.4.2 Viscosity measurements

Viscosity of the liquid samples was measured using a Brookfield DVT rotational viscometer with the SC4-18 spindle fitted. This is shown in Figure 3.4. This instrument has a manufacturer error of $\pm 1.0\%$ of the measurement range used and has a stated repeatability with $\pm 0.2\%$. The SC4-18, which is a small sample adapter was used for all measurements. This SC4-18 has a maximum shear rate of 264 s^{-1} .



Figure 3.4: Brookfield viscometer used for all viscosity measurements.

Viscosity is the measurement of a fluid resistance to deformation by stress. This can be measured by shear stress or by tensile stress and the knowledge obtained from viscosity testing is used to predict a fluid's performance. For example inks, paints and foods can be tested for viscosity and this will show the flow deformation character of an individual solution which allows the manufacturer to predict how a liquid will

behave under certain conditions. Table 3.16 shows the setting used for the viscosity measurements.

Table 3.16: Setting used for the viscosity measurements

Torque (%)	Speed (rpm)	Shear Speed (rpm)	Shear Rate (s ⁻¹)	Temperature (°C)
50 %	25	Between 20.79 and 23.21	33000	20.8

3.4.3 Differential scanning calorimetry (DSC)

A Mettler DSC-HP 1, Differential scanning calorimeter (DSC) was used to detect the glass transition temperature. The glass transition (T_g) is the temperature at which an amorphous polymer will become soft when heated or brittle when cooling. It can be used to help predict how a polymer will react when processed since it shows changes in the mechanical properties such as strength, hardness, brittleness and elongation. DSC is commonly used to detect first and second order transitions in polymers. These are energy transfer effects due to enthalpy (H) changes from phase transitions or chemical reactions that may occur in the sample. The definition of enthalpy is:

$$H = U + pV. \quad [3.2]$$

Where: H = enthalpy, U = the internal energy of the system, p = pressure, V = volume.

Therefore:

ΔH = change in enthalpy. $\Delta H > 0$ = endothermic, so heat is absorbed by the system

$\Delta H < 0$ = exothermic, heat is given out by the system.

When using a DSC heat is applied to the sample at constant pressure. The heat flow to the analyte sample and a reference are recorded as a function of temperature. In this case an empty DSC pan, which is a 40 μ l aluminium sample holder was used as a reference. Both the sample and reference start at the same temperature. The temperature of both sample and reference is increased at the same rate to give a value for enthalpy change.

The annealed films of the 100 % PEDOT:PSS, the 97 % PEDOT:PSS (1:30), 97 % PEDOT:PSS (1:35) and 98 % PEDOT:PSS (1:40) samples were tested using DSC. To obtain the film without the substrate the 100 % film was cured as a solid as described in Section 3.3.2.1 and the PEDOT/ TWEEN 80/MEK films were annealed onto glass slides and scraped off. Results of this experiment are detailed in Section 4.2.2.

3.4.4 Surface energy of the substrate

Surface energy is a measure of how a droplet will wet onto a substrate. This can be measured by using contact angle measurements from which the surface energy of the substrate can be calculated. For the substrates used in this PhD the contact angle was measured using a controlled volume of three different liquids according to British standard BS EN 828:2013 (British Standard, 2013) and an Attension Optical Tensiometer. See Figure 3.5. This method is known as Sessile Drop Analysis and involves using a syringe containing the liquid analyte suspended from the Optical Tensiometer, which measures exactly how much liquid is being dispensed. As the droplet of liquid falls onto the substrate the Optical Tensiometer calculates the surface energy of the substrate using the angle of the droplet on the substrate surface.



Figure 3.5: Attension Optical Tensiometer

To achieve accurate results three different liquids need to be compared for the calculation. Liquids compared were water, diiodomethane and ethylene glycol. Polar liquids, for example water and ethylene glycol, will have higher energy than a non-polar liquid, such as diiodomethane. Figure 3.6 shows how the different surfaces can affect the angle and wetting of the liquids. The lower the surface energy of the substrate is, the less it will wet which means a liquid applied to it will form droplets rather than a homogeneous film over the substrate surface. If the substrate has a high surface energy then it becomes easier to spread the liquid over the surface of the substrate. When wetting takes place on a substrate the surface tension of the liquid balances that of the substrate.

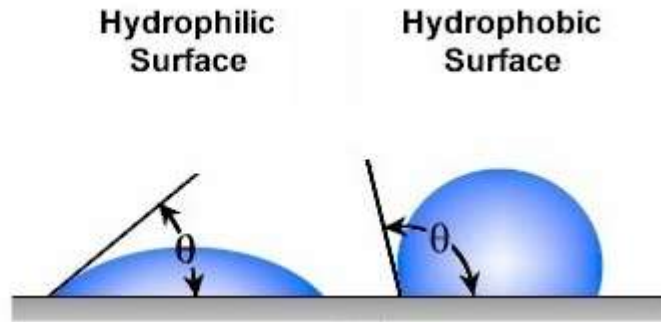


Figure 3.6: The surface energy of the substrate affects how a liquid will spread.:

The wettability of a liquid in contact with a solid surface typically has a drop shape. The angle of the drop is the angle formed by the tangent at the triple point, which is in effect the point where wetting occurs. In order to measure the surface energy, the baseline must be maintained. This is the straight line which goes through the triple point as shown in Figure 3.7. The triple point is where according to the British standard: “the solid, the liquid and the gas phases coincide with each other” and where the baseline intersects the angle of the droplet. The contact angle (θ) is the angle of the droplet next to the baseline, which forms a tangent to the drop and must also go through one of the triple points. When a contact angle = 0° this indicates complete wetting of a substrate. The surface energy of a material is defined using Young’s formula (British Standard, 2013, Ebnesajjad and Landrock, 2015)

$$\gamma S = \gamma SL + \gamma L \cdot \cos \theta \quad [3.3]$$

where:

γS = surface free energy of the solid plastic substrate

γL = surface tension of the liquid in equilibrium with air (deionised water, ethylene glycol or diiodomethane)

γ_{SL} = interfacial energy of the solid plastic substrate in contact with the liquid at contact angle (θ),

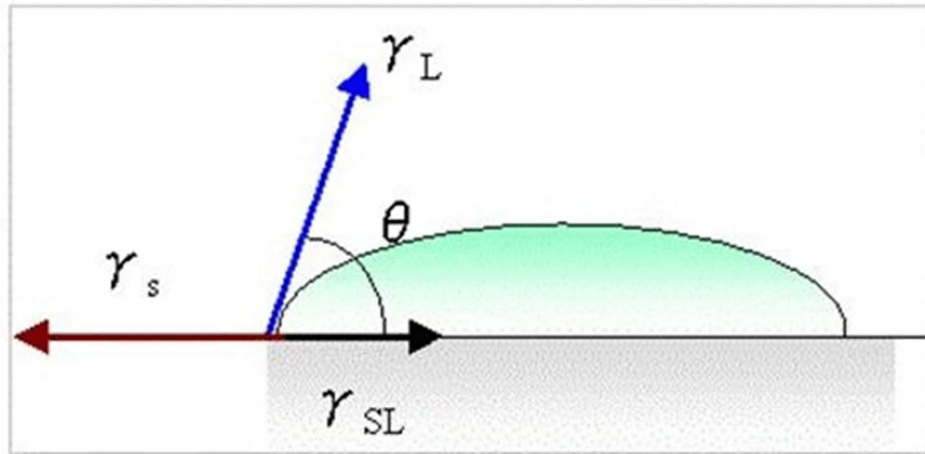


Figure 3.7: The measurement of surface energy using Sessile Drop Analysis (British Standard, 2013)

To perform the measurement, each liquid in turn was dispensed from a syringe, onto the flat sample. The software measured the left hand and right hand contact angles and from this the OWRK/Fowkes calculation (Biolinscientific manual) was performed. This gave a value for the contact angle of the substrate.

Since each substrate listed in Table 3.17 has a different surface energy this means that droplets of liquid will wet differently on the substrates.

Table 3.17: Surface energies of polymer substrates

Surface Energy (mNm). 20 °C at STP	Plastic	Reference
44.6	PET	(Ebnesajjad and Landrock, 2015)
30.1	PP	
34.2	PC	

If the substrate deviates from ideal, which is the case in this PhD, a close approximation to the literature value is the best result that can reasonably be obtained. The ideal system would also be free from draughts, which the laboratory where these measurements were performed was not.

Both PP and PC have a low surface energy. This can cause problems with adhesion of PEDOT to these substrates. For good wetting to occur the surface energy of the liquid needs to be lower than, or the same as, the surface energy of the substrate. This will allow the liquid to be able to adhere to the surface so it can form a homogeneous film, which can then be annealed.

PET was later chosen for the substrate due to results described in Chapter 4. As more TWEEN 80 surfactant was added to the solutions the contact angle reduced to 0 °C hence there are only results for the higher PEDOT concentration samples and not for the higher TWEEN 80 concentration samples.

3.4.5 Electrical conductivity testing

Two types of electrical testing were performed on the samples, Keithley 6517b resistivity and Jandel RM3000 four-point-probe. Using a Keithley high resistivity 6517b meter the resistivity was measured, using a Jandel RM3000 four-point-probe the sheet resistance and bulk resistivity were measured. Each method will be described separately and has advantages and disadvantages in its use. Conductivity was not measured but relates to resistivity by the following equations where it can be seen that the inverse of resistivity is conductivity. This means the lower the resistivity the better the material conducts electricity.

Where:

$$V = I \times R \quad [3.4]$$

V = voltage (V), I = current (amps), R = Resistance (Ω m)

And:

$$R = \rho L/A \quad [3.5]$$

L = length (m), A = Cross sectional area of the sample (m^2), ρ = resistivity (Ωm),

And:

$$\sigma = 1/\rho \quad [3.6]$$

σ = Conductivity (S m^{-1}).

Due to the low conductivity of the PEDOT:PSS samples all conductivities are reported in Siemens per centimetre (Scm^{-1}) as is used in much of the literature rather than in S m^{-1} .

3.4.5.1 Bulk resistivity

Bulk or volume resistivity using a Jandel four point probe, was measured directly in Ωcm . This is a measure of the resistance of the material regardless of the shape or size. Therefore, it is the intrinsic measurement of electrical conductivity of the material. Using a current of 10 nA applied to the sample the resistivity was measured by the instrument. Ten readings were taken over the course of one minute in order to take an average and to try to minimize errors.

3.4.5.2 Sheet resistance

Sheet resistance, is commonly used in characterisation of semiconductor materials. It is measured in Ω square (Ωsq) using a four-point-probe. Again, a 10nA current was applied to the samples and the reading of resistivity was measured directly by the Jandel instrument. Sheet resistance is only used for measurement of 2D systems such as thin films and it is assumed that the film is of uniform. It can be measured directly using a four-point-probe system. Sheet resistance does not vary regardless of the size of the sample so can be used to

compare samples that differ greatly in size. The name ohms square is due to the assumption that a square sheet with resistance of $10\ \Omega_{\text{sq}}$ will have a resistance of $10\ \Omega$. Really Ω square (Ω_{sq}) is simply Ω , but the square is added so it is known this is a measurement of sheet resistance (University of Berkley). (Jandel Engineering). The term Ω_{sq} is often used to distinguish the difference between a film of material and a solid such as a piece of wire. The samples flickered which is assumed to be caused by the molecules of water and possibly ammonia which are adsorbed from the air and which adhere to the surface of the polymer film and interfere with characterisation of the material.

Sheet resistance is defined as:

$$R_s = \pi / \ln 2 (\Delta V / I) \quad [3.7] \text{ (Blythe, 1984)}$$

Where: R_s is the sheet resistance of the sample (Ω_{sq}), $\pi / \ln 2$ is a geometric correction factor. The geometric correction factor only applies when the sample thickness is less than 0.1 of the ratio of the probe spacing. Since the thinnest sample film measured was $1\ \mu\text{m}$ thick and most were more than this all samples measured were within range so $\pi / \ln 2$ is considered as zero (Jandel Engineering). This means the correction factor can be ignored and results obtained do not need this adjustment.

It was of importance to measure sheet resistance because the only measure of the amount of conductivity of the starting material, which was supplied with the PEDOT:PSS was that of sheet resistance.

3.4.5.3 Four-point-probe

The use of a four-point-probe apparatus is one of the most widely used instruments for the measuring the resistivity of semiconductors. The Jandel

RM3000 four-point-probe has 4 linear probes which are spaced at 0.5 mm apart and it is able to supply constant currents between 10 nA and 99.99 mA. Figure 3.8 shows the Jandel RM3000 four-point-probe system.



Figure 3.8: The Jandel RM3000 four-point-probe (Jandel Engineering)

The Jandel four-point-probes consist of a platform and a meter attached to a PC. The sample was placed onto the test platform. There is a digital meter which generates a constant current and displays the sheet resistance (Ωsq). 10nA current was applied to the sample and 10 readings of sheet resistance were taken over the period of one minute. From this an average was calculated and also the standard deviation. However, the minimum and maximum readings were plotted instead of standard deviations to ascertain the range of readings which had a tendency to instability. The only exception to this was the 99 % PEDOT:PSS sample, which in every set of

samples measured had a stable reading. This is of relevance later in Chapter 6. Figure 3.9 shows the set-up of the four-point-probe resistivity configuration.

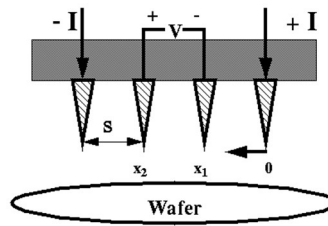


Figure 3.9: Measurement of sheet resistivity using a Four-point-probe (University of Toledo, 2011)

For the material to be measurable using a four-point-probe, the probes need to make contact with it. It needs to be homogeneous and ideally uniformly doped. All four probes must be in contact with the material. The two outer probes produce the current source and the two inner probes measure the potential difference across the surface of the material. The four-point probe was used to avoid interference from contact resistance since this system removes errors from the probe resistance and the contact resistance between each probe and from the spreading resistance under each probe.

The sample must also be electrically insulated from the substrate. Since the substrate was PET this was not a problem. In the case of the samples measured in this project care was taken not to puncture the thin film on the surface of the substrate with the four probes. A silicon wafer was used to calibrate the instrument. The current is assumed to flow along the plane of the sheet of film rather than flowing perpendicular to it. The four-point-probe system is relevant only when the sample is in the form of a thin wafer or film. This is the case with the PET film substrate coated with different concentrations of PEDOT:PSS/ TWEEN 80/MEK. Results of the four-point-probe testing can be found in Sections 4.3.5 to 4.3.5.3 and 4.4.2. When measuring using a four-point-probe the current (I) is set.

In this case a current of 10 nA was used for all measurements. The instrument gave a reading in ohms directly from the measurement. This was recorded. In order to ensure accuracy ten measurements were taken over one minute and these values were averaged in order to plot them.

3.4.5.4 Two-point probe

A two-point probe testing method was devised using a Keithley 6517b high resistivity meter. Differences between measuring using the four-point probe and the Keithley 6517b included the fact the four-point-probe uses a constant current (10 nA) to measure resistivity directly. The Keithley 6517b uses DC voltage which is set for each experiment and measures the current from which the resistivity can be calculated using equation [3.4] as explained in Section 3.4.5.

The Keithley 6517b was found to be giving a measurement of the surface resistivity of the material rather than a bulk resistivity. This was believed to be due to both the facts that:

- PEDOT:PSS films conduct along the plane sheet rather than through it;
- the adsorbed contaminant molecules of water and ammonia caused interference with resistivity measurements meaning surface not bulk resistivity was being measured.

The voltage applied to the samples was varied using 1 V, 2 V, 5 V, 10 V, 20 V, 30 V, 40 V and 50 V since it was of interest to see how the PEDOT:PSS responded at higher voltages. Most of the literature uses applied potentials of between 0.5-1.5 V. Therefore, it was interesting to explore how they behave at the higher unknown applied potentials. To check the equipment was set up correctly a 219 Ω resistor was measured before each session. Samples were cut into 1cm square pieces to standardise the test. The probes were attached at two

points across the 1cm square of sample. A variable DC Voltage was applied to the samples and 6 repeat measurements of current, on each sample, were conducted at the given voltage applied with a Keithley 6571b as shown in Figure 3.10.



Figure 3.10: The Keithley 6517b High resistivity meter

With the Keithley 6517b meter, the voltage applied was known with the current being measured. Using: $R=V/I$ the resistivity was calculated.

The readings were unstable, however there is a 20 % error margin inherent in the instrument so this would account for the variability of results. The instability is caused by background currents in the material. The background current is caused by piezoelectric effects and polarization effects inside the polymer as well as internal capacitive elements from static electricity. Since these interferences can cause a bigger current than that caused by the applied voltage this makes measurements unstable and increases measured resistivity. The Keithley is also a two probe

measurement method so interferences from resistance from the probes and equipment itself also creates inaccuracies in measured readings.

Using a Keithley 6517B meter, resistivity was measured on all viable samples. Some of the samples had suffered from delamination so only those samples with an intact surface area were tested. The samples were tested in random order with randomized applied potential. This is because it is possible that the changes that were happening were due to the applied voltage change rather than the change in concentration of the reagent species. Results of electrical testing using a Keithley can be found in Sections 4.2.8, 4.3.3, 4.3.4, 4.4.3 and 4.5.2.

3.4.6 Optical Microscopy

The film thickness and surface quality of a range of the samples made were measured using various microscopes. Samples for the optical microscopy were cut, mounted in resin and the surface was polished to show the thickness of the PEDOT films. This is shown in Figure 3.11.



Figure 3.11: Microscopy samples were mounted in resin and polished

3.4.7 Scanning Electron Microscopy (SEM)

A Hitachi TM3030 benchtop SEM, was used to look at the surface of films. This instrument has a gun voltage of 5 kV or 15 kV and a magnification of up to 60,000. An image was obtained to generate Figure 4.2. No sample preparation was needed since the polymer coating was conductive.

3.4.8 Profilometer

An Alicona IFM G5 Vc5 Profilometer, as shown in Figure 3.12, was used to measure the profilometry of the surface of the films. It was also found to give good images of the cellulose modified surfaces.

The Alicona Profilometer uses a non-contact, optical measurement system based on Focus-Variation. It automatically collects a number of data points and analyses these to give the surface profile of the material.



Figure 3.12: Alicona profilometer

The Alicona uses the standard parameters: Ra, Rq, Rz to measure the roughness profile of a sample.

Ra is the average roughness value. Rq is the Root-Mean-Square roughness of the profile. Rz is the average peak to valley height of the roughness profile. The Alicona also measures Rt and Rmax. Rt is the maximum peak to valley height of the roughness profile. Rmax is the maximum peak to valley height of the roughness profile within a sampling length.

Rz is most useful for measuring the roughness profile of random structures.

To calculate the roughness of a sample the Alicona takes several measurements at different points on the sample and then uses the mean value as shown in Figure 3.13.

Using these measurements the average roughness is calculated.

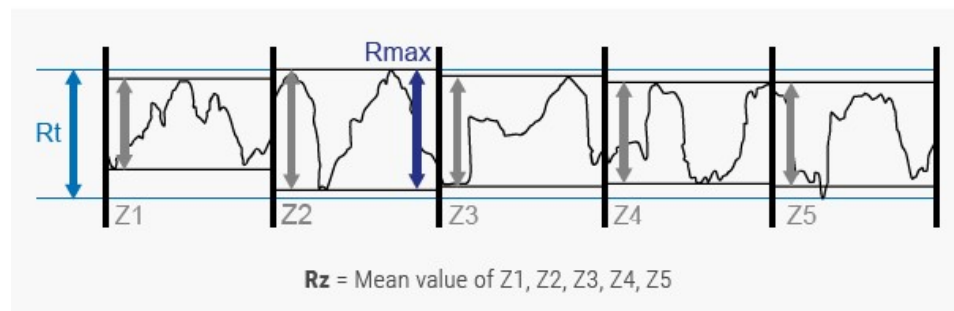


Figure 3.13: Alicona calculation of Rz (adapted from <http://www.alicon.com>)

3.4.9 Spectroscopy

Spectroscopy makes use of the interaction between matter and the electromagnetic spectrum. It involves study of the electronic transitions from ground state to a higher excited level where:

$$\Delta E = h\nu. \quad [3.8]$$

and:

$$\nu = f/\lambda \quad [3.9]$$

where:

ΔE = The change in energy level, h = Planck's constant, ν = a photon of light, f = frequency of the wave of light (Hz), λ = wavelength (m/s)

Four different types of spectroscopy were used for this project. These were ultra violet-visible (UV-Vis) spectrophotometry, Infra red (IR) and Raman spectroscopy. Nuclear magnetic Resonance (NMR) was also attempted but gave no results so this was abandoned.

Spectroscopy uses the inelastic scattering of monochromatic light. Absorption and transmittance spectroscopy both use light from an incident light source which is split into the relevant wavelength using a monochromator or grating. Monochromators are used for UV, Raman and IR spectroscopy. The light passes through the monochromator where it is split. One beam then goes to the sample detector while the other hits the reference detector. The instrument then compares the sample to the reference. Absorbance relates to transmittance where:

$$A = \log_{10} I_0/I \quad [3.10]$$

$$T = I/I_0 \quad [3.11]$$

Therefore:

$$A = \log_{10} 1/T \quad [3.12]$$

A = Absorbance, T = transmittance, I_0 = the intensity of incident light, I = the intensity of transmitted light

3.4.9.1 Ultra violet-Visible spectrophotometer (UV-Vis)

Absorbance spectroscopy using UV-Vis spectrum was used, where the light source used had light in the visible and the near UV and near- infrared (NIR) regions. The UV-Vis spectrophotometer works by using UV, visible, and NIR light to promote an energy level change in the electrons residing in a molecule. In order to do this the photon of energy $h\nu$ must be exactly the same energy as the energy difference between two different orbitals such as the band gap difference between the HOMO and LUMO levels (Skoog, West *et al.*, 1992). This is known as an electronic transition.

Using a Cary 60 spectrophotometer, as shown in Figure 3.14, the UV-Visible spectrum was recorded.



Figure 3.14: The Cary 60 UV-Vis spectrophotometer

Liquid samples of TWEEN 80 (100 %), and TWEEN 80 with MEK were recorded. The samples containing PEDOT:PSS whether 100 % PEDOT:PSS or a solution mixed with surfactant and MEK were all recorded using a glass slide coated with the annealed solution. The absorbance spectrum from 200 nm to 900 nm was scanned in order to see if there were any detectable differences between different

concentrations of PEDOT and in an attempt to detect any charge carriers which according to Chapter 2, it should be possible to do.

3.4.9.2 Fourier Transform Infra Red (IR)

In IR spectroscopy the interaction of molecular species with infrared radiation takes place. IR can yield data for both transmittance and absorption. Usually it is transmittance that is used. IR is used to identify functional groups. IR relies on different chemical species absorbing energy in different parts of the IR spectrum. The IR instrument used for the analyses was a Bruker Tensor 27 fitted with a total internal reflection crystal and this is shown in Figure 3.15.



Figure 3.15: The Bruker Tensor 27 FTIR

This type of IR is known as Attenuated Total Reflection (ATR). The sample must be in contact with the ATR crystal for analysis to take place. The ATR crystal is shown in Figure 3.16.

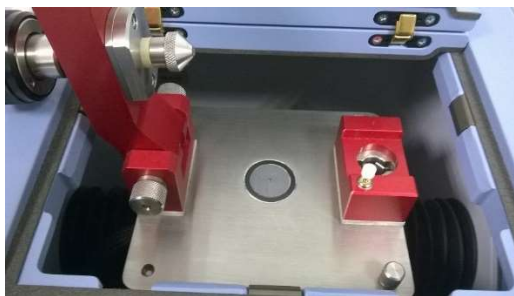


Figure 3.16: The ATR crystal inside the FTIR

ATR uses total internal reflection to analyse the sample. A beam of light is passed through crystal and it is reflected off the internal surface of the ATR crystal by the sample. The reflected light is collected by a detector which produces the spectrum. The sample must at all times remain in contact with the ATR crystal.

IR was found to be of use when analysing PEDOT and was used to try to determine if the samples are in a conductive, or oxidised state, by studying differences in the functional groups. The solid samples were initially made using the PET substrate as described in Section 3.2.5. However, the spectrum was indistinguishable which was believed to be due to the PET spectrum interfering. They were then made using glass slides as the substrate, and were analysed by scraping the film off the surface and using ATR but this was also unsuccessful in obtaining spectra. In the end potassium bromide (KBr) discs were made of each sample from the scrapings ground up with dried KBr. KBr is invisible in the IR spectrum so only the analyte is observed when using this method. IR was used to attempt to distinguish between the materials and to try to determine if there is an aromatic-quinoid transition. The IR spectrum in most cases showed a sloping baseline. It is possible to use the software to correct this but it was decided to leave it since it denotes electrical conductivity (Shimadzu Scientific Instruments).

3.4.9.3 Raman Spectroscopy

Raman spectroscopy uses the energy from the laser to excite and analyse molecules so that photons of light are scattered at either higher or lower energy than the incident photons. The energy difference (ΔE) occurs because there is a change in the polarization of the molecule. This gives similar information about the structure and functional groups as IR does. Raman was used to try to find differences between the different concentrations of PEDOT to try to find out how the structure changes with the onset of conductivity enhancement. Raman was used since it may help to detect the quinoid structure and show how the structure differs from the aromatic structure.

A Renishaw RE04 in Via Raman microscope was used as shown in Figure 3.17. Raman is very similar to IR in that it relies on vibrations from the molecule interacting with light from a laser. Two different lasers were used. Both lasers are in the IR region. At the start of the experiments, the 785 nm laser was used. This was chosen because it was in the IR region and results were needed to analyse the fingerprint region of the spectrum for sulphur since this was virtually impossible to see in NIR. The 785 nm laser was used with a 1200 grating. Since other researchers (Sakamoto, Okumura *et al.*, 2005) have used a 633 nm laser to analyse PEDOT further experiments were done using the 633 nm laser.



Figure 3.17: The Renishaw Raman RE04

3.4.10 Synchrotron Small Angle Xray Scattering (SAXS) and Wide Angle Xray Scattering (WAXS)

Four samples were analysed at the I22 beamline of Diamond Synchrotron which is based in Oxfordshire. A synchrotron uses magnets and radio frequency waves to accelerate charged particles (electrons) along a stainless steel tube. The electrons emit light of various wavelengths and strength depending upon the experiment. The beamline used a see Figure 3.18, and was set up in Isotropic mode with an attached Linkam DSC, see Figure 3.19 (a) and (b), for SAXS/WAXS with a 1.9 m camera. This gave a q range of 0.01-0.85 \AA^{-1} at 12.4 keV.

The value of q is related to 2θ or d spacing since:

$$q = 2\pi / d \quad [3.13] \quad (\text{U.S Department of Energy}).$$

From the Bragg equation:

$$n\lambda = 2d\sin\theta \quad [3.14]$$

where: n = a positive integer λ = wavelength of the incident wave, d = lattice spacing of atoms in the crystal, θ = the angle of incidence.

WAXS gives information on the crystallinity of the sample whereas SAXS gives information on molecular structure of the sample such as bonding and molecular order within the molecule. Figure 3.18 shows how the SAXS attaches to the WAXS.

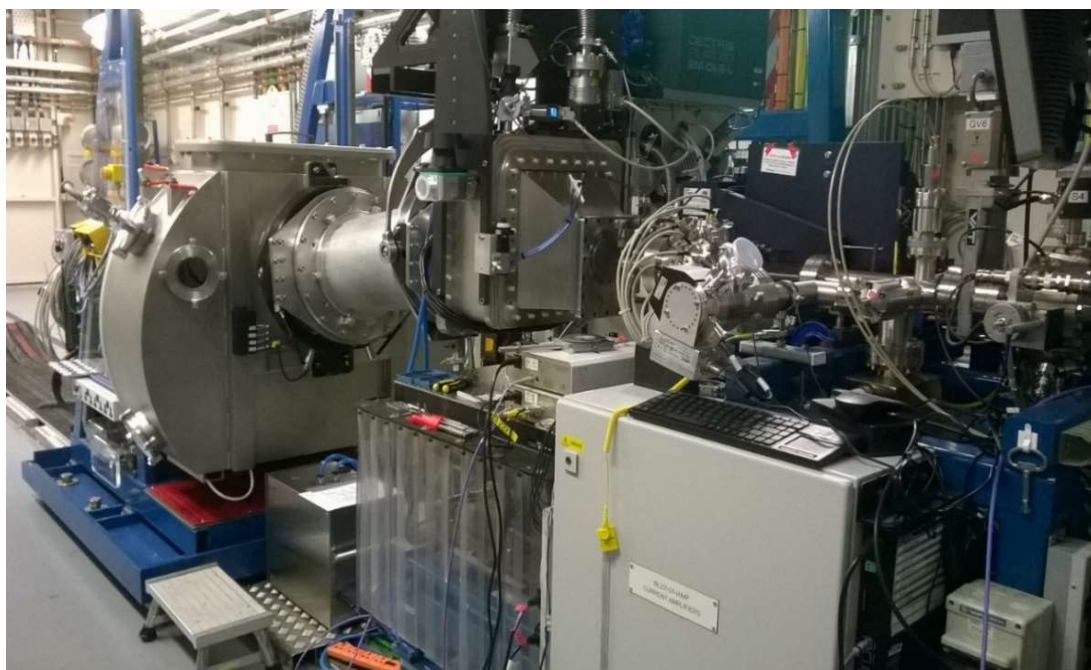


Figure 3.18: Diamond Synchrotron showing Pilatus WAXS and SAXS

Figure 3.19 shows the Linkam DSC.(a) which was attached to the SAXS.

There is a window (b) which allows the synchrotron Xrays to pass through the sample to the SAXS.

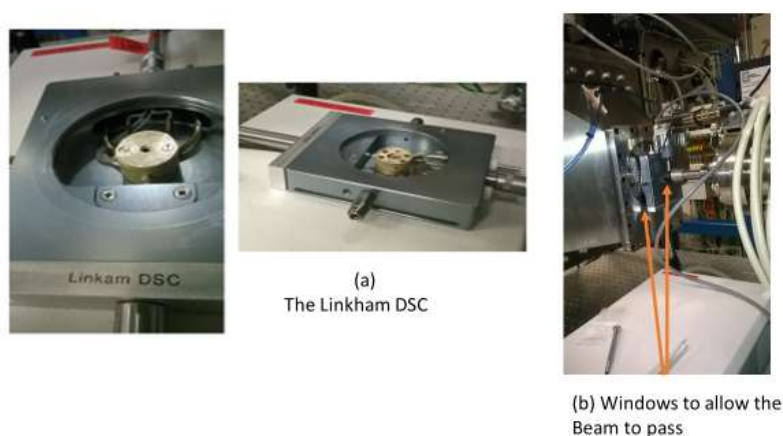


Figure 3.19: Diamond Synchrotron showing (a) Linkham DSC and (b) shows the location of the windows which allow the beam to pass through the sample

Samples were prepared by punching holes in DSC lid and base pans. These were covered with a Mylar window which allows x-rays to penetrate to the sample. The sample was put inside and then the DSC pan was closed. This is shown in Figure 3.20.

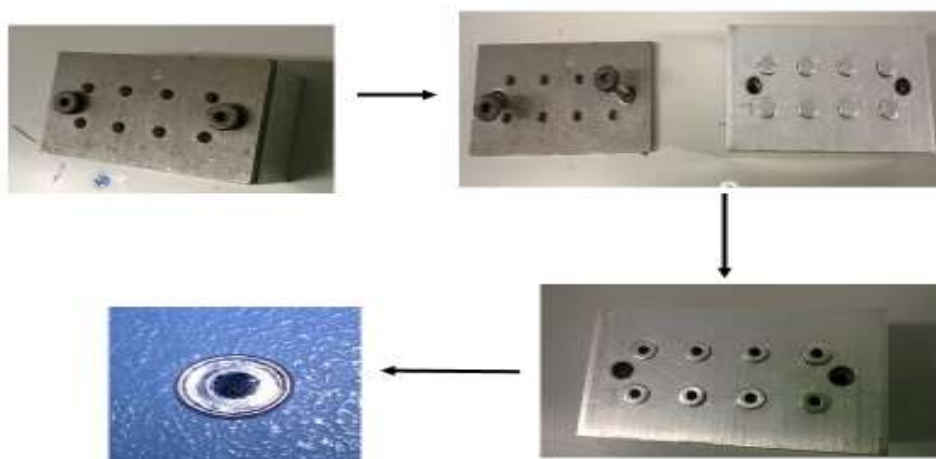


Figure 3.20: Sample preparation for the Synchrotron

The samples taken to Diamond Synchrotron were the 100 % PEDOT:PSS annealed film, the 97 % PEDOT:PSS film and the 99 % PEDOT:PSS film. A fourth liquid sample

was also analysed. This was the 100 % PEDOT:PSS. To keep the liquid PEDOT:PSS within the DSC pan washers were used between the mylar windows. No results of interest were obtained using this technique.

3.4.11 Nuclear Magnetic Resonance (NMR)

Proton Nuclear Magnetic Resonance (NMR) spectroscopy uses a magnetic field and can be used to show conformational changes within a molecule. Molecules which do not have a spin of $\frac{1}{2}$ do not absorb NMR so are used as solvents for this technique. If a magnetic field is applied to a sample an energy transfer takes place between the ground state to a higher energy level. This can be used to analyse conformational changes within the molecule. NMR was used in an attempt to discover if the PEDOT molecule changed in conformation when in the conductive state or between different concentrations of PEDOT:PSS. The liquid 100 % PEDOT:PSS was mixed with deuterated water (D_2O) solvent but no results were obtained. The 97 % PEDOT:PSS sample was also trialled using NMR no useful results were obtained using this form of analysis.

3.5 Conclusions

This chapter has explained the materials, manufacturing methods and characterisation techniques used in this research. NMR and Xrays were not used for this PhD since no useful results were obtained from these analyses.

4.0 Results

4.1 Introduction

This section begins by explaining the scoping experiments which were undertaken in order to proceed to optimising the samples. The results from the scoping experiments are found in Section 4.2. Results from the scoping experiments informed the rest of the project and details the results from further experiments to optimise the PEDOT films and the characterisation results.

Table 4.1 shows designations used to differentiate between the different solutions and films manufactured.

Table 4.1: Designations used for analysis of films and solutions

PEDOT:PSS (%)	Additives (%)		Solution Ratio Designation	PEDOT:PSS Film Designation Electrical (%)	Additives in Film Designation (%)
	TWEEN 80	MEK			
90.91	2.27	6.82	1:10	91	9.0
93.75	1.56	4.69	1:15	94	6.3
95.24	1.19	3.57	1:20	95	4.8
96.15	0.96	2.88	1:25	96	3.9
96.77	0.81	2.42	1:30	97	3.2
97.22	0.69	2.08	1:35	97	2.8
97.56	0.61	1.83	1:40	98	2.4
98.04	0.49	1.47	1:50	98	2.0
98.59	0.35	1.06	1:70	99	1.4
98.90	0.27	0.82	1:90	Eliminated	1.0
100	0.00	0.00	100	100	0.00

4.2 Scoping

The scoping experiments were performed in order to determine the optimal materials and manufacturing processing for the materials.

4.2.1 Conductive polymers

After initial scoping experiments showed most of the PEDOT analogues were very difficult to process only two of the PEDOTs were taken forward. These were PEDOT:PSS (1.1 %) in water (also known as Orgacon) and PEDOT:PEG 0.8 - 2 wt. % in nitromethane, 90-95 wt. %, isopropanol, 0.2 - 0.8 wt. %, ethanol, 4 - 8 wt. % (also known as Aedotron™ TM-P3 polymer). It was found to be impossible to spray the [PEDOT:OTs] propylene carbonate and the [PEDOT:OTs] nitromethane which were eliminated from further study since both types of PEDOT:OTs blocked the nozzle of the airbrush. This was probably due to the particles agglomerating in solution. Sonication of the solution was found to slightly improve this but even after sonicating the solution still started to agglomerate after 20-30 minutes.

Although both PEDOT:PEG and PEDOT:PSS are electrically conductive, the PEG analogue proved to be harder to make into films. Therefore, PEDOT:PSS was eventually chosen due to its ease of processing as well as procurement. A further advantage was that PEDOT:PSS could be obtained easily in an aqueous dispersion. Using water as the dispersant, gives the final product a reduced environmental impact compared to solvent based systems. Since this is growing area of wider environmental concern, this was advantageous to this PhD project.

The conductive polymers were agglomerating despite being sonicated and blocked the airbrush. After preliminary scoping investigations which are detailed in 3.3.2, only PEDOT:PSS was taken forward for further experiments since it was only PEDOT:PSS and PEDOT:PEG analogues that showed any resistivity readings.

The reason for choosing PEDOT:PSS over PEDOT:PEG was:

- There was very little difference found in the resistivity of PEDOT:PEG to PEDOT:PSS.
- PEDOT:PSS is more widely commercially available and usually cheaper than PEDOT PEG so better for bulk applications.
- PEDOT:PSS gave slightly more homogeneous film quality to that of PEDOT:PEG.

For these reasons PEDOT:PEG was eliminated from further study.

4.2.2 Solid cast 100 % PEDOT:PSS samples

The experiment was performed as detailed in Section 3.3.2.1. At the start of the experiment the sample weighed 30.001 g. At the end the sample weighed 0.336 g. It was found the paper case samples gave no conductivity results at all. The resistivity was out of range of the Keithley equipment used. Since there was no current registering it was impossible to calculate the resistivity. With the paper samples the PEDOT solution completely impregnated the paper case so no thickness was measurable for this film either. The silicon cake gave a current measurement of 11.72 mA. However, results are unreliable since as seen in Figure 4.1, the film was far from being homogeneous. The conclusion is that under normal laboratory conditions it is impossible to obtain a homogeneous thin film or thick film of 100 % PEDOT:PSS using this particular analogue as supplied by Sigma unless additives are used which then results in a solution which is not 100 %.



Figure 4.1: (Left) The paper cased samples, (Right) Silicon cake case sample of 100 % PEDOT:PSS after annealing

4.2.3 Substrate selection

Wetting was a problem with all samples except paper. Paper showed little or no conductivity and burned easily in the oven during the annealing process. Resistivity measurements were out of range for the Keithley and all other equipment. It was impossible to check most samples for conductivity since the samples were either a sticky gel even after days of leaving to anneal or completely delaminated. Often samples peeled off the substrate and adhesion was non-existent. Paper was eliminated as a viable substrate since it showed no conductivity and poor film quality. PP and PC were eliminated due to delamination of the films and poor film quality. Only PET and glass remained as viable substrates to take forward in this PhD project. PET was chosen as the bulk polymer and glass because it is of interest in a large amount of research into thin films.

4.2.4 Surface energy

The contact angle of PET was measured using a sessile drop method as described in Section 3.4.4 and was found to be 47.45 mN/m using the OWRK/Fowkes calculation. From Table 3.8 this is a close result to that of the literature.

4.2.5 Manufacturing techniques

Different manufacturing methods had been trialled and some were eliminated during the scoping. The metal particles and carbon particles without exception caused the airbrush to block up so no further experiments were performed incorporating these additives.

4.2.6 Pipetting

Using a benchtop SEM the samples made using pipetting were found to contain 0.15- 0.3 mm bubbles in the film shown in Figure 4.2.

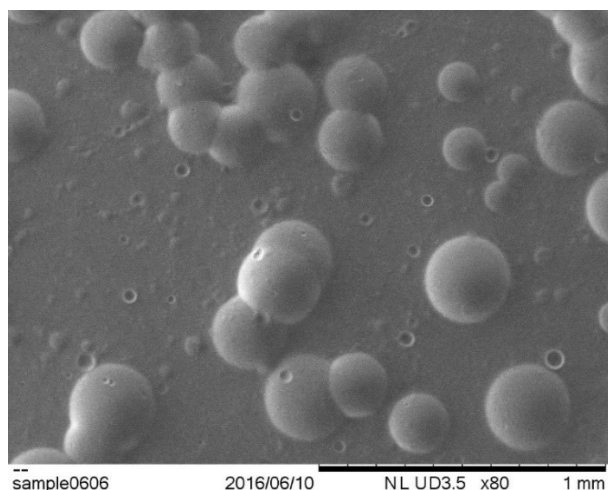


Figure 4.2: Benchtop SEM of the sample showing what appears to be bubbles on the surface of the PEDOT/TWEEN 80/MEK film

The pipetted samples were found to have far higher resistivities than the identical samples made using the other methods. It is assumed that the higher resistivity is caused by the presence of the bubbles in the annealed films which cause the current to flow less efficiently through the samples. This is then causing a lower conductivity due to the presence of the annealed bubbles. The pipetting method was not taken forward after the initial experiment proved it to be non-viable. Pipetting gave a very uneven film, which remained sticky and peeled off the substrate completely in most cases. Since the pipetted film was uneven electrical measurements were unreliable. All electrical results from pipetted samples were too inconsistent to continue experimenting with this method of application.

4.2.7 Spraycoating and Dipcoating

From the initial trials, no adhesion was achieved and all samples delaminated. An example of the problem with wetting of samples in order to produce a homogeneous films is shown in Figure 4.3.

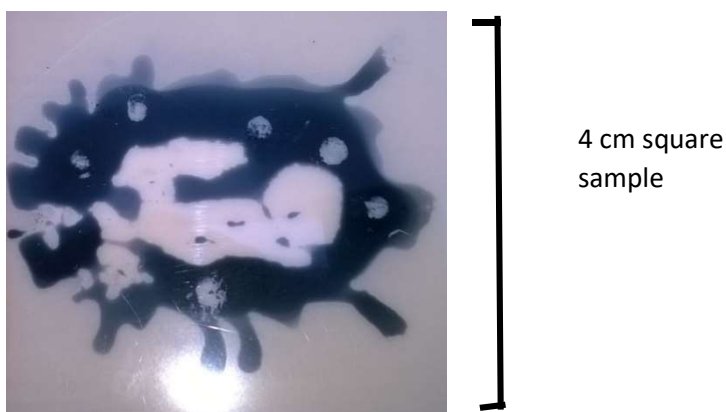


Figure 4.3: 100 % annealed PEDOT:PSS sprayed onto PET film does not wet well.

Spray coating gave a slightly better film but still delaminated. Most but not all solutions were found to block the spraycoater. Dip coating gave uneven films with a graduating

thickness due to gravity during the manufacturing process but using the central areas gave consistent samples. Spincoating while giving a thinner film delaminated and had no adhesion to the substrate. A film was needed that was compatible with the substrate. In order to achieve compatability additives were explored. Adhesion and substrate wetting was improved using a surfactant and thoroughly cleaning the substrate prior to application of the PEDOT-mixture.

4.2.8 Conductivity of the 100 % PEDOT:PSS

Attempts to obtain a 100 % film without a substrate had proved impossible. The 100 % PEDOT:PSS applied to PET has a very imperfect film quality. This changes little regardless of manufacturing method used so this must be noted when analysing this data. Conductivity of the 100 % PEDOT:PSS annealed onto PET was measured as a thin film using a Jandel four point probe and Keithley 6517b two point probe resistivity meter as shown in Table 4.2.

Table 4.2: Average sheet resistance results of 10 readings taken over 1 minute using the Jandel four point probe at 10nA for the 100 % sample

Manufacturing method	Average(Ω/sq)
Dipcoated	4255
Spraycoated	4082
Spincoated	4880

For the Keithley 6517b the samples were tested at 1,2,5,10,20,30,and 40 V. Resistivities are shown for the samples in Table 4.3.

Table 4.3: Average resistivity results of 5 samples using the Keithley 6517b for the 100 % sample at different applied potential differences

Manufacturing method	1 V	2 V	5 V	10 V	20 V	30 V	40 V
	Ω	Ω	Ω	Ω	Ω	Ω	Ω
Dipcoated	34602	34157	34499	49086	33873	34076	34708
Spraycoated	5188	4832	52965	49707	47013	48388	34757
Spincoated	5421	2304	50403	50169	24892	75011	59722

4.2.9 TWEEN 80 Surfactant and MEK

From the results of the scoping experiments most potential additives for wettability and conductivity enhancement were eliminated leaving just TWEEN 80 and MEK for further experiments since the scoping had shown conductivity enhancement, as well as improved wettability of substrate. TWEEN 80 was found to improve wettability of glass, PET, PP and PC when mixed with the solvents and gave a more even homogeneous film. However, once annealing was completed the film in most cases shrunk and delaminated. For example, the film was still on the surface of the PP substrate but no longer covered it. Although addition of TWEEN 80 to PEDOT:PSS improved the wetting of PP with ethanol as solvent, the film never actually dried, and remained as a sticky residue. There was a lot of delamination of the film from the PP samples during annealing but the droplet effect seen in Figure 4.3 was slightly improved. TWEEN 80 with a PC substrate gave some improvement over PP and the film did not delaminate during annealing at 120 °C however, the quality of the film was not homogeneous. This led to elimination of both PC and PP as substrates. PET also remained sticky but had a much better film quality and homogeneity and delaminated least. It was concluded that PET was the best substrate to take forward and to try to optimise the film for conductivity testing. This made sense being the substrate with highest surface energy and the best wetting as was explained in Section 3.4.4. The

TWEEN 80 and the solvent mixed perfectly with no phase separation and gave wettability. This was measured visually by noting if the solution gave an even and homogeneous coverage on the substrate. It was also found that when measuring the surface energy of annealed samples of PET coated in higher concentrations of PEDOT:PSS with TWEEN 80 and MEK that the surface energy was zero indicating the TWEEN 80 and MEK was altering surface energy and allowing a good wetting to give a homogeneous film on the substrate. It was also noted that when the TWEEN 80 solutions made using MEK were stored they did not separate into two phases. Propanol, Butan-1-ol and Butan-2-ol, Hexane and Water were discounted as possible solvents. This left Ethanol and MEK and a 50:50 mixture of ethanol and MEK. It was found that MEK gave much better films than either the 50:50 mixture or the Ethanol so the optimum solvent for improving wettability was the MEK. However, because addition of the surfactant affects the drying of the surface of the film and the film remains sticky this caused the films to stick to sample bags and in some cases to peel off the substrate, which was a problem for testing. The TWEEN 80 films were able to be tested for electrical conductivity and were found to have actually slightly enhanced the conductivity of the film from what was achieved with the 100 % PEDOT:PSS. An example of the improved film quality is shown in Figure 4.4 which shows a much improved film quality to Figure 4.3.



Figure 4.4: The spraycoated PEDOT:PSS solution on PET showing better wetting with addition of surfactant

4.2.10 Adhesion

Even after cleaning the substrates thoroughly and using a surfactant to improve wettability as described in Section 3.3.1, there was still a problem with adhesion since in all samples the thin films of PEDOT were either delaminating completely on to sample storage bags or scratching very easily when being tested. No adhesion improvement was found with the surface modifiers such as CMC and PVA and the films all delaminated from the substrate and did not stay on the substrate long enough to get any conductivity results. Wetting and delaminating were major issues and most samples could not be tested for conductivity. Addition of TWEEN 80 surfactant and MEK to PEDOT:PSS was found to slightly improve wetting, adhesion and final film quality. This is described in Section 4.2.9.

4.2.11 Conclusions from scoping

Once the selection of materials had been finalised the rest of the project concentrated on optimising the solutions and the performance of the thin films of PEDOT:PSS.

In conclusion:

- PET was chosen as the bulk polymer and glass was chosen because it is of interest in a large amount of research into thin films.
- All the conductive polymers except for PEDOT:PSS were eliminated from further study.
- MEK was found to be the best solvent closely followed by ethanol.
- TWEEN 80 improved film quality, wetting and slightly improved adhesion although adhesion is still a problem.

Further questions to be investigated now include:

- Could the starting material be further enhanced using the additives TWEEN 80 and MEK?
- What is the optimum amount of each additive to enhance the conductivity of PEDOT:PSS.
- The starting material has a sheet resistance of $<100 \Omega/\text{sq}$ according to manufacturer but this was measured using a four point probe, as between 4082 to 10872 Ω/sq depending on the manufacturing technique. How do the different techniques affect this result?
- Solve outstanding adhesion problems.

- What is the mechanism of conductivity, which may be discernible from spectroscopy. How does PEDOT conduct electrically?
- Consider processing routes for bulk application. Conductive PEDOT:PSS films may eventually lead into further research which can feed into a bulk manufacturing program if an enhancement in processing is identified. What is the best manufacturing technique to maintain low resistivity but allow for transfer to bulk applications?

4.3 Optimisation of the films

It was concluded that The samples produced in Sections 4.2.6 and 4.2.7 had been of poor film quality but the addition of the additives, TWEEN 80 and MEK, gave a better, more homogeneous film which could be measured for electrical conductivity. The conclusion was that the films need to be optimised for adhesion, film quality and electrical conductivity. As described in Section 3.3.3, the solutions were applied to PET as a thin film by three different methods: spraycoating , dipcoating and spincoating in order to compare manufacturing methods. Having made solutions as described in Section 3.2.5, the properties of pH and viscosity were investigated. The annealed films were characterised using four-point probe and two-point probes as well as spectroscopically. These methods are described in Sections 3.4.5.3 and 3.4.5.4. From the results of these experiments the film quality was further optimised by altering the concentration of TWEEN 80 and MEK. Once the film quality and electrical conductivity had been optimised the solid films were characterised.

4.3.1 pH

The reported pH of the starting material is pH <2.5. In order to check this and to see if the additives would make any changes to the original pH, the solutions were made

up as previously described in Chapter 3. The buffers used to calibrate the equipment were pH 7.01 \pm 0.01 @ 25 °C and pH 4.01 \pm 0.01 @ 25 °C. Measured pH of the PEDOT:PSS/TWEEN 80/MEK solutions are shown in Figure 4.5.

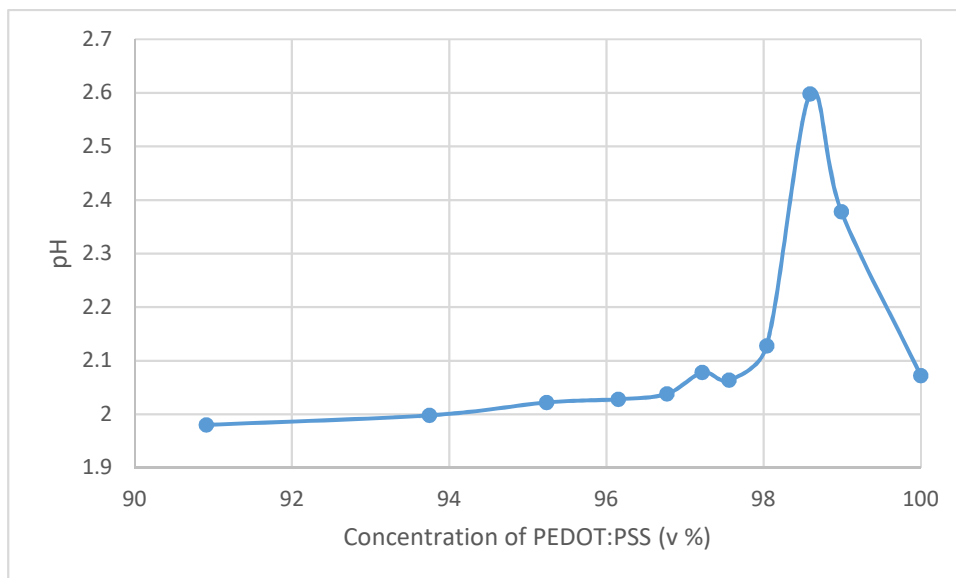


Figure 4.5: Measured pH showing the concentration of PEDOT:PSS in each solution

4.3.2 Viscosity measurements

Viscosity measurements were taken for all the solutions. Table 3.16 shows the settings used for these measurements. Figure 4.6 shows the viscosity of the solutions. The reported viscosity stated by Sigma for the 100 % PEDOT:PSS was 30- 100 centipoise (cP) at 20 °C. Viscosity measurements were repeated 6 times and showed an average viscosity of 69.77 cP for 100 % PEDOT:PSS which is within the stated range.

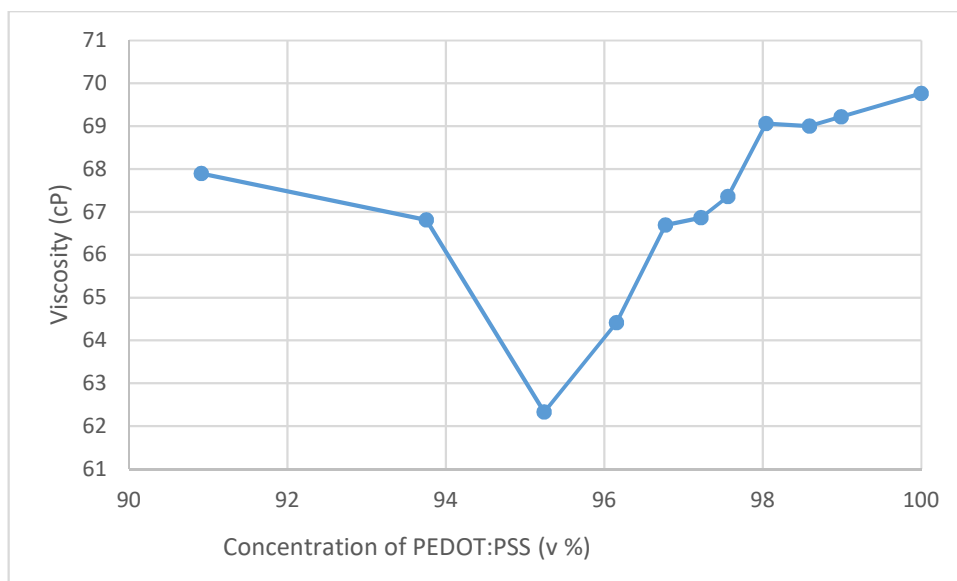


Figure 4.6: Viscosities for the PEDOT:PSS/TWEEN 80/MEK solutions at 21 °C

Average measured viscosity for the 100 % TWEEN 80 solution was found to be 37.4 cP.

4.3.3 Spraycoating

The procedure for spraycoating is described in Section 3.3.3.1. All the higher concentration samples with 98 to 99 % PEDOT:PSS, found in Zone 3 as later explained in, Section 5.3.1.1 and the 100 % PEDOT:PSS, show very poor film quality and even with addition of the surfactant, the film quality still requires improvement. As the surfactant concentration is increased so the film quality also increases up to a maximum at which point it becomes very sticky. When measured, the contact angle was zero, for these higher surfactant films. The 91 to 94 %, samples are conductive but they were also very sticky or rubbery which caused them to stick onto other surfaces such as poly bags used for storage and transportation as well as measuring equipment. As the concentration of PEDOT:PSS increases the samples become more brittle since they delaminate easily off the substrate. The conductivity of the

spraycoated samples was measured as detailed in Section 3.4.5. Figure 4.7 shows the poor film quality achieved with the spraycoated samples.

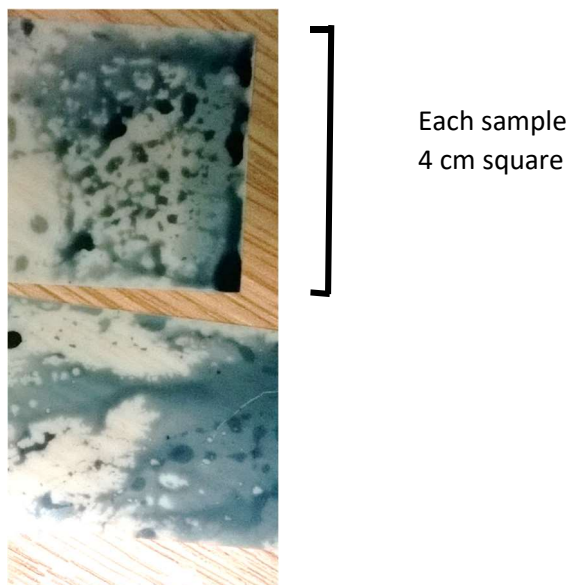


Figure 4.7: Spraycoated 99 % PEDOT:PSS (bottom) and 100 % PEDOT:PSS (top)

Results are shown in Figures 4.8-4.12 which shows the different sample sets of spraycoated samples which were tested using a Keithley 6517b.

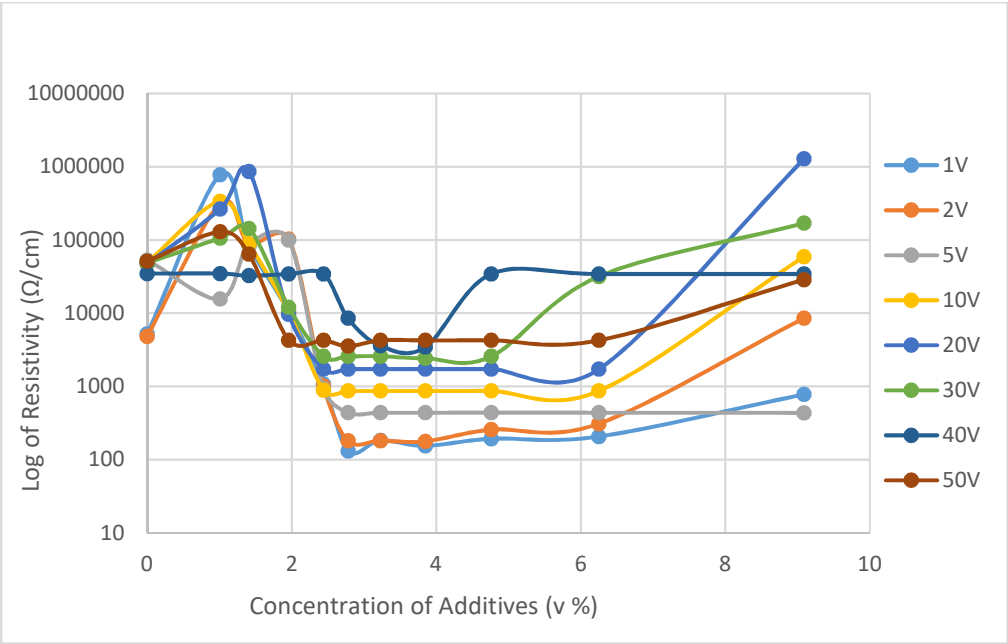


Figure 4.8: Spraycoated Set 1 resistivity at various voltages using Keithley 6517b

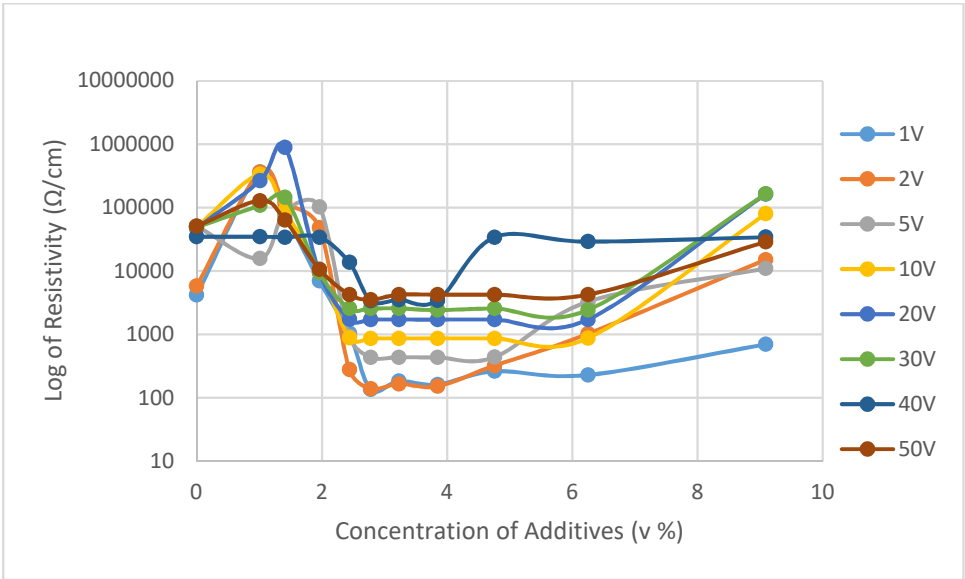


Figure 4.9: Spraycoated Set 2 resistivity at various voltages using Keithley 6517b

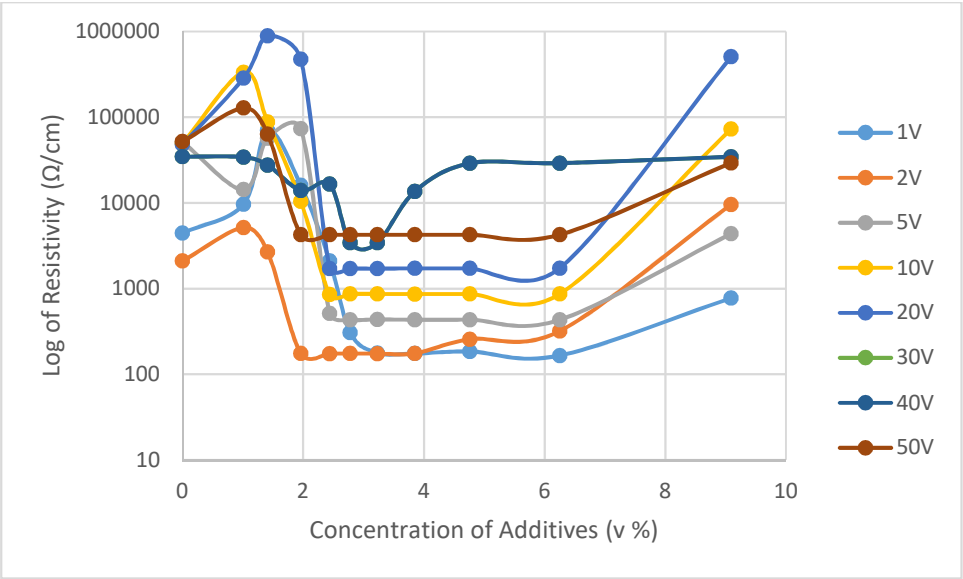


Figure 4.10: Spraycoated Set 3 resistivity at various voltages using Keithley 6517b

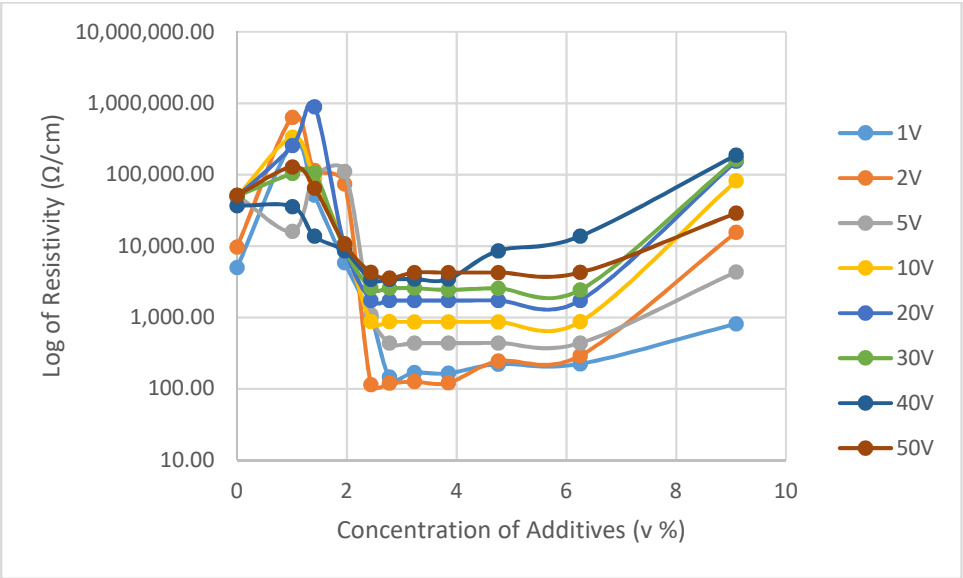


Figure 4.11: Spraycoated Set 4 resistivity at various voltages using Keithley 6517b

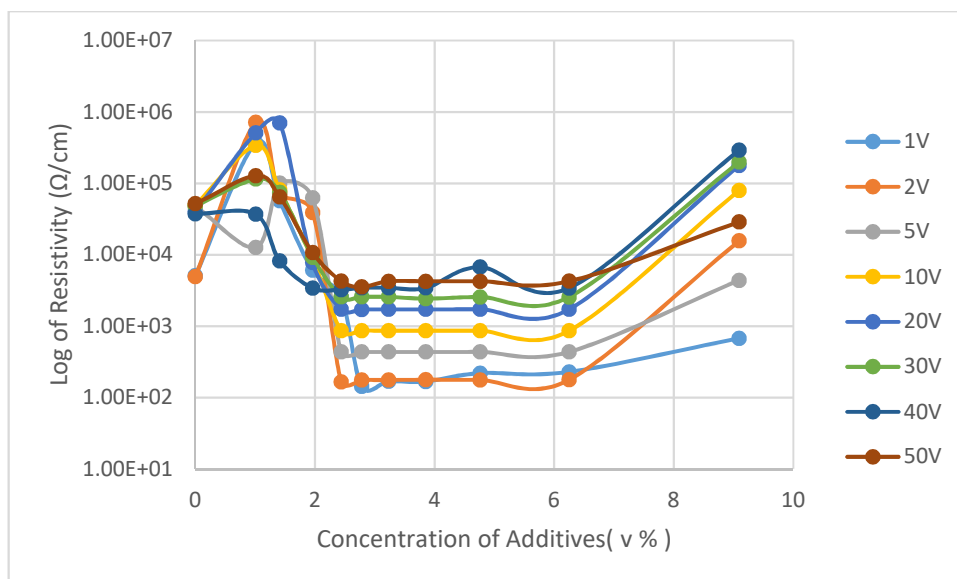


Figure 4.12: Spraycoated Set 5 resistivity at various voltages using Keithley 6517b

Having obtained 5 sets of samples that verified the electrical results were repeatable, three representative samples were chosen. This is explained in Section 5.3.1.1. These were: the 100 % PEDOT:PSS starting material, the 97 % PEDOT:PSS sample, and the 99 % PEDOT:PSS sample that measured as the most stable electrically, although this was not as conductive as the 97 % PEDOT:PSS sample. The other samples were eliminated due to film delamination problems and unstable resistivity results. It had been discovered that the 99 % PEDOT:PSS sample, when measured electrically, was stable whereas the other samples were unstable over a range of values. In order to eliminate error from the measurements, the samples were measured in a random order. This was repeated for each set of samples.

The three representative samples that had been chosen were then plotted at each applied potential difference. These are shown in Figures 4.13 to 4.20. The different sets of samples were all made identically but at different dates in order to show repeatability of experiments and repeatability of results.

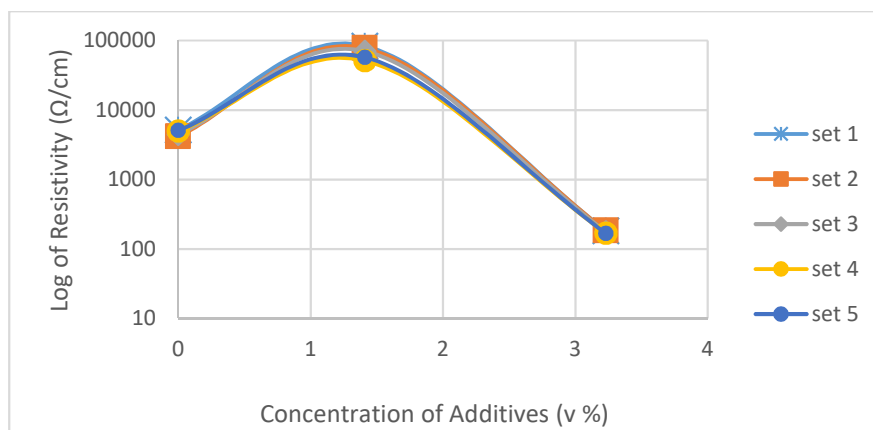


Figure 4.13: Average resistivity values for sets 1-5 for the 97 % PEDOT:PSS , 99 % PEDOT:PSS and 100 % film samples at 1 V – Spraycoated

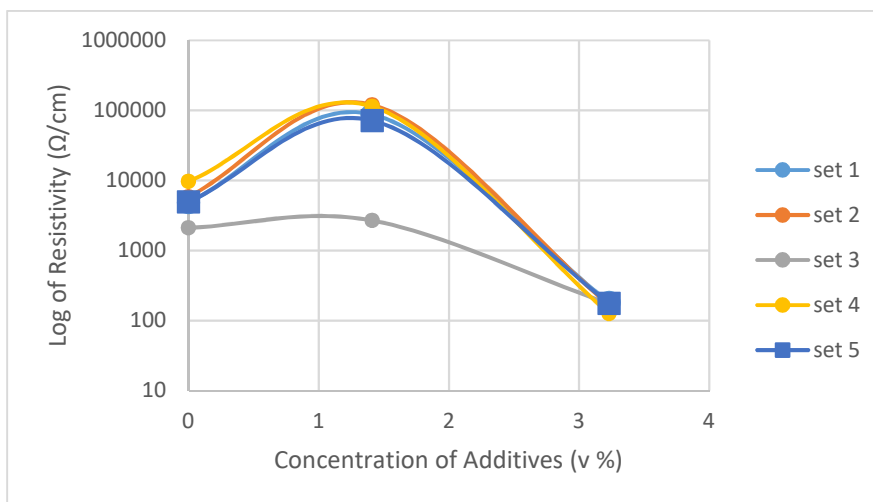


Figure 4.14: Average resistivity values for sets 1-5 for the 97 % PEDOT:PSS, 99 % PEDOT:PSS and 100 % film samples at 2 V – Spraycoated

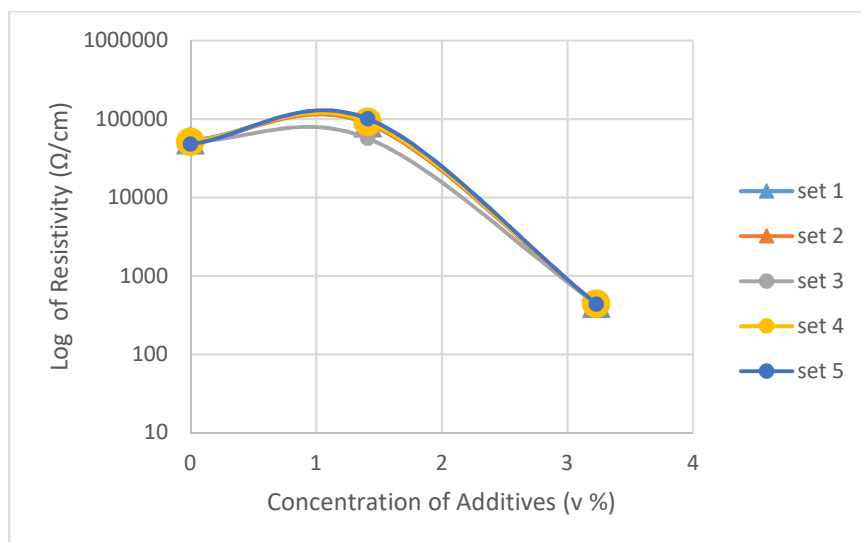


Figure 4.15: Average resistivity values for sets 1-5 for the 97 % PEDOT:PSS, 99 % PEDOT:PSS and 100 % samples at 5 V – Spraycoated

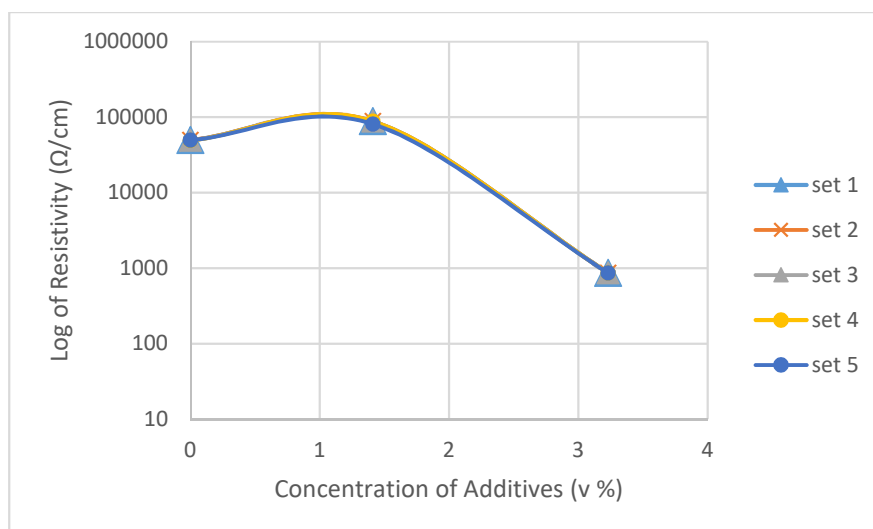


Figure 4.16: Average resistivity values for sets 1-5 for: 97 % PEDOT:PSS, 99 % PEDOT:PSS and 100 % film samples at 10 V – Spraycoated

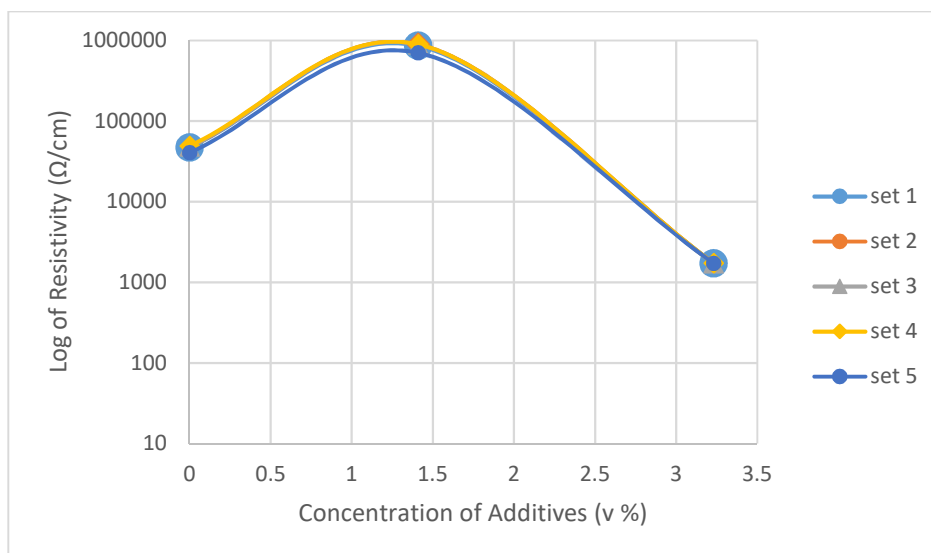


Figure 4.17: Average resistivity values for sets 1-5 for the 97 % PEDOT:PSS, 99 % PEDOT:PSS and 100 % film samples at 20 V – Spraycoated

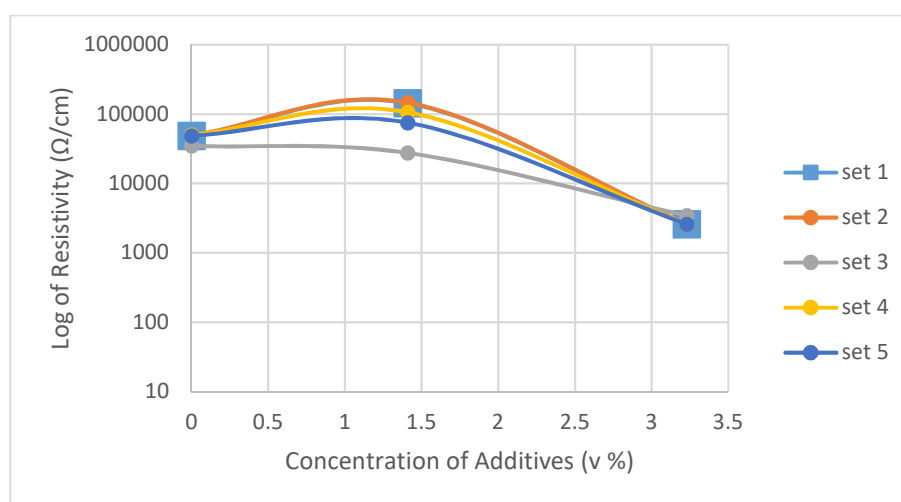


Figure 4.18: Average resistivity values for sets 1-5 for the 97 % PEDOT:PSS, 99 % PEDOT:PSS and 100 % film samples at 30 V – Spraycoated

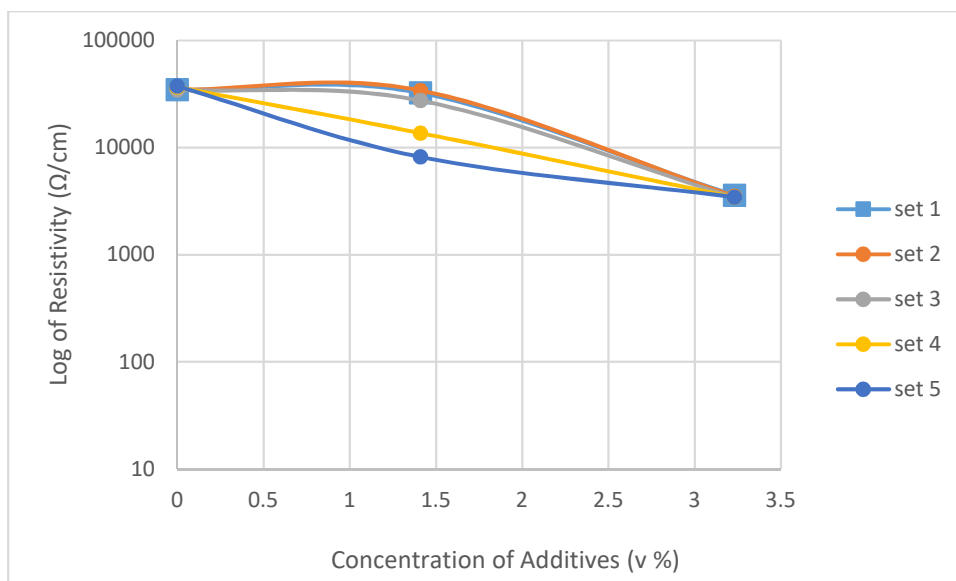


Figure 4.19: Average resistivity values for sets 1-5 for the 97 % PEDOT:PSS, 99 % PEDOT:PSS and 100 % film samples at 40 V – Spraycoated

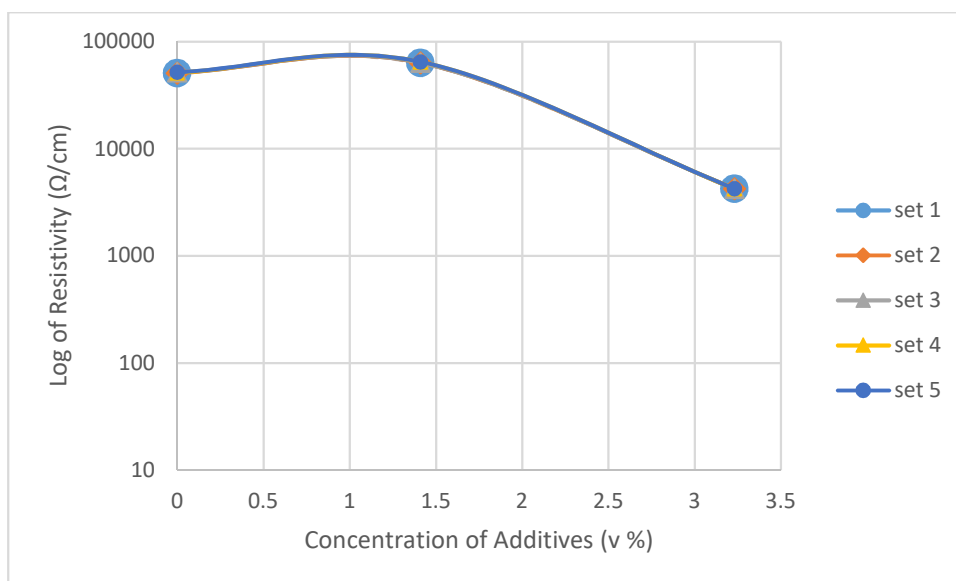


Figure 4.20: Average resistivity values for sets 1-5 for the 97 % PEDOT:PSS, 99 % PEDOT:PSS and 100 % film samples at 50 V – Spraycoated

4.3.4 Dipcoating

The procedure for dipcoating is described in Section 3.3.3.2. Figure 4.21 shows the good quality dipcoated 97 % PEDOT:PSS film on the left (1) with the 99 % PEDOT:PSS film in the centre (2) with the poor sample coverage and the scratches

on the surface of the sample which occurred even inside a sample bag. On the right in Figure 4.21 (3), is the dip-coated 100 % PEDOT:PSS film on PET substrate showing how the solution beads even with surfactant added and how it dries with an unhomogeneous surface. This uneven beading means it is difficult to get reliable conductivity results. For conductivity measurements a small 1 cm square was drawn on the reverse of the sample as guide for electrical characterisation tests. The resistivity was measured as detailed in Section 3.4.5. Note that set 1 of the dipcoated samples was only tested up to 40 V since at that time this was the maximum measurement and then this set became too scratched to use. All the other samples were tested up to 50 V since the decision was taken to see what effect the higher voltage would have.

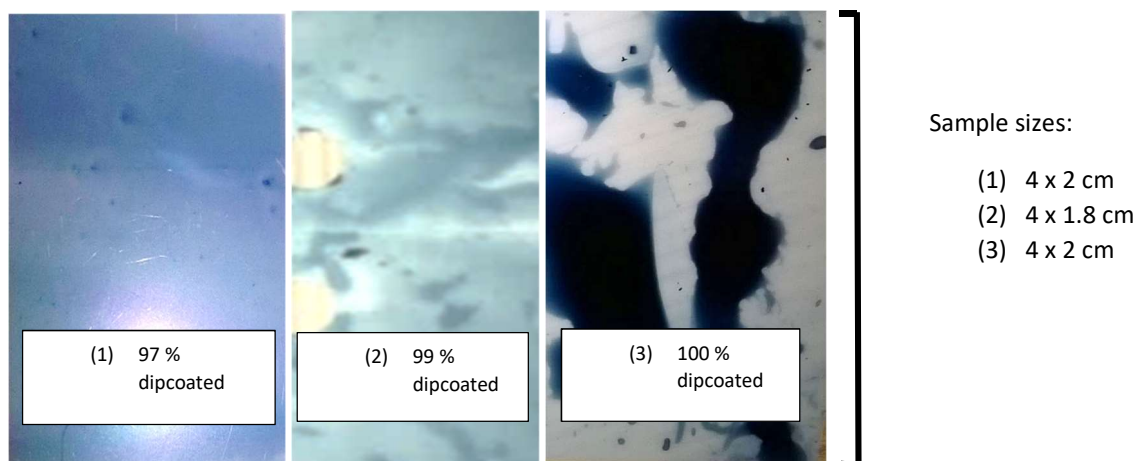


Figure 4.21: The dip-coated samples on PET, Left (1) 97 % PEDOT:PSS , 99 % PEDOT:PSS centre (2), right (3) 100 % films of PEDOT:PSS

Figures 4.22 to 4.26 show results of the resistivity testing using the Keithley 6517b.

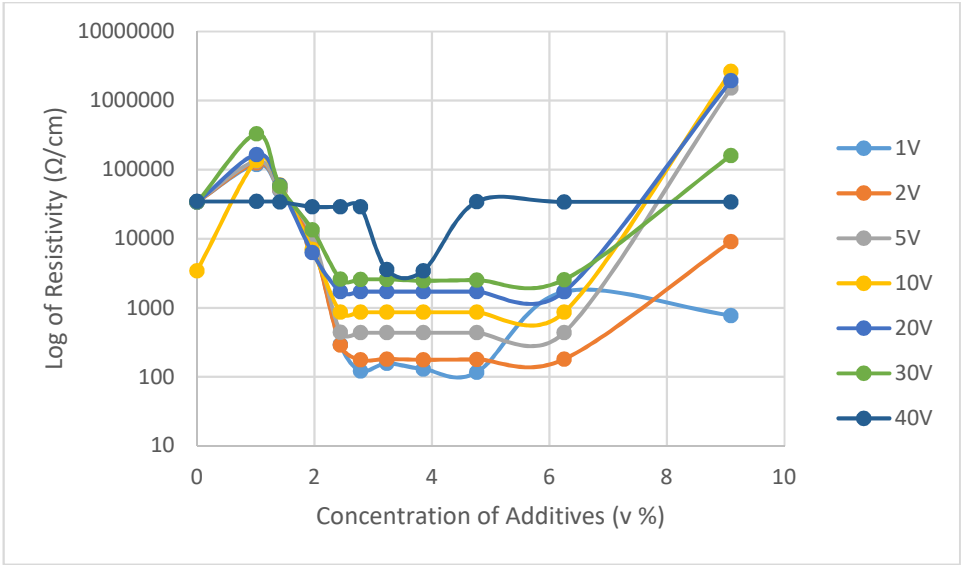


Figure 4.22: Dipcoated Set 1 resistivity at various voltages using Keithley 6517b

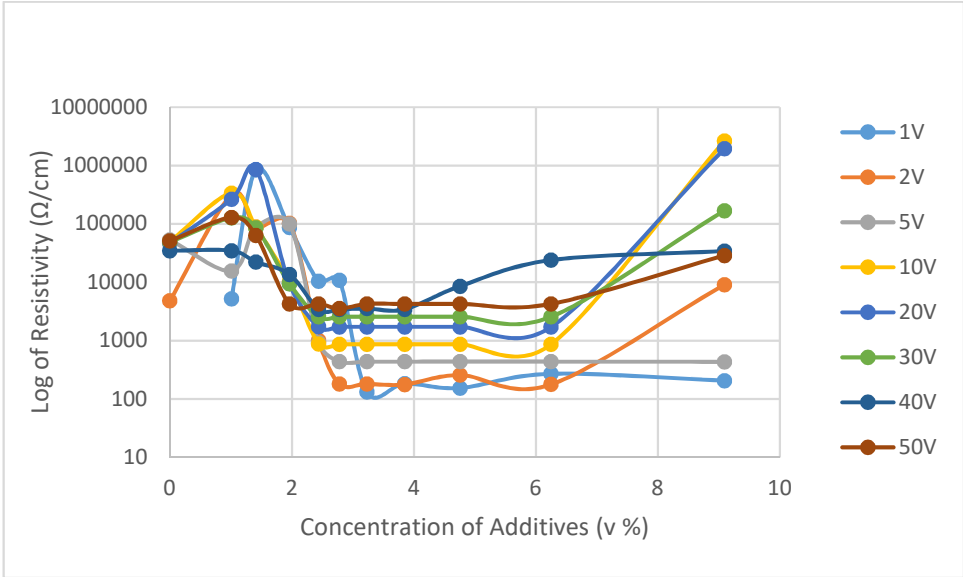


Figure 4.23: Dipcoated Set 2 resistivity at various voltages using Keithley 6517b

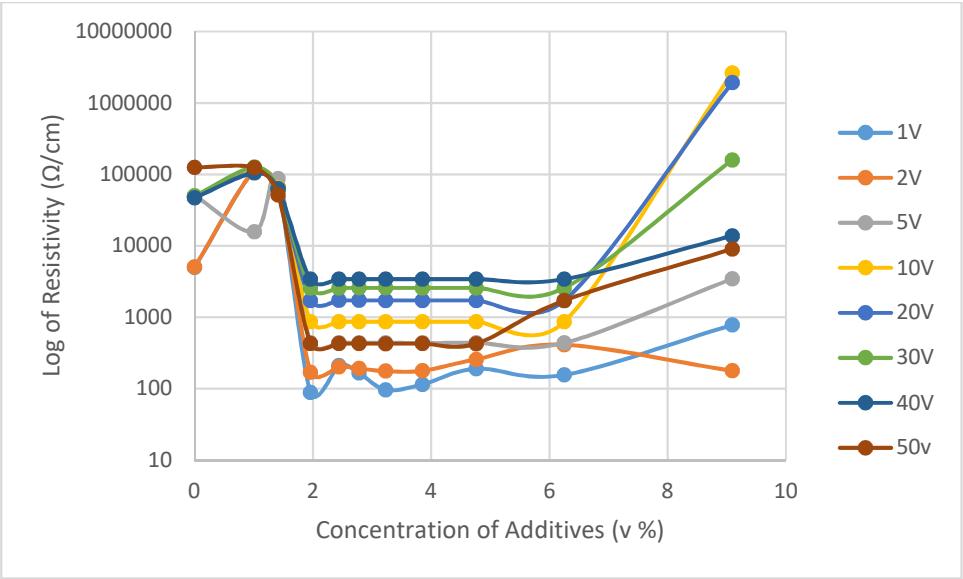


Figure 4.24: Dipcoated Set 3 resistivity at various voltages using Keithley 6517b

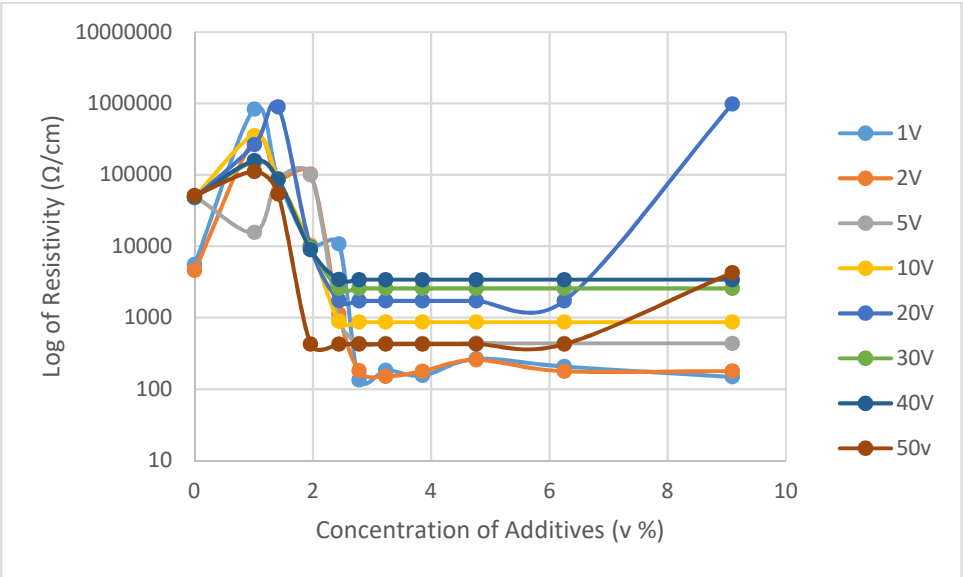


Figure 4.25: Dipcoated Set 4 resistivity at various voltages using Keithley 6517b

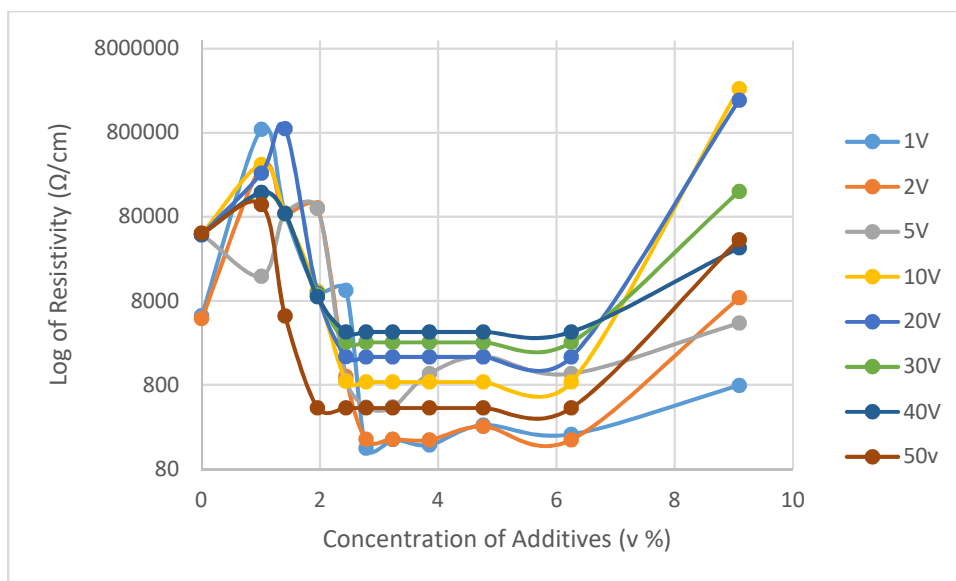


Figure 4.26: Dipcoated Set 5 resistivity at various voltages using Keithley 6517b

The three representative samples of most interest were then plotted without the rest of the samples. This is shown in Figures 4.27 to 4.34.

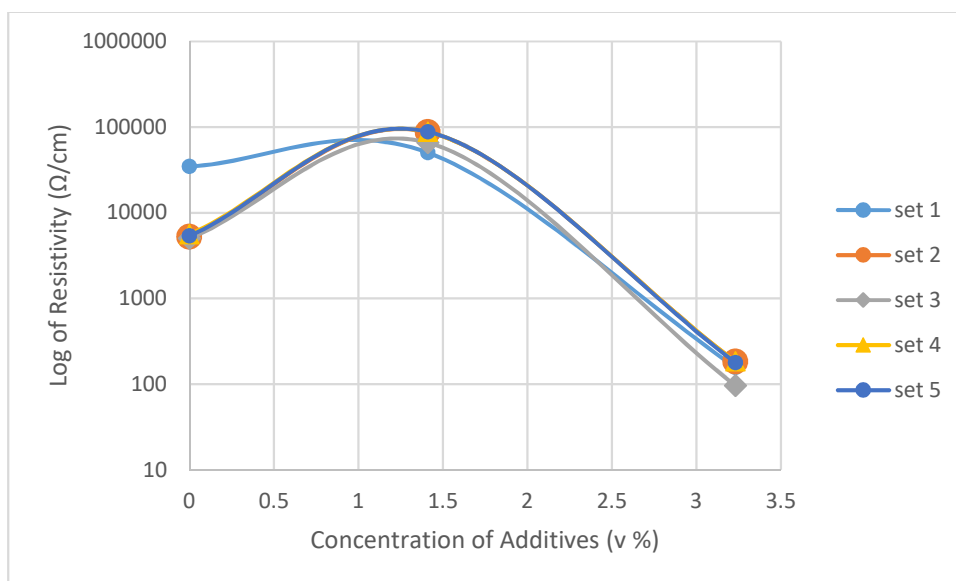


Figure 4.27: The average for the 97 % PEDOT:PSS 99 % PEDOT:PSS and 100 % PEDOT:PSS resistivity at 1 V using Keithley 6517b

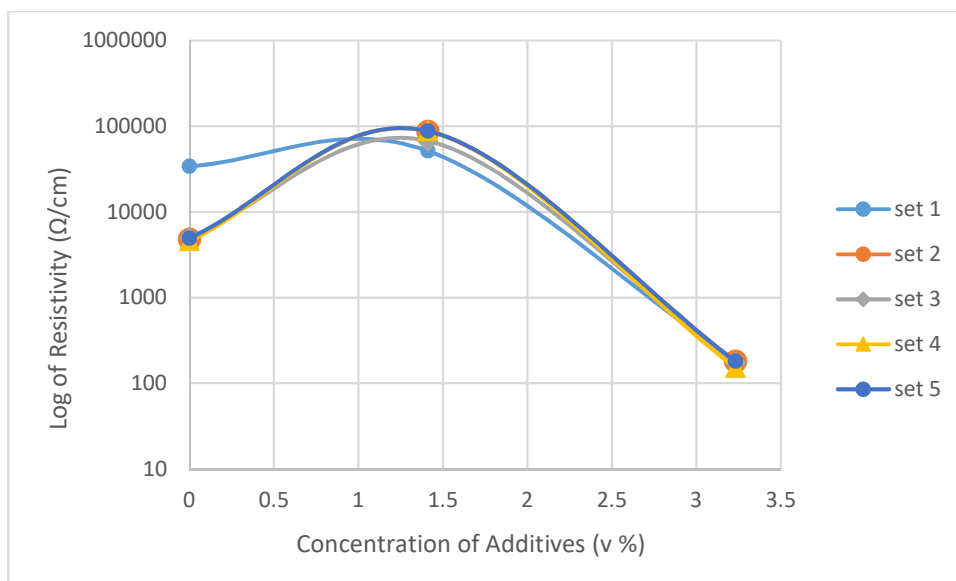


Figure 4.28: The average for the 97 % PEDOT:PSS 99 % PEDOT:PSS and 100 % PEDOT:PSS resistivity at 2 V using Keithley 6517b

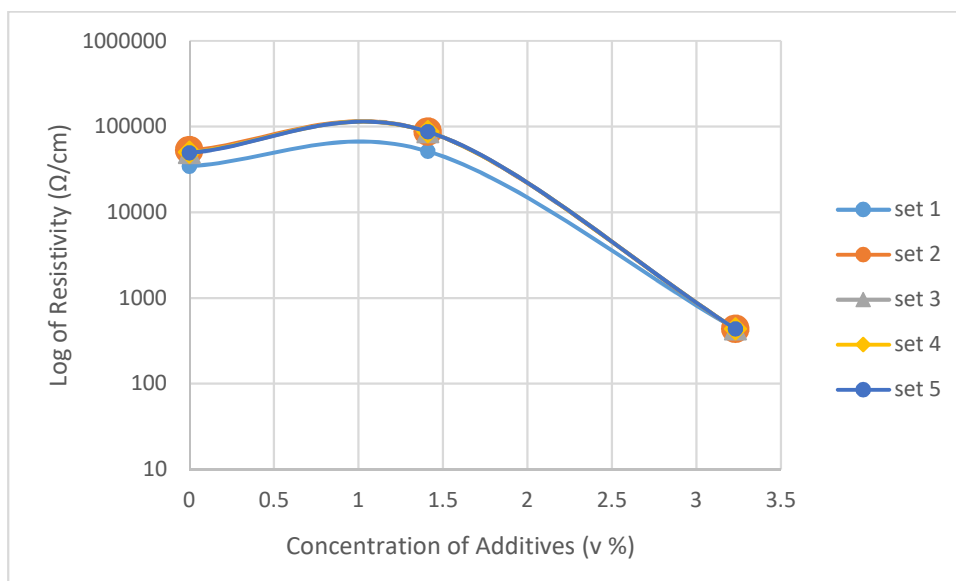


Figure 4.29: The average for the 97 % PEDOT:PSS, 99 % PEDOT:PSS and 100 % PEDOT:PSS at 5 V for dipcoated sets 1-5 using Keithley 6517b

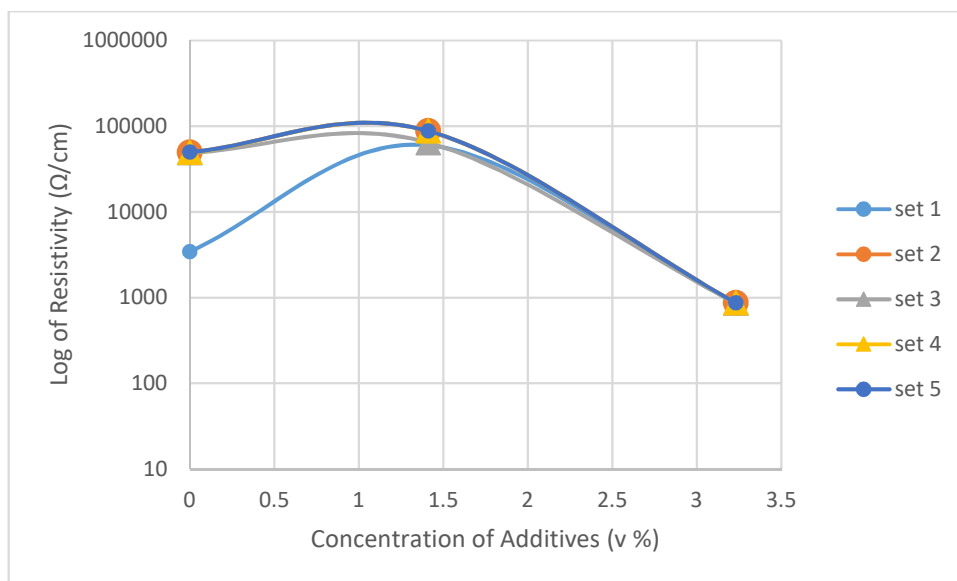


Figure 4.30: The average for the 97 % PEDOT:PSS, 99 % PEDOT:PSS and 100 % PEDOT:PSS dipcoated sets 1-5 at 10 V

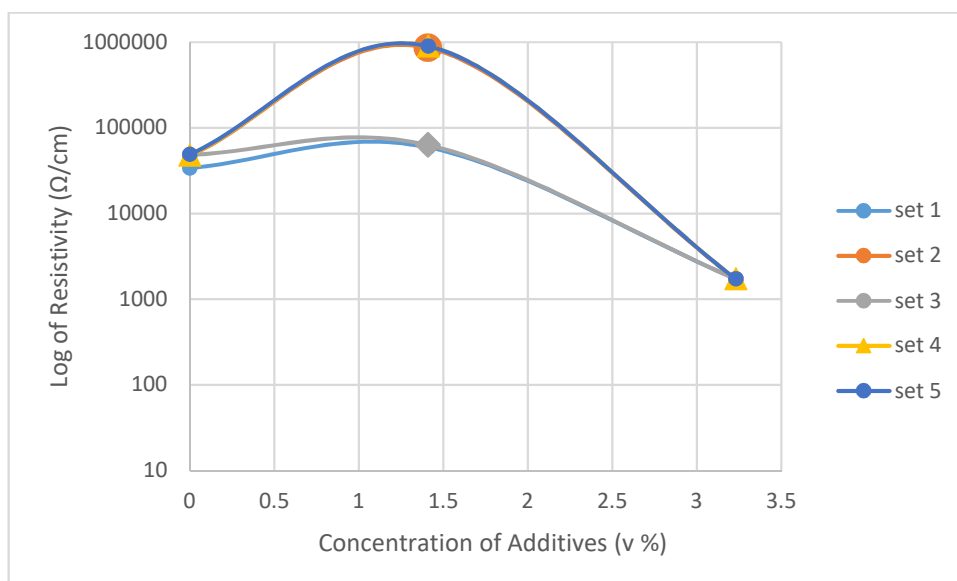


Figure 4.31: The average for the 97 % PEDOT:PSS, 99 % PEDOT:PSS and 100 % PEDOT:PSS dipcoated samples at 20 V

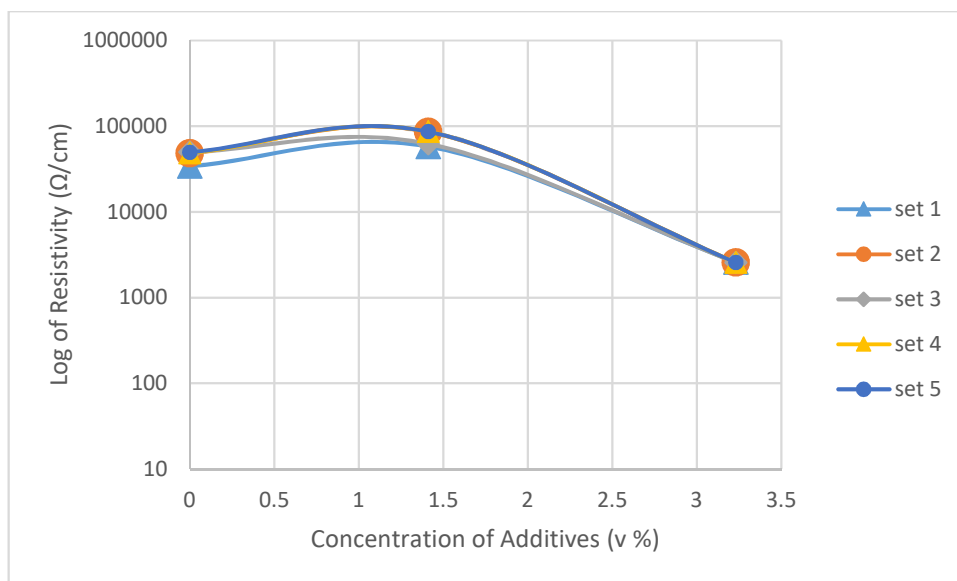


Figure 4.32: The 97 % PEDOT:PSS , 99 % PEDOT:PSS and 100 % PEDOT:PSS for dipcoated sets 1-5 at 30 V

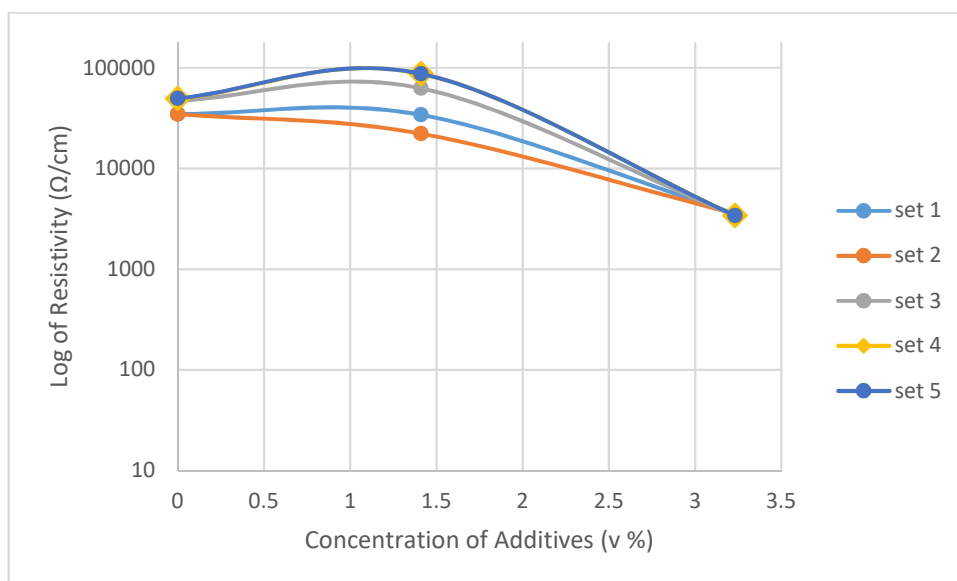


Figure 4.33: The average for the 97 % PEDOT:PSS, 99 % PEDOT:PSS and 100 % PEDOT:PSS dipcoated sets 1-5 at 40 V

Figure 4.34 does not include sample set 1 since the decision to test up to 50 V was taken after this set had become too scratched and damaged to continue testing accurately.

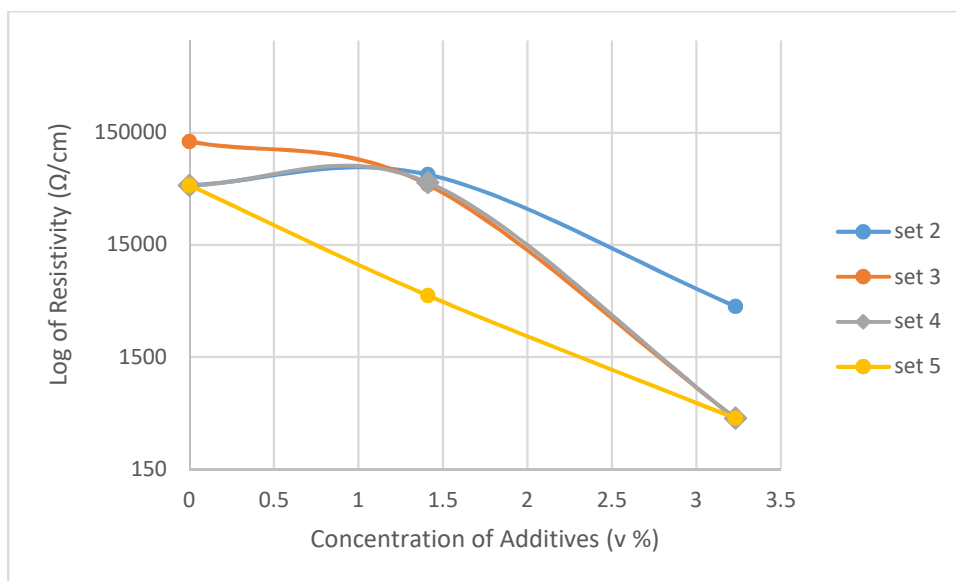


Figure 4.34: The average for the 97 % PEDOT:PSS, 99 % PEDOT:PSS and 100 % PEDOT:PSS dipcoated sets 2-5 at 50 V

To see how resistivity of each sample set varied for the same concentration of sample with different applied potential the values were then plotted as shown in Figures 4.35 to 4.37.

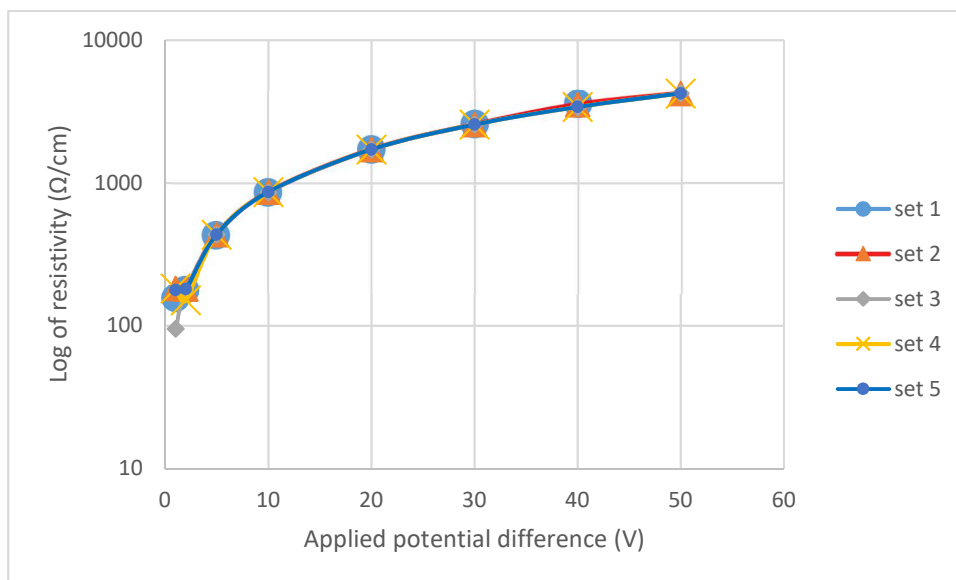


Figure 4.35: Measured resistivity vs applied voltage for the 97 % PEDOT:PSS, dipcoated PEDOT:PSS film samples

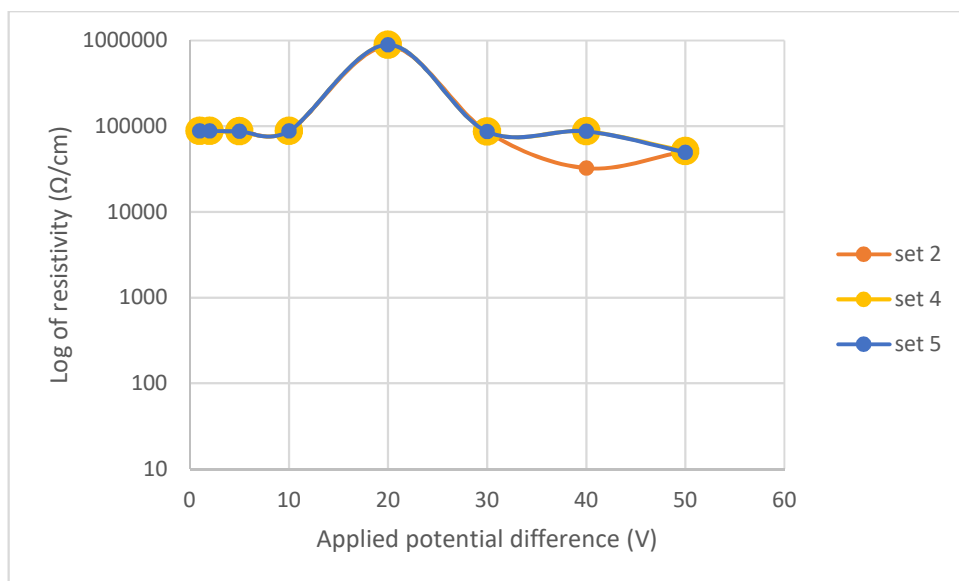


Figure 4.36: Measured resistivity vs applied voltage for 99 % PEDOT:PSS dipcoated PEDOT:PSS film samples

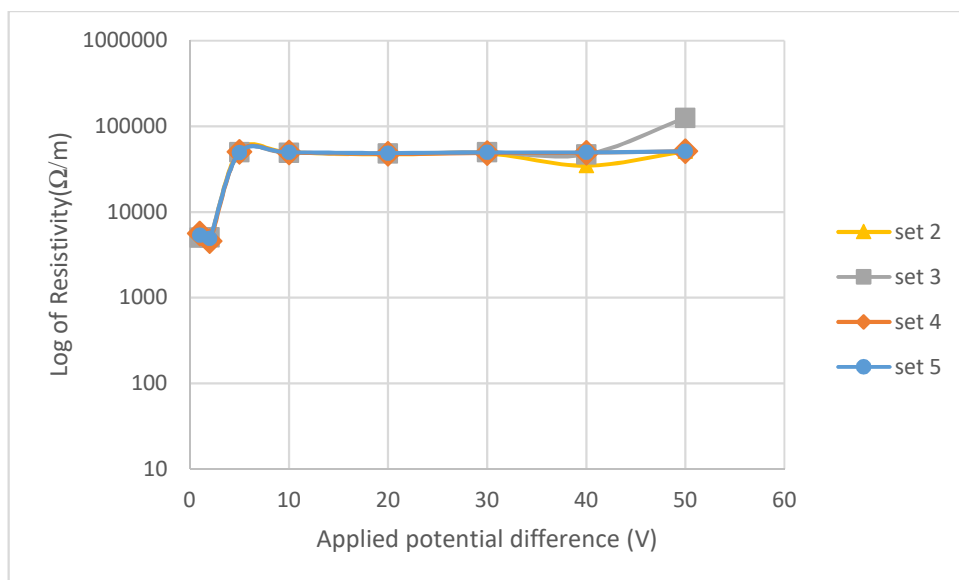


Figure 4.37: Measured resistivity vs applied voltage for the 100 % dipcoated PEDOT:PSS samples

4.3.5 Electrical measurements

Resistivity measurements were taken for every viable sample using the four-point probe and two point probe methods described in Section 3.4.5. Original results for these experiments can be found in the Appendix.

4.3.5.1 Four-Point-Probe – dipcoated samples

When using the four-point-probe as described in Section 3.4.5.3, the readings were somewhat unstable so in order to take this into account 10 readings were taken over 1 minute and then the average reading was plotted. Tables 4.4 and 4.5 show examples of the results obtained using a four-point-probe with these settings.

Table 4.4: An example of the sheet resistance results from measuring with the Jandel four-point-probe

(%) PEDOT:PSS	Mean Resistivity (Ωsq)	Minimum Resistivity (Ωsq)	Maximum Resistivity (Ωsq)
91	198	111	289
94	2382	2253	2659
95	2459	2060	2931
96	2606	2359	3010
97	3352	3100	3520
97	2517	2088	2835
98	2703	2175	3120
98	4882	4495	5156
99	29559	29360	29760
99	228402	227360	229560
100	4255	4012	4423

Table 4.5: An example of the results for bulk resistivity obtained from the Jandel four-point-probe

PEDOT:PSS (%)	Mean Resistivity (Ωcm)	Minimum Resistivity (Ωcm)	Maximum Resistivity (Ωcm)
91	27	24	30
94	287	239	341
95	108	102	119
96	118	110	129
97	216	182	289
97	111	102	119
98	138	125	149
98	716	671	770
99	4127	4106	4172
99	11519	11500	11540
100	201371	188780	218890

Figure 4.38 shows the sheet resistance of the dipcoated samples showing the minimum and maximum values. Figure 4.39 shows the Bulk resistivity.

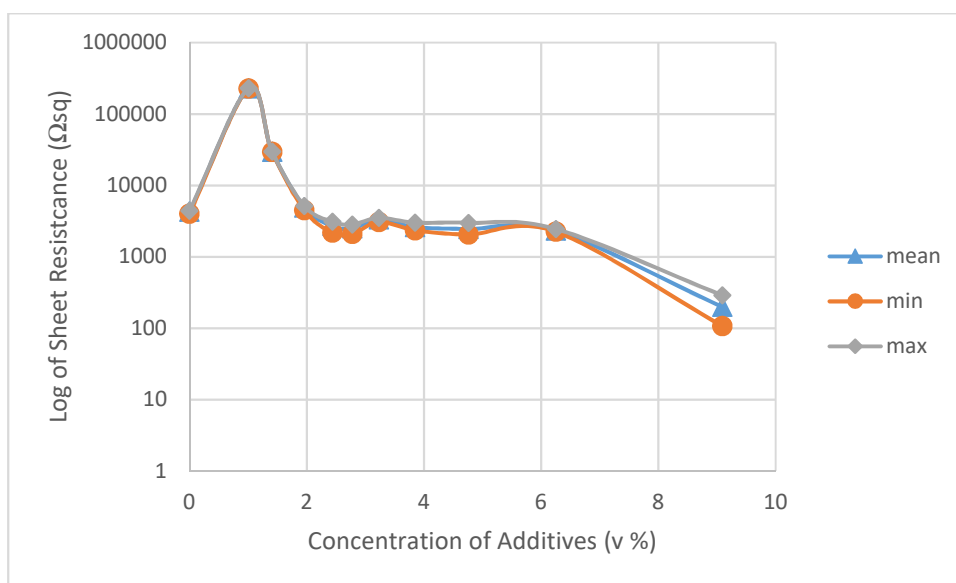


Figure 4.38: Sheet resistance of dipcoated sample showing mean, minimum and maximum results obtained using a four-point probe at 10 nA

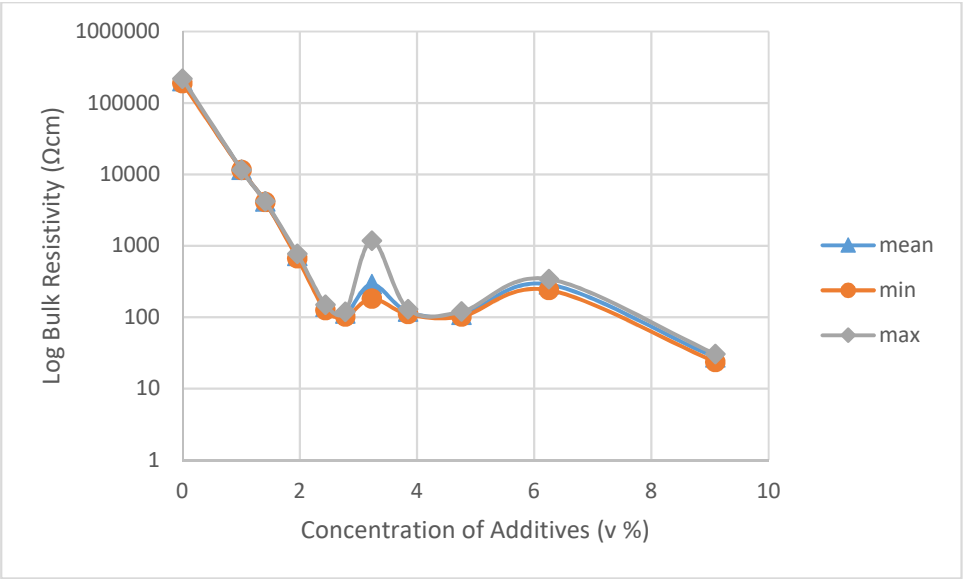


Figure 4.39: Bulk resistivity of the dipcoated samples using a four-point probe at 10nA

4.3.5.2 Four-Point-Probe – spraycoated samples

The sheet resistance and bulk resistivity of the spraycoated samples was measured in an identical way to that of the dipcoated samples. This is shown in Figures 4.40 to 4.41.

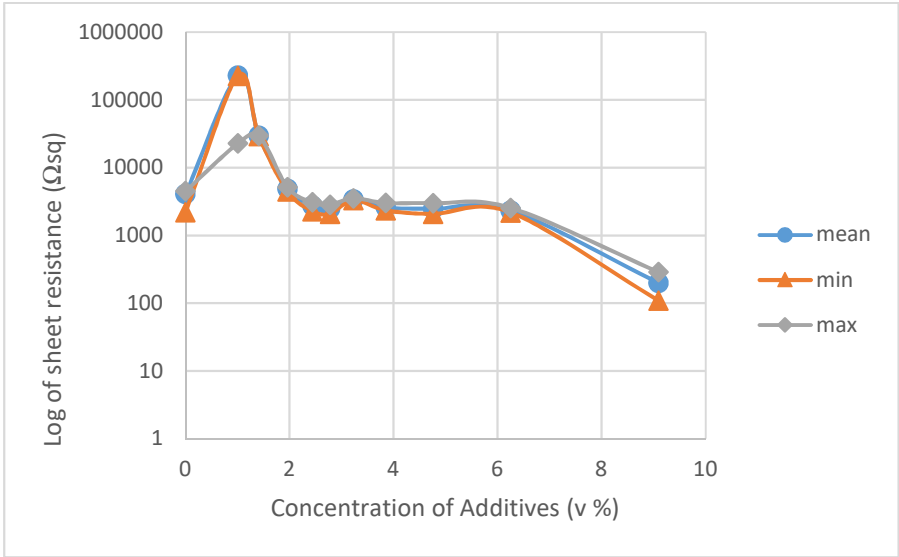


Figure 4.40: Sheet resistance of the spraycoated samples

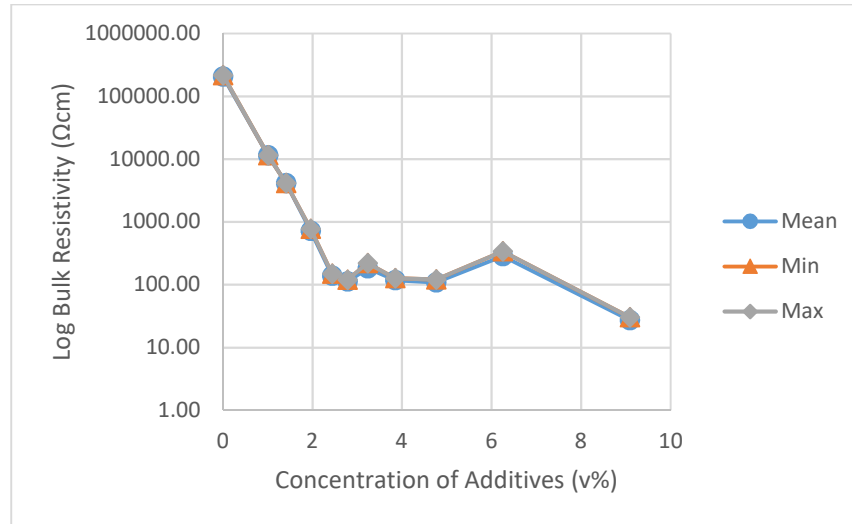


Figure 4.41: Bulk Resistivity of spraycoated samples

4.3.5.3 Four-Point-Probe – spincoated samples

By the time spincoating was conducted, only the 97 % PEDOT:PSS sample and the 99 % PEDOT:PSS and 100 % samples were manufactured using spincoating since by this time the rest of the sample set had been eliminated. Figure 4.42 shows the sheet resistance of the spincoated samples.

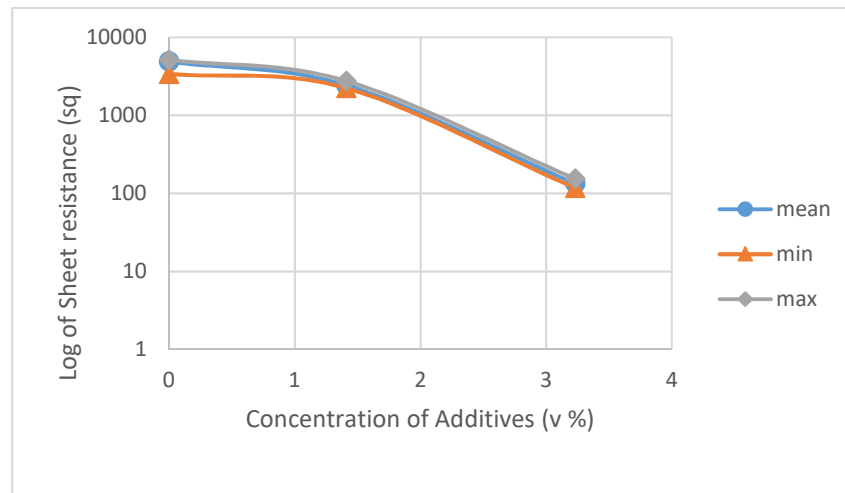


Figure 4.42: Sheet resistance of the spincoated samples

Figure 4.43 shows the spincoated bulk resistivity measurements.

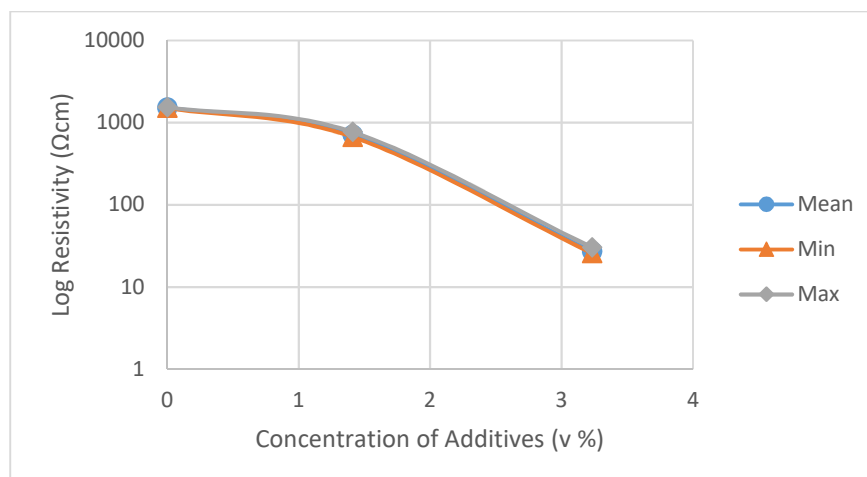


Figure 4.43: Bulk resistance of the spincoated samples

4.3.6 Film Thickness using Optical microscopy

Many authors claim sample layer thickness is important to conductivity of individual samples, so it was of importance to determine the range of thicknesses being produced by each manufacturing technique. To obtain sample thickness the samples were mounted in resin, polished and observed using an optical microscope as described in Section 3.4.6.

4.3.6.1 Spraycoated Film Thickness

Figure 4.44 shows examples of the film thickness measured of the spraycoated samples. The range of film thickness of the PEDOT:PSS for the electrically tested spraycoated samples was from 3.49 to 4.65 μm .

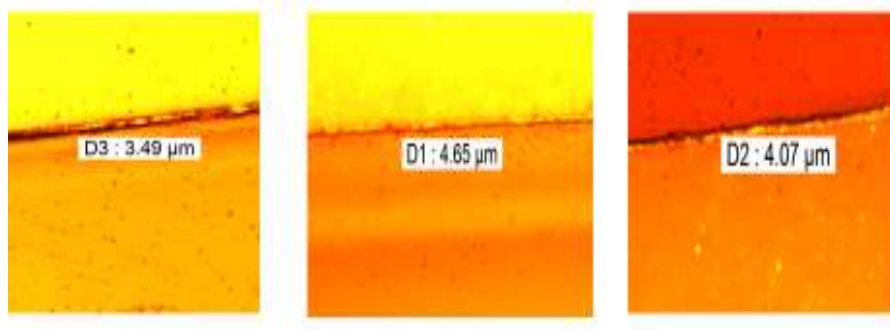


Figure 4.44: The range of film thickness for the electrically tested spraycoated samples.

4.3.6.2 Dipcoated Film Thickness

Dipcoating was trialled as described in Section 3.3.3.2. When manufacturing by dipcoating, the effects of gravity means that if the same amount of liquid is applied to the same sized PET film and left to hang for the same amount of time, once the PEDOT mixture has been annealed the film thickness varies within a repeatable amount. By taking the same portion of the PET film for testing on every sample and also measuring the film thickness on every sample variabilities can be controlled.

Due to the nature of the manufacturing method, dipcoated samples range in thickness from an average of 4 μm at one end up to an average of 18 μm at the other end. When choosing which dipcoated samples to measure for resistivity the decision was taken to exclude all samples at the extreme ends of the samples. This left the mid-section which gave a good even coverage and the thickness was in the region of 7-10 μm . In the end samples of an average of between 7.56 to 8.22 μm were very reproducible and these were chosen for further characterisation. Figure 4.45 shows examples of the film thickness measurements of the dipcoated samples.

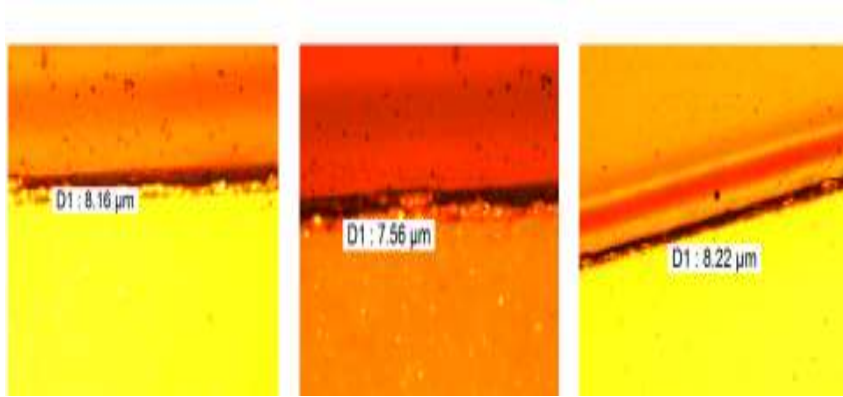


Figure 4.45: Measured film thickness of the dipcoated samples

4.3.7 Spincoating

Results from the spraycoated and dipcoated samples was in accordance with the Literature Review finding that conductivity and film thicknesss may be connected. To explore this hypothesis further spincoating was trialled as described in Section 3.3.3.3.

4.3.7.1 Spincoated Film Thickness

The spincoated samples were of reliably constant thickness at the centre of the spincoated area with splashes at the edges. The central part of the 100 % PEDOT:PSS sample had a film thickness with an average thickness of 2 μm as shown in Figure 4.46. However, the quality of the film was very irregular.



Figure 4.46: Film thickness measurement of the 100 % PEDOT:PSS spincoated sample

The 97 % and 99 % spincoated samples had an average film thickness of between 1-2 μm thick as shown in Figure 4.47.

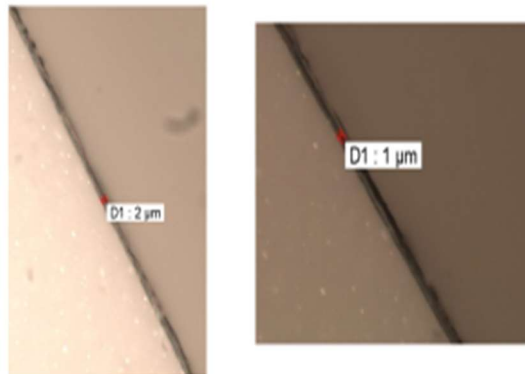


Figure 4.47: The film thicknesses measurements of 97 % and 99 % unmodified, spincoated samples

When the 97 % or 99 % sample was measured at several points the same measurement was obtained, which shows the film thickness was reasonably uniform with this manufacturing technique with sample thickness of 1-2 μm .

4.3.7.2 Resistivity of spincoated samples – Keithley 6517b

Using the Keithley 6517b meter the resistivity was measured as described in Section 3.4.5.4. This is shown in Figures 4.48 to 4.52.

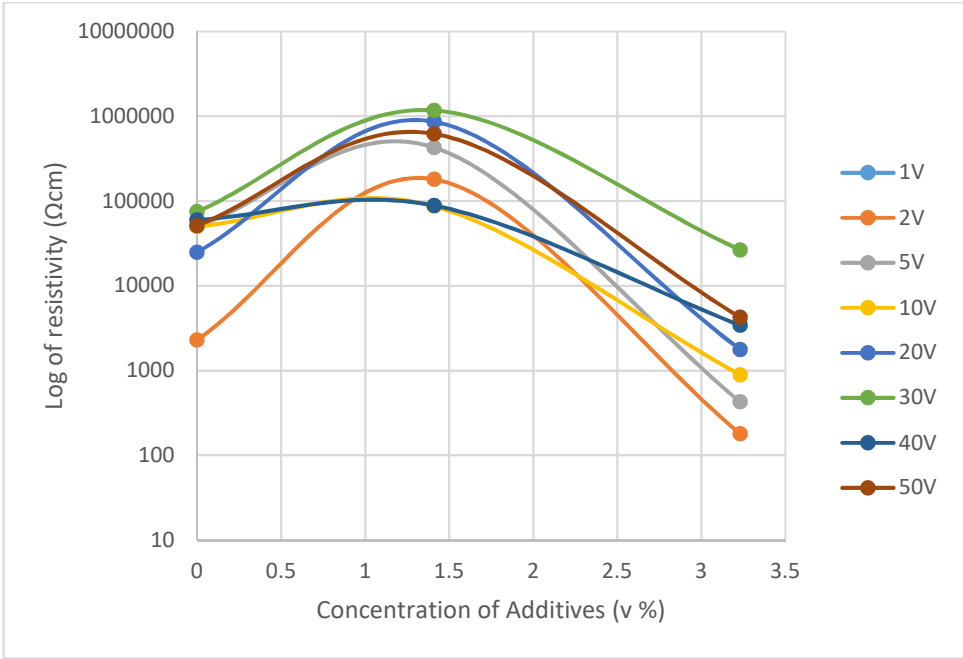


Figure 4.48: Resistivity of spincoated set 1 with no surface modification

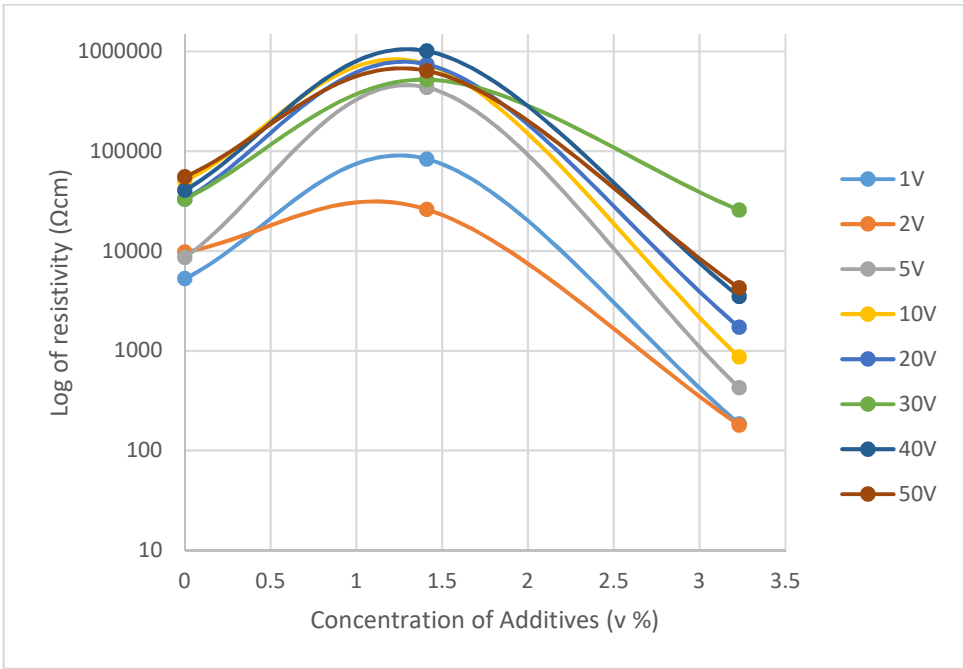


Figure 4.49: Resistivity of spincoated set 2 with no surface modification

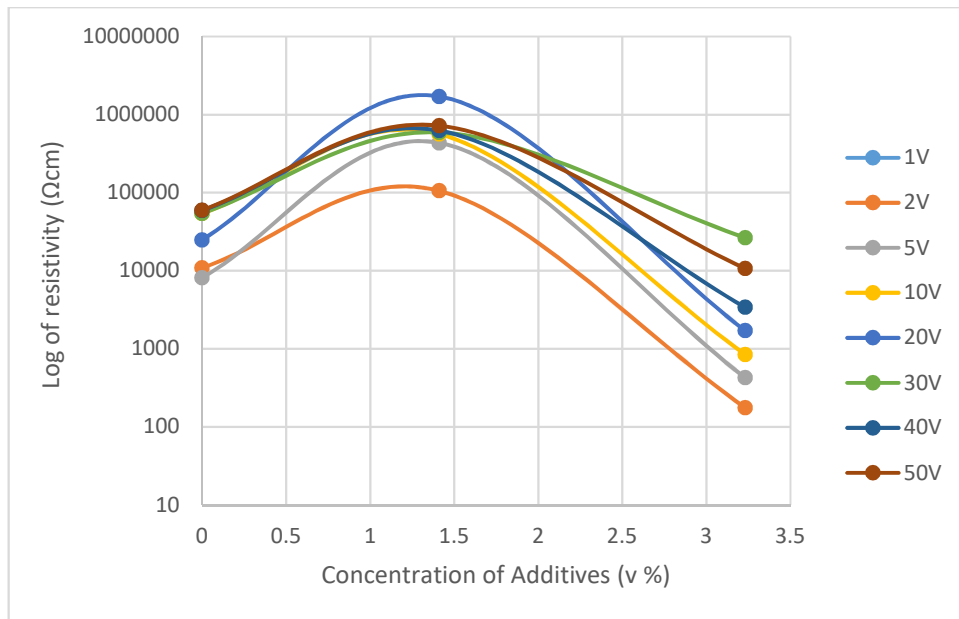


Figure 4.50: Resistivity of spincoated set 3 with no surface modification

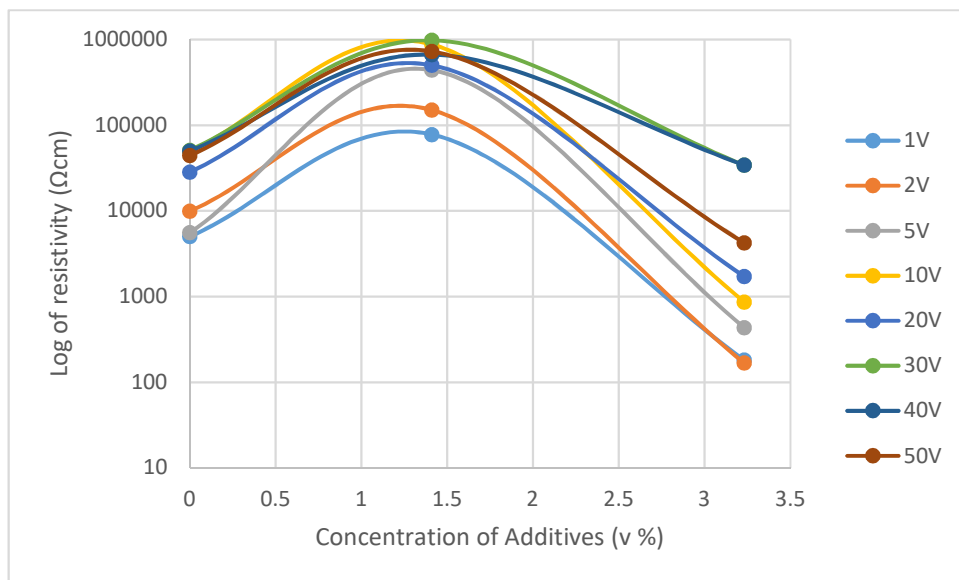


Figure 4.51: Resistivity of spincoated set 4 with no surface modification

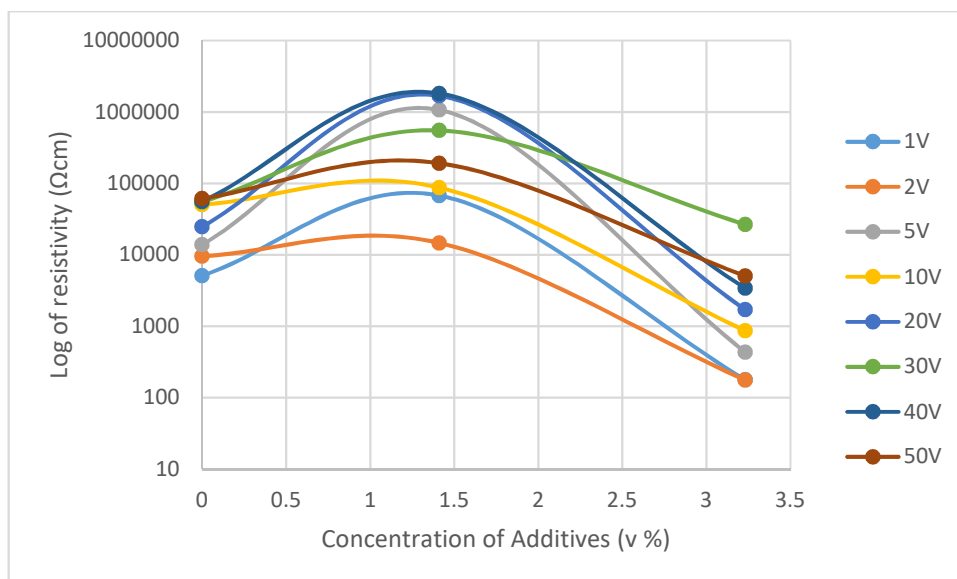


Figure 4.52: Resistivity of spincoated set 5 with no surface modification

4.4 Adhesion Studies

The reason for this work is film delamination means it would be impossible to utilize the results of this research for any industrial projects in the future. Although the film quality had been improved with addition of surfactant and MEK, the adhesion of the films to the substrate was still a major issue so attempts to rectify this were made.

Chemical and physical methods of modifying the substrate were trialed as described in Section 3.3.4.

4.4.1 Chemical modification

Chemical modification to the substrate involved spincoating of different solutions of cellulose and PVA to try to get better adhesion of the PEDOT:PSS and prevent the film from delaminating. From Table 4.6 the lowest resistivity was achieved with hydroxyethyl cellulose and methyl cellulose. However, hydroxymethyl cellulose samples delaminated. The research continued with methyl cellulose since this gave the best film quality and amongst the highest resistivity results. The substrate could

be bent 180 degrees in both directions and the polymer remained conductive. The film did not delaminate. Figure 4.53 shows the 97 % PEDOT:PSS film sample after chemical modification using methyl cellulose. There are what appears to be small holes or bubbles visible in the surface of the film

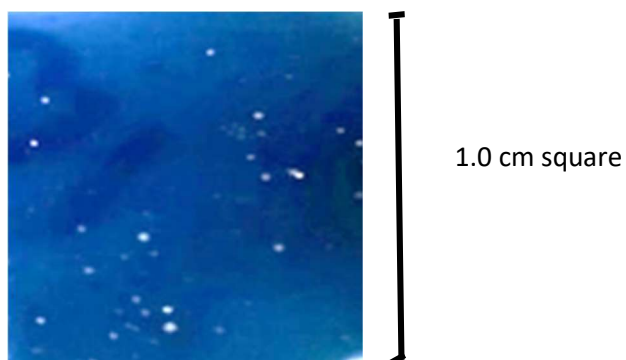


Figure 4.53: The 3 % Additives, 97 % PEDOT:PSS (1:30) ratio sample after chemical modification using methyl cellulose.

Despite this the sample has relatively low resistivity when compared with the other samples as is shown in Table 4.6

Table 4.6: Chemical modification of PET showing the Keithley resistivity results and bending of samples

Number	CAS number	Chemical	Water (g)	Modification chemical (g)	Concentration spray coated	BENDING Y/N	DELAMINATION? Y/N	Resistivity at 40V 0.5cm between probes
1	9004-57-3	Ethyl cellulose	10.029	0.0574	0.6%	Yes	NO	38 GΩ
2	9004-67-5	Methyl cellulose	10.021	0.0588	0.6%	Yes	NO	8.65 GΩ
3	9004-32-4	Carboxymethylcellulose sodium salt	10.014	0.0548	0.5%	Yes	NO	60 GΩ
5	9004-62-0	Hydroxyethyl cellulose	10.035	0.0548	0.5%	Yes	NO	6.2 GΩ
6	9002-89-5	PVA MW 89000-98000:99% hydrolysed	10.076	0.1022	1%	Yes	NO	31 GΩ

4.4.2 Four-point-probe measurements of the chemically modified substrate, spincoated sample sets

In order to compare the chemically modified samples with the original unmodified spincoated samples the sheet resistance and bulk resistivity of the samples was measured. This is shown in Figures 4.54 and 4.55.

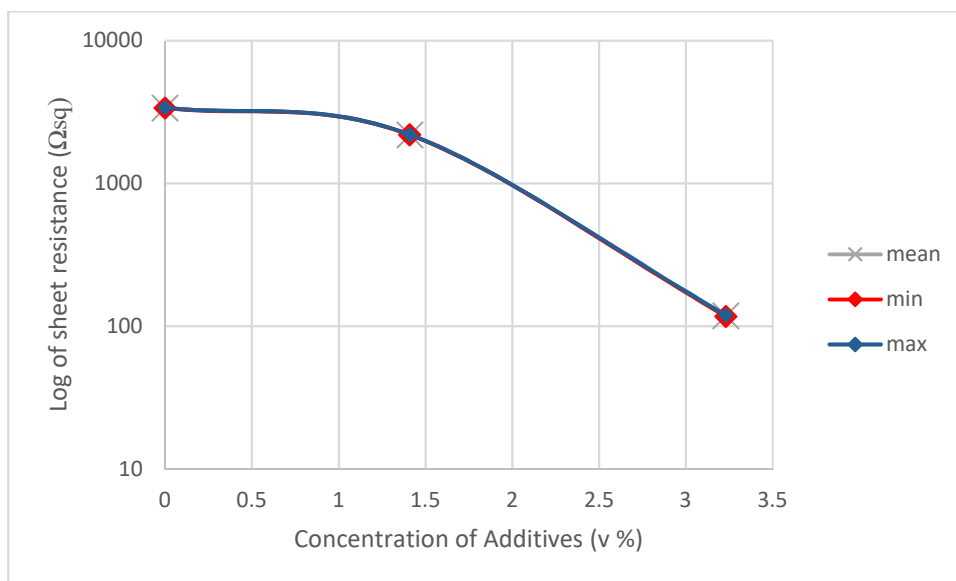


Figure 4.54: Sheet resistance of the chemically modified samples

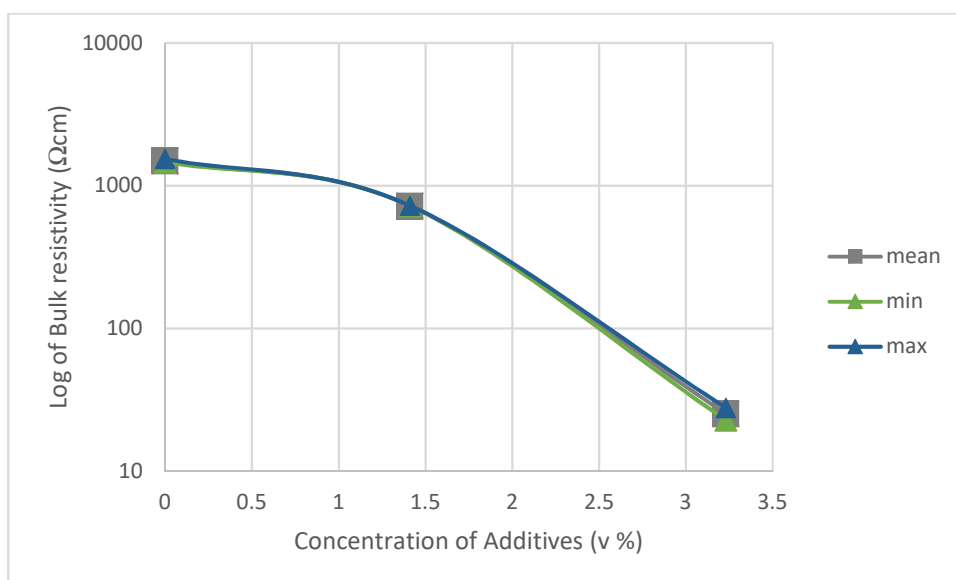


Figure 4.55: The bulk resistivity of the chemically modified sample

4.4.3 Two-point probe resistivity of the chemically modified substrate, spincoated sample sets

Electrical testing of the cellulose modified substrate showed good electrical results when tested using the Keithley 6517b which correlate reasonably well with the unmodified sample sets but the delamination problems were much reduced. Resistivity using spincoating as the method of manufacture has proven both the chemically modified sample and the unmodified film sample have similar resistivities for the 97 % PEDOT:PSS sample and 100 % PEDOT:PSS however the resistivity of the 99 % PEDOT:PSS film has increased using this method of manufacturing. This is shown in Figures 4.56 to 4.60.

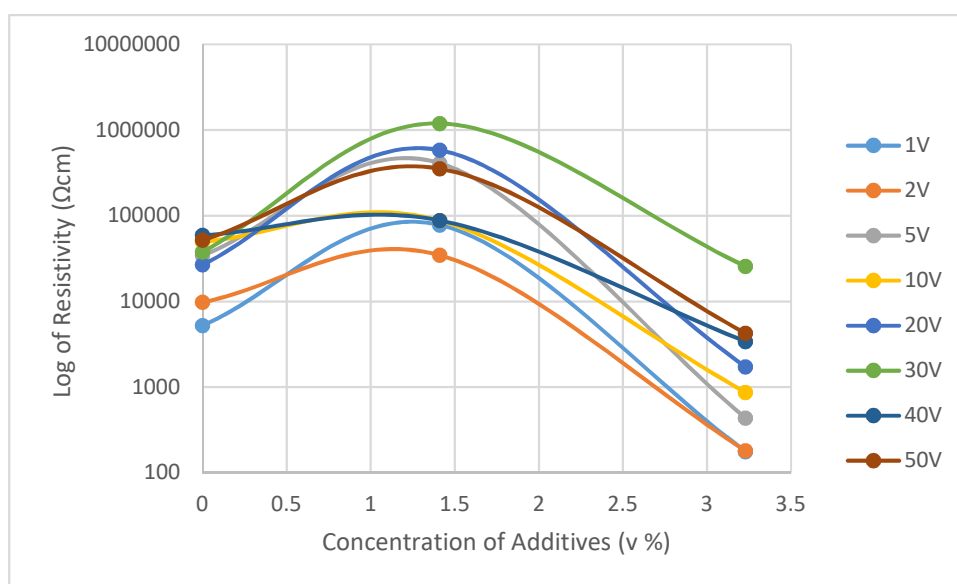


Figure 4.56: Resistivity of the chemically modified substrate samples set 1

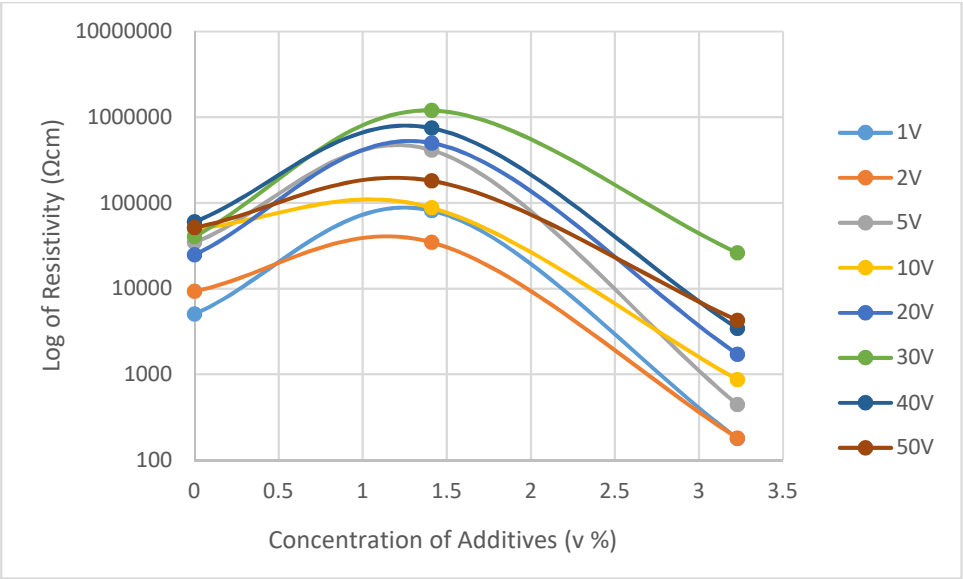


Figure 4.57: Resistivity of the chemically modified substrate sample set 2

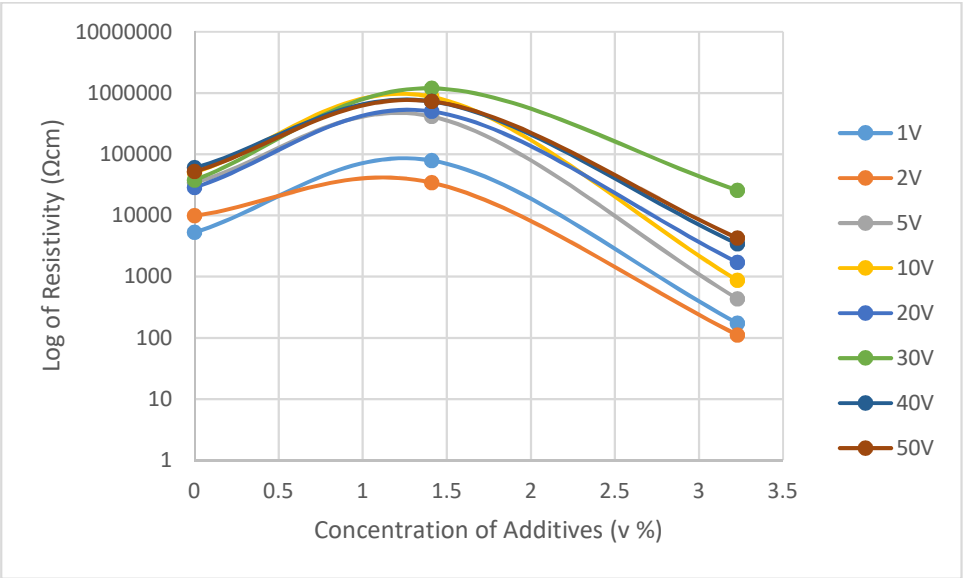


Figure 4.58: Resistivity of the chemically modified substrate sample set 3

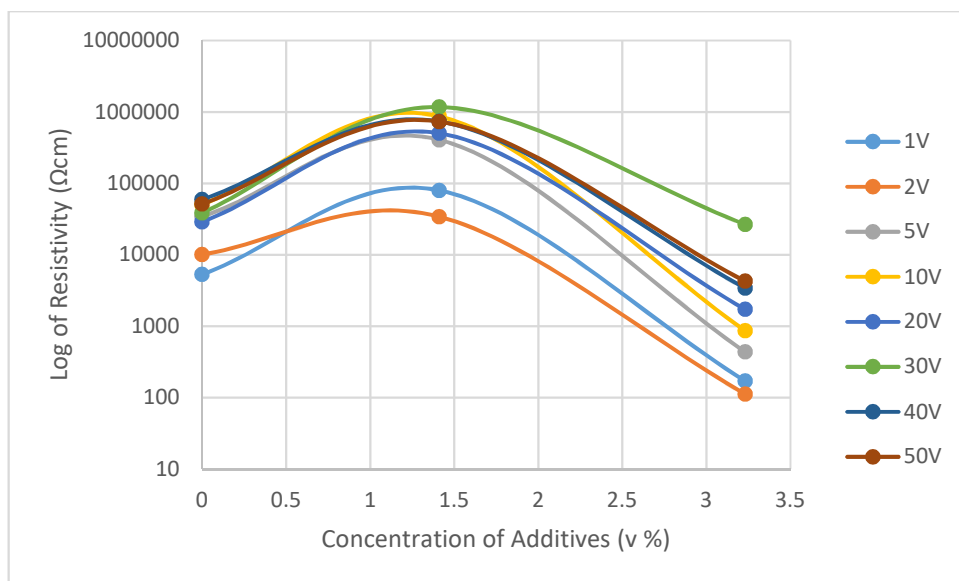


Figure 4.59: Resistivity of the chemically modified substrate sample set 4

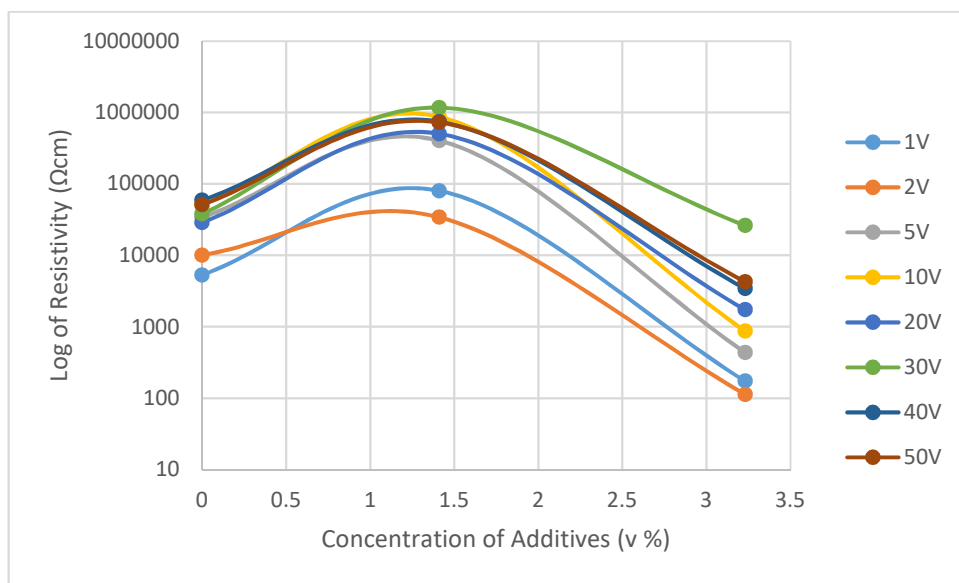


Figure 4.60: Resistivity of the chemically modified substrate sample set 5

4.4.4 Methyl cellulose studies with water

According to the literature, the PEDOT:PSS is known to be hygroscopic so it is of interest to know how the cellulose behaves when in contact with water in order to see how any roughness profiles may change. To see if there was any difference when the cellulose was in contact with water, the methyl cellulose coated samples, without a coating of PEDOT solution or PEDOT:PSS, were immersed in water for 1 minute and then measured using an Alicona profilometer. This was in an attempt to duplicate the water absorption which happens over time with absorption of water molecules from the air. All samples were measured using x 20 magnification on the profilometer. The surface of the sample before immersion in water is shown in Figure 4.61.

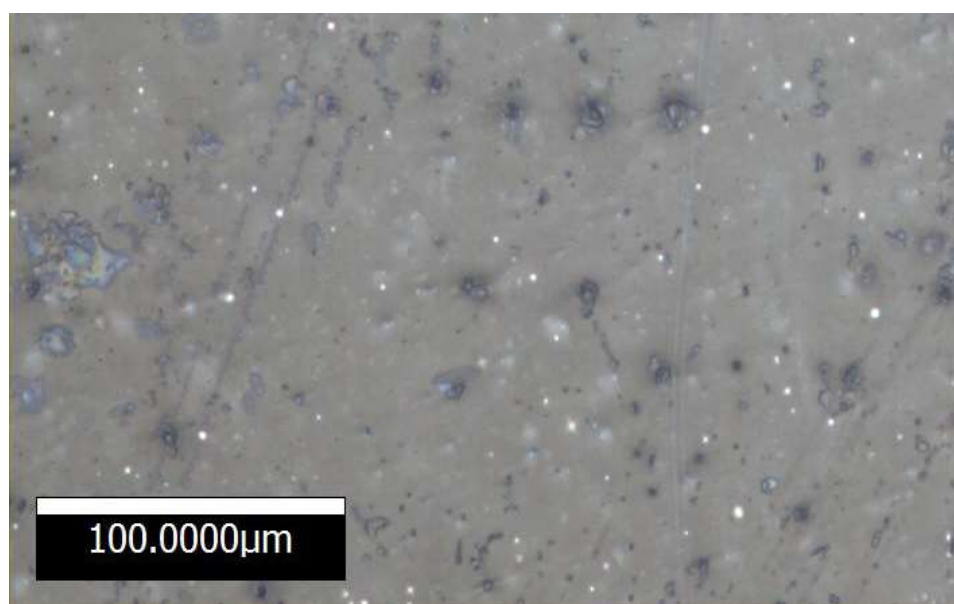


Figure 4.61: The surface of chemical modification using methyl cellulose on a PET substrate x 20 magnification – No water immersion

The un-treated sample has an intact edge as shown in Figure 4.62, before immersion the edge of the cellulose is intact.

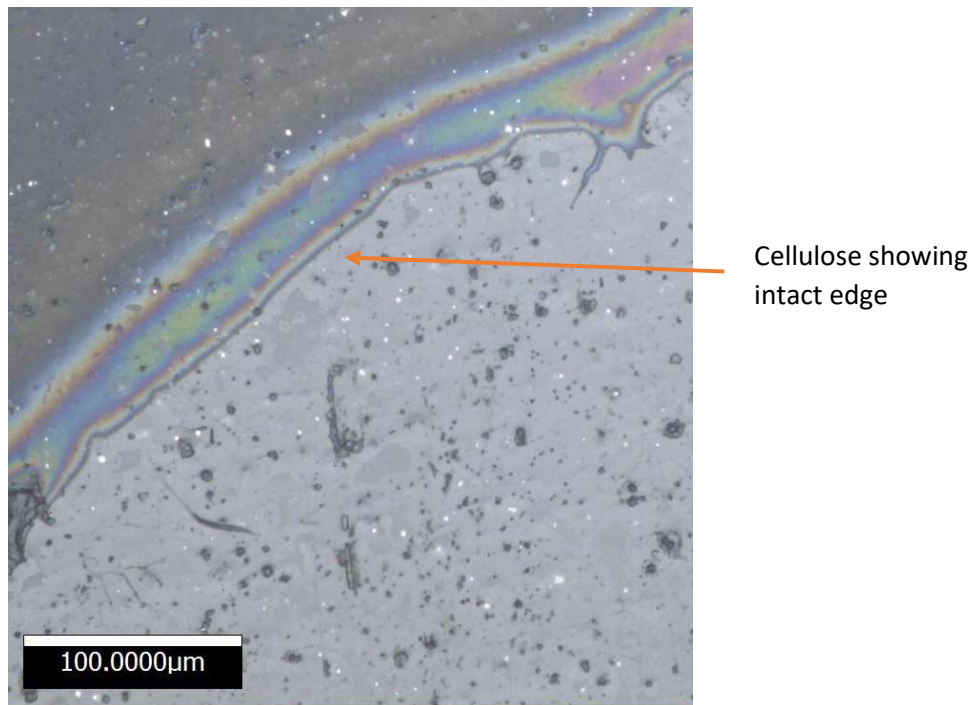


Figure 4.62: Chemical modification with methyl cellulose showing the edge where the chemical modification ends x 20- before water immersion

After the cellulose was immersed in water the edge of the cellulose is breaking where the film has swollen in water. This is shown in Figure 4.63. This means as the sample ages and the PEDOT:PSS and the cellulose gain water from the atmosphere the layers will probably swell and fracture which will impinge on the conductivity of the sample. Of course it must be remembered that the experiment allowed a fast intake of water into the cellulose rather than the slower humidity up-take that would occur over time with absorbing water from the air. For these images the Alicona was used just as a microscope to capture the images. It was also used to measure surface roughness as detailed in Sections 4.4.6 and 4.4.7.

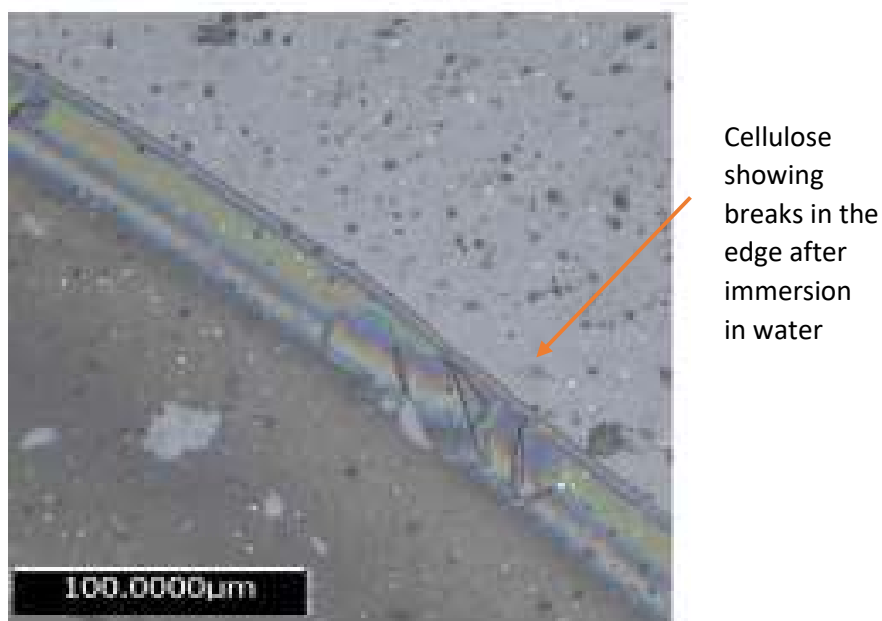


Figure 4.63: The edge of the cellulose after immersion in water on PET substrate x 20 magnification

4.4.5 Mechanical Abrasion

Abrasion was used as the physical surface modification in order to see if this would improve adhesion of the PEDOT:PSS films. Mechanical abrasion was applied using the Taber abrader as described in Chapter 3. PET was abraded using the Taber abrader for 0 to 1000 cycles. All the samples were spincoated with PEDOT:PSS/TWEEN 80/MEK solutions and annealed. They were then then assessed for delamination. The samples with 100-400 cycles showed the least delamination with the 0-100 and the 600-1000 cycles all showing delamination. To make a comparison the unabraded substrate was also coated with the same solution.

4.4.6 Roughness studies of non-abraded samples

All the non-abraded samples regardless of the manufacturing technique including the spincoated samples with a methyl cellulose modification had a roughness of 23.64 μm . Methyl cellulose then did not alter roughness of the samples.

4.4.7 Roughness of the PET

The samples that were taken forwards after mechanical abrading were those which underwent 100-400 cycles of abrasion with the best samples with respect to final film quality being the 100 and 200 abrasion cycles. The other samples were excluded since they all either showed defects in the film once it was annealed or suffered from delamination of the film from the substrate. In order to understand more about the abraded samples some roughness studies were performed using the Alicona profilometer. Figure 4.64 shows the 400 cycles spincoated 97 % PEDOT:PSS film sample with visible scarring from the abrasion.

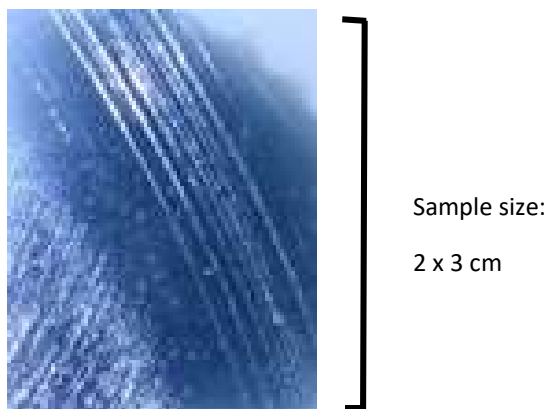


Figure 4.64: The 400 cycles spincoated 97 % PEDOT:PSS film sample showing visible scarring from the abrasion

The polymer delaminates from this surface. Where the ring of abrasion occurs the film does not delaminate whereas on the other parts of the PET the sample delaminates. Table 4.7 shows the roughness results from the profilometer measurements conducted.

Table 4.7: Results of mechanical abrasion with uncoated sample

SPEED (RPM)	NUMBER OF CYCLES	ROUGHNESS Rz (μm)	BENDING	DELAMINATION
0	0	10.3	N/A	N/A
72	10	1.1	Yes	Yes
72	20	1.1	Yes	Some scratches easily
72	50	1.2	Yes	Some scratches easily
72	100	1.1	Yes	NO
72	200	1.3	Yes	NO
72	400	1.3	Yes	NO
72	600	1.5	Yes	Some
72	800	1.0	Yes	Yes
72	1000	1.1	Yes	Yes

4.5 Electrical resistivity measurements adhesion modified samples

Electrical resistivity measurements were performed on spincoated samples which had the modified substrates to compare them with pristine substrate samples

4.5.1 Four-point-probe measurements of abraded spincoated samples

In order to compare the abrasion treatment with the rest of the samples the abraded samples were tested for sheet resistance and bulk resistivity. These are shown in Figures 4.65 and 4.66.

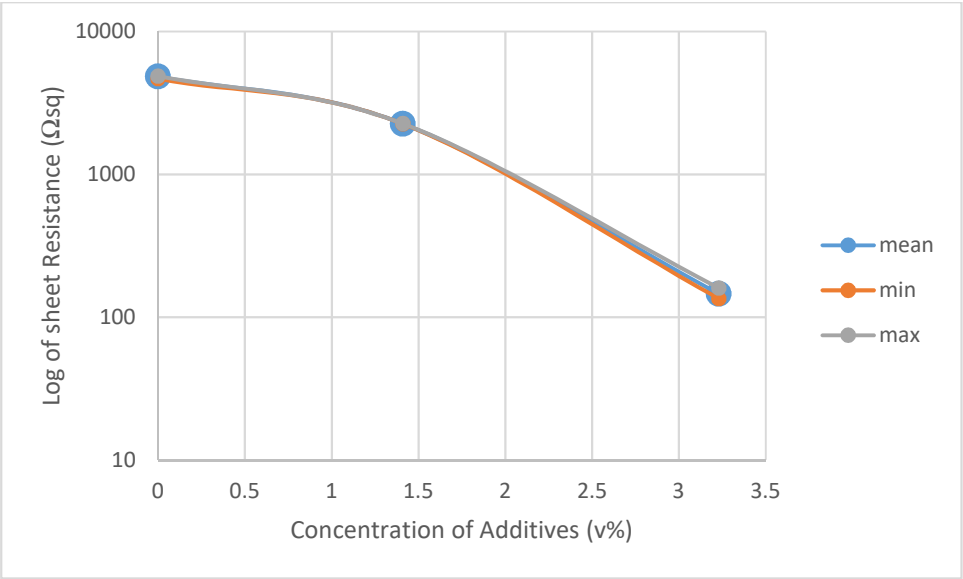


Figure 4.65: Sheet resistance of the Mechanically abraded samples

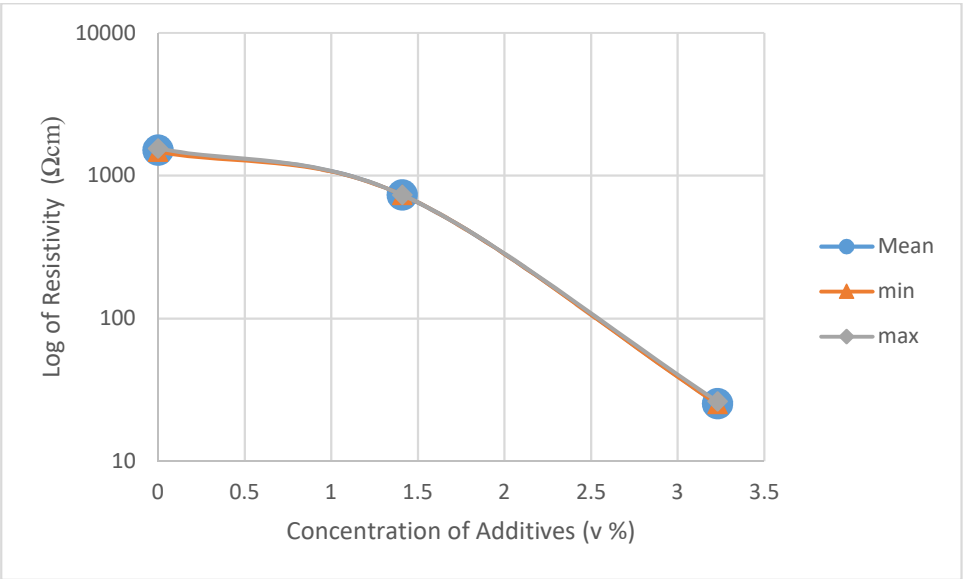


Figure 4.66: Bulk resistivity of the mechanically abraded samples

4.5.2 Two-point probe measurements of abraded spincoated samples

Abraded samples show a similar results pattern to the unabraded samples as showing in Figures 4.67 to 4.71.

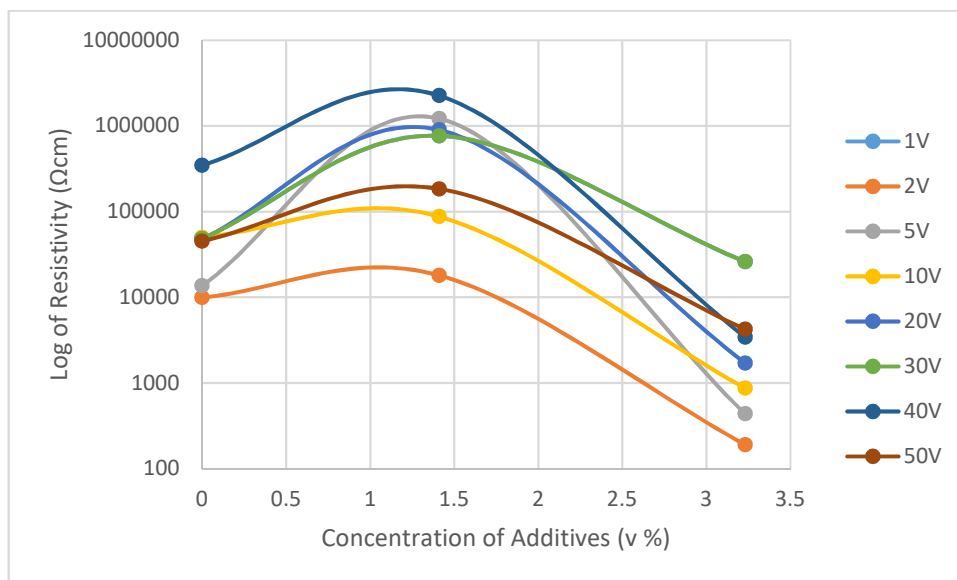


Figure 4.67: Abraded samples set 1 Keithley results

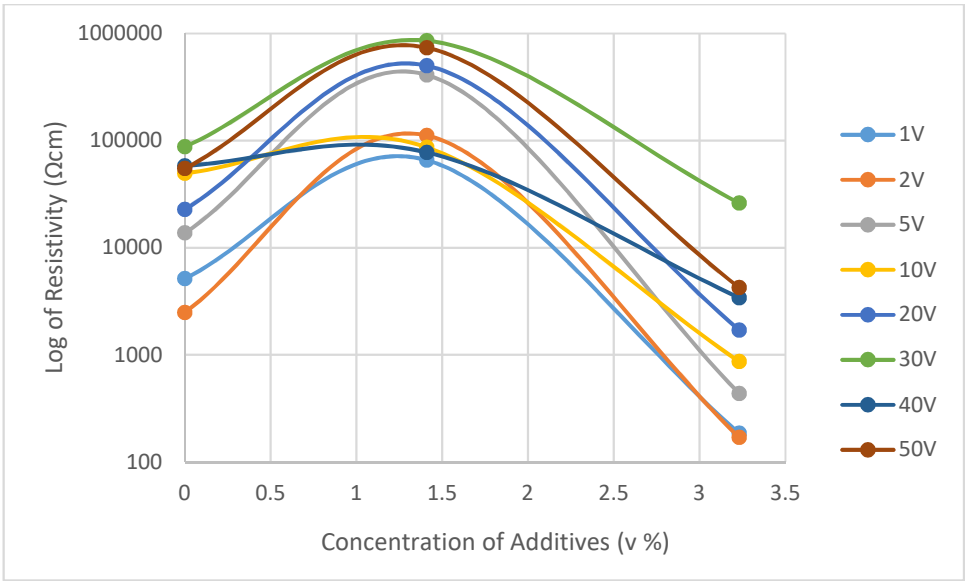


Figure 4.68: Abraded samples set 2 Keithley results

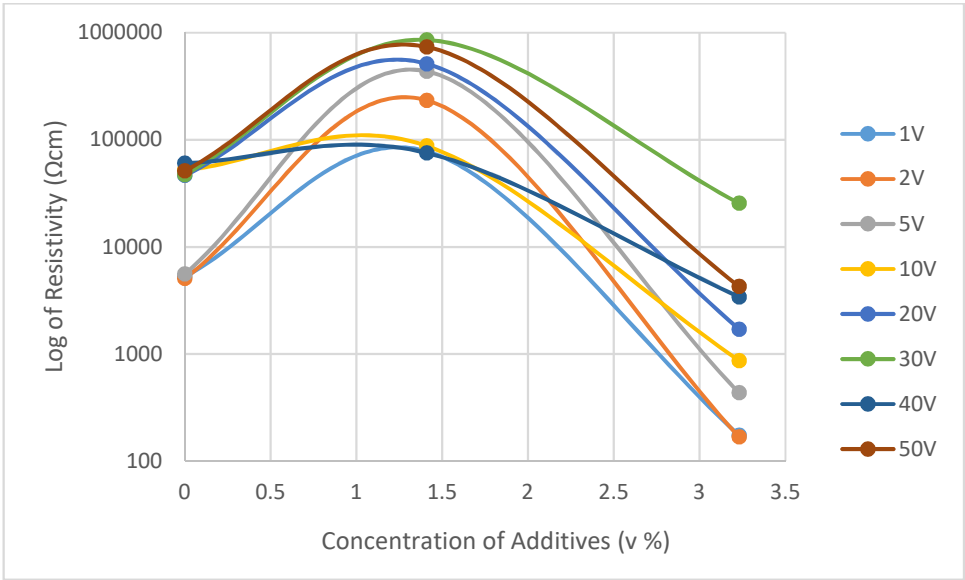


Figure 4.69: Abraded samples set 3 Keithley results

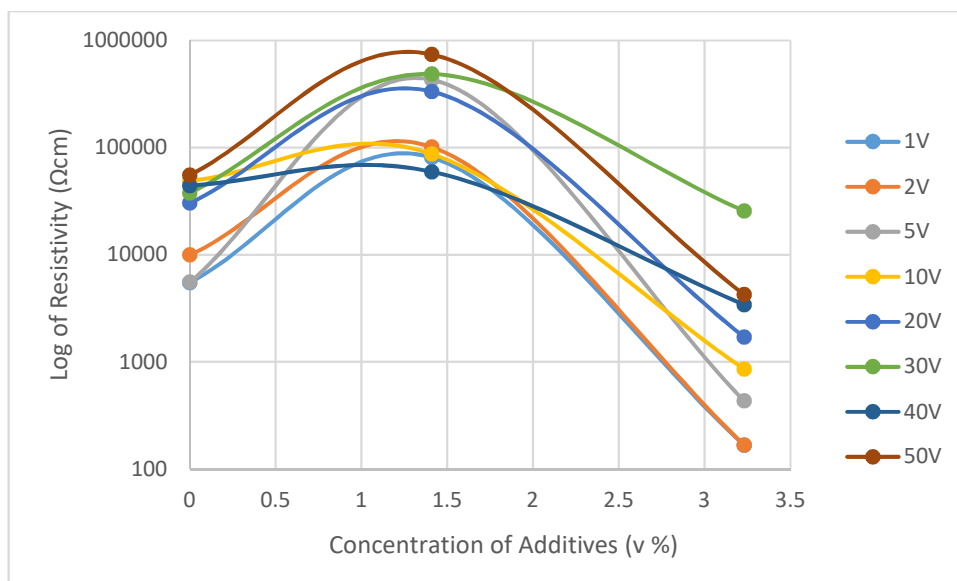


Figure 4.70: Abraded samples set 4 Keithley results

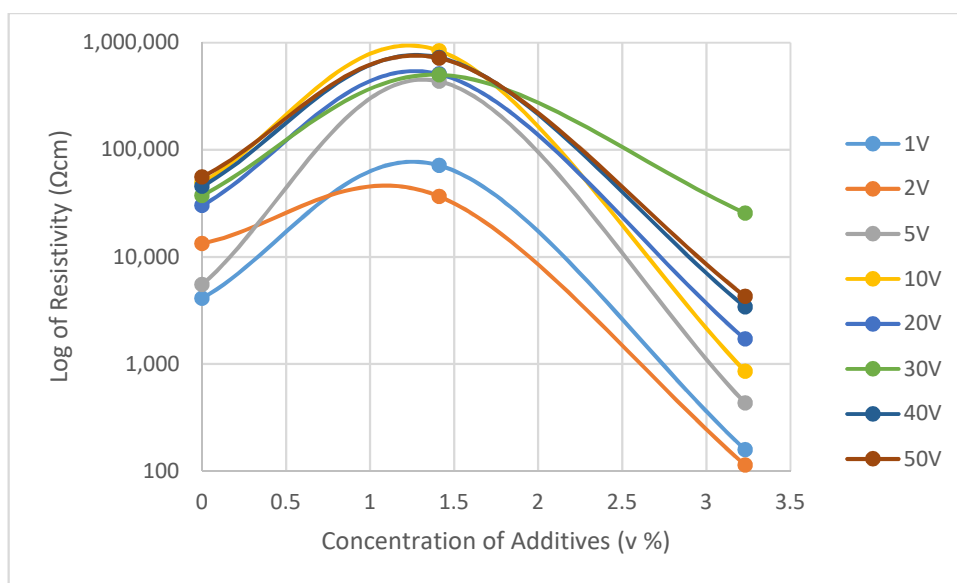


Figure 4.71: Abraded samples set 5 Keithley results

4.5.3 Film thickness of the abraded samples

The mechanically abraded samples were measured for film thickness, roughness and quality using the profilometer. An average of five measurements for each sample were taken which are shown in Table 4.8. The abraded samples were found to have

slightly thicker films than chemically modified samples. However, the surface of the PET was abraded away so this means the surface would have been lower than the surrounding area. The film coated the surface since the abraded area acted as a well to contain the PEDOT. The abraded samples did solve the adhesion problems and show similar resistivity to the chemically modified samples. No further investigation of abrasion was undertaken.

Table 4.8: Spincoated samples with mechanical Abrasion modification to the substrate. Note there are no results for some samples due to total delamination

Modification description (cycles)	Film Composition (%)	Film composition Ratio	Average thickness (μm)
100	3 % Additives: 97 % PEDOT:PSS	1:30	52
100	1 % Additives: 99 % PEDOT:PSS	1:70	49
100	100 % PEDOT:PSS	100 %	49
200	1 % Additives: 99 % PEDOT:PSS	1:70	12
200	100 % PEDOT:PSS	100 %	15
200	3 % Additives: 97 % PEDOT:PSS	1:30	11
400	100% PEDOT:PSS	100 %	34
400	1 % Additives: 99 % PEDOT:PSS	1:70	29
400	3 % Additives: 97 % PEDOT:PSS	1:30	31
600	3 % Additives: 97 % PEDOT:PSS	1:30	33
600	100 % PEDOT:PSS	100 %	32
600	1 % Additives: 99 % PEDOT:PSS	1:70	29
800	1 % Additives: 99 % PEDOT:PSS	1:70	20
800	3 % Additives: 97 % PEDOT:PSS	1:30	19
800	3 % Additives: 97 % PEDOT:PSS	1:30	18
600	100 % PEDOT:PSS	100 %	23
1000	1 % Additives: 99 % PEDOT:PSS	1:70	41
1000	100 % PEDOT:PSS	100 %	41

4.5.4 Film thickness of the chemically modified samples

The chemically modified samples were spincoated. All film thicknesses were measured and recorded for each type of chemical modification performed. The different types of cellulose used made a difference to film thickness. The samples which had been spincoated with the chemical modifier methyl cellulose all had an average film thickness of 2-3 μm regardless of the concentration of PEDOT:PSS. The sample with methyl cellulose modification was immersed in epoxy resin as described in Section 3.4.6 so that the film thickness could be measured using optical microscopy. The sample in Figure 4.72 is the 100 % PEDOT:PSS on a methyl cellulose modified PET substrate.

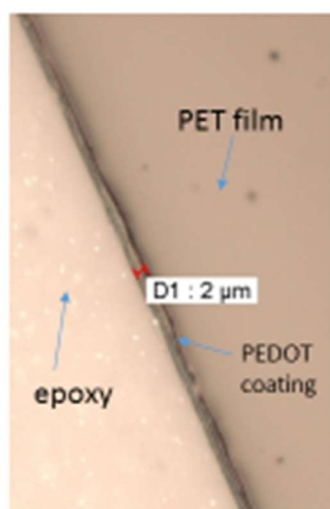


Figure 4.72: The mounted 100 % PEDOT:PSS spincoated film was immersed in epoxy and the film was measured using optical microscopy

Ethyl cellulose gave delaminated films probably due to the water content in the PEDOT:PSS. This is because ethyl cellulose is hydrophobic, so is better solvated in an organic solvent rather than in water. The film thicknesses were quite a bit thicker than the methyl cellulose films with an average of between 6-7 μm whereas the methyl cellulose had an average film thickness of 1-2 μm . This is probably due to the films

detaching from the substrate since all samples made using ethyl cellulose delaminated. This could be because when mounted air pockets formed which would have been filled with the epoxy mounting material and so make the film measurements appear to be thicker. A similar problem occurred with samples modified with hydroxyethyl cellulose which also delaminated, so measurements for film thickness were again difficult to achieve with accuracy and precision. However these samples had lower resistivity than the methyl cellulose samples as shown in Table 4.9. This may be a modifier worth considering for further investigation at a future date but this was beyond the scope of this PhD. Film thickness of hydroxyethyl cellulose measured between 2 μm and 3 μm regardless of the PEDOT concentration. The spincoated samples shown in Figure 4.73 show the gradual improvement achieved as different surface modifications were trialled. From top to bottom: CMC (a), PVA (b) and methyl cellulose substrate modifier (c)

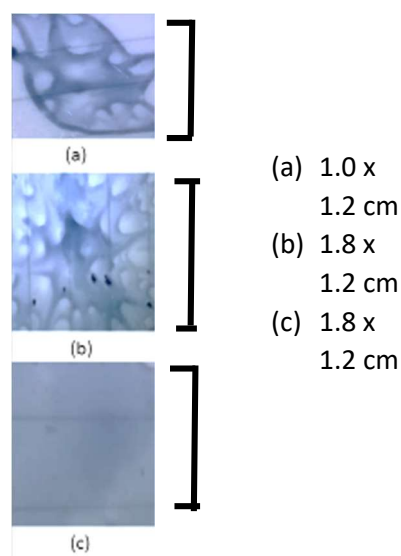


Figure 4.73: Spincoated 97 % PEDOT:PSS film samples on cellulose showing how the method was improved to give good films. CMC (a), PVA (b) and methyl cellulose substrate modifier (c)

A homogeneous coverage was now obtained using the 97 % PEDOT:PSS sample along with the methyl cellulose surface modifier. Even the 100 % PEDOT:PSS

solution wetted far more evenly than the non-chemically treated substrate. Also no delamination occurred so there was far better adhesion to the substrate than without modification, and electrical conductivity was maintained in all samples. The 99 % PEDOT:PSS sample with ethyl cellulose, measured using the profilometer had a film thickness of 6 μm . These films delaminated. The 99 % PEDOT:PSS sample had a varying film thickness of between 5-7 μm over all samples made. Figure 4.74 shows the 97 % PEDOT:PSS spincoated, methyl cellulose modified sample using the profilometer and a x 20 magnification and shows the film surface is quite uneven.

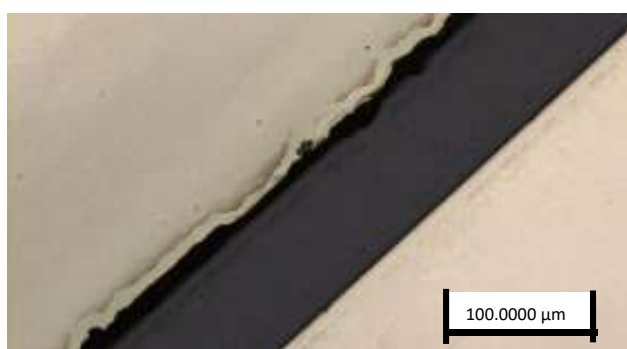


Figure 4.74: Alicona measurement (x 20) of the 97 % PEDOT:PSS film sample

Methyl cellulose was the most promising modifier for the substrate surface. This was closely followed by PVA and CMC but these both gave thicker films and higher resistivity. Hydroxyethyl cellulose gave the lowest resistivity but the films delaminated. Little difference was found in film thickness or film quality between the other analogues of cellulose used to modify the surface. In the end methyl cellulose was chosen because it gave the best 97 % PEDOT:PSS results with lowest resistivity of the films that had the best adhesion. The methyl cellulose samples also had much thinner films and it did not delaminate.

Table 4.9 lists the samples measured with the film thicknesses achieved.

Table 4.9: Average thickness of 5 samples using spincoated samples with chemical modification

Modification description	Film composition (%)	Film composition Ratio	Average Thickness (μm) (X 20)	Film quality
Ethyl cellulose	3 % Additives: 97 % PEDOT:PSS	1:30	5-6	delaminates
Ethyl cellulose	1 % Additives: 99 % PEDOT:PSS	1:70	5-7	delaminates
Ethyl cellulose	100 % PEDOT:PSS	100 %	4-11	delaminates
Methyl cellulose	100 % PEDOT:PSS	100 %	2-3	homogeneous
Methyl cellulose	1 % Additives: 99 % PEDOT:PSS	1:70	2-3	homogeneous
Methyl cellulose	3 % Additives: 97 % PEDOT:PSS	1:30	2-3	good
Hydroxyethyl cellulose	100 % PEDOT:PSS	100 %	2-3	delaminates
Hydroxyethyl cellulose	1 % Additives: 99 % PEDOT:PSS	1:70	2-3	delaminates
Hydroxyethyl cellulose	3 % Additives: 97 % PEDOT:PSS	1:30	2-3	delaminates
PVA	100 % PEDOT:PSS	100 %	3-7	reasonable film
PVA	1 % Additives: 99 % PEDOT:PSS	1:70	2-7	reasonable film
PVA	3 % Additives: 97 % PEDOT:PSS	1:30	2-7	good
CMC	3 % Additives: 97 % PEDOT:PSS	1:30	5-11	good
CMC	1 % Additives: 99 % PEDOT:PSS	1:70	5-11	reasonable film
CMC	100 % PEDOT:PSS	100 %	5-11	reasonable film

4.6 Spectroscopy

The Literature review had identified that spectroscopy may be used to determine the conformational changes of the PEDOT molecules and to track any charge carriers which may be present.

4.6.1 Ultra Violet (UV) Spectroscopy

Ultra violet spectra were recorded of each solution between 200 and 800 nm as described in Section 3.4.9.1. Results are shown in Figures 4.75 to 4.78. These spectra show results in terms of the concentration of PEDOT:PSS present in each sample.

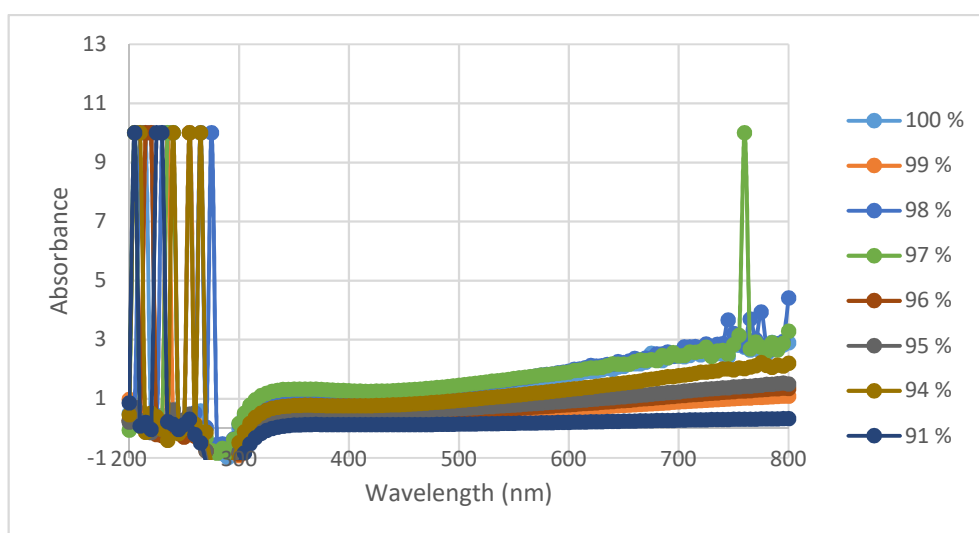


Figure 4.75: UV spectra of all ratios of PEDOT:PSS/TWEEN 80/MEK and 100 % PEDOT:PSS

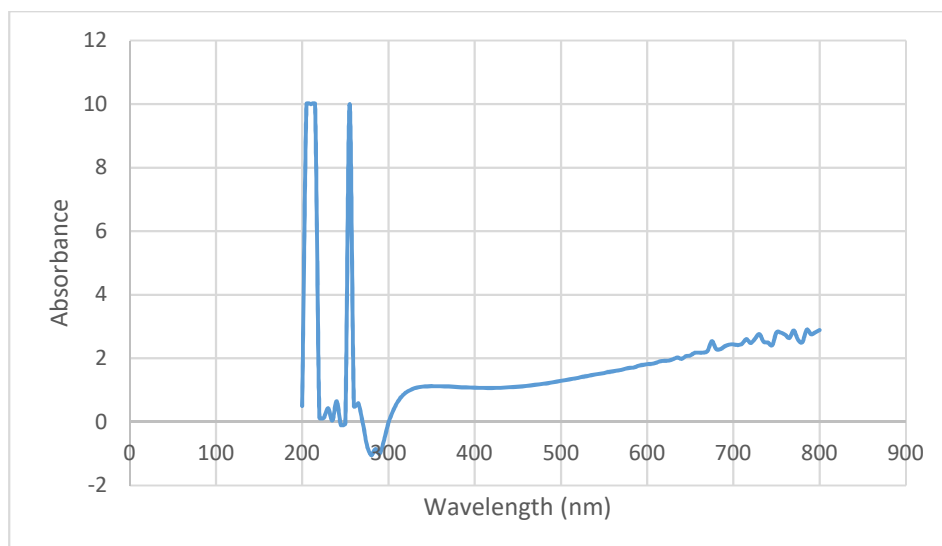


Figure 4.76: UV spectrum of 100 % PEDOT:PSS

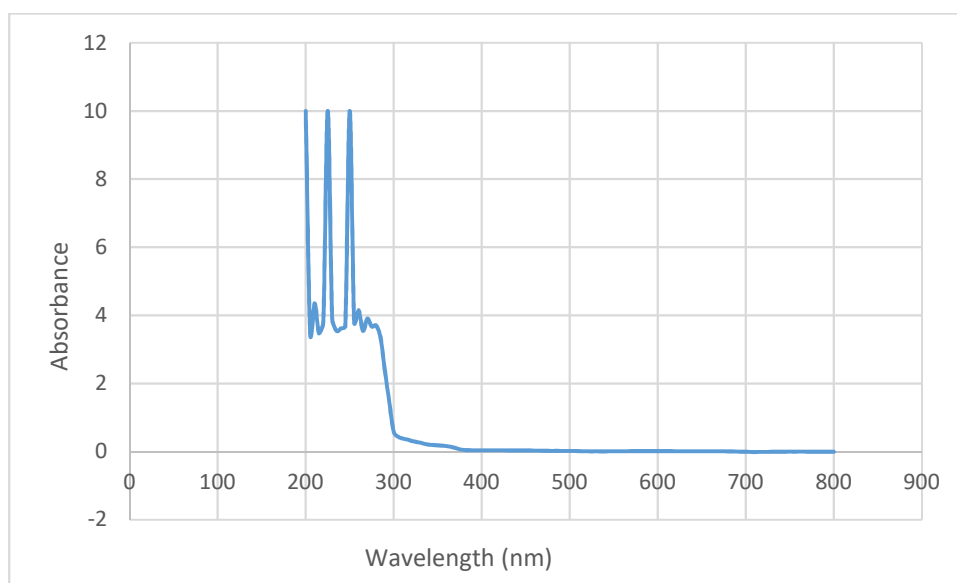


Figure 4.77: UV spectrum of TWEEN 80 + MEK solution

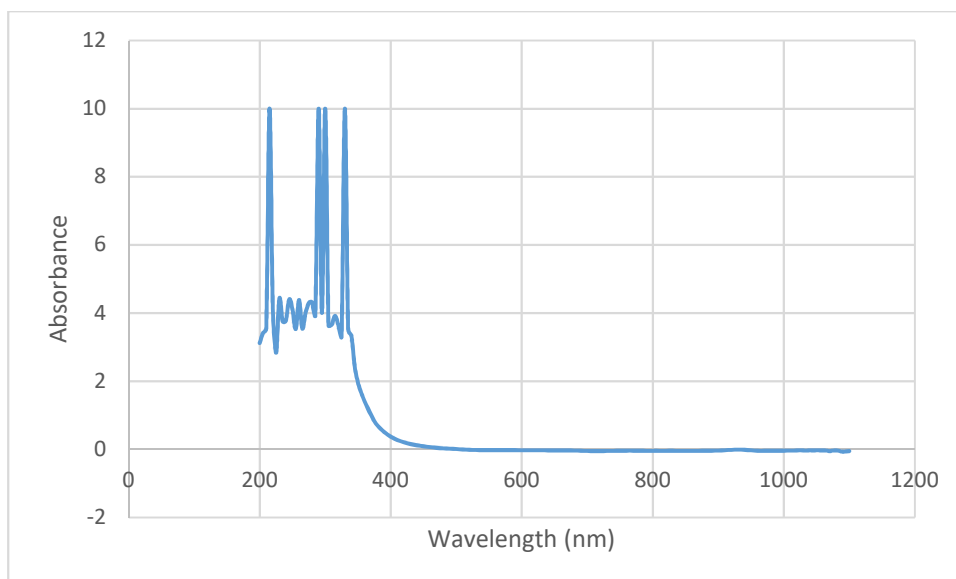


Figure 4.78: UV of 100 % TWEEN 80

4.6.2 Infra red (IR)

IR was found to be of use when analysing PEDOT in order to show whether the polymer is in a conductive or oxidised state. This is done by studying the signature of the functional groups. Procedures are explained in Section 3.4.9.2. The solid samples were initially made using the PET substrate but the spectrum was indistinguishable, which was believed to be due to the PET interfering with the test. The samples were then made with glass slides as the substrate, and were analysed by scraping the film off the surface and using Attenuated Total Reflectance (ATR) but this was also unsuccessful in obtaining spectra. In the end Potassium Bromide (KBr) discs were made of each sample. Table 4.10 lists the composition of the sample with an identification which is used for the graphs.

Table 4.10: Table of identification names for samples

Sample composition	Number used on IR graphs
6 % Additives: 94 % PEDOT:PSS (1:15)	15
5 % Additives: 95 % PEDOT:PSS (1:20)	20
4 % Additives: 96 % PEDOT:PSS (1:25)	25
3 % Additives: 97 % PEDOT:PSS (1:30)	30
3 % Additives: 97 % PEDOT:PSS (1:35)	35
2 % Additives: 98 % PEDOT:PSS (1:40)	40
2 % Additives: 98 % PEDOT:PSS (1:50)	50
1 % Additives: 99 % PEDOT:PSS (1:70)	70
100 % PEDOT:PSS	100

It must be remembered that despite the composition in Table 4.10 showing 3 % additives for both the 30 and 35 samples the actual concentration of these two samples is not identical. Further information on the exact composition of all the samples can be found in Section 3.2.5. Figure 4.79 shows the IR spectrum of 100 % annealed PEDOT:PSS.

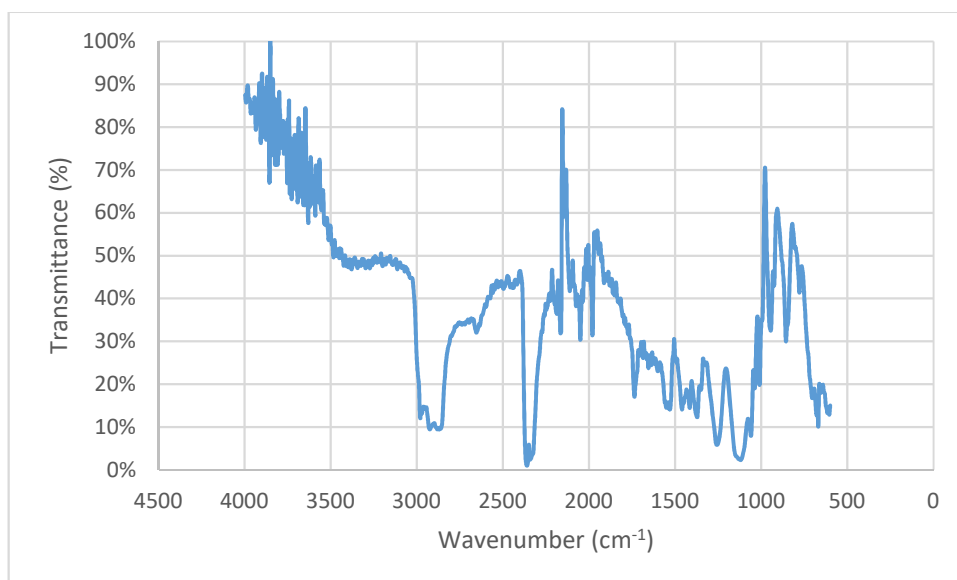


Figure 4.79: 100 % PEDOT:PSS solid annealed film as a KBr Disc showing full scanning range

Figure 4.80 shows the films made using the PEDOT:PSS/TWEEN 80/MEK mixtures. A few of the samples exactly overlay onto a different sample so only those that show are included.

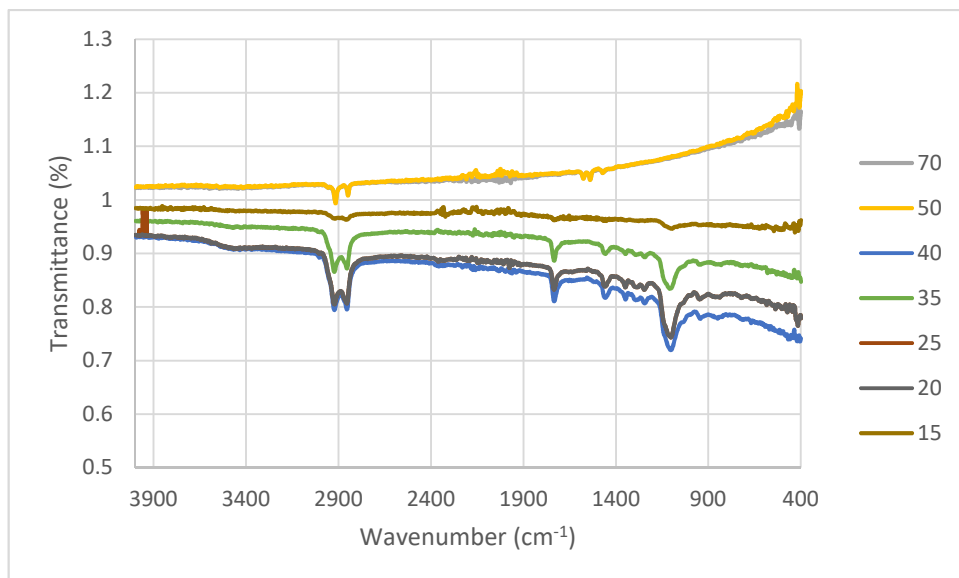


Figure 4.80: IR of the annealed films from 4000 to 500 cm^{-1}

An IR of PET was also collected as shown in Figure 4.81.

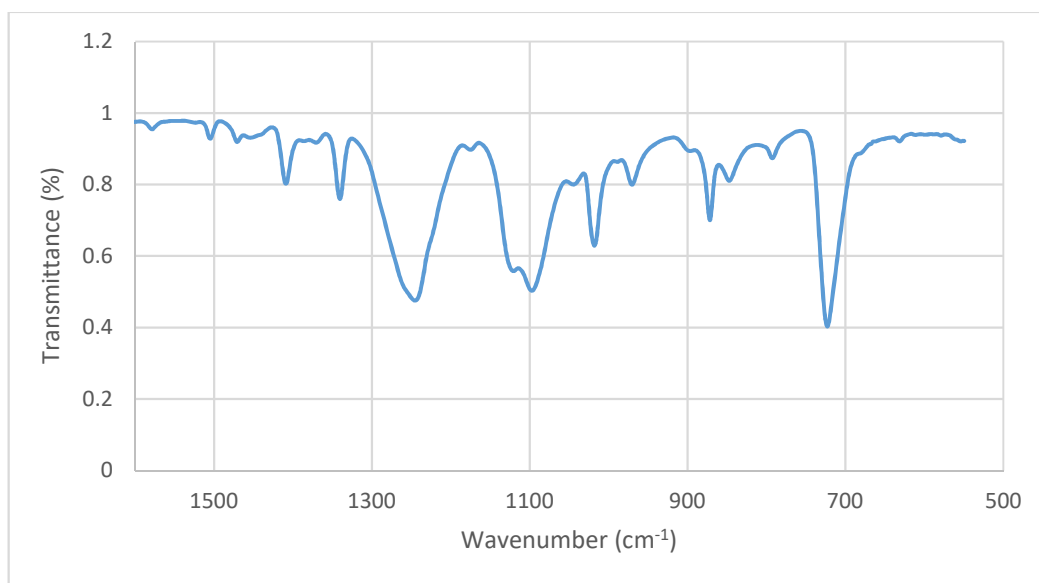


Figure 4.81: IR of the PET film used as substrate

An attempt was made to try and track the charge carriers and conformational changes by using a piece of PET with a hole cut into it and to apply a potential difference across the samples. Assuming the charge carriers caused changes to the functional groups then IR should be able to detect this. This method produced no results. Possibly this was due to the fact the PET stopped the sample from contacting the NIR. The PET was included in the experiment in order to shield the NIR instrument from the applied potential difference. However, it also stopped the sample from registering at all with the NIR instrument. As can be seen from Figures 4.81 and 4.82 there is very little difference found in the PET spectrum making it impossible to reliably track any changes.

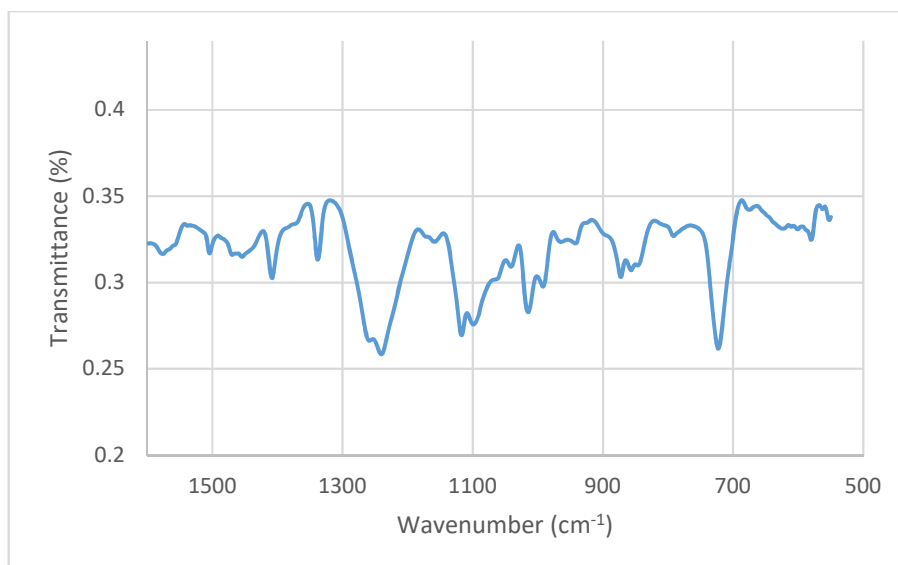


Figure 4.82: IR of 100 % PEDOT:PSS film through hole in insulating PET film in order to do electrical testing

4.6.3 Raman

The samples were measured using Raman spectroscopy using two different wavelengths as described in Section 3.4.9.3.

4.6.3.1 The 785 nm laser

A few experiments were performed which recorded the Raman spectrum using a 785 nm laser. Figure 4.83 shows the Raman spectrum of all samples measured.

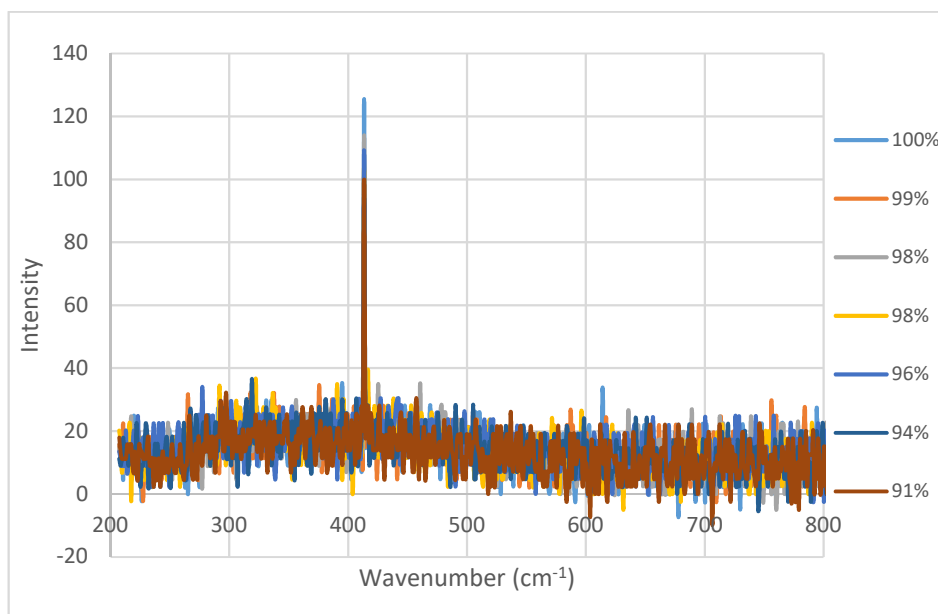


Figure 4.83: The full Raman spectra for all samples

Figure 4.84 shows the expanded spectrum.

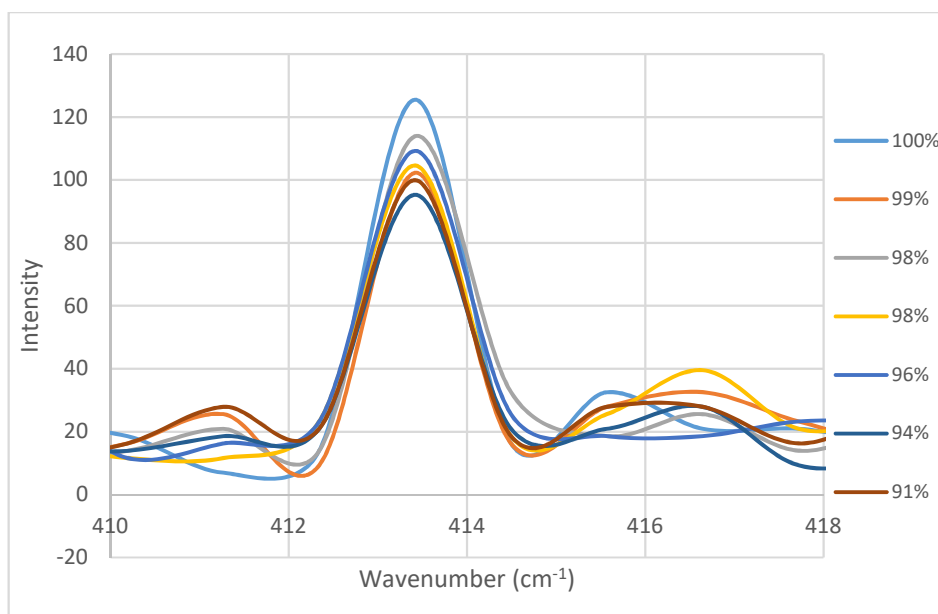


Figure 4.84: Raman spectra illustration showing changes in peak height at 413 cm⁻¹

Figure 4.85 shows the: 98 % PEDOT:PSS sample measured using a 785 nm laser.

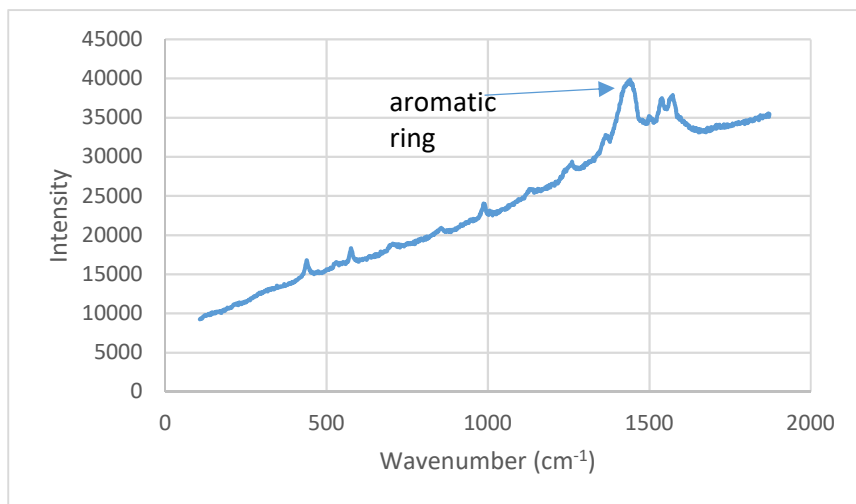


Figure 4.85: Raman spectrum of the 98 % PEDOT:PSS film sample at 785 nm

4.6.3.2 The 633 nm laser

Further experiments were performed on a different spectrometer using a 633 nm laser, which is in the IR region of the spectrum since the literature indicated IR was of most use for analysis of charge carrier effects in PEDOT as described in Chapter 2.

Figure 4.86 shows the traces obtained from some of the experiments conducted.

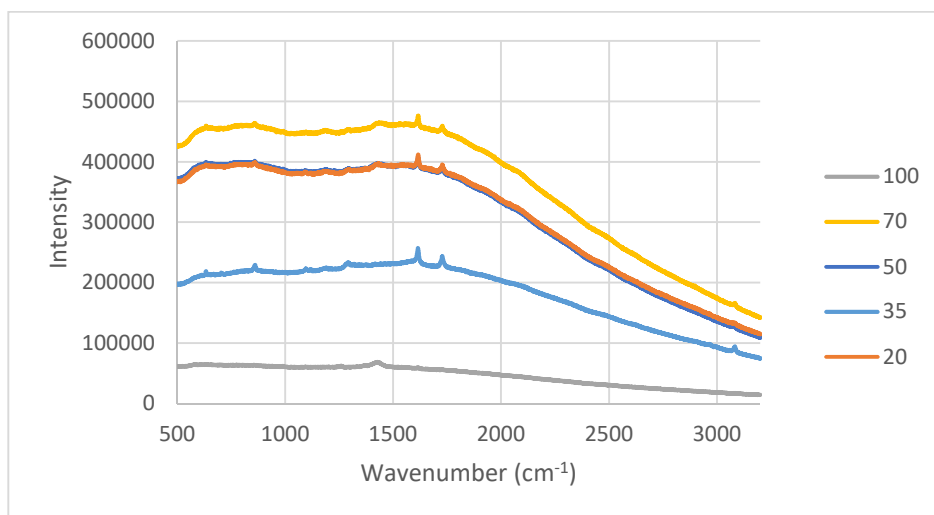


Figure 4.86: Raman spectra of all conductive samples using the 633 nm laser.

4.6.4 Nuclear Magnetic Resonance (NMR)

NMR has been used previously to analyse PEDOT (Kim, Kim *et al.*, 2009). In an attempt to see if the PEDOT molecule changes in conformation between the conductive form and the non-conductive form NMR was used. It has been assumed that when the molecule is ionised it could be altering the functional groups present. In turn this may help to confirm ionisation or to track conformational changes within the PEDOT polymer. The results were however inconclusive. PEDOT:PSS does not appear to show up in NMR despite literary references which describe that it does.

4.6.5 Synchrotron

An attempt was made to duplicate the annealing process where the sample is annealed at 120 °C in an oven under air. To duplicate the procedure a DSC attached to a synchrotron was used. Because the experiment was run with a Rapid Access Beamtime Application the equipment had to be used as already set-up. Unfortunately, the synchrotron was operating close to the allowed count so results were difficult to obtain. To optimise the experiment needs to be re-run with a different q value. As explained in Chapter 3, from the Bragg equation $n\lambda=2d\sin\Theta$, where: n = a positive integer λ = wavelength of the incident wave, d = lattice spacing of atoms in the crystal, Θ = the angle of incidence.

The value of q is related to 2θ or d spacing since $q = 2\pi / d$, (U.S Department of Energy).

At one point it was unclear if the sample which was a liquid could have leaked out of the DSC pan which was situated on its side to join to the synchrotron. However analysis after the event was carried out and the DSC pan was cut in half and analysed

under an Alicona microscope to see if there was PEDOT:PSS inside the cut pan, this is shown in Figure 4.87. As shown there is a dark residue inside the pan which is assumed to be the remains of the annealed PEDOT:PSS.

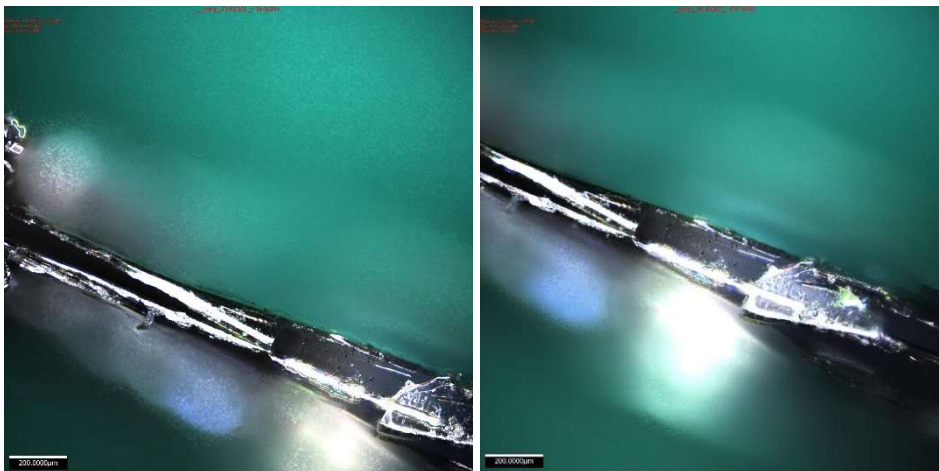


Figure 4.87: DSC pan cut in half to see if there was any PEDOT:PSS left inside after synchrotron/DSC analysis. There is a black residue which must be the remains of the PEDOT:PSS

Due to the inconclusive results from this experiment no further testing was attempted with the synchrotron. No crystallinity was found to be present therefore no metallic state was occurring in the PEDOT molecules as had previously been found by other researchers.

4.7 Thermal analysis using Differential Scanning Calorimetry (DSC)

The literature value for the glass transition (T_g) of 100 % PEDOT:PSS was found to be 102 °C for PEDOT so having a copolymer of PSS should lower the T_g . (http://shodhganga.inflibnet.ac.in/bitstream/10603/3499/11/11_chapter%205.pdf.)

As described in Section 3.4.3, Differential scanning calorimetry (DSC) was performed, to characterise the films made and to compare to the 100 % PEDOT:PSS to see what, if any changes had occurred to the thermal profile of the sample films.

Figure 4.88 shows how the glass transition temperature is affected by the addition of TWEEN 80 surfactant and MEK.

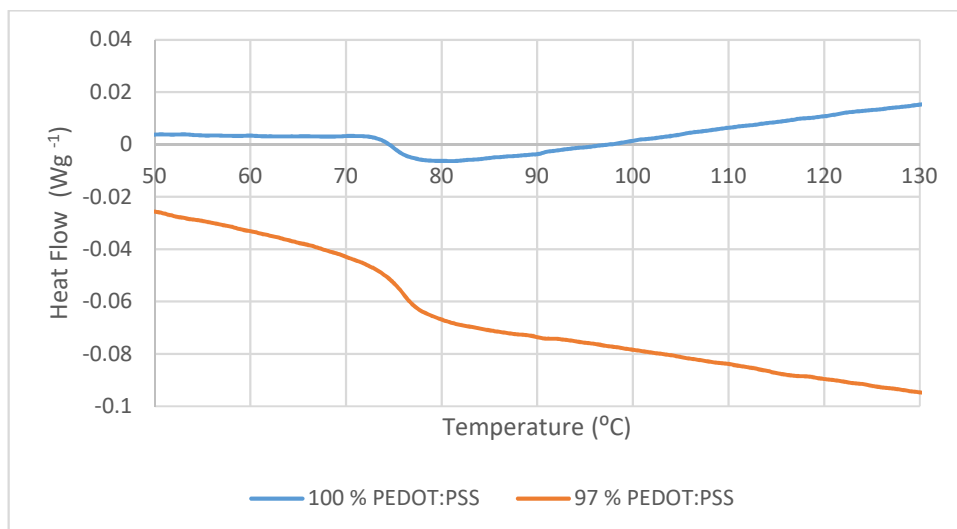


Figure 4.88: The Glass transition temperature of the 100 % PEDOT:PSS film sample and of the 97 % PEDOT:PSS film sample

The rest of the samples measured show a glass transition temperature as shown in Table 4.11.

Table 4.11: Measured Glass transition using DSC

Sample	Sample composition (%)	Onset of the Glass transition (T _g) (°C)	Midpoint of the Glass transition (T _g) (°C)	Endpoint of the Glass transition (T _g) (°C)
100 %	100 % PEDOT:PSS	85.46	75.51	77.22
1:40	2 % Additives 98 % PEDOT:PSS	83.99	75.01	78.00
1:35	3 % Additives 97 % PEDOT:PSS	83.42	75.76	78.06
1:30	3 % Additives 97 % PEDOT:PSS	77.61	70.95	73.39

4.8 Conclusions

Chapter 4 has detailed the results obtained and the progression from the scoping experiments through to an improvement of film quality and of adhesion, which was the major problem for the PhD. Several methods of characterisation were trialled but discarded since they gave no relevant results. Different manufacturing methods were compared to decide which would be most viable for bulk manufacturing. The starting material had a low reported conductivity of $<100 \text{ } \Omega/\text{sq}$. This was measured at 4082 to 10872 Ω/sq using a four point probe. Additives improved conductivity of most of the samples with the spincoated samples having the lowest resistivity. The addition of TWEEN 80 surfactant with MEK additives to PEDOT:PSS was intended to improve both conductivity and wettability, which it achieved. It did not deal with the adhesion problems. This is further discussed and explained in Chapter 5.

Chapter 5 will consider several factors:

Adhesion was the major problem for the entire project. By using chemical and physical surface modification adhesion problems were finally solved. However, how this affects conductivity is discussed.

The mechanism of conductivity is of great importance. The spectroscopy experiments aimed to show how PEDOT:PSS conducts electrically and this will also be discussed.

Film thickness is of importance to conductivity, so measurements of film thickness were performed and this will also be analysed.

Thermal analysis was performed with an aim to discover how PEDOT:PSS stands up to heat processing and so to estimate if it can be used for bulk processing.

5.0 Analysis

5.1 Introduction

The aim of the PhD was to enhance the conductivity of PEDOT:PSS for use in mass polymer manufacturer routes. Different methods of manufacture were investigated, (as described in Section 3.3), to produce thin films of doped and undoped PEDOT:PSS. A further aim was to try to clarify the mechanism of charge transfer occurring in this material. Performance at high voltages has not previously been reported and was also studied here. In order to assess if these aims have been achieved, this chapter presents the analysis of the experimental work.

In order to differentiate effectively between the samples Table 5.1 lists the sample codes and contents which is used in the following analyses. Depending on which is the most relevant the designations shown in Table 5.1 are used to identify the individual samples. Some of these samples were eliminated in the later research carried out but are still shown in earlier results.

Table 5.1: Designations used for analysis of films and solutions

PEDOT:PSS (%)	Additives (%)		Solution Ratio Designation	PEDOT:PSS Film Designation Electrical (%)	Additives in Film Designation (%)
	TWEEN 80	MEK			
90.91	2.27	6.82	1:10	91	9.0
93.75	1.56	4.69	1:15	94	6.3
95.24	1.19	3.57	1:20	95	4.8
96.15	0.96	2.88	1:25	96	3.9
96.77	0.81	2.42	1:30	97	3.2
97.22	0.69	2.08	1:35	97	2.8
97.56	0.61	1.83	1:40	98	2.4
98.04	0.49	1.47	1:50	98	2.0
98.59	0.35	1.06	1:70	99	1.4
98.90	0.27	0.82	1:90	Eliminated	1.0
100	0.00	0.00	100	100	0.00

5.2 Solutions

The solutions are analysed separately to the film samples.

5.2.1 pH and viscosity

Figure 4.5 shows the pH of the different solutions. Previous work on the pH of PEDOT by Elschner (Elschner, Kirchmeyer *et al.*, 2011) confirms that the highest conductivity in PEDOT:PSS systems occurs between pH 0-3 so the results shown in Figure 4.5 are in accordance with this with the most conductive samples all measuring a pH of 2.03-2.08 \pm 0.01.

There is no significant change until the peak at the 1:70 solution. Analysis of pH shows a rise from pH 1.99 for the 1:10 solution to pH 2.6. for the 1:70 solution. The calibration of the pH meter has an error margin of \pm 0.01 which means this could be a real result rather than an error, however, this sample is also the least conductive with only 1 % additives so therefore a less doped sample. It may be, that the less conductive sample is in the aromatic form, or it could be that the aromatic conformation has caused the solution to have a higher pH which stabilises the aromatic structure and may therefore be an indication that a greater proportion of PEDOT:PSS is present in the aromatic form.

At the lower pH, the solutions may be losing PSSH. The peak is probably caused by the PSSNa changing to PSSH and thereby becoming slightly more acidic, due to the H⁺ from water displacing the Na⁺ atoms. The 98.59 % solution is found At the high point, which is least acidic sample, so this is the point at which there is the most PSSNa in solution.

Figure 4.6 shows the viscosity of the solutions. As the concentration of PEDOT:PSS is reduced, the surfactant concentration rises. There is probably a dilution effect

occurring from 100 % down to 95 % PEDOT:PSS. After this the dilution is inducing aggregation of the particles which continues to increase viscosity as the surfactant concentration rises. It may also be indicative of a rheological effect caused by a chemical change. However, at this point there is no evidence to support this theory. When measuring the PEDOT-mixtures, as shown in Figure 4.6, there was slight dip at a PEDOT concentration of 95 %, however there was very little change in viscosity regardless of the concentrations. As the concentration of PEDOT:PSS is reduced, the surfactant concentration rises. There is probably a dilution effect occurring from 100 % down to 95 % PEDOT:PSS. After this the dilution is inducing aggregation of the particles which continues to increase viscosity as the surfactant concentration rises. It may also be indicative of a rheological effect caused by a chemical change. However, at this point there is no evidence to support this theory. Attempts to alter the viscosity by addition of sulphuric acid (AR) to the solutions to see if pH could be related to change in viscosity gave no definitive results.

5.3 Film Properties

Film quality was enhanced using TWEEN 80. This has a similar structure to sorbitol which is known to enhance conductivity so it could be enhancing the conductivity as well as improving film quality. There is no doubt that the film quality must make a difference to the overall conductivity since, if the particles do not connect the current cannot flow. By producing a more homogeneous film this would be expected to cause better conductivity. It appears that as the surfactant concentration increases so also does the quality of the film produced.

5.3.1 Bulk and surface resistivity

The aim of this project was to enhance the conductivity of 100 % PEDOT:PSS, therefore an analysis of electrical performance is required. At the start of the project

a full set of samples was analysed which had a range of concentrations of additives from 9 % down to zero. The designations of the samples is shown in Table 5.1.

5.3.1.1 Sheet Resistance

The initial measurements of sheet resistance as found with the four-point-probe, could be grouped into three distinct Zones of resistivity as shown in Figure 5.1. Table 5.2 shows the samples in different designated Zones. From Table 5.1, there are two samples which can be designated 98 % and two samples which can be designated as 99 %.

Table 5.2: Zones of conductivity

	PEDOT:PSS (%)	
Zone 1	91 – 94	eliminated
Zone 2	95 – 98	97.56 % is most conductive
Zone 3	99 – 100	98.04 % eliminated 98.59 % taken forward 99 % eliminated

The 99 % sample has high resistivity and showed unreliable results. This is probably due to the very poor film quality in relation to the Zone 2 samples so this was eliminated.

The 98.59 % sample was taken forward for further research since it was the most stable of all samples measured although having higher resistivity than those samples included in Zone 2 and from now was designated as the 99 % sample.

The 98.04 % sample was eliminated since this sample showed unreliable resistivity results despite being similar in resistivity to Zone 2 samples.

The 97.56 % sample which was taken forward for further research was from now on designated as 98 %.

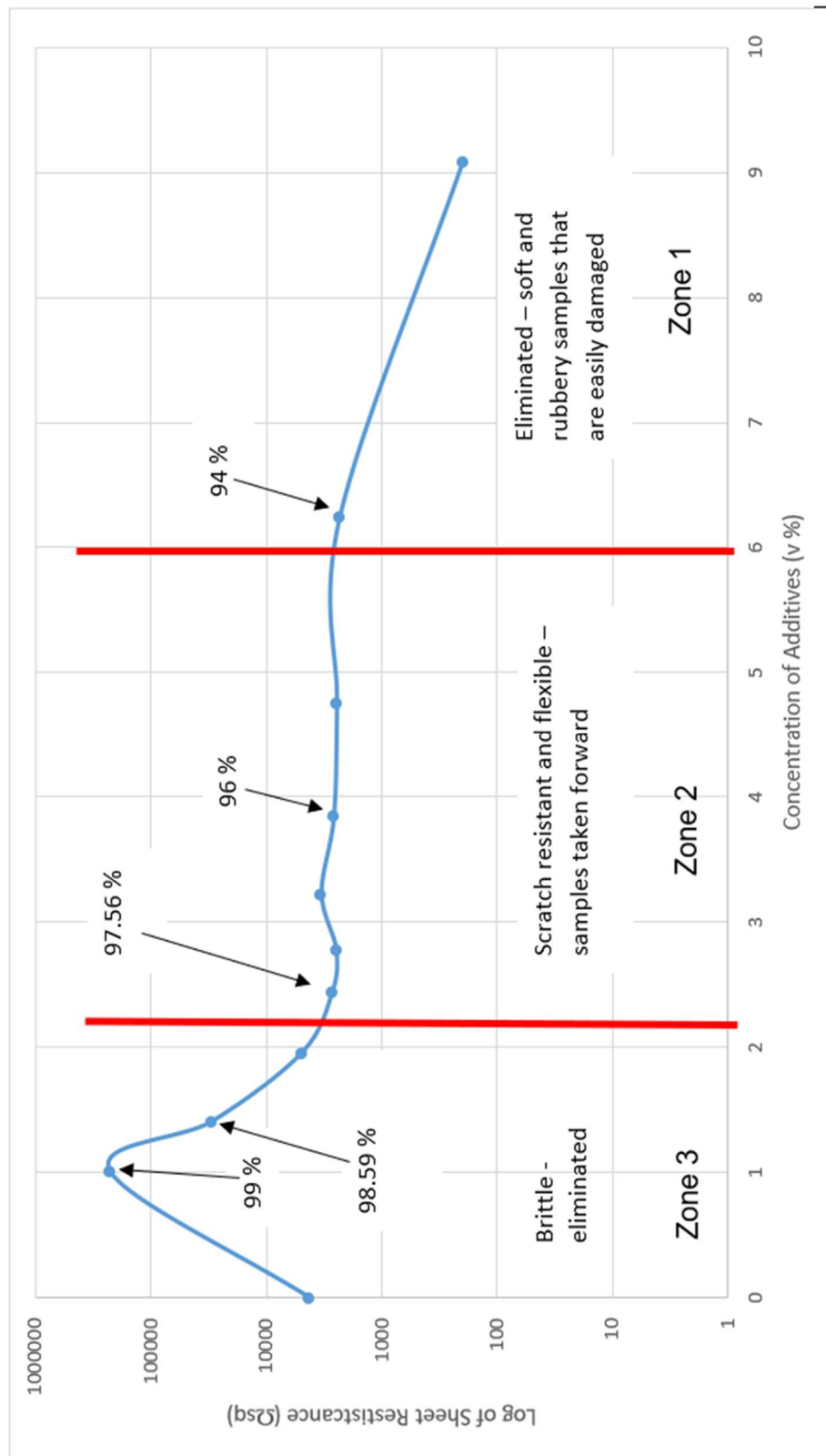


Figure 5.1 Sheet resistance of the PEDOT:PSS samples using a four-point probe at 10 nA

Zone 1 contains the 91 % and 94 % PEDOT:PSS samples. This region of the graph has the highest surfactant content and the films became damaged very easily due to the samples being soft and rubbery which caused them to stick onto test equipment and storage bags. A similar problem was found with the 94 % sample. For this reason the 91 and 94 % samples were eliminated from further study despite having the highest conductivities.

The 95 % to 98 % samples were more durable with the 97 % samples being the most durable with increased scratch resistance. As the surfactant content rises so the durability falls. The 100 % PEDOT:PSS to 99 % PEDOT:PSS was brittle as has been previously reported in the literature and did not stick well to the substrate. As more additive is added the PEDOT:PSS becomes more soft and pliable. Because the 100 % PEDOT:PSS has such brittle films, care was taken when measuring not to damage the surface of the samples. The samples with enhanced conductivity also had better handleability. In Zone 2, samples were all very similar in resistivity to 100 % PEDOT:PSS. These had a wider range of concentrations but little difference was found between the samples with respect to resistivity testing, however, IR showed some important differences as will be explained in 5.5. The samples found in Zone 2 ranged in concentration from 95-98 % of the original 1.1 % dispersion of PEDOT:PSS present in the samples. These had a similar resistivity to each other and lower resistivity than the 100 % PEDOT:PSS. Zone 3 ranges from 99-100 % of the original dispersion of PEDOT:PSS present the final sample film. At this point it is worth noting that the film sample at the edge of Zone 2 and the adjacent film sample in Zone 3 both round down to a PEDOT:PSS concentration of 98 % of the original PEDOT:PSS dispersion. However, there is a repeatable resistivity result with the

Zone 2 sample where the Zone 3 samples have far more irregular results, so the Zone 3 sample was eliminated from further study

The relative amount of additives included in the samples clearly makes a great deal of difference. At either end, the resistivity is high in relation to Zone 2, which shows best conductivity (lower resistivity) in all cases. The range for highest conductivity seems to be between 4 % and 2 % additives. The Zone 3 sample shows an increase in resistivity with lowering of the additives. Partly this will be due to the poorer film quality since the lower the concentration of surfactant, the worse the film quality. This could be the real reason for enhancement of conductivity. Better film coverage will mean better contact between the PEDOT particles. It is known that sorbitol and its derivatives and close relatives, as discussed in Chapter 2, can be used to dope PEDOT:PSS. The mechanism by which the conductivity of PEDOT is increased is not completely understood and this may vary depending on the exact structure of the dopant.

5.3.1.2 Bulk resistivity

Bulk resistivity, as measured using the four-point-probe, shown in Figure 5.2, falls steadily as surfactant concentration is increased. Using the same three Zones of conductivity, it can be seen that the bulk resistivity of the 98 % sample is slightly higher than the rest of the Zone 2 samples. However, this sample is of interest spectroscopically as described in Section 5.5.

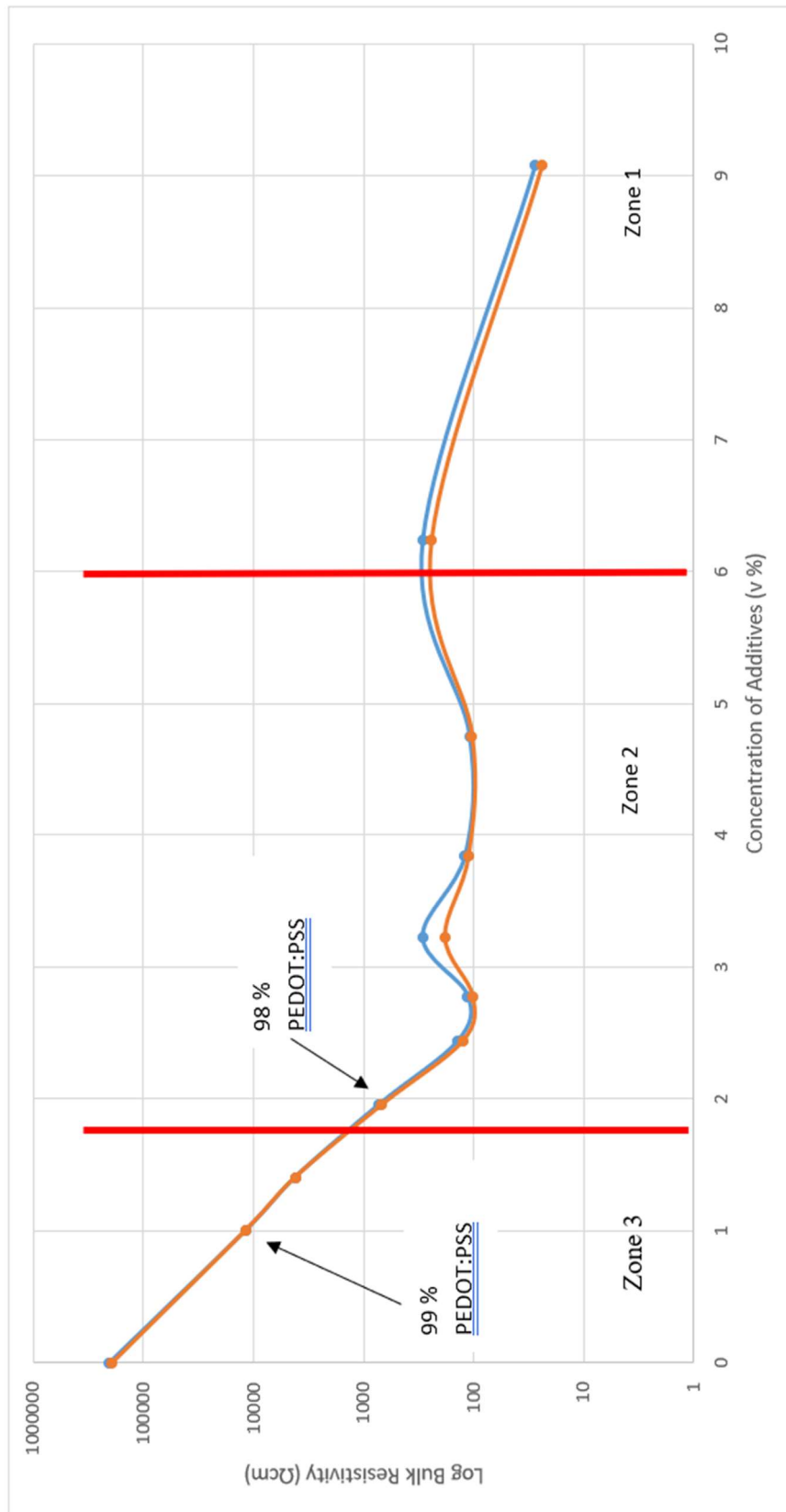


Figure 5.2: Bulk Resistivity of PEDOT:PSS using a four-point probe at 10nA

There is a difference between the results for bulk and surface resistivity of the 99 % samples shown on Figures 5.3 and 5.4, where the surface resistivity rises but the bulk resistivity falls along with addition of additives. This rise in surface resistance is probably caused by contaminant molecules such as water and possibly ammonia adhering to the surface of the film and raising the surface resistivity, or related to the surface roughness of the film, since the bulk resistivity is much lower. The shape of the two graphs is also completely different with the bulk measurements being more conductive. Since the results were repeated several times with new samples and the same results were obtained repeatedly this is not an error but must be the result of differences in the surface to bulk properties.

5.3.1.3 High Voltage Testing

The spraycoated samples and dipcoated samples measured using a Keithley 6517b, as described in Chapter 3, all have very similar profiles. These are shown individually in Sections, 4.3.3 and 4.3.4. A typical example is shown in Figure 5.3. This Figure also shows the surface resistance measured using the four-point-probe. The Keithley gave the results as current which was then converted to resistivity using equation 5.1 as explained in Section 3.4.5, since the voltage applied was known. For the four-point probe, the current was known and the resistivity was measured. To compare the two techniques, the voltage was calculated using equation 5.1 since the four-point-probe had a known current and measured values for the resistivity.

$$V=I/R \quad [5.1]$$

Figure 5.3 shows a graph of dipcoated set 2 (but all the spraycoated and dipcoated graphs are very similar) measured using the Keithley 6517b, with the sheet resistance, measured using a Jandel four-point-probe.

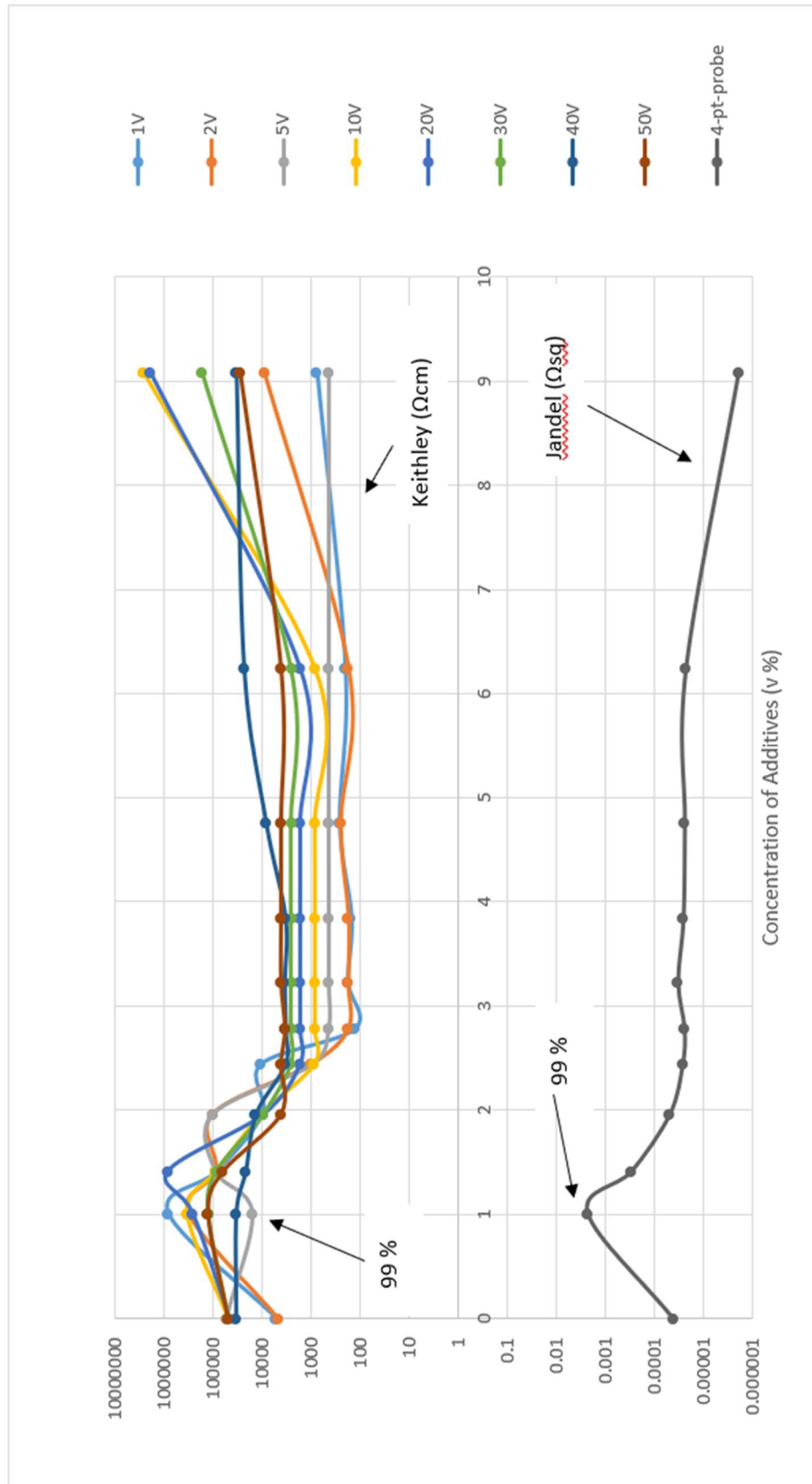


Figure 5.3: A typical profile of the samples using a Keithley 6517b at different applied potential differences with the surface measurements from the Jandel four-point-probe

There are some minimal differences in the profiles of the samples with respect to the applied voltage when measuring using the Keithley. It is obvious when looking at Figure 5.3 that the Keithley results must be giving measurements for surface resistance rather than bulk resistivity since the graphic profile of both the Keithley at all voltages and the calculated voltage profile for the Jandel are the same shape. In both cases regardless of voltage or current the resistivity of the 99 % sample peaks. This is more than likely due to this sample having a poor film quality whereas the rest of the samples all have a similar resistivity to that of the 100 % PEDOT:PSS. Resistivity for the rest of the samples falls with increased addition of surfactant. Since film quality improves at the same rate it is likely the resistivity becomes lower due to improved film forming.

Dipcoated sample set 2 has a measured current and calculated resistivity at each applied voltage. Results are shown in Tables 5.3 to 5.5. All sets of dipcoated and spraycoated results were very similar.

Table 5.3: An example of the current measured using the Keithley two point probe at 1- 5Volts.

% of PEDOT:PSS	100	99	99	98	98	98	97	97	96	95	94	91
Potential Difference (V)	1	1	1	1	1	1	1	1	1	1	1	1
Current (I) (Ampere)	0.000190	0.00001	0.000011	0.000096	0.000093	0.007500	0.005480	0.006460	0.003780	0.004840	0.001290	
Resistivity (Ω)	5263	100000	88495	10395	10752	133	182	155	265	207	775	
% of PEDOT:PSS	100	99	99	98	98	97	97	96	95	94	91	
Potential Difference (V)	2	2	2	2	2	2	2	2	2	2	2	
Current (I) (Ampere)	0.000400	0.00006	0.000023	0.000020	0.001980	0.011050	0.011040	0.011270	0.007790	0.011240	0.000220	
Resistivity (Ω)	5000	312500	87719	10256	1010	181	181	177	257	178	9090	
% of PEDOT:PSS	100	99	99	98	98	97	97	96	95	94	91	
Potential Difference (V)	5	5	5	5	5	5	5	5	5	5	5	
Current (I) (Ampere)	0.000100	0.000319	0.000057	0.000050	0.005420	0.011460	0.011440	0.011460	0.011390	0.011460	0.011450	
Resistivity (Ω)	5000	15674	87412	100806	923	436	437	436	440	436	437	

Table 5.4: An example of the current measured using the Keithley two point probe at 10- 30 Volts

% of PEDOT:PSS	100	99	99	98	98	97	97	96	95	94	91
Potential Difference (V)	10	10	10	10	10	10	10	10	10	10	10
Current (I) (Ampere)	0.000 201	0.000 30	0.0001 14	0.000965	0.011310	0.011540	0.011530	0.011560	0.011530	0.011540	0.000004
Resistivity (Ω)	4975 ₁	334448	88028	10362	884	866	867	865	867	866	2631578
% of PEDOT:PSS	100	99	99	98	98	97	97	96	95	94	91
Potential Difference (V)	20	20	20	20	20	20	20	20	20	20	20
Current (I) (Ampere)	0.000 420	0.0000 75	0.0000 22	0.002030	0.011560	0.011630	0.011630	0.011630	0.011620	0.011630	0.000010
Resistivity (Ω)	4761 ₉	265251	892857	9852	1730	1719	1720	1719	1721	1719	1941747
% of PEDOT:PSS	100	99	99	98	98	97	97	96	95	94	91
Potential Difference (V)	30	30	30	30	30	30	30	30	30	30	30
Current (I) (Ampere)	0.000 600	0.0001 97	0.0003 47	0.003180	0.011640	0.011680	0.011680	0.011690	0.011680	0.011690	0.000178
Resistivity (Ω)	5000 ₀	152284	86455	9433	2577	2568	2568	2566	2568	2567	168539

Table 5.5: An example of the current measured using the Keithley two point probe at 40-50 Volts

% of PEDOT:PS S	100	99	99	99	97	97	96	95	94	91
Potential Difference (V)	40	40	40	40	40	40	40	40	40	40
Current (I) (Ampere)	0.001150	0.001150	0.001170	0.001170	0.001169	0.001172	0.011610	0.001170	0.001169	0.001165
Resistivity (Ω)	34782	34782	34188	34188	34217	34129	3445	34188	34217	34335
% of PEDOT:PS S	100	99	99	99	98	97	96	95	94	91
Potential Difference (V)	50	50	50	50	50	50	50	50	50	50
Current (I) (Ampere)	0.000978	0.000380	0.000784	0.011720	0.011720	0.011750	0.011750	0.011750	0.011750	0.001750
Resistivity (Ω)	51124	131578	63775	4266	4266	4255	4255	4255	4255	28571
% of PEDOT:PS S	100	99	99	98	98	97	96	95	94	91
Potential Difference (V)	40	40	40	40	40	40	40	40	40	40
Current (I) (Ampere)	0.001150	0.001150	0.001170	0.001170	0.001169	0.001172	0.011610	0.001170	0.001169	0.001165
Resistivity (Ω)	34782	34782	34188	34188	34217	34129	3445	34188	34217	34335

Most notable is the results at 40 V. In every case this gives a different shaped curve indicating that it could be at this voltage that degradation begins to occur in the samples. The samples still remained conductive but had much higher resistivity however the 50 V applied potential gave the same shape curve as the lower applied potentials. All samples regardless of the method used to manufacture them, showed three Zones of conductivity. Using results as explained in Section 5.3, most samples were eliminated from further study leaving just three representative samples for further research. Spincoated samples were only made in the concentrations chosen to represent the two Zones of most interest. The results from measuring the resistivity of the spincoated samples at high voltage are shown in Section 4.3.7.2. A typical example is shown in Figure 5.4.

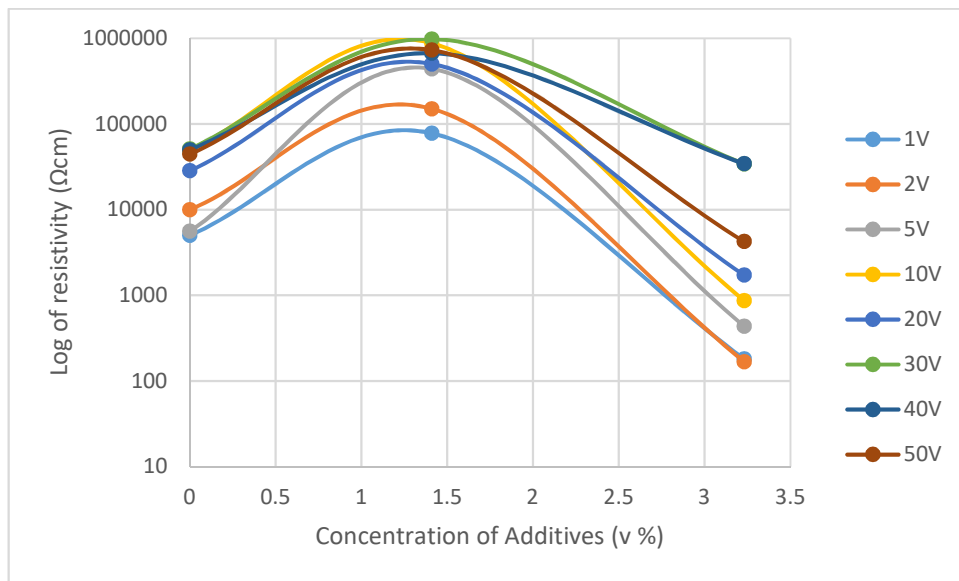


Figure 5.4: Resistivity of the 97 %, 99 % and 100 % dipcoated samples with unmodified substrates at different applied potentials using Keithley 6517b

Looking at individual voltages all profiles are again quite similar. Choosing just one applied potential difference, the similarities can be seen in Figures 5.5 and 5.6.

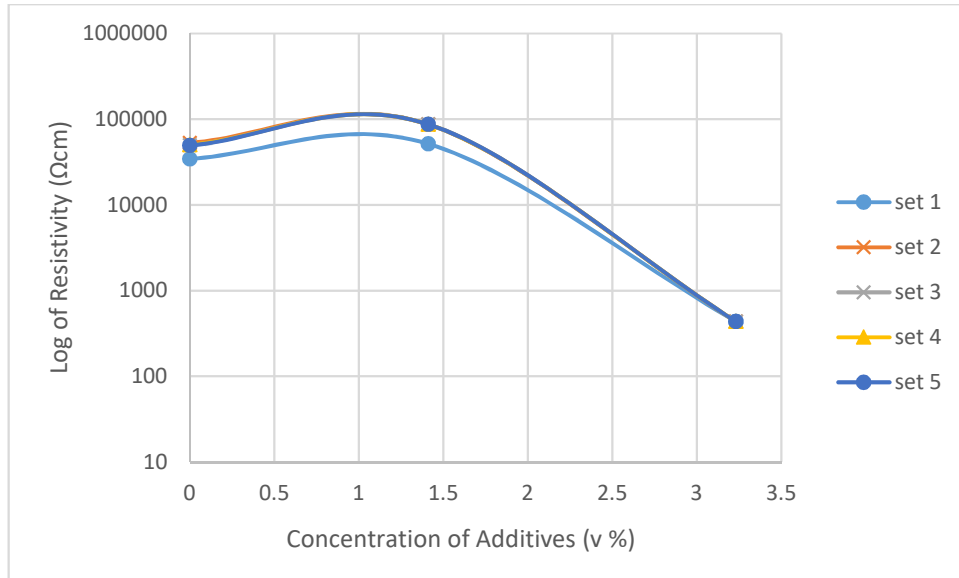


Figure 5.5: Resistivity of the 97 %, 99 % and 100 % dipcoated samples at 5V

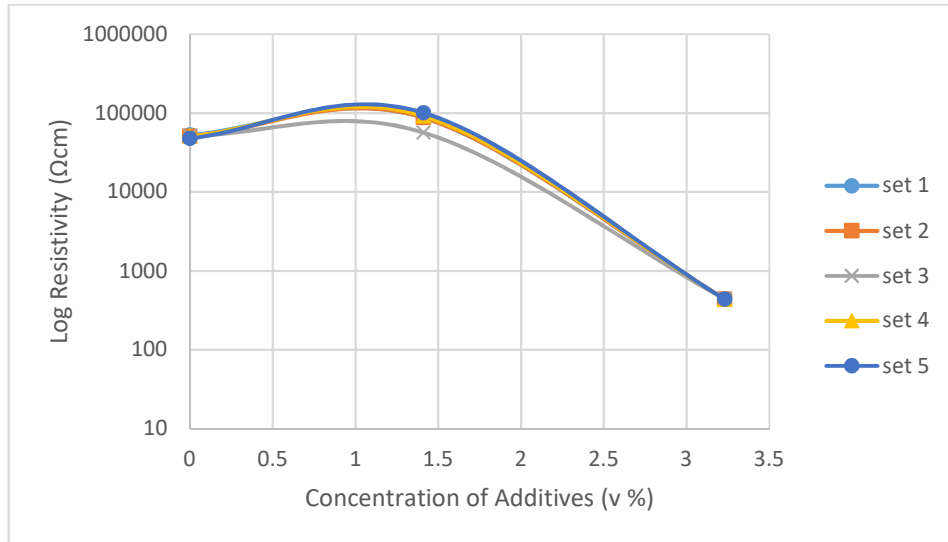


Figure 5.6: Resistivity of the 97 %, 99 % and 100 % spraycoated samples at 5V

Figures 5.4 to 5.6 are representative of the trends observed in all samples at all applied voltages. In all cases the Zone 2 sample has the lowest resistivity. This sample also has the best film quality. It can also be seen that regardless of the

manufacturing methods the resistivity rises with a rise in applied potential difference. An example of this is shown in Figure 5.7.

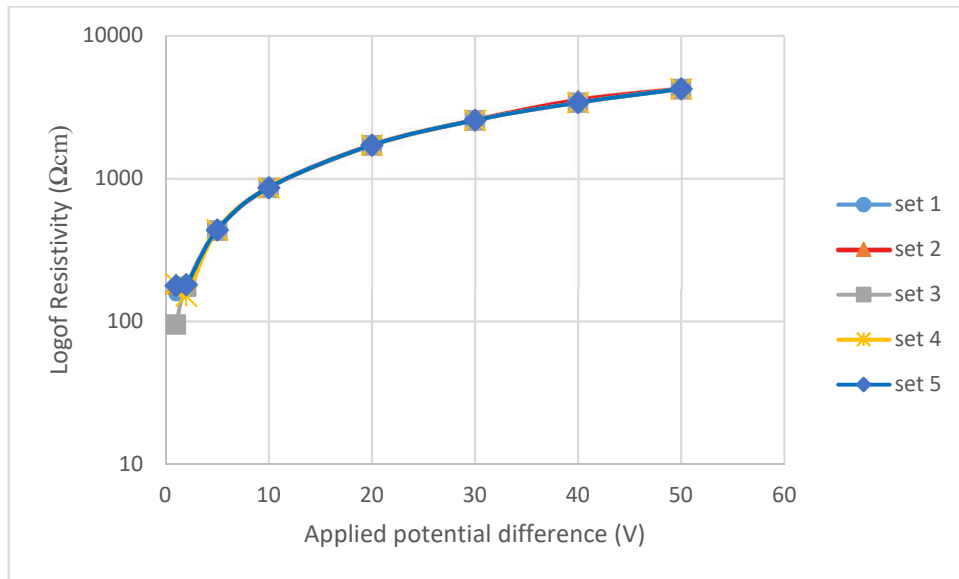


Figure 5.7: The rise in resistivity with increasing applied Voltage for the 97 % dipcoated samples

5.4 Manufacturing Routes

Relative to spraycoating and dipcoating, spincoating did not aid in improving adhesion to the substrate and the same problems were found with the film quality. Two methods of modifying the substrate surface were attempted. Chemical modification with several reagents and mechanical abrasion.

The best reagent was found to be methyl cellulose. This was spincoated onto the substrate as detailed in Chapter 3, and then this modified substrate was coated with the PEDOT- mixtures as per the previous samples. Electrical resistivity results were similar in trend but slightly lower in resistivity to those with both dipcoating and spraycoating, with the unmodified spincoated samples having lower resistivity and all spincoated samples being lower than those made by dipcoating and spraycoating.

The spincoated samples had a thinner film thickness and lower resistivity than the thicker samples from the other manufacturing methods as shown in Table 5.6.

Table 5.6: Film thicknesses of different manufacturing techniques

Manufacturing technique	Film thickness (μm)
Spraycoated	3.49-4.65
Dipcoated	7.59-8.22
Spincoated	1-2
Chemically modified	2-3
Physically modified	11-52

It was impossible to measure the film thickness of the methyl cellulose itself since it could not be seen by optical microscopy or by SEM so the only way to measure this was to calculate it using the results from both the unmodified samples and those chemically modified with an additional layer of PEDOT–mixture. The film coating from the unmodified samples was measured at 1-2 μm with for six samples an average of 1.67 μm . For the unmodified samples when taking an average over 6 samples the thickness of the film was 2.67 μm .

Therefore using this information:

[Chemically Modified samples] – [unmodified samples] = thickness of the cellulose coating.

$$2.67 \mu\text{m} - 1.67 \mu\text{m} = 1 \mu\text{m}$$

So the calculated film thickness of the methyl cellulose coated samples can be assumed to be an average of 1 μm .

The abraded samples had a film thickness of between 11-52 μm so these were far thicker than the other spincoated samples. However since by abrading the PET it

was worn away this residual film thickness is actually much less. However, actual thickness was not ascertained since the film quality and resistivity of the chemically modified samples was superior to the abraded samples.

5.4.1 Sheet resistance of the modified samples

Three representative samples were chosen to measure sheet resistance. The three samples of most interest which had been identified as the 97 %, 99 % additives and 100 % PEDOT:PSS, (which was the benchmark), were applied to a modified substrate using mechanical abrasion or methyl cellulose. They were tested to compare them with the unmodified samples. Figures 5.8 and 5.9 show the spraycoated samples and dipcoated samples are virtually identical and show the same trend for sheet resistance. When plotted on one graph the samples overlay each other, therefore, the sheet resistance is virtually identical. This perhaps helps to show the consistency in the methods underpinning this research.

In all cases the same trend in resistivity with concentration is present regardless of the manufacturing method. The 1 V applied potential difference gives the lowest resistivity with resistivity rising with each increase in potential difference applied.

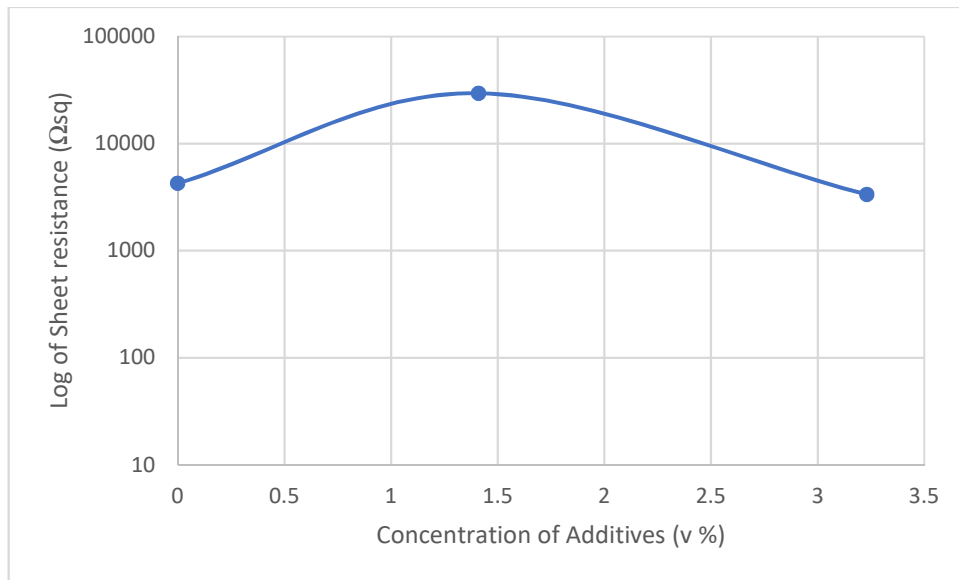


Figure 5.8: The sheet resistance of the dipcoated samples

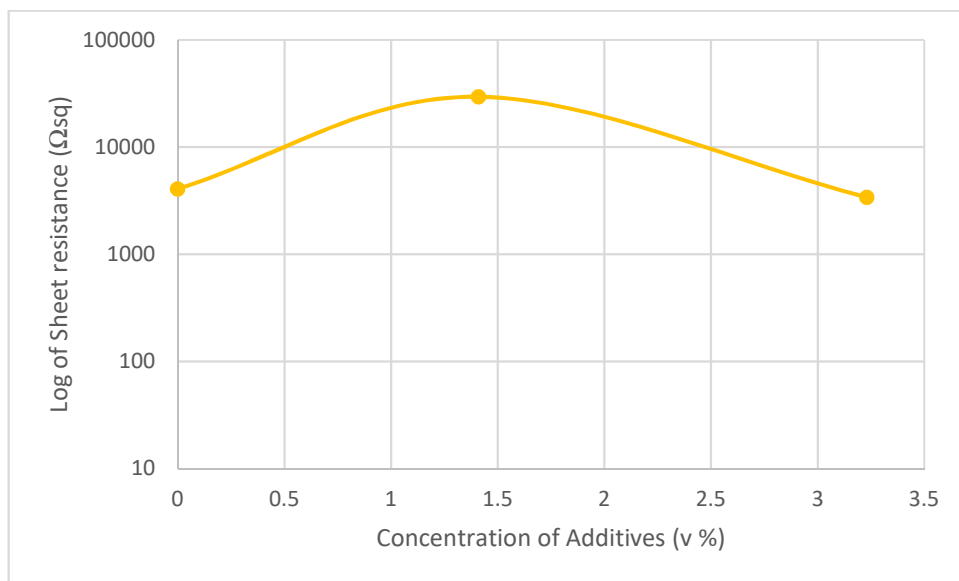


Figure 5.9: The sheet resistance of the spraycoated samples

An example of the trend of the spincoated samples with no chemical modification is shown in Figure 5.4 and shows the samples using an applied potential difference of between 1 to 50 V. The trend, as found in the dipcoated and spraycoated samples remains the same using the four-point-probe as shown in the sheet resistance

measurements in Figure 5.10. Methyl cellulose gives a more homogeneous film but slightly thicker film than spincoated untreated samples which is still electrically conductive and gives good adhesion to PET.

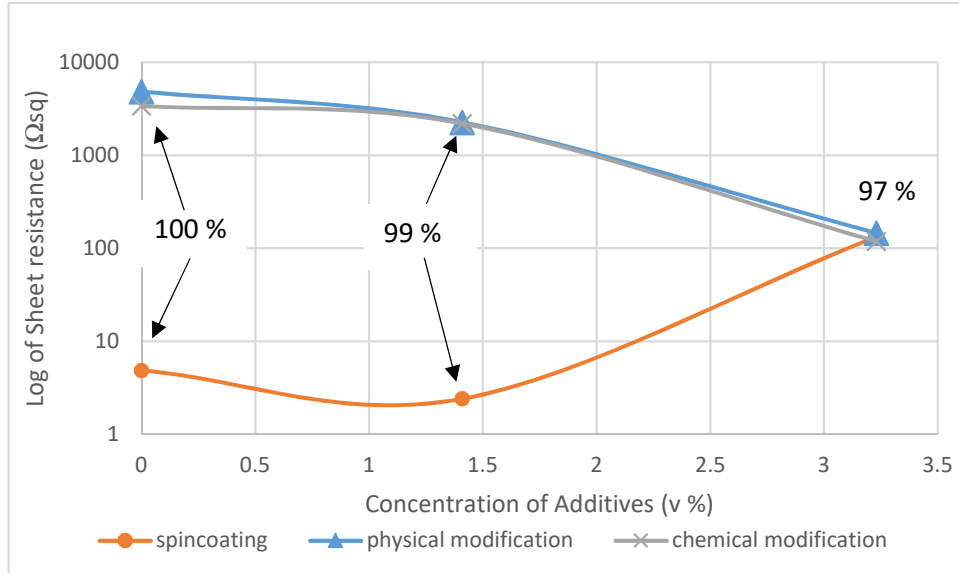


Figure 5.10: Comparison of sheet resistance the spincoated samples

The unmodified spincoated 100 % sample has lower sheet resistance than the rest of the 100 % samples and a lower sheet resistance than the doped samples. The shape of the graph in Figure 5.10 shows the sheet resistance rises as the additive concentration increases. However, since the 100 % sample suffered from lack of good adhesion to the substrate, the best samples shown in Figure 5.10 are the chemically and physically modified spincoated samples. These spincoated samples have very similar same sheet resistance, since they virtually overlay one another as shown in Figure 5.10. The exception to this is the 99 % PEDOT:PSS spincoated but unmodified sample which had the lowest sheet resistance and showed an improvement on the starting material. This is shown in Figure 5.10. This was also found to be the most stable sample when measuring with stable readings. All the rest of the samples were unstable when measured. However, both the chemically and physically modified samples had the lowest resistivity at the 3 % additives despite

being different in film thickness as shown in Table 5.6. Film thickness and resistivity are believed to be related, with thinner films giving lower resistivity. It would appear there is a point above which the film thickness makes little difference somewhere between 3.4 and 7.5 μm . This could explain why the dipcoated and spray coated samples are so similar for electrical characterisation.

The sheet resistance of the spincoated samples in relation to that of the other manufacturing techniques is much lower. This is probably due to the improved film quality and the thinner film of the spincoated samples so the spincoating manufacturing method produces the lowest resistivity films although resistivity does rise slightly when the surface of the substrate is treated with either chemical or physical modification. It could also be because the spincoating technique causes the polymer chains to align which will increase conductivity. This would link with previously reported research where it was suggested in Section 2.5.2 in the work of Denneulin, Bras *et al*, (Denneulin, Bras *et al.*, 2011) that PEDOT chains may align.

5.4.2 Bulk resistivity of the modified samples

Figures 5.11 and 5.12 shows the bulk resistivity measured using a four-point-probe. The spincoated samples are all so similar that again the lines overlay. The spincoated samples are all clearly lower resistivity for all concentrations used to make the samples than those made using the other manufacturing methods.

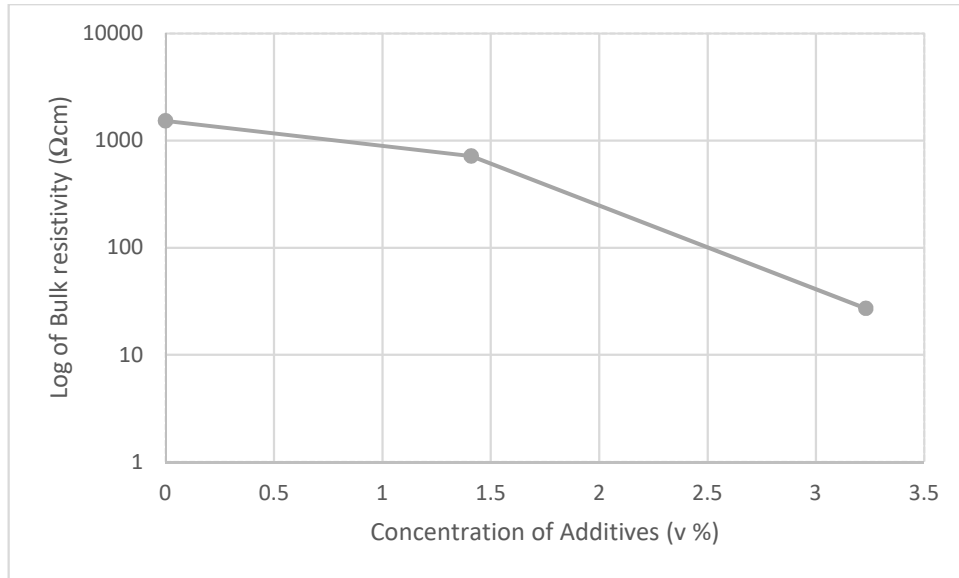


Figure 5.11: Bulk resistivity of the unmodified spincoated samples

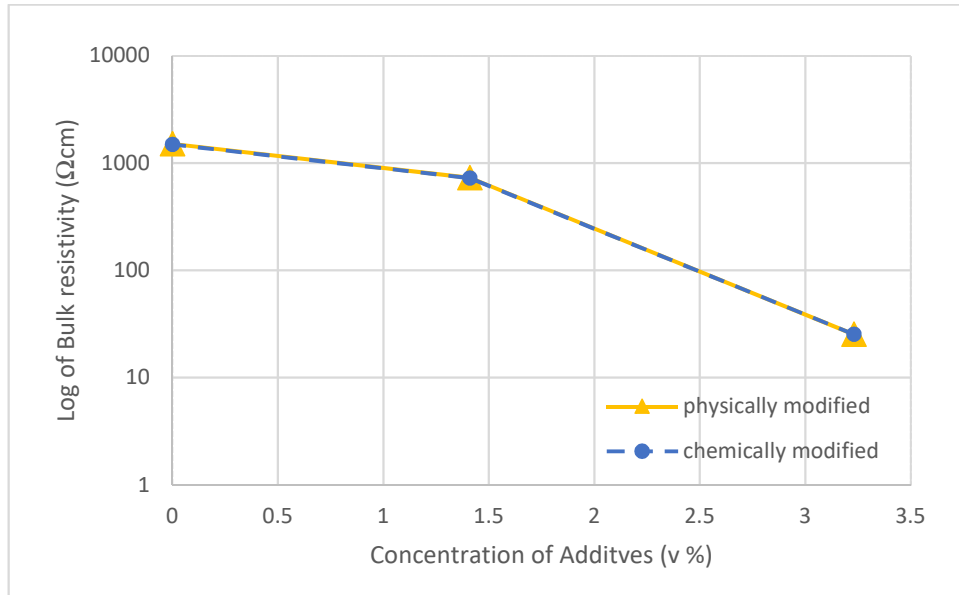


Figure 5.12: Comparison of bulk resistivity of the chemically and physically modified spincoated samples

As with sheet resistance the spincoated films, being much thinner and of better film quality than those of the spraycoated and dipcoated samples all have far lower resistivity. In all cases the samples improve in bulk resistivity with the increase in additive concentration regardless of the method used to manufacture the sample.

This proves:

- The TWEEN 80/MEK additive in some cases improves the conductivity of the PEDOT:PSS used in this PhD project.
- Both film thickness and film quality is related to the conductivity of the samples. A homogeneous surface is required which will allow the charge carriers to have a pathway for movement. Since the charge carriers move across the film rather than perpendicular to it the thinner films have better conductivity.
- Chemical or physical substrate modification of PET slightly raise the resistivity but are needed to improve film adhesion to the substrate.
- The 97 % PEDOT:PSS spincoated sample with a modified substrate (by either modification method) is the best candidate to carry forward for any further research into bulk applications of this conductive polymer.
- There is evidence to support PEDOT:PSS may align during processing with spincoating enhancing conductivity.

5.4.3 High voltage of the modified samples

Chemical and physical modification both work as an adhesion promotor for PET substrates, coated with films of PEDOT:PSS containing the additives TWEEN 80 and MEK. Chemical modification using methyl cellulose gives the least variable results but mechanical abrasion of the surface does also work. Both methods give very similar resistivity results. Figures 5.13 to 5.15 show the results of measurements using a Keithley 6517b.

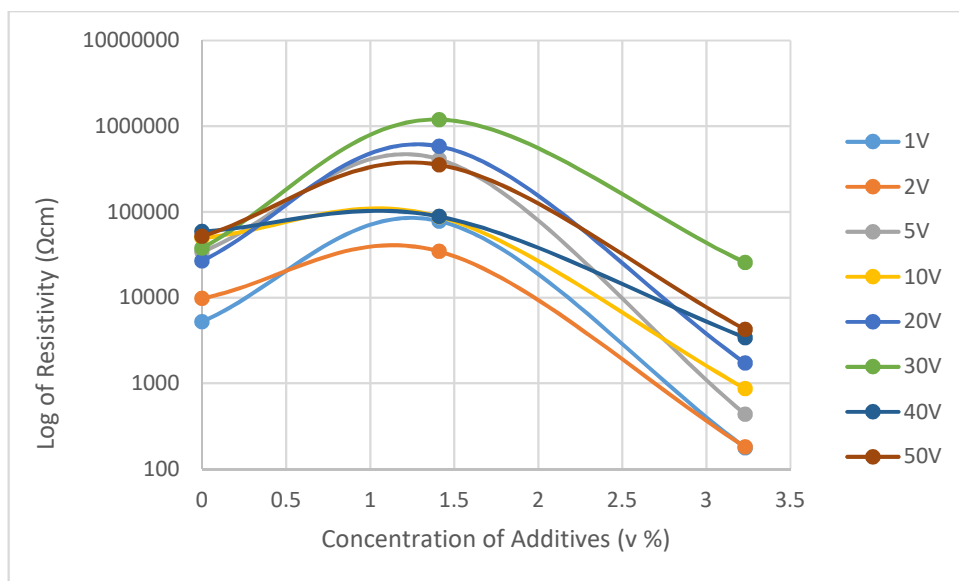


Figure 5.13: The Resistivity of the chemically modified spincoated samples using the Keithley 6517b

The abraded results shown in Figure 5.15 show greater variability than the chemically modified results as seen in Figure 5.15. This is regardless of the applied potential difference.

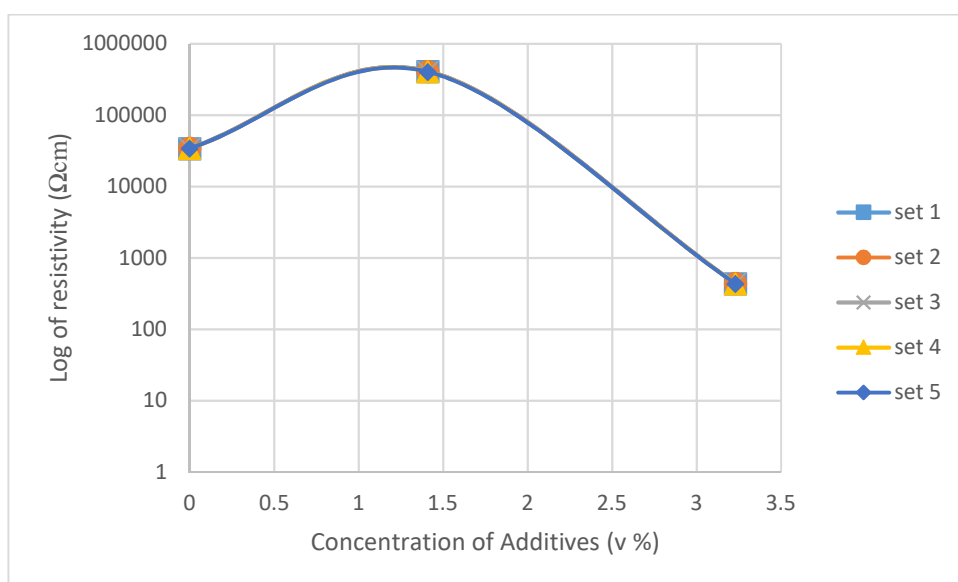


Figure 5.14: Chemically modified spincoated samples at 5 V

Mechanical abrasion is most useful up to 400 cycles but 100 or 200 cycles gives the best film quality. Higher or lower amounts of abrasion cycles resulted in film delamination from the PET substrate due to lack of adhesion and a lowering of conductivity. However, as seen in Figure 5.15 the results are less repeatable than those of the chemical modification.

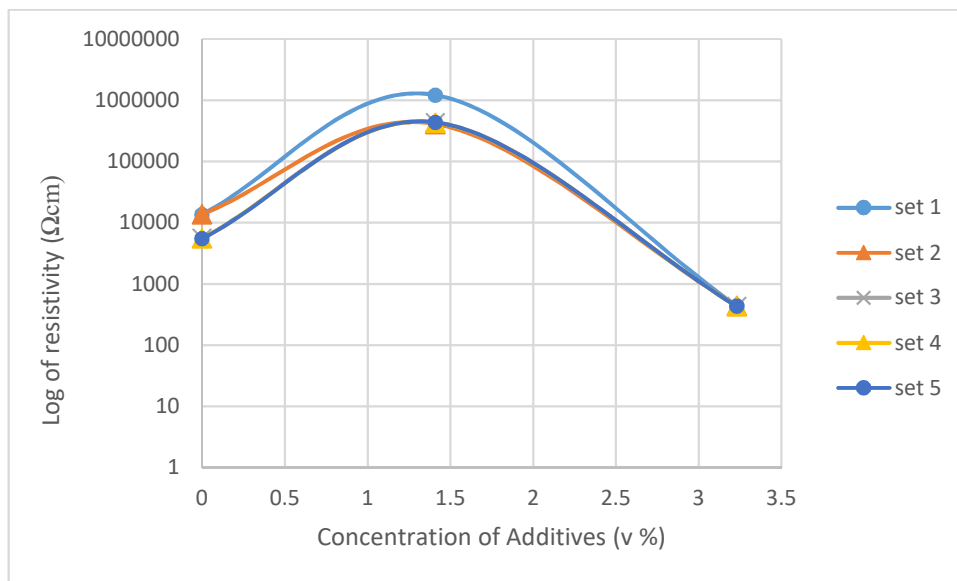


Figure 5.15: Abrasion modified spincoated samples at 5V using Keithley 6517b

Any further work could use either of these modifiers for the substrate but the methyl cellulose would give better electrical repeatability. The spincoated modified samples although 1 μm thicker than the unmodified samples are the better samples to go forward into a bulk processing application since without the modification there is no adhesion to the substrate.

5.5 Spectroscopy

Individual samples were analysed in order to find indicators of the conductive mechanisms.

5.5.1 Ultra Violet (UV) spectroscopy and Charge carriers

A UV investigation of specific samples was performed in order to compare any differences found. Figures 5.16 and 5.17, show a peak at around 760 nm in two samples. The peak in the 97 % PEDOT:PSS is at 760 nm and the 3 peaks in the 98 % PEDOT:PSS samples are at 744, 765 and 774 nm. Abdulla (Abdulla and Abbo, 2012) attributed peaks occurring at around 750 nm to radical dications or bipolarons, being formed. However, this was in polypyrrole not in PEDOT:PSS. Nabid (Nabid, Asadi *et al.*, 2010) found polarons at 750 nm in PEDOT and states this is indicative of conductive PEDOT and shows in UV when in the conductive state. Arias-Pardilla (Arias-Pardilla, Gimenez-Gomez *et al.*, 2012) and Feng (Feng, Li *et al.*, 2007) also identified polarons at 750 nm in PEDOT. Neutral polymer chains absorb UV at 600 nm. No peaks were found around 600 nm or above 774 nm. This means, assuming UV is picking up charge carriers at 744 to 774 nm, the chain is not in a neutral configuration. Chains in the polaron state according to several researchers, absorb in IR. Several authors also state that the polaron state is a radical cationic state (Bredas, Themans *et al.*, 1984, Bubnova, Khan *et al.*, 2014). As discussed in the Literature Review, removal of the electron to form a radical cation also changes the geometric structure of the molecule to give a quinoid structure rather than an aromatic structure. This can be detected using IR and UV techniques.

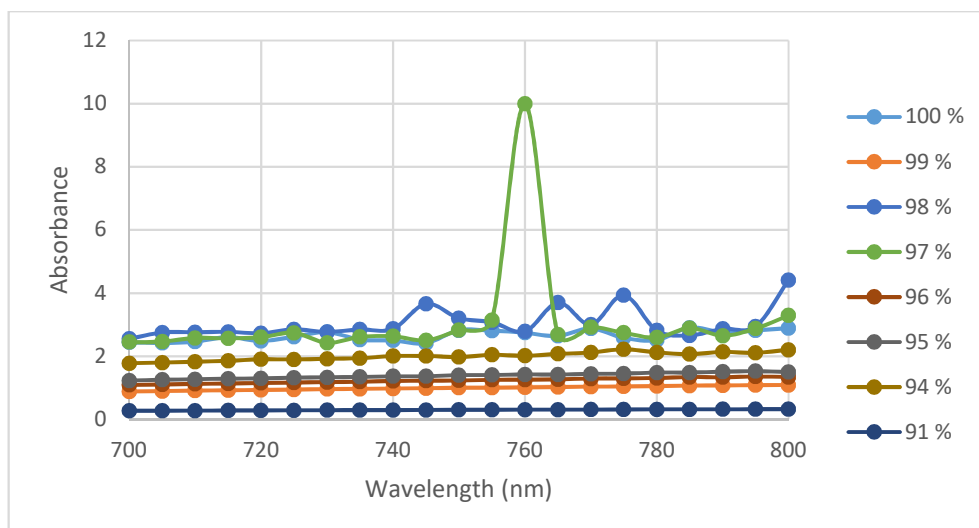


Figure 5.16: UV Spectra showing all solutions at 700-800 nm

Comparison of the original data generated by the instrument, with that in Figure 5.16 showed the original data to be very noisy at the lower wavelengths. This is shown in Figure 4.75. However, the peaks shown in Figures 5.16 – 5.17 were still found to be present in the original data. Due to the high levels of noise the region below 350 nm was ignored for the purposes of analysis so only the region from 350 nm to 800 nm were analysed.

The original data still shows similar peaks around 760nm to those shown in Figure 4.75. The peaks were detected in two of the samples. The 97 % sample had only a very small peak but the 98 % sample had several definite peaks which may confirm the presence of polaron charge carriers being detected at this wavelength. Due to the noise effect shown in Figure 4.75 it is difficult to say for certain of this shows detection of polarons.

It could be that the doping with TWEEN 80 and MEK has caused a change in geometry of the PEDOT molecules possibly due to swelling (Bredas and Street, 1985) of the particles due to treatment with the solvents. A search of the literature has shown

nothing in either TWEEN 80 or in PEDOT:PSS to identify what these peaks can be. However, Meng (Meng, Perepichka *et al.*, 2003) did detect bipolarons in sorbitol doped polythiophene at 760 nm with a stated bandgap of 1.63 eV. The 100 % samples of PEDOT:PSS, TWEEN 80 show no peaks here. Neither do any of the other samples.

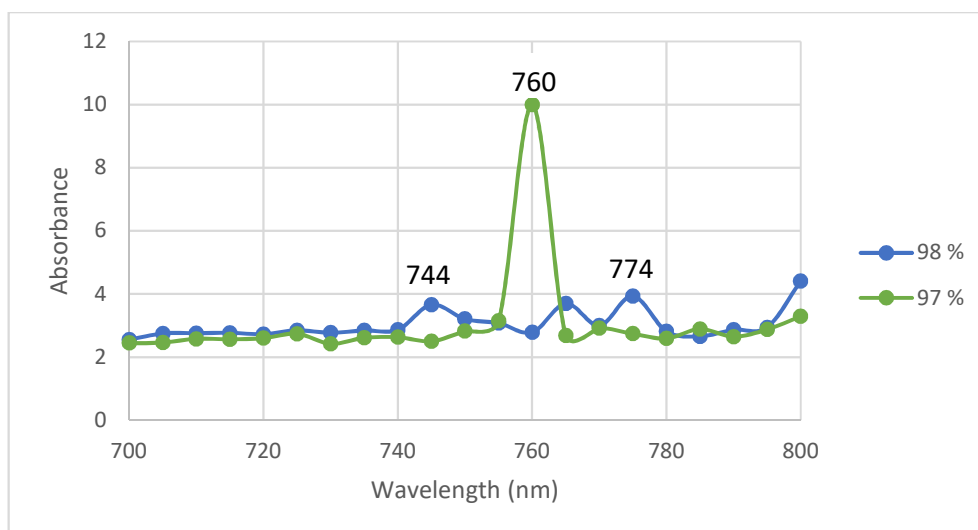


Figure 5.17: UV spectra of 97 % PEDOT:PSS sample and: 98 % PEDOT:PSS sample

Han (Han and Foulger, 2004) states that in oxidised and doped, conjugated polymers, a peak at a wavelength of 777 nm shows the detection of polaron and bipolarons where they are elevated from the VB band to an intergap band below the CB band. Han references the seminal work of Bredas (Brédas, Wudl *et al.*, 1987) and DeLongchamp (DeLongchamp and Hammond, 2001) here. This is pretty close to the peaks detected in the 97 % PEDOT:PSS and the 98 % PEDOT:PSS samples shown in Figure 5.17. Since no other references have been found to explain these peaks it must be concluded that these peaks probably show detection of polaron or of bipolaron activity. According to the research paper by Bredas (Bredas and Street, 1985) who, when using polypyrrole as the model, there is a possibility of two different

optical transitions when bipolarons are present on a conjugated polymer chain. Both of these occur below the band-gap transition. These are from the valance band to the lower bipolaron level and from the VB to the higher bipolaron level. Using the equations 1-4 it is possible to calculate the band gaps as showing in the spectra in Figure 5.17:

$$\Delta E_{(j)} = hf \quad [5.1]$$

$$f = \frac{v}{\lambda} \quad [5.2]$$

$$\Delta E_{(j)} = h \frac{v}{\lambda} \quad [5.3]$$

$$\Delta E_{(eV)} = \frac{h \cdot v}{Q_e \lambda} \quad [5.4]$$

Table 5.7 explains the symbols and calculations in equations 5.1 - 5.4.

Table 5.7: Table of symbols

Symbol	Term	Value	Unit
ΔE	Energy change of electron during transition	s	J or eV
h	Plancks Constant	6.626×10^{-34}	J.s
f	Frequency of absorbed light/photon	To Be Calculated	Hz
v	Speed of Light	2.998×10^8	m/s
λ	Wavelength of absorbed light/photon	Measured Value	nm
Q_e	Charge of an electron	1.609×10^{-19}	C

An example of the calculation:

$$\Delta E = [6.626 \times 10^{-34} / 1.609 \times 10^{-19}] [2.998 \times 10^8 / 760 \times 10^{-9}]$$

$$\Delta E = [4.118 \times 10^{-15}] [3.96 \times 10^{14}]$$

$$f = 3.96 \times 10^{14} \text{ Hz}$$

$$\Delta E = 1.62 \text{ eV}$$

Using this equation the band gap that shows in the UV spectra for samples 97 % PEDOT:PSS and 98 % PEDOT:PSS can be calculated. This is shown in Table 5.8:

Table 5.8: Table of band gaps for the samples in Figure 5.17

λ		ΔE
nm	m	eV
760	7.60×10^{-07}	1.62
744	7.44×10^{-07}	1.66
774	7.74×10^{-07}	1.60
799	7.99×10^{-07}	1.55

Both the 97 % PEDOT:PSS and 98 % PEDOT:PSS samples show peaks at 744 nm and 760 nm and 774 nm, the 97 % PEDOT:PSS sample shows a small peak at 799 nm and a large peak at 760 nm. The peak 799 nm is however right at the edge of the spectra so could continue further beyond where the equipment was able to measure. The peaks are also wide with the 97 %, 760 nm peak stretching from 755 to 760 nm. The other peaks are similarly wide.

A search of the literature has not identified any peaks that normally occur in PEDOT at 744, 760, 774 and 799 nm. Several authors have stated the polaron or bipolaron transition can be detected in various materials (including polymers, and composites) at around 777 nm using UV so this is an interesting result (Brédas, Wudl *et al.*, 1987, DeLongchamp and Hammond, 2001, Han and Foulger, 2004). The calculations show a band gap for these samples of 1.55 -1.66 eV which again is very close to the value stated by Kvarnstrom who states PEDOT has a low bandgap of approximately 1.6- 1.7 eV (Kvarnström, Neugebauer *et al.*, 1999). Pei (Pei, Zuccarello *et al.*, 1994) found the neutral form of PEDOT had a 1.5 eV band gap and the doped form had a 1.6- 2.0 eV band gap. Although this paper dates back to 1994, it was cited in 2013 by Ouyang (Ouyang, 2013a, Ouyang, 2013b). Ashery (Ashery, Said *et al.*, 2016)

believed doping to occur in three stages and that when a 1.5 eV band gap occurred the bipolaron state existed and PEDOT behaves as a metal. De Longchamp (DeLongchamp and Hammond, 2001) states that the most commonly stated band gap for PEDOT is at 1.6 eV. De Longchamp also found that at 860 nm bipolaron charge carriers were detected and at 654 nm polarons were detected in oxidised PEDOT. However, DeLongchamp was using a composite of PEDOT mixed with polyaniline so it would be expected that this would give slightly different results. It is still of interest that these two stated wavelengths show charge carriers in a PEDOT composite and they are very similar to the wavelengths detected in Figure 5.17. It seems likely that only polarons exist in the samples shown in Figure 5.17. This is in accordance with the findings of Zykwiniska (Zykwiniska, Domagala *et al.*, 2003), who found that at low doping levels polarons were the main charge carrier and at higher levels it was bipolarons. It could be that the 97 % PEDOT:PSS and 98 % PEDOT:PSS samples are at the optimum doping for TWEEN 80, and that at lower doping level such as the 99 % PEDOT:PSS sample which is very stable with higher resistivity and higher pH, and that this would be deemed the lowest doping level. This does not account for the conductivity of the 97 %, 95 % or 94 % PEDOT:PSS samples which all conduct similarly as those in Figure 5.19 but show no sign of polaron activity. These samples must therefore conduct by a different mechanism or the polarons are generated so fleetingly they cannot be detected by UV.

Gao (Gao, Liu *et al.*, 2002) believed the bipolaron charge carrier was the dominant structure in conducting polythiophenes of which PEDOT is a family member.

Bredas (Bredas and Street, 1985) found that the absorptions between the gap levels disappear (with ESR) as the doping level was raised and the absorptions change to one single larger peak. Similarly, with the samples shown in Figure 5.16 as the doping level rises the peaks disappear. The 98 % PEDOT:PSS sample has several smaller

peaks, the 97 % PEDOT:PSS sample has two of which one is larger and then as the concentration of the surfactant rises so the peaks get smaller and disappear. Bredas attributes this to the transition of the polaron to a bipolaron.

Although, the exact mode of measurements are different, it is of interest to note that the 98 % PEDOT:PSS sample shown in Figure 5.17 has peaks at 744, 760, 774, and 799 nm, whereas the 97 % PEDOT:PSS sample has a large peak at 760 nm and a small peak at 799 nm. Both of these solutions have enhanced conductivity when referenced to the 100 % PEDOT:PSS material. This could indicate evidence of the transition between the polaron state to bipolaron state at the change in concentration of PEDOT:PSS between the 98 % PEDOT:PSS and 97 % PEDOT:PSS samples. Also interesting is the fact the 98 % sample is right at the edge of Zone 2 and has a slightly higher resistivity than the rest of the Zone two samples and yet this sample shows what appears to be polaron or bipolaron activity.

Bredas experimented with several other conducting polymers including polythiophene, the parent molecule of PEDOT, and found very similar results. Polythiophene, unlike polypyrrole, is believed to attain metal-like conductivity. Bredas believes this to be due to the merging of the upper and lower bipolaron bands in the VB and CB levels. When a p-type of doping is achieved this means the new level will be formed in the VB and this will be empty. It must also be remembered that Bredas was measuring polythiophene and not the more stable PEDOT. As explained by Bredas (Bredas and Street, 1985) at higher dopant concentration the peaks from bipolarons get smaller and disappear. This may explain why the higher surfactant samples show no polaron or bipolaron peaks. Bredas also found the bipolaron peaks disappear as the dopant concentration is increased. The conductive 94 % to 96 % PEDOT:PSS samples show no defined peaks, but only much smaller peaks hinting at a change in mechanism at this point. This indicates the mechanism of conductivity

probably changes with the concentration of the solutions. All the other samples are missing the peaks that could be representing the presence of polarons/.bipolarons. It is assumed that the rest of the Zone 2 samples, conduct using a hopping mechanism rather than the polaron/bipolaron mechanism detected in the 97 % PEDOT:PSS and the 98 % PEDOT:PSS Zone 2 samples. It is believed bipolarons are the major charge carriers in doped PEDOT systems. However the spectra obtained found evidence of what is probably polarons not of bipolarons. It can be concluded that the Cary 60 UV-Vis detects the propagation of polaron charge carriers in some samples at these wavelengths.

5.5.1.1 PSS identification

Every sample regardless of the concentration of additives contains PSS. All samples also have a large peak at 205-264 nm which although it shifts slightly, seems to be an identical shaped peak and can be attributed to both TWEEN 80 and PEDOT:PSS. This explains the noisy peak observed on every sample in this region, but means it is of no use in identifying species of interest. PSS and any changes occurring in the PSS could not therefore be detected using the method.

5.5.2 Vibrational spectroscopy

Using the films which were previously annealed onto glass slides and then scraped off and ground with dried KBr to form discs the samples were analysed using IR.

5.5.2.1 Infra red

In most PEDOT:PSS analyses, the region which is of most interest is that between 500-1600 cm^{-1} , so for the purpose of this PhD thesis, this is the region that will be studied in most detail. According to Han, (Han and Foulger, 2004), PEDOT:PSS can be recognised by peaks found at 1600 cm^{-1} and below. Although there are peaks at

3593 and 3471 and 3332 cm^{-1} these are attributed to CH_2 and the C-H of the aromatic ring groups and the O-H at 3000-3900 cm^{-1} (Cristovan, Nascimento *et al.*, 2006). There is normally no OH group expected in PEDOT:PSS, however they are present in TWEEN 80 and also in water which may be present even after annealing. Most of the IR spectra have a slanting baseline. This is shown in Figure 5.18. While it is possible to alter this and correct it, it is of note to discover that a slanting baseline in ATR is often indicative of a conductive sample (Shimadzu Scientific Instruments).. This is particularly the case when the baseline slopes to the right where, as is conventional in IR, the wavenumber increases from left to right.

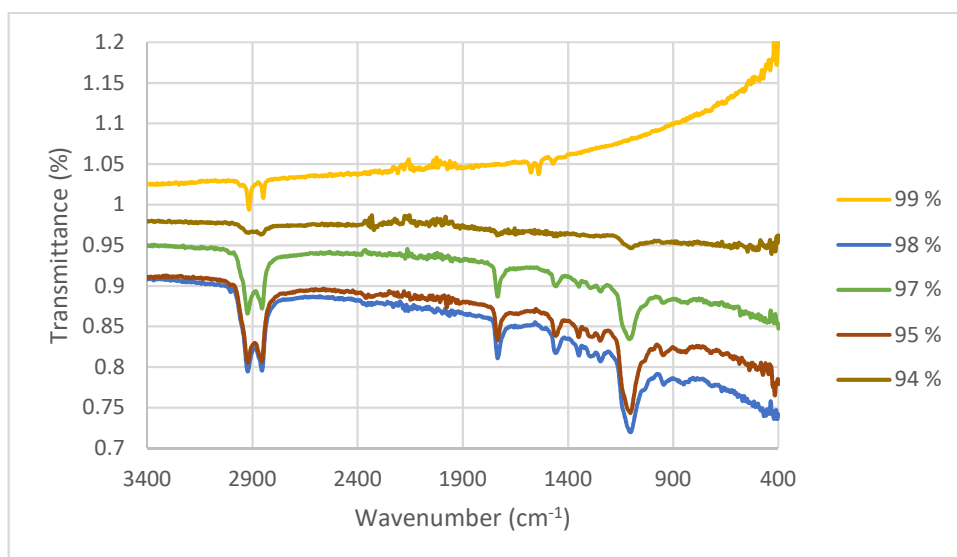


Figure 5.18: KBr discs of the PEDOT /TWEEN 80/MEK annealed films from 4000 to 500 cm^{-1}

Figure 5.18 shows a carbonyl in most samples at around 1700 cm^{-1} and a wide COC and SO_2 peak at around 1100 cm^{-1} . However, some samples are missing both of these peaks. This will be discussed further in Sections 5.5.2.3 and 5.5.2.4. Note that the lower surfactant samples do not have the carbonyl peak. This means the PEDOT ring may have ruptured or that one or both of the two oxygen groups at the 3 and 4 positions may have become protonated in order to become OH groups. Alternatively,

the higher pH of these samples is causing an aromatic structure which does not allow for conformational change to the more conductive quinoid form. Or perhaps the aromatic form is causing the higher pH. This is discussed further in Sections 5.5.2.3 and 5.5.2.4

5.5.2.2 Aromatic and aliphatic CH groups.

The following spectra are analysed using the information found in Table 5.9. As is shown, there are differences in the interpretations of the functional groups in the spectra collected by different research groups. For example Han *et al* agree with Friedel *et al* that the C=C group is around 1600 cm^{-1} . However, Friedel denotes this is due to the PSS groups whereas Han simply says it is due to the aromatic C=C groups which may also apply to the C=C in PEDOT. The different research groups also identify different functional groups at the same place in a spectrum making it difficult to tie down a definite analysis of any one functional group in a spectrum.

Table 5.9: Table of functional group analysis by IR using different literary reports.

Research group	Functional group	Wavenumber (cm ⁻¹)	Description
Han (Han and Foulger, 2004)	C-O-C	1234	Stretch of ethylenedioxy in ring
		1068	
	C-C, C=C	1357	Stretch of quinoid tautomer of thiophene ring
	C-S	989	Stretch in thiophene ring
		856	
		700	
	C-H	3000-3070	Stretch of the C-H groups of PSS
	C=C, C=C-H	1500-1600	Stretch and out of plane bending
		950-1225	2 or 3 bands due ring torsion
		730-770	
		680-720	
Friedel (Friedel, Keivanidis <i>et al.</i> , 2009)	C-O-C	1240	Stretch of ethylenedioxy in ring
	C-C, C=C	1350	Thiophene ring deformation
	C=C, C=C-H	1600	PSS ring, Stretch and out of plane bending
	H ₂ SO ₄	<600	Sulphuric acid
	S=O	1180	Vibration
	O-S-O	1030	Vibration
	Unassigned peak	1542	Unassigned peak possibly due to deformation of the phenyl rings to which the S-O groups attach in PSS
	C=C, C=C-H	1530-1560	Aromatic ring Stretch
	C-H	3186	Ring vibration
		3151	
	Doping Induced band	1529	Doping Induced band- not assigned
	C=C	1469	C=C vibration
		1437	
	Doping Induced band	1415	Doping Induced band- not assigned
	C-C	1381	Vibration
	SO ₂	1339	Asymmetric stretching
		1296	Inter-ring vibrations
	C=C, COROC	1176	Vibrations
	SO ₂	1132	Stretching
	COROC	1070	Vibrations
		1045	
Cristovan (Cristovan, Nascimento <i>et al.</i> , 2006).	O-H	3000-3900	OH group

Different researchers also describe functional groups differently and designate for example COROC at 1176 and 1070-1045 cm⁻¹ (Sandoval, Suárez-Herrera *et al.*, 2015) whereas Han and Friedel both identify COC at 1234 and 1240 cm⁻¹ respectively

(Friedel, Keivanidis *et al.*, 2009, Han and Foulger, 2004). In reality both groups are describing the ethylenedioxy groups but from different angles as shown in Figure 5.19. However, there is actually only a small difference between the ranges and all samples shown in this report have a prominent COC peak between 1000 and 1200 cm^{-1} which may mean a contribution from both functional groups. For ease of explanation, in this thesis, this is described as the COC group.

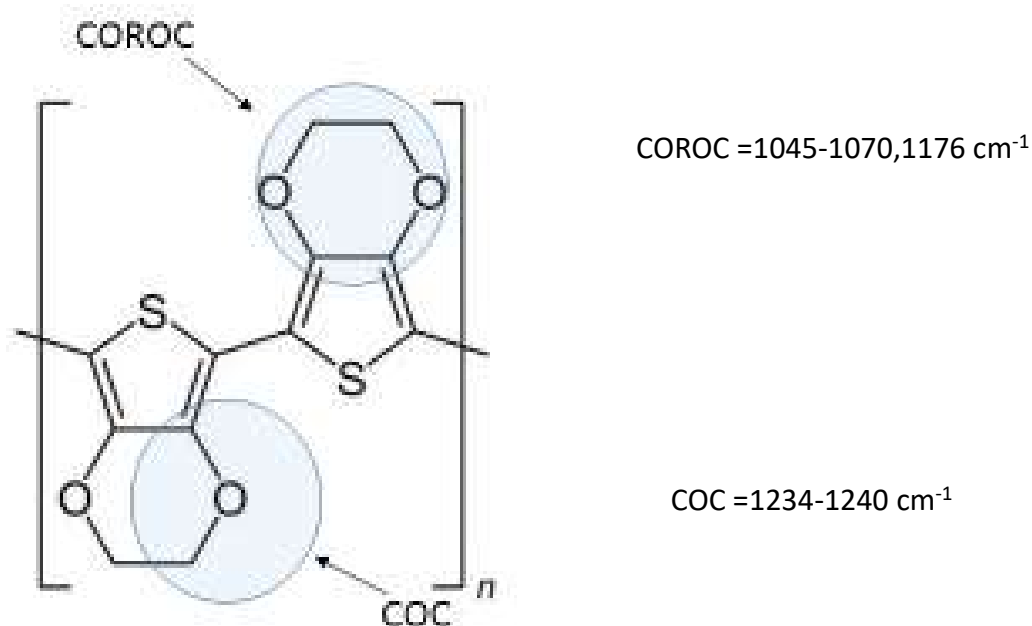


Figure 5.19: The difference between COC and COROC

In 100 % PEDOT:PSS, which is shown in Figure 5.20, the aromatic CH peak is found above 3000 cm^{-1} . This is confirmed by the research groups listed in Table 5.9. The aliphatic CH peak is usually large as is shown in Figure 5.20, which shows a doublet at 2857 cm^{-1} due to the aliphatic CH groups on PEDOT, PSS and TWEEN 80 as well as any MEK which could still be present after annealing. The small peak at 2349 cm^{-1} is due to the presence of CO_2 .

Friedel's thiophene ring deformation which occurs at 1360 cm^{-1} correlates with Han's C-C and C=C stretch of the quinoid tautomer at 1357 cm^{-1} . Friedel found what is described as an unassigned peak at 1542 cm^{-1} and Sandoval found what is described as a doping induced band at 1529 cm^{-1} . This may be another region where the quinoid form of PEDOT is located. However, Han identified the quinoid groups at 1357 cm^{-1} . Sandoval found a second doping induced band at 1415 cm^{-1} which is again not assigned to any particular group but probably belongs to either C=C or C-C. The different chemical environments have affected the exact position of the appearance of the functional groups. However, they are close enough to be able to identify similar functional groups in Figures 5.20 to 5.29.

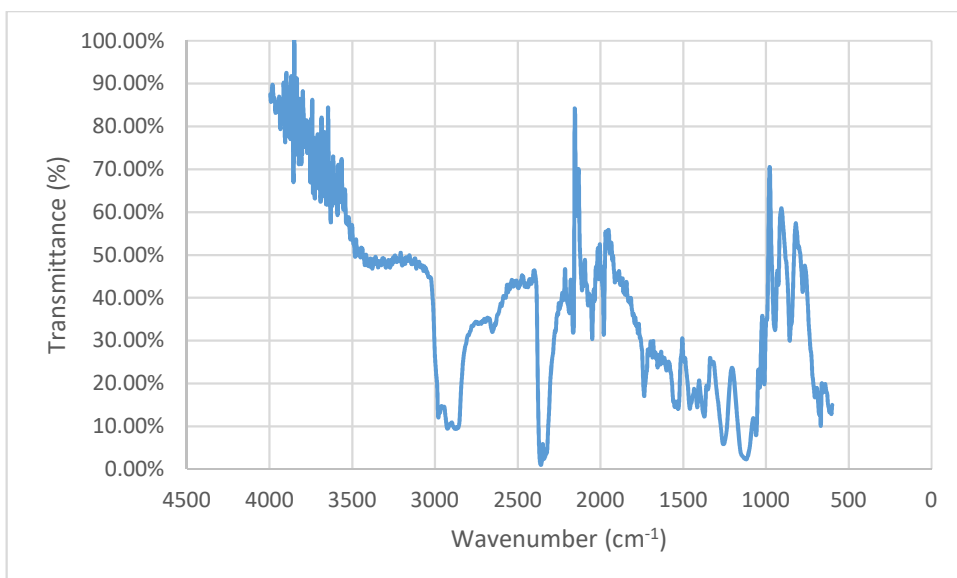


Figure 5.20: IR of the 100 % PEDOT:PSS

The peaks found in 100 % PEDOT:PSS are listed in Table 5.10.

Table 5.10: Functional groups found in 100 % PEDOT:PSS annealed film

Wavenumber(cm^{-1})	Functional group	Explanation	References
3000-4000	CH or OH	stretch of the C-H groups in PSS or OH groups in either water or in TWEEN 80.	Han (Han and Foulger, 2004), Sandoval (Sandoval, Suárez-Herrera <i>et al.</i> , 2015) both found this peak in PSS.
2655, 2362	C-H	aliphatic	
1736	C=O	Carbonyl group due to the two oxygens on the ring structure at 3,4 positions.	
1655	C=C	C=C alkene	
1529-1502	C=C	C=C aromatic	
1458	CH	Aromatic ring bending	
1415	CH	Is this also due to the quinoid structure?	
1372- 1380	CH or C=C	Quinoid	(Han and Foulger, 2004)
1258	C-O-C	Stretch of ethylenedioxy in ring	(Han and Foulger, 2004)
1119	SO ₂		(Friedel, Keivanidis <i>et al.</i> , 2009)
1060	COROC vibration		(Sandoval, Suárez-Herrera <i>et al.</i> , 2015)
1038	O-S-O stretching		(Friedel, Keivanidis <i>et al.</i> , 2009, Sandoval, Suárez-Herrera <i>et al.</i> , 2015)
856	C=C BEND		
669	SH/C-C	Could be SH or C-C	

The vibration found at 3000-4000 cm^{-1} was attributed by both Han and Sandoval to be due to the CH bonds of the PSS molecules however this could also be caused by OH groups. The peaks between 1980 and 2165 cm^{-1} are likely noise peaks as you don't tend to have anything absorbing in this region.

At 1458 cm^{-1} there is a peak representing the stretching mode of the aromatic C=C and C-C groups which are found in the PEDOT ring structure.

5.5.2.3 Carbonyl (C=O) peak

All of the more conductive Zone 2 samples have a definite carbonyl group in IR. PEDOT:PSS should not have a carbonyl peak. In Figure 5.20 showing the full IR spectrum for 100 % PEDOT:PSS, there is a carbonyl group at 1736 cm^{-1} . This is believed to be caused by the presence of the two COC groups in the PEDOT ring structure. Most references find a peak at 1638-1655 for the CH groups but not a carbonyl. There was a study on over-oxidised polythiophenes (Barsch and Beck, 1996) which found the over-oxidised polymers had a carbonyl which was part of terminal COOH groups which can form under certain conditions such as at very high pH. However, the measured pH was not as high, Barsh overoxidised at pH14, and for these to form the polymer should be losing conductivity and this has not been found to have been the case with the least conductive samples being those which do not have the carbonyl group. In Figure 5.21, the carbonyl in the Zone 2 samples moves as the PEDOT concentration surfactant decreases from 1729 to 1733 cm^{-1} . This may be due to the influence of the different chemical environments of different samples which change with increasing surfactant and MEK concentration.

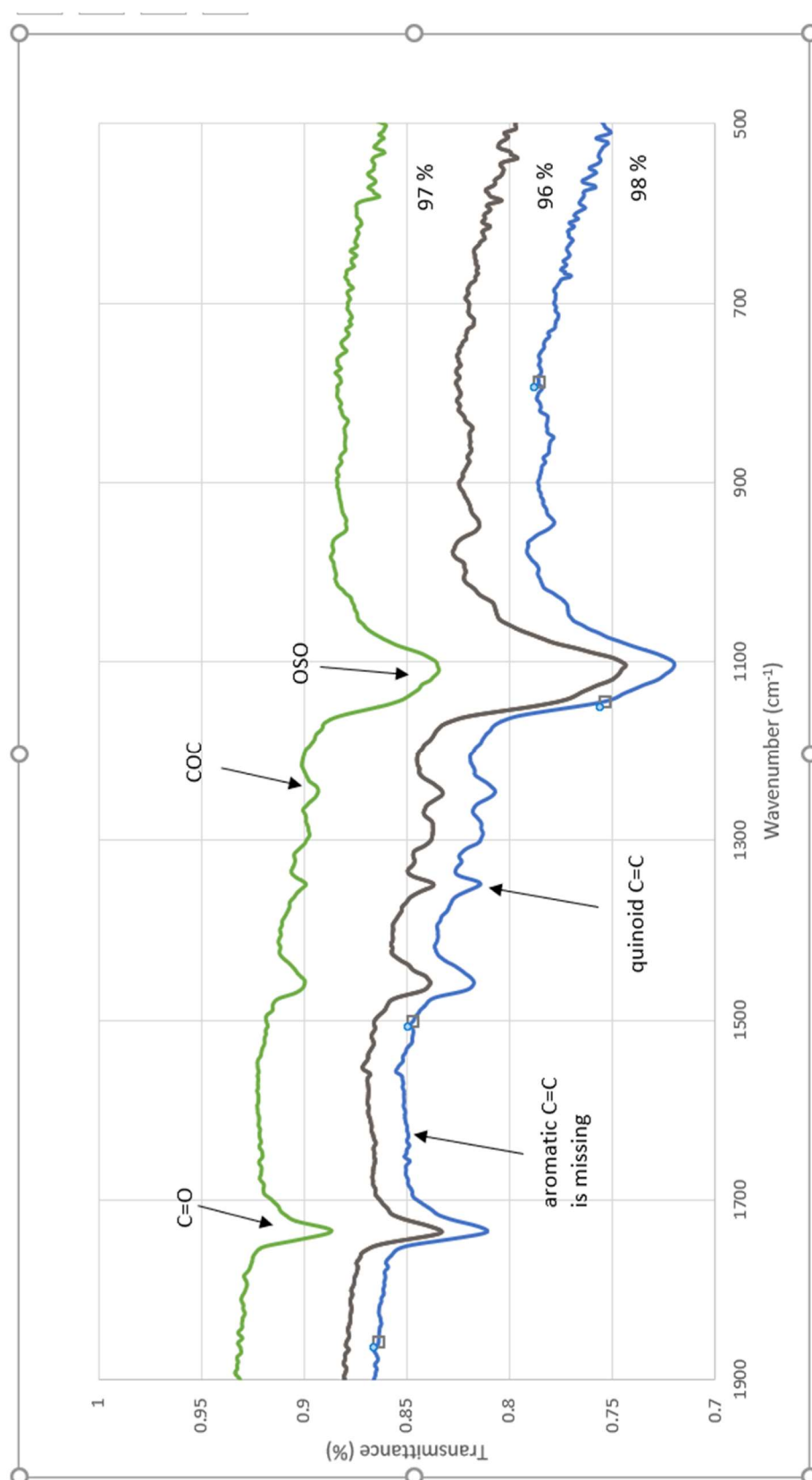


Figure 5.21: The samples in the conductive region (The 98 %, 97 % and 96 % PEDOT:PSS samples) from 1900 to 500 cm^{-1}

It should be noted, that the 99 % PEDOT:PSS sample, (Figures 5.22 and 5.23) show no carbonyl peaks around 1700 cm^{-1} , so these have disappeared either due to rupture of the rings or to protonation causing OH groups. Alternatively, it could be that the $\text{C}=\text{O}$ is a temporary arrangement and therefore it has not formed at all hence it is not detected. If the $\text{C}=\text{O}$ group forms to stabilise the moving electrons in a quinoid structure by donating unpaired electrons from the O atoms to the carbon this may form a stable arrangement when the molecule is in the quinoid form.

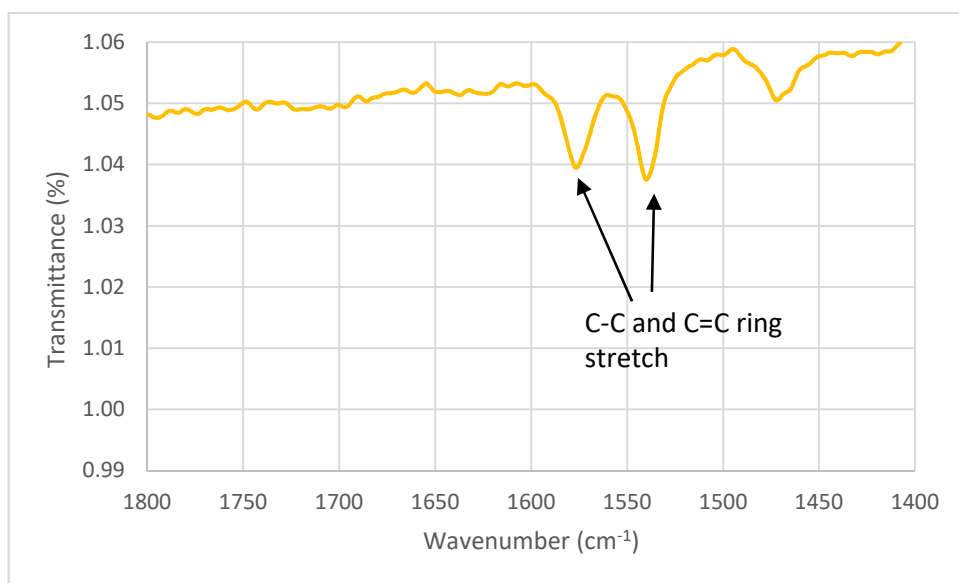


Figure 5.22: IR showing carbonyls are not present in these Zone 3 samples

Due to the fact the ring structure may rupture it is also necessary to look above the 3000 cm^{-1} region to determine if the carbonyl groups present on the ring structure may have become protonated. There is the suggestion of an OH peak at $3417\text{--}3500\text{ cm}^{-1}$ as shown in Figure 5.23 which would confirm this assumption. This is present in both of the less conductive Zone 3 samples, the 98 % PEDOT:PSS and the 99 % PEDOT:PSS samples. However, this OH peak is also present to a lesser

extent in the rest of the samples and may be due to bound water molecules which have been incompletely removed during annealing.

It would be expected that since there is no amine group in PEDOT:PSS that no amine peak should be present. However, it was noted by Jönsson (Jönsson, Birgersson *et al.*, 2003) that even pristine PEDOT:PSS absorbs nitrogen from the atmosphere. This means that PSS absorbs the ammonia gas from the atmosphere in the presence of water. This leads to the formation of the complex PSS.NH_4^+ (Jönsson, Birgersson *et al.*, 2003). So this peak, or part of this peak, found in Zone 3 samples at around $3000 - 3500\text{cm}^{-1}$ may in actual fact be due to the presence of the complex PSS.NH_4^+ rather than simply to either water or the OH peak of hydrated ether groups from the PEDOT ring structure. Since the PEDOT:PSS used for these experiments was solvated in water this possibility must be kept in mind. Ammonia produces peaks as shown in Table 5.11.

Table 5.11: Table of IR absorptions of Ammonia

3534 cm^{-1} (IR intensity = 0.052) (Raman active)	N-H symmetric stretching (Purdue University)
3464 cm^{-1} (IR intensity = 0.073) (Raman active)	N-H asymmetric stretching (Purdue University)
3464 cm^{-1} (IR intensity = 0.073) (Raman active)	N-H asymmetric stretching (Purdue University) (e)
1765 cm^{-1} (IR intensity = 1.1×10^{-6}) (Raman active)	H-N-H scissoring (Purdue University) (e)
3100-3500	Amines (Royal Society of Chemistry)

OH peaks are wider and larger in general than ammonia peaks which may help to distinguish between the two. Figure 5.23 shows what could either be an ammonia or an OH group.

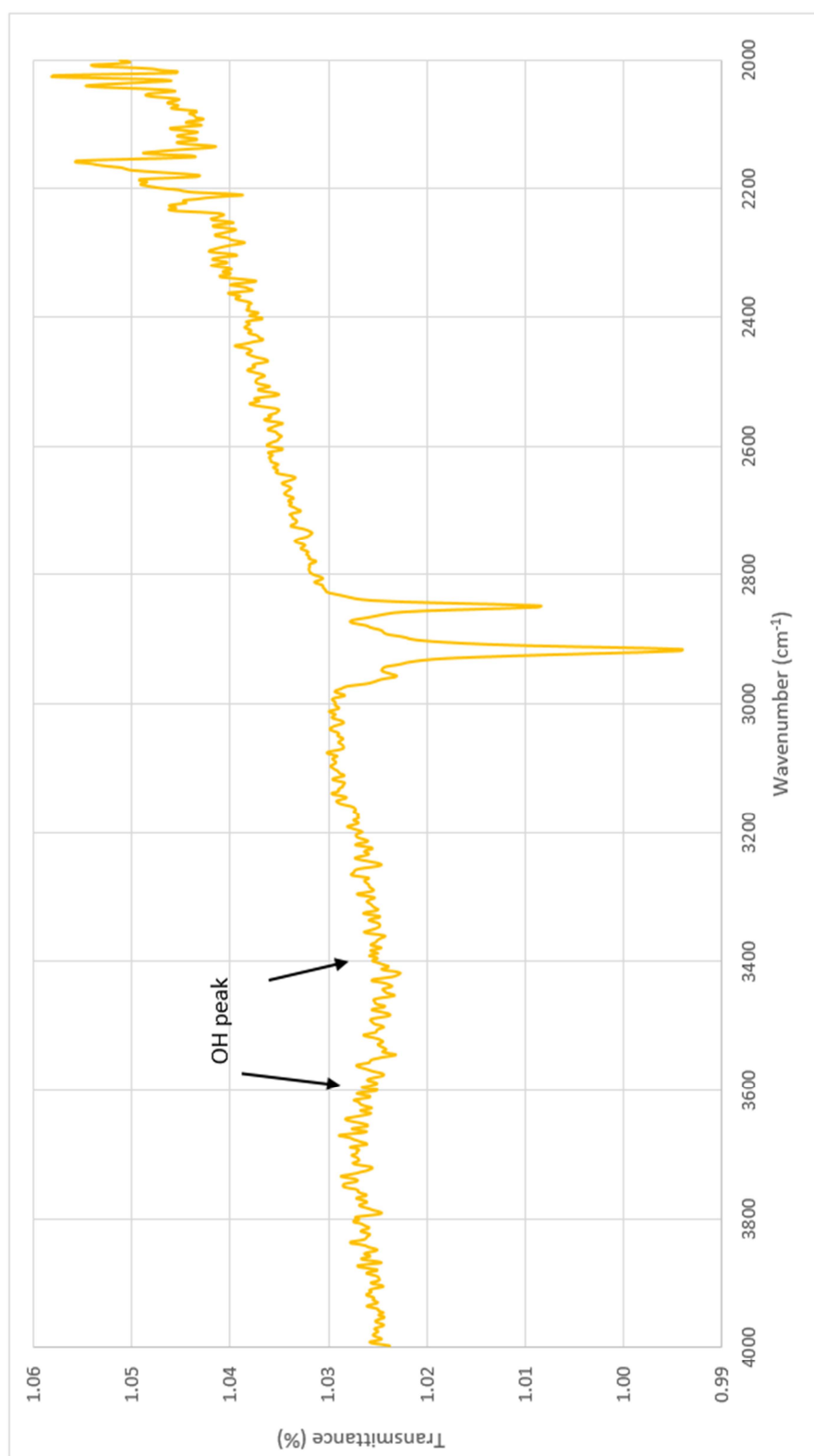


Figure 5.23: IR of the Zone 3 samples showing a possible OH peak.

The peak is wide but is not large. Since the carbonyl was not found to exist in this sample it is more likely that the peaks found around 3400 cm^{-1} are caused by OH groups. Ammonia usually gives more defined peaks but if both ammonia and OH were present this could still account for this peak. It seems that as the samples lose conductivity they also lose the carbonyl peak. However, it is more likely that the peak comes from the OH of water since if there is any ammonia present it must come from absorbed water molecules, which would mask the peak from ammonia regardless.

5.5.2.4 C-O-C groups

All the researchers listed in Table 5.9, found the C-O-C group in the wavenumbers 1240, 1176, 1070 and 1045 cm^{-1} . As stated by Friedel (Friedel, Keivanidis *et al.*, 2009), this functional group is generally used to identify PEDOT. As seen in the IR spectra shown in Figures 5.24 and 5.25, there is a wide peak between $1190 - 1009\text{ cm}^{-1}$. This can be attributed to the vibrations from the COC ethylenedioxy group in the ring attached at points 2 and 3 of the thiophene ring in PEDOT and to the SO_2 groups. Because the peaks are merging together it is difficult to separate the two peaks.

The COC functional group is the most prominent identifiable peak found in the IR spectra in Zone 2 samples as well as in the 100 % PEDOT:PSS. This is also shown in Figure 5.21 where the peak around 1700 cm^{-1} in the mixtures of PEDOT with TWEEN 80 and MEK is due to the two dioxy structures at the 3 and 4 positions. It could however be caused by MEK which contains a carbonyl group. In theory the annealing step should remove the MEK however it could be that there are traces remaining or that the MEK has reacted in some way with the other reagents in the mixture. However, this is for further study and beyond the scope of this thesis. Similarly, the COC groups may be forming a temporary C=O bond due to either

donation of unpaired electrons into the ring structure to help to stabilise the quinoid state but this is also something for further research to identify. Figure 5.24 also shows how the spectra changes with a change in mixture of the samples.

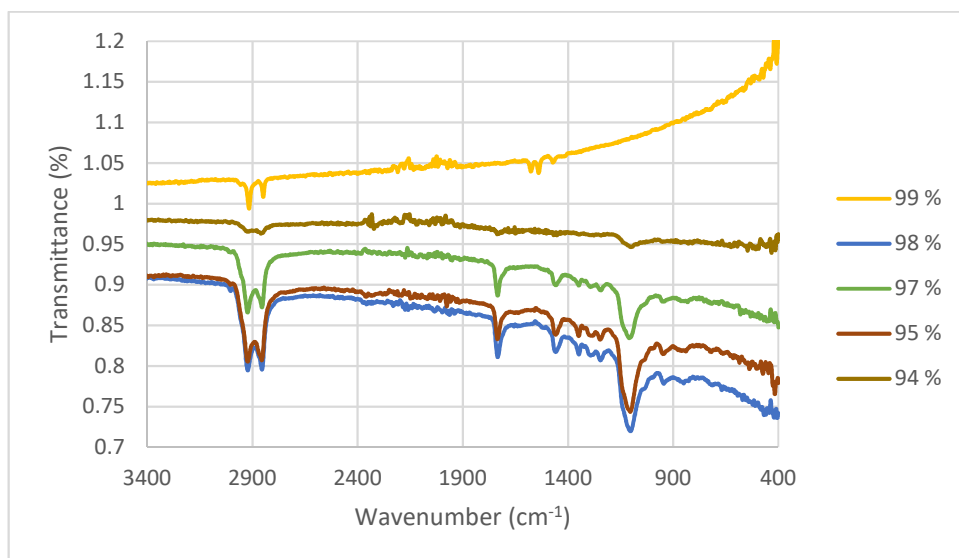


Figure 5.24: The IR spectra of 94 %, 96 %, 97 % and 98 % PEDOT:PSS samples in the most conductive region

At 1193-1123 cm^{-1} there is a COC bond adjacent to a large SO_2 peak in the 96 % PEDOT:PSS sample, 97 % PEDOT:PSS and 98 % PEDOT:PSS samples shown in

Figure 5.25. It is not present in the Zone 3, 99 % samples with the exception of 100 % PEDOT:PSS.

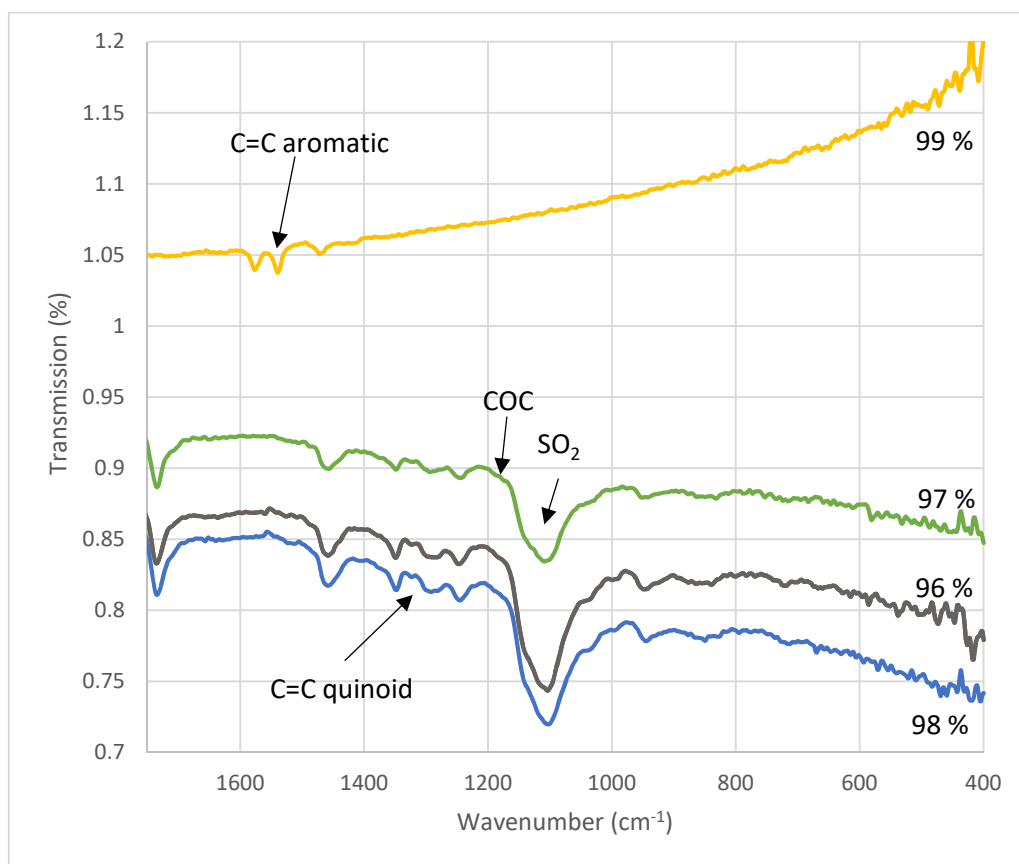


Figure 5.25: IR spectra between 1700 and 400 cm^{-1} for 99 %, 98 %, 97 % and 96 % PEDOT:PSS

There is a small peak at 1346 cm^{-1} attributed by Liu (Liu, Kim *et al.*, 2011) to come from the C-C of the thiophene ring shown in Figures 5.21 and 5.25. These are the most conductive Zone 2 samples. They have a COC group and a carbonyl.

Figure 5.26 shows the full spectrum of the 96% PEDOT:PSS, 97 % PEDOT:PSS, and 98 % PEDOT:PSS, enhanced conductivity samples, found in Zone 2. Detection of polaron activity was discovered in the 97 % PEDOT:PSS, and 98 % PEDOT:PSS, samples using UV. However, it was not shown in the 96 % PEDOT:PSS sample despite the obvious similarity in the IR spectra so despite them showing different

excitations with UV they are seen to be almost identical using IR. As discussed the less conductive samples have no carbonyl or COC group. The 98 % PEDOT:PSS sample is at the border of Zone 2. The less conductive, Zone 3 sample is shown in Figure 5.27.

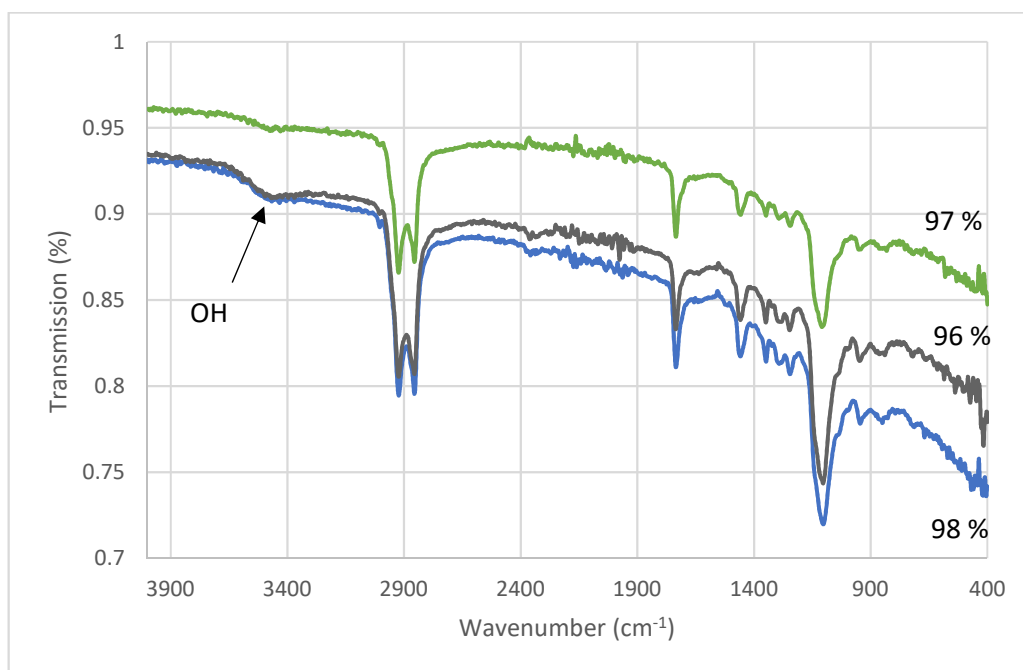


Figure 5.26: The full spectra of 96 % PEDOT:PSS, 97 % PEDOT:PSS, and 98 % PEDOT:PSS samples

Note that Figure 5.26 shows the both the carbonyl peak at around 1700 cm^{-1} and COC/SO₂ peaks at 1100 cm^{-1} . The lower surfactant samples such as the 99% PEDOT:PSS sample shown in Figures 5.25 and 5.27, do not have the carbonyl peak or COC and SO₂ peak. This peak is not present in the top sample shown in Figure 5.25. This suggests that either the PEDOT ring has ruptured causing one or both of the two oxygen groups at the 3 and 4 positions may have become protonated in order to become OH groups or they are not forming a temporary carbonyl hence the aromatic structure prevails over the quinoid. Figure 5.27 also shows a Zone 3, 99 % PEDOT:PSS sample which has no COC/SO₂ or carbonyl group but instead has a different peak to the other samples found as doublet at 1538 cm^{-1} . This is believed to

be an aromatic C=C group and shows this sample is not in the quinoid form so is unlikely to be as conductive. It is not present in the enhanced Zone 2 samples so this is probably the point at which the conformational change takes place where the samples change from aromatic to quinoid.

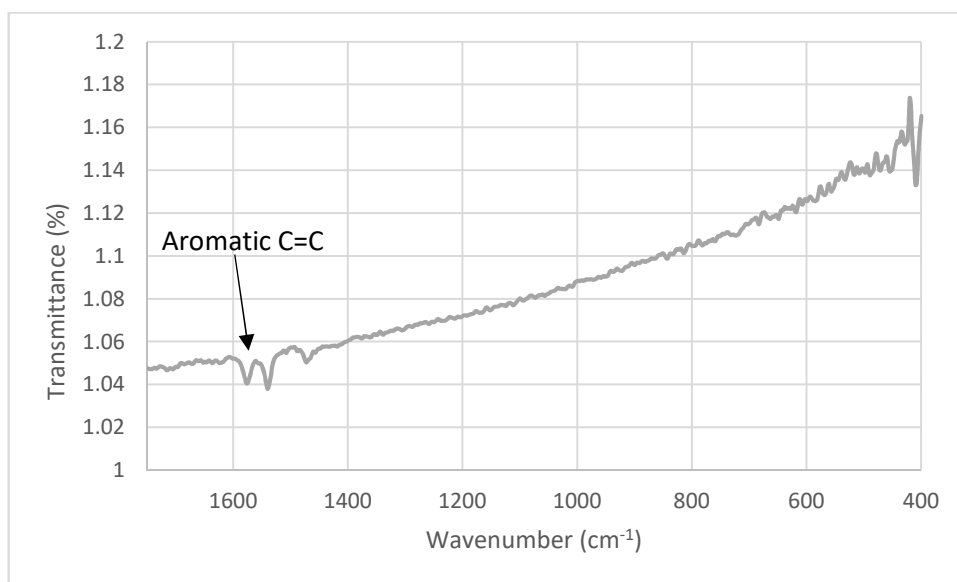


Figure 5.27: IR of the C=C aromatic peaks in the 99 % PEDOT:PSS Zone 3 sample at 1540 and 1575 cm^{-1}

It may also mean the formation of a temporary carbonyl group is necessary to stabilise the now energetic quinoid form and the samples which conduct need to be in the right conformation to allow formation of a carbonyl in order to allow the rest of the molecule to become quinoid and therefore conductive. This is also the sample with highest pH so this could be stopping formation of the carbonyl group and therefore formation of a quinoid structure. Or the aromatic form could be causing a higher pH.

5.5.2.5 Aromatic-quinoid transition

From the literature most researchers report the quinoid peak to be between 1300 - 1460 cm^{-1} and the aromatic C=C to occur around 1600 cm^{-1} . In all enhanced conductivity Zone 2 samples there were peaks found in this region. Han and Foulger (Han and Foulger, 2004) identified the quinoid group to be found at 1357 cm^{-1} in doped

PEDOT:PSS. However, this was a different analogue of PEDOT:PSS and in a different chemical environment. There are multiple peaks in the 100 % PEDOT:PSS, Figure 5.28 between $1372 - 1380 \text{ cm}^{-1}$ which are believed to be due to the C=C and C-C of the aromatic-quinoid transition. The presence of these peaks show the 100 % PEDOT:PSS is in the conductive state. However, there are also C=C peaks around 1600 cm^{-1} which belong to the aromatic form of PEDOT and the 100 % sample also shows these so not all sites on the polymer have been ionised which is as expected. There is a noticeable change as the Zone 2 samples change to Zone 3 and the number of quinoid to aromatic groups alters as shown in Figure 5.25, with the Zone 2 samples having far more peaks in this region.

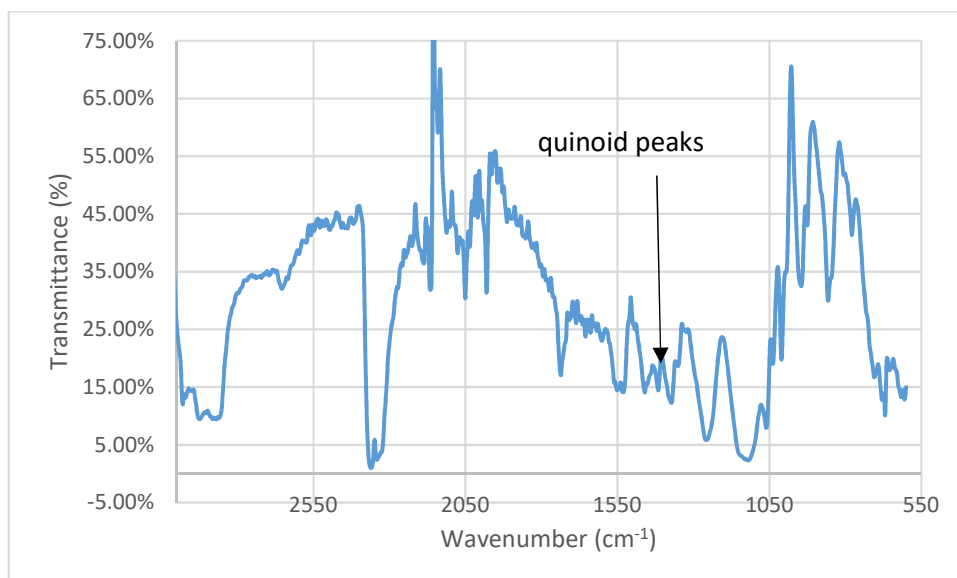


Figure 5.28: IR of 100 % PEDOT:PSS showing the the quinoid group peaks .

There is also a peak at 1415 cm^{-1} . Several researchers as shown in Table 5.9, have found peaks in doped analogues of PEDOT in this area but no one seems to have made any definite assumptions as to what causes this peak in PEDOT:PSS. It is simply described as a “doping induced peak”. Doping is used to cause the molecule to become more conductive. This entails generation of charge carriers, which are more likely to be present and to flow through the material if the molecules are in

quinoidal form. However, methyl and methylene alkanes also appear at this region so this is could also caused by methyl end groups on the polymer chains. This could then mean the chains are breaking and this peak appears as shorter molecular weight chains occur.

Peaks found at 1357 cm^{-1} were attributed by Han (Han and Foulger, 2004) to the C - C and C = C of the quinoid structure of PEDOT, as the thiophene ring transforms from the aromatic to quinoid structure, when generating charge carriers. These can be seen in Figures 5.21, 5.24, 5.25, and 5.28. Since, in order to conduct electrically the structure should be in the quinoid form this peak is important. Friedel reports this just as thiophene ring deformation rather than saying directly it is due to the transition between the aromatic and the quinoid tautomers. However, depending on how it is analysed ring deformation could mean a conformational change from the aromatic to the quinoid, or it could simply mean twisting and bending of the ring. Maybe Friedel failed to pick-up on the possibility his research had shown the transition from aromatic to quinoid. It is concluded in this research that the quinoid form probably shows in IR between $1300\text{-}1460\text{ cm}^{-1}$ and that both forms are present in all except the doped Zone 3 samples. The aromatic form was found in the Zone 3 samples as is shown in Figures 5.22 and 5.23.

5.5.2.6 Sulphur groups and the fingerprint region

According to Nasybulin (Nasybulin, Wei *et al.*, 2012) the conductivity depends of the amount of the PSS present. Elschner (Elschner, Kirchmeyer *et al.*, 2011) believes the PSS takes no part in the charge transport and is only present to provide a template for the dispersal of the PEDOT and to aid film forming properties. Whichever is correct, it would be ideal to be able to distinguish the PSS from the PEDOT in the IR spectrum. However, sulphur groups are difficult to see in IR, as shown in Figure 5.29,

being mainly in the fingerprint region. Where they can be seen, they exist at the same places as other more prominent groups. Sun (Sun, Zhao *et al.*, 1998) states that the SH group occurs at $1245\text{--}1255\text{ cm}^{-1}$. The antisymmetric stretching of the group occurs at 1212 , 1223 and 1245 cm^{-1} . This area shows both the COC group and the OSO groups which merge together. This large peak is shown in Figure 5.25. The antisymmetric of the SO's, occurs around $580\text{--}550$ and at 490 cm^{-1} . Since the molecule measured by Sun is not PEDOT:PSS there will be slight differences in the exact appearance of the same group but this is the approximate region where sulphur groups show in IR.

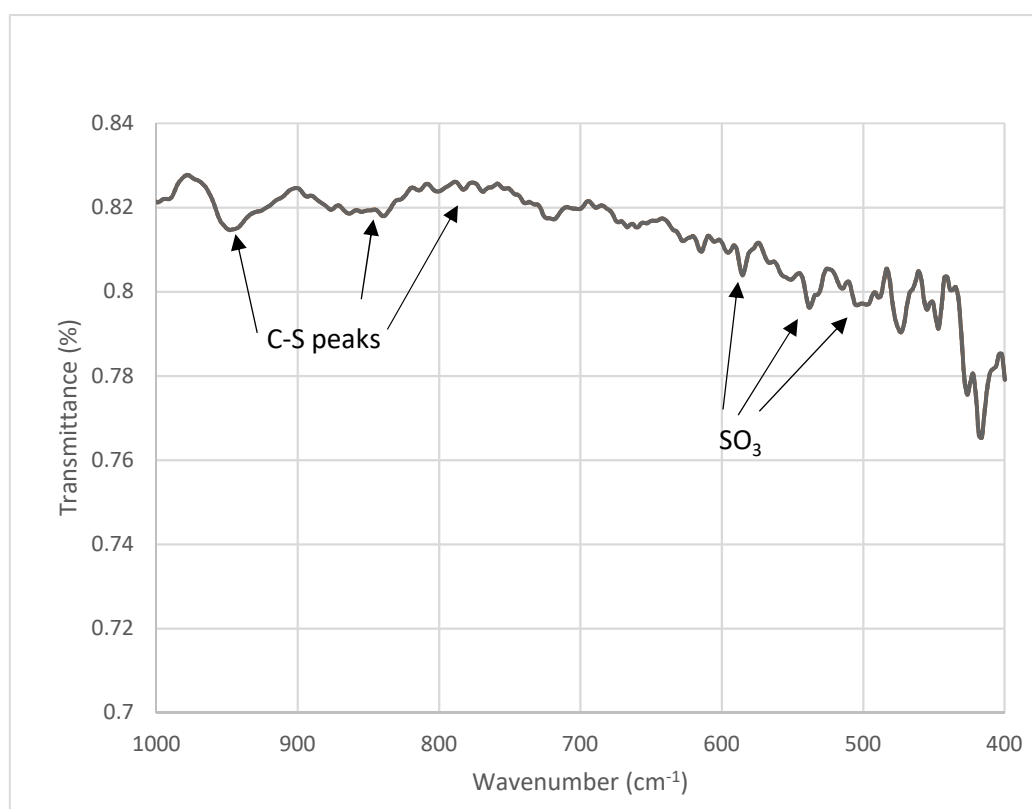


Figure 5.29: IR of the 97 % sample possibly showing C-S peaks and SO₃

In Sun's molecules SO₃ occurs as 559 and 495 cm^{-1} , whereas it is impossible to say for certain it shows in the spectra here. There are peaks in this area as shown in Figure 5.29, which could be attributed to the sulphur groups, but this remains

uncertain. Sun states that absorptions within the 550-600 cm^{-1} area can be assigned to several different functional group absorptions.

Cristovan (Cristovan, Nascimento *et al.*, 2006) analysed PSS but this was not part of PEDOT:PSS, using IR. Since the attached molecule is not PEDOT the absorptions will vary slightly although they would be expected to occur in approximately the same region. H-PSS film was found to absorb with symmetrical stretching of the molecules of C-C at 1590 cm^{-1} , S-O at 1175 cm^{-1} , O-S-O at 1000-1030 cm^{-1} . Friedel (Friedel, Keivanidis *et al.*, 2009) also found the SO vibration to occur at 1180 cm^{-1} with the O- S-O vibration found at 1030 cm^{-1} . Unfortunately, this is in the same region as the C-O-C peak so it is very difficult to say for certain the O-S-O peak Friedel found is in fact the same peak seen in these spectra. Friedel observed a disappearance of the sulfonic acid group which occurs in Friedels spectrum at below 600 cm^{-1} . Friedel also found a peak at 1542 cm^{-1} which Friedel believed was due to the deformation of the C=C groups within the aromatic ring structure to which the S-O groups attach in PSS. The sulphur groups give only weak intensities of peaks because according to Fichou (Fichou, Horowitz *et al.*, 1990) when analysing polythiophene, there is a very small amount of sulphur atoms in relation to carbon atoms. For this reason it is difficult to see sulphur peaks to the extent that other functional groups can be observed. It was concluded that it was impossible to know for certain if there was any change to the sulphur groups since peaks in this region were complicated and could not be identified for certain.

5.5.3 Raman

According to Tran-Van (Tran-Van, Garreau *et al.*, 2001) the Raman positioning of functional groups are very similar to that of IR, Tran-Van used Raman to determine the π -bonds in PEDOT. Similar functional groups occur at similar wavenumbers in

Figures 4.83 and 4.84 a peak was found in all samples at 413 cm^{-1} regardless of the concentration of PEDOT:PSS but reduces in size as the amount of PEDOT:PSS is reduced as is seen. Kalagi (Kalagi and Patil, 2016) identifies PSS at 436 cm^{-1} which is caused by the SO_2 group bending. Kalagi found an increase in intensity and sharpness with increasing thickness of PEDOT:PSS with the peak at 1409 cm^{-1} and the peak at 1246 cm^{-1} became stronger. Since the films become more uneven as the amount of surfactant is decreased a similar effect may be occurring here. It is therefore believed that the peak shown in Figure 4.83 and 4.84 is PSS. Kalagi believed that since PEDOT is a non-degenerate polymer then no soliton charge carriers are likely to exist so the only charge carriers in PEDOT can be polarons and bipolarons. There was no evidence found for the charge carriers at 733 nm . Like the IR spectra all the Raman scans have a sloping baseline. Since Raman is part of the IR spectrum it is assumed that this is due to the samples being conductive as was the case with the IR.

The Raman spectrum of the 98 % PEDOT:PSS sample shown in Figure 4.85 has an aromatic peak and Figure 5.30 shows evidence of $\text{C}=\text{C}$. This is a Zone 2 sample which is conductive. Luo (Luo, Billep *et al.*, 2013) states that the peak that appears at 1510 cm^{-1} is due to the de-doping of PEDOT. The 98 % PEDOT:PSS sample shows a peak at 1520 cm^{-1} so may show signs of being de-doped. However, this sample also showed evidence of polarons in UV.

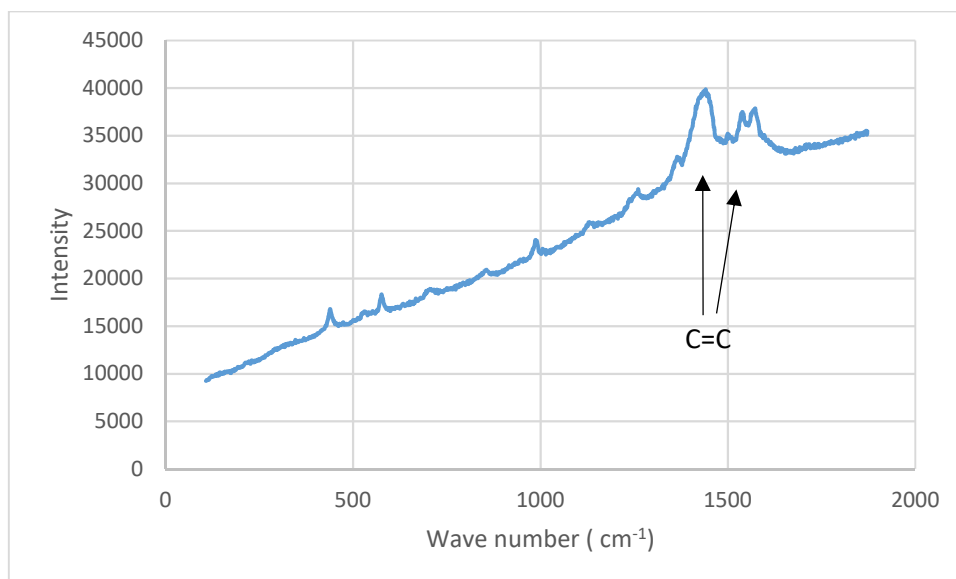


Figure 5.30: Raman of the 98 % PEDOT:PSS sample using 785 nm laser

According to Kalagi (Kalagi and Patil, 2016) there are five peaks in the 633 nm Raman spectra which identify PEDOT:PSS. These are shown in Table 5.12 as reported by Kalagi (Kalagi and Patil, 2016).

Table 5.12: Raman peaks found in spectra of PEDOT:PSS (Kalagi and Patil, 2016)

Wavenumber cm ⁻¹	Functional group
1521	C=C asymmetric vibrations
1407	C=C symmetric vibrations
1361 shoulder	C-C stretching deformations
1246	C-C in-plane symmetric stretching
1409	Thiophene ring

Kalagi further states that the region from 1400-1500 cm⁻¹ identifies the aromatic-quinoid forms of PEDOT. Because there are two extreme benzenoid and quinoid structures possible and also varying degrees in between each structure there are different absorptions. The quinoid structure has the highest energy so it is therefore,

less likely to be observed since staying in the quinoid form is less favourable to the PEDOT molecule.

Sakamoto (Sakamoto, Okumura *et al.*, 2005) used Raman at 633 nm and found that when the polymer was oxidised the peak at 1254 cm^{-1} disappears. When reduced the peak at 1424 cm^{-1} gets larger. There are also other changes where peaks move slightly with each spectrum. However, the differences stated by Sakamoto are so tiny it is difficult to say for sure that they are not simply due to a slightly different chemical environment as would be the case with Infrared analysis.

Luo (Luo, Billep *et al.*, 2013) found that the band found at around 1436 cm^{-1} shifts to a lower wavenumber when PEDOT is de-doped and a new peak occurs at 1510 cm^{-1} . Again there is such a small difference it is difficult to say for certain that this confirms anything. Figure 4.86 shows a slight difference between the 100 % and conductive samples with a new peak appearing at 3094 cm^{-1} which gets bigger with increasing surfactant concentration which may suggest the formation of the quinoid structure.

Analysis of the 97 % PEDOT:PSS spectrum shown in Figure 5.31 is tabulated in Table 5.13.

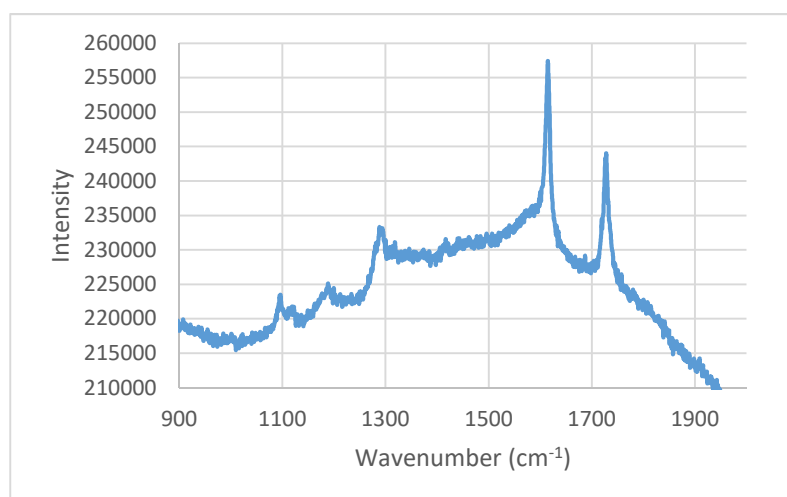


Figure 5.31: Raman spectra using 633 nm laser of the 97 % PEDOT:PSS, Zone 2 sample

Table 5.13 Raman analysis of the 97 % PEDOT:PSS sample:

Wavenumber cm^{-1}	Functional group	Reference
632	$\nu(\text{C-S})$ aliphatic 630– 790 cm^{-1} from PSS	(Horiba.com, Kalagi and Patil, 2016)
860	$\nu(\text{C-S})$ aromatic 1080 - 1100 cm^{-1} , 3000 - 3100 cm^{-1}	(Horiba.com, Kalagi and Patil, 2016)
1098	$\nu(\text{C=S})$ 1000 - 1250 cm^{-1} $\nu(\text{CC})$ alicyclic, aliphatic chain vibrations 600 - 1300 cm^{-1} , $\nu(\text{CC})$ aromatic ring chain vibrations 1000 cm^{-1}	(Horiba.com)
1193	$\nu(\text{C=S})$ 1000 - 1250 cm^{-1} $\nu(\text{CC})$ alicyclic, aliphatic chain vibrations 600 - 1300 cm^{-1} , $\nu(\text{CC})$ aromatic ring chain vibrations 1000 cm^{-1}	(Horiba.com)
1288	$\nu(\text{C=S})$ 1000 - 1250 cm^{-1} $\nu(\text{CC})$ alicyclic, aliphatic chain vibrations 600 - 1300 cm^{-1} , $\nu(\text{CC})$ aromatic ring chain vibrations 1000 cm^{-1}	(Horiba.com)
1419	Thiophene ring, $\delta(\text{CH}_2)$ $\delta(\text{CH}_3)$ asym 1400 - 1470 cm^{-1}	(Horiba.com) (Kalagi and Patil, 2016)
1613	$\nu(\text{CC})$ aromatic ring chain vibrations 1580, 1600 cm^{-1} , 1450, 1500 cm^{-1} ,	(Horiba.com)
1728	C=O 1680 - 1820 cm^{-1}	(Horiba.com)
3082	$\nu(\text{C-H})$ 3000 - 3100 cm^{-1} , Aromatic – quinoid transition	(Horiba.com)

In the 97 % PEDOT:PSS sample there is a band which could be attributed to the aromatic-quinoid transformation (Horiba). The peak at 3082 cm^{-1} that is present in all samples but is much larger in the 97 % PEDOT:PSS sample shown in Figure 5.32. Since this sample was shown to have polarons in UV this peak would confirm the likelihood of their presence.

Literature sources analyse the 200-2000 cm^{-1} wavenumbers when investigating PEDOT. When using the literature (Horiba.com) to analyse the samples this peak is the best way to distinguish the quinoidal transition. Since it also only occurs in the

Zone 2 samples it is likely this represents the proof of the aromatic to quinoid conformational changes and the conductive state where polarons or bipolarons exist.

The peak in this region is caused by the =C-H functional group. This functional group is of course present in every sample. Since the same 97 % PEDOT:PSS sample also showed the polaron peak in UV it can be concluded that the 97 % PEDOT:PSS sample conducts using a polaron mechanism. This peak is larger in this sample than in the other Zone 2 samples which suggests this is caused by changes in the numbers of =C-H groups when this sample is being measured. Other than this peak there is very little difference between any of the samples.

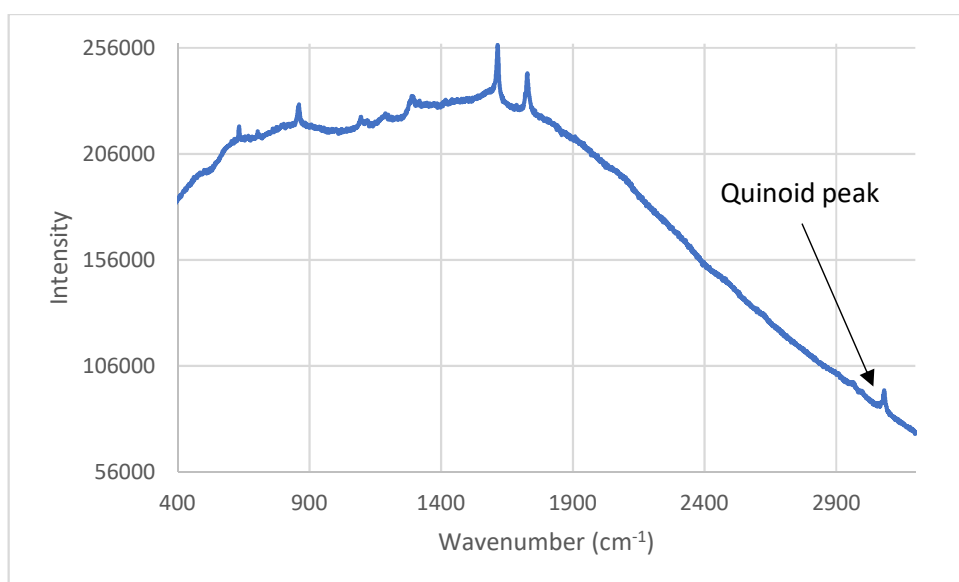


Figure 5.32: Raman scan at 633 nm on the 97 % PEDOT:PSS sample

The Raman spectrum of the 94 % PEDOT:PSS sample is different to that of most of the samples and is shown in Figure 5.33.

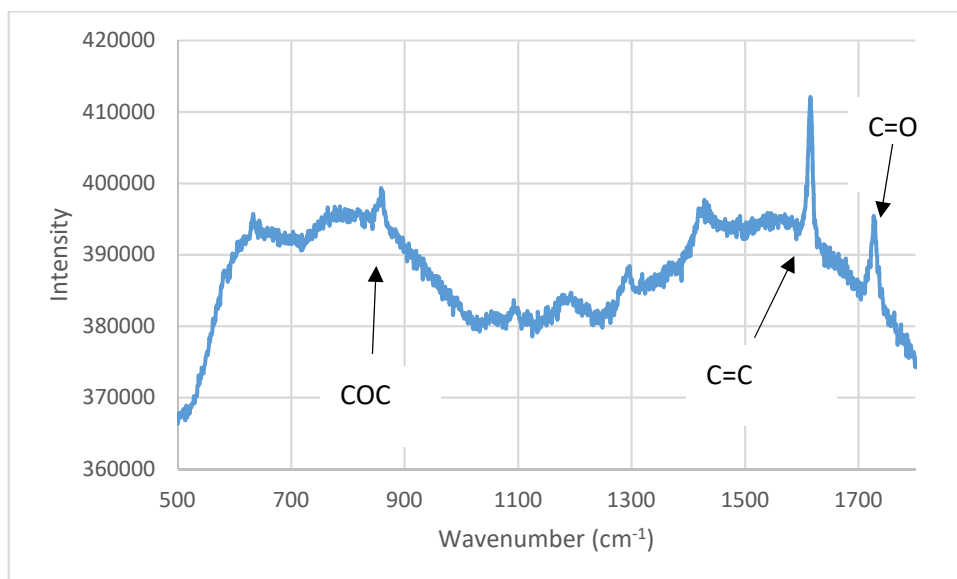


Figure 5.33: Raman of the 94 % PEDOT:PSS sample

Table 5.14 lists the analysis of the Zone 2, 94 % PEDOT:PSS sample. Note that at around 1610 cm⁻¹ the C=N peak also occurs (between 1610 - 1680 cm⁻¹(Horiba.com)) and although PEDOT:PSS as a molecule does not contain any nitrogen, as was established by Jönsson (Jönsson, Birgersson *et al.*, 2003) PEDOT can absorb ammonia from water in the atmosphere.

Table 5.14: Raman spectrum using 633 nm laser and the 94 % PEDOT:PSS sample

Wavenumber (cm ⁻¹)	Functional group	Reference
635	$\nu(\text{C-S})$ aliphatic 630 – 790 cm ⁻¹ from PSS	(Horiba.com, Kalagi and Patil, 2016)
862	$\nu(\text{C-O-C})$ 800 -970 cm ⁻¹	(Horiba.com, Kalagi and Patil, 2016)
1099	$\nu(\text{C-S})$ aromatic 1080 - 1100 cm ⁻¹	(Horiba.com, Kalagi and Patil, 2016)
1100.99	$\nu(\text{C-S})$ aromatic 1080 - 1100 cm ⁻¹	(Horiba.com, Kalagi and Patil, 2016)
1179	$\nu(\text{C-C})$ alicyclic, aliphatic chain vibrations 600 – 1300 cm ⁻¹ , $\nu(\text{C=S})$ 1000 - 1250 cm ⁻¹	(Horiba.com)
1201	$\nu(\text{C-C})$ alicyclic, aliphatic chain vibrations 600 – 1300 cm ⁻¹ , $\nu(\text{C=S})$ 1000 - 1250 cm ⁻¹	(Horiba.com)
1300	$\nu(\text{C-C})$ alicyclic, aliphatic chain vibrations 600 – 1300 cm ⁻¹	(Horiba.com)
1432	$\delta(\text{CH}_2)$ $\delta(\text{CH}_3)$ asym 1400 - 1470 cm ⁻¹	(Horiba.com)
1616	$\nu(\text{C=C})$ 1500 - 1900 cm ⁻¹ C=N 1610cm ⁻¹	(Horiba.com)
1729	$\nu(\text{C=C})$ 1500 - 1900 cm ⁻¹ $\nu(\text{C=O})$ 1680 - 1820 cm ⁻¹	(Horiba.com)

This this may explain why the 94 % PEDOT:PSS sample is borderline with Zone 1, since degradation from water absorption could be the problem. The rest of the samples show no unusual peaks and all are pretty much the same.

In conclusion, the 94 % PEDOT:PSS sample seems to have a nitrogen peak from ammonia and the 97 % PEDOT:PSS sample has what appears to be aromatic to quinoid transition peaks which would confirm polaron presence.

5.6 Thermal analysis

Thermal analysis using DSC was performed to characterise the films made and to compare to the 100 % PEDOT:PSS to see what, if any changes had occurred to the

thermal profile of the sample films. This is described in Section 3.4.3 and the results can be seen in Figure 4.88.

5.6.1 Thermal analysis using Differential scanning calorimetry (DSC)

The glass transition temperature is shown in Figure 4.88 and shows how the glass transition temperature (T_g) is affected by the addition of TWEEN 80 surfactant and MEK. The rest of the samples measured show a glass transition temperature as shown in Table 5.15.

Table 5.15 The glass transition of different samples using DSC:

Sample	Sample ratio Additives to PEDOT:PSS	Onset of the Glass transition (T_g) ($^{\circ}\text{C}$)	Midpoint of the Glass transition (T_g) ($^{\circ}\text{C}$)	Endpoint of the Glass transition (T_g) ($^{\circ}\text{C}$)
100 %	100 %	85.46	75.51	77.22
98 % PEDOT:PSS	1:40	83.99	75.01	78.00
97 % PEDOT:PSS	1:35	83.42	75.76	78.06
97 % PEDOT:PSS	1:30	77.61	70.95	73.39

The T_g is shifting with the change in concentration of the TWEEN 80 surfactant from 0 % to 3 %. The temperature of the onset of the T_g seems to be lowering and the peak seems to be widening as the PEDOT:PSS concentration is lowered. This could be due to a plasticising effect occurring, which would also account for why the samples became sticky as the PEDOT:PSS concentration is reduced and the TWEEN 80 concentration increased.

Using DSC PEDOT alone has a T_g of 102 $^{\circ}\text{C}$ (Shodhganga, Chapter 5,

PREPARATION AND PROPERTIES OF PEDOT

http://shodhganga.inflibnet.ac.in/bitstream/10603/3499/11/11_chapter%205.pdf).

However the PEDOT:PSS measured for this project has a T_g of between 75.51- 85.46 °C of the entire range of transition is recorded. So the PSS part of the molecule lowers the T_g considerably. The TWEEN 80 then further lowers the T_g . Evangelos (Evangelos, Sotirios *et al.*, 2012, Fehse, Meerheim *et al.*, 2008, Skotheim and Reynolds, 2006, Yoshioka and Jabbour, 2006) believe that PEDOT:PSS has a variable glass transition temperature since there is very strong ionic bonding between the PEDOT and the PSS. The additives cause a plasticising effect, which lowers the T_g further. When the additives are mixed with the PEDOT:PSS there is a change in the chemical and physical structure which leads to higher conductivity. Evangelos also used an analogue of PEDOT:PSS that had the same ratio of components 1:5:2 (PEDOT:PSS:Na) as the PEDOT:PSS used for this research.

5.7 Conclusions

Many researchers have stated that it is difficult to manufacture a homogeneous thin or thick film from PEDOT:PSS. To achieve this some kind of additive is generally used. Many of the additives have been found to aid in film forming and to enhance conductivity. However, the additives also lead to better connectivity between the conductive particles. The enhanced dispersal then allows for the particles of PEDOT to touch better and so may really enhance conductivity simply because the film coating made is more homogeneous.

From the analysis of experiments performed in Chapter 4, several assumptions can be made:

- 100 % PEDOT:PSS is virtually impossible to manufacture, from a dispersion, into a homogeneous film without some kind of additive.

- The addition of additives, TWEEN 80 and MEK, as dopants, enhance the conductivity of PEDOT:PSS at certain percentages. Resistivity is enhanced at an additive concentration of 2.4-6.3 %.
- 100 % PEDOT:PSS applied as a thin film, is less conductive than the TWEEN 80 and MEK doped PEDOT applied as a thin film.
- The additives slightly improved wetting but did not fully deal with the adhesion problem since adhesion was not satisfactory on PET substrates. Adhesion was a major problem for the entire project. By using chemical and physical surface modification adhesion problems were finally addressed. However, this slightly reduced conductivity.
- The best concentrations for film formulation was found to be the 95 % PEDOT:PSS solution to 98 % PEDOT:PSS solution with a chemical substrate modification using methylcellulose. Chemical modification affects conductivity because methyl cellulose is not conductive. This slightly reduces the final conductivity.
- pH may affect both conductivity and stability. The highest resistivity samples (98.59 %) also had highest pH.
- Viscosity decreases with addition of additives until a minimum at 95 % PEDOT:PSS when agglomeration occurs or other unknown mechanisms cause an increase in viscosity.
- The processing route used affects resistivity. Spincoating is best, probably due to the polymers aligning during application, which gives better conductivity. Dipcoating gives slightly better electrical resistivity measurements than spraycoating. Dipcoating, probably uses gravity to cause alignment of the polymer chains, but to a lesser extent than spincoating. Spraycoating has the least likelihood of alignment of the polymer chains.

Therefore with respect to alignment:

spincoating > dipcoating > spraycoating

Although spincoating is the best method of manufacture it is the hardest to scale up to a bulk application. Therefore for future bulk applications dipcoating probably provides the best solution.

- The most electrically stable sample when performing electrical characterisation was the 98.59 % PEDOT:PSS film, however this also had higher resistivity than all the Zone 2 samples.
- High voltage studies confirm the films can be retested and the same results obtained over several measurements indicating that previous research stating PEDOT:PSS decays at higher potentials is incorrect when applied to this research.
- UV spectroscopy experiments confirmed the presence of polaron charge carriers in two samples, the 97.22 % and 97.56 % PEDOT:PSS made using the 1:35 and 1:40 ratio of PEDOT:PSS to TWEEN 80/MEK solutions.
- IR proved that the Zone 2 enhanced conductivity samples have both a carbonyl and a COC group whereas the Zone 3 samples tested (98.59 %) made using the 1:70 ratio of PEDOT:PSS to TWEEN 80/MEK lose this and gain an OH peak. This suggests either that in the Zone 3 samples the ring is rupturing and the oxygen atoms are being protonated or that in the Zone 2 samples the two COC groups are stabilising the quinoid structure by becoming temporary carbonyls.
- IR and Raman show what is believed to be quinoid peaks, which are necessary for PEDOT to be in the conductive state. IR proved the aromatic C=C group is present in the higher resistivity, 98.59 % samples but the quinoid C=C group is the most prevalent in all the Zone 2 (95-98 %) samples. Since

this also occurred in the 97.22 % and 97.56 %, Zone 2 samples in which polarons were detected using UV, this probably confirms polaron charge carriers are present. However, it does not explain how the 95.24 %, 96.15 % and 96.77 % samples, which are also in Zone 2, conduct since no polarons were detected in these samples and yet resistivity is very similar to the 97.22 % and 97.56 % samples. Table 5.16 shows all the Zone 2 samples and lists the samples in which charge carriers were detected using UV.

Table 5.16: Charge carriers detected by UV in Zone 2 samples

PEDOT:PSS (%)	Additives (%)		Charge carriers in UV
	TWEEN 80	MEK	
95.24	1.19	3.57	Not detected
96.15	0.96	2.88	Not detected
96.77	0.81	2.42	Not detected
97.22	0.69	2.08	polarons
97.56	0.61	1.83	polarons

- Jönsson (Jönsson, Birgersson *et al.*, 2003) have stated that PEDOT loses conductivity due to the ammonia in air and water. Ammonia is difficult to detect using IR due to the OH peak which is in the same region and which masks the ammonia peak. The 94 % sample analysed using Raman showed the C=N peak at 1610 cm^{-1} . Other investigators have overlooked the presence of nitrogen in the PEDOT:PSS IR spectra but this would explain why PEDOT:PSS has a short electrical shelf life and decays in air. Further study is needed to prove ammonia is present.
- At high doping levels the additives had plasticised the PEDOT:PSS. Thermal analysis was performed to discover how PEDOT:PSS stands up to heat processing for future bulk applications. This would account for why many of the samples have an increasing stickiness as the concentration of the TWEEN

80 rises. It would also explain how the higher TWEEN 80 concentration samples have better wetting to substrates and also why they easily peel off the substrate onto sample bags and equipment.

6.0 Shelf-life / Degradation studies

No references were found where the shelf-life of PEDOT samples was assessed. Therefore, an initial shelf-life analysis was performed to see how the PEDOT:PSS film samples studied here changed over a period of time with these particular dopants.

6.1 Sample life of the dipcoated samples

In order to gauge the long term shelf-life of the PEDOT:PSS film samples on PET, the same four-point-probe measurement was performed as described in, Section 3.4.5. Dipcoated samples were chosen since at the start of the shelf-life experiments these provided the highest quality coatings, therefore presenting the most appropriate choice to provide repeatable results over the lifetime of the samples.

Therefore, sheet resistance at 10 nA of the unmodified and annealed dipcoated samples was measured. The dipcoated samples were then re-measured every few weeks and the results from each measurement were recorded. Figure 6.1 shows results of all the samples that were made at the start of the experiments and those made at 16 weeks. Only one set of the dipcoated samples was measured for shelf-life studies but 10 readings for each measurement were taken, at regular intervals for

a total of 62 weeks of measuring. All samples were stored in poly-bags in a box, in the dark, at ambient conditions under air.

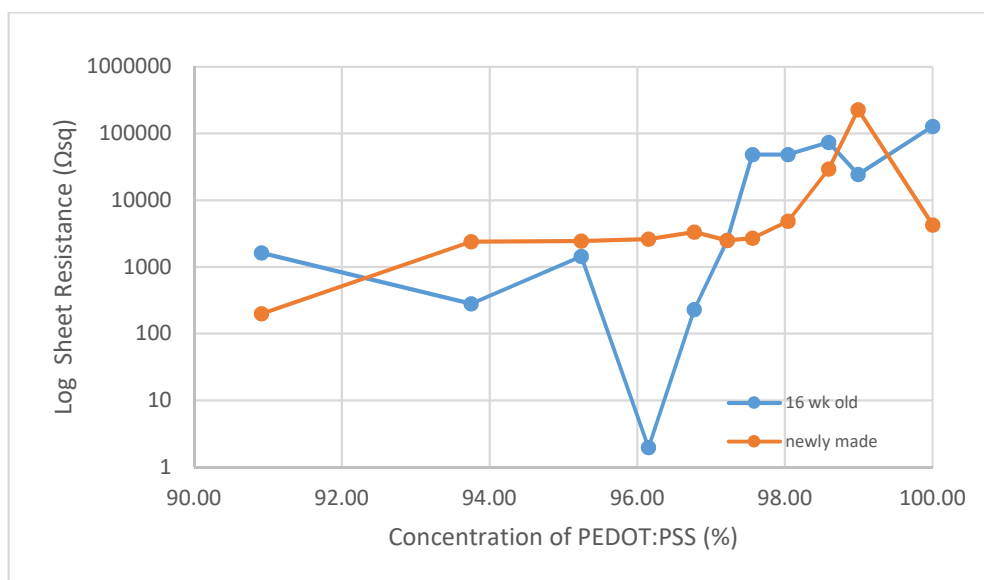


Figure 6.1: Average Sheet Resistance of the dipcoated samples over 16 weeks of storage

Figure 6.1 shows the difference in sheet resistance with concentration between the newly made samples, in orange, and the stored 16 week old samples, in blue, for all samples made in the set from the lowest concentration at 91 % PEDOT:PSS up to 100 % PEDOT:PSS. There is a sudden dip at a concentration of 96 % PEDOT:PSS. The 97 % sample also has lower sheet resistance after 16 weeks. Since only one set of samples was tested it is not known at this time if this is repeatable.

After this initial measurement the shelf life resistivity of the samples was measured every few weeks to track changes. However, from this point on most samples were eliminated from further study. This was due to the subsequent findings of the author

previously reported in chapter 6 and of the three samples of most interest that were identified as the 97 %, 99 % and 100 % PEDOT:PSS.

Figure 6.2 shows the three chosen samples plotted against the number of weeks to illustrate how they change over the entire time they were tracked. There is a trend with all samples showing rising sheet resistance with storage. The 99 % sample, which was the most stable sample all the way through the previous experiments, shows the least change in sheet resistance with both 100 % PEDOT:PSS and the 97 % enhanced sample showing a similar trend. Therefore, the 99 % sample and is the most stable when stored and after 35 weeks outperforms the 100 % sample becoming more conductive.

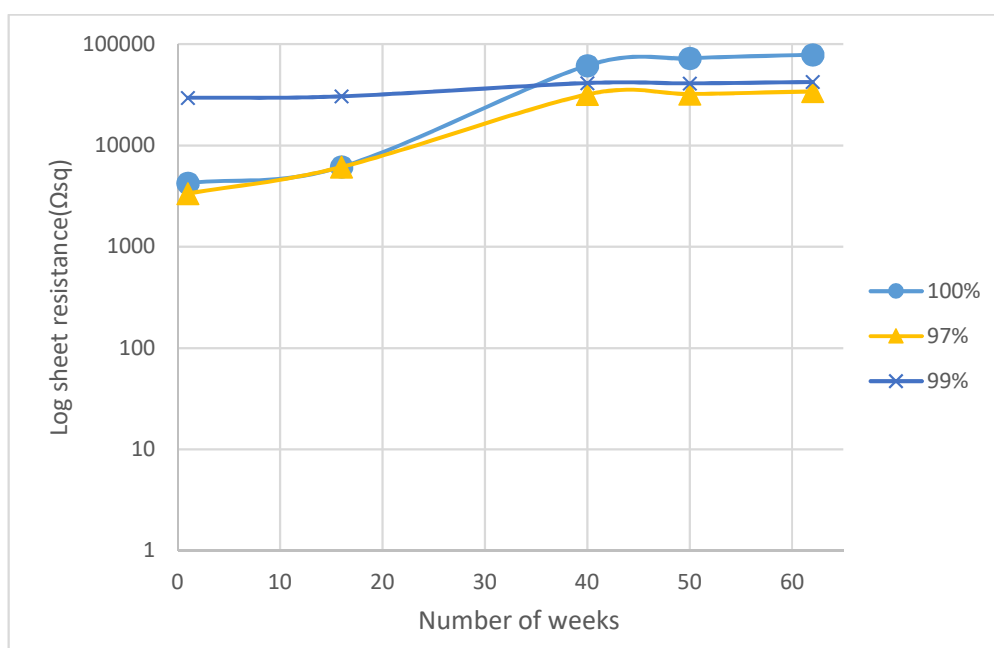


Figure 6.2: Sheet resistance (Ωsq) of samples over 62 weeks

Figure 6.3 shows the stored samples measured at 40 V using a Keithley 6517b over 62 weeks and shows a similar shape to the surface resistivity measurements shown in Figure 6.2, with the 97 % sample remaining the most conductive and the 100 % sample approaching the 99 % sample.

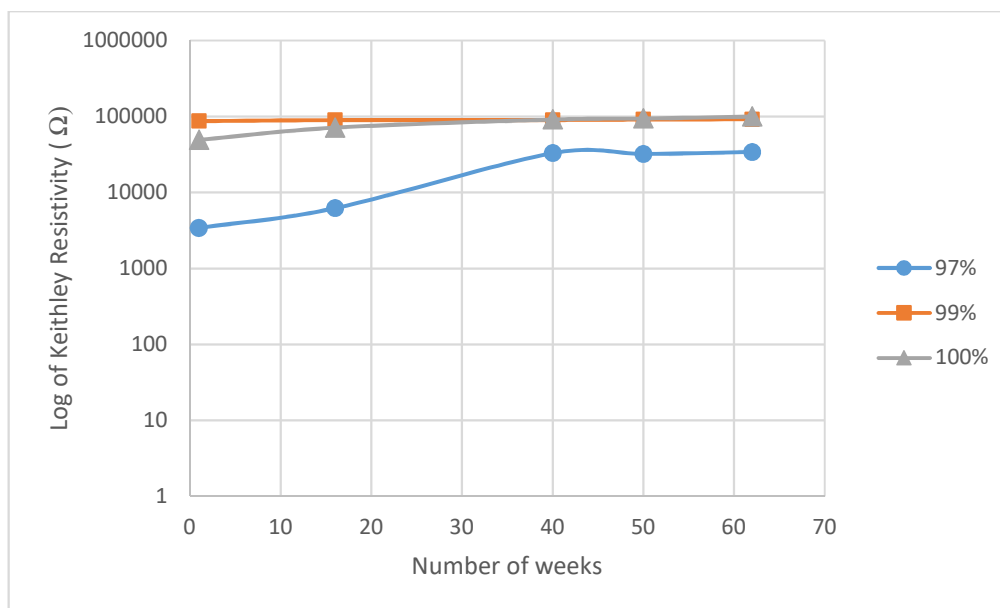


Figure 6.3: Keithley resistivity of samples measured at 40 V over 62 weeks

Figure 6.4 shows the difference in bulk resistivity, measured using the four-point-probe, with concentration between the newly made samples, in orange, and the stored 16 week old samples, in blue, for all samples made in the set from the lowest concentration at 91 % PEDOT:PSS up to 100 % PEDOT:PSS. The resistivity of the 100 % sample was found to be an order of magnitude more conductive after 16 weeks possibly due to the polymer chains relaxing or aligning better but was still less conductive than all the other doped samples. Again, the majority of the samples were not tested further and only the chosen three samples were tested for the rest of the testing period.

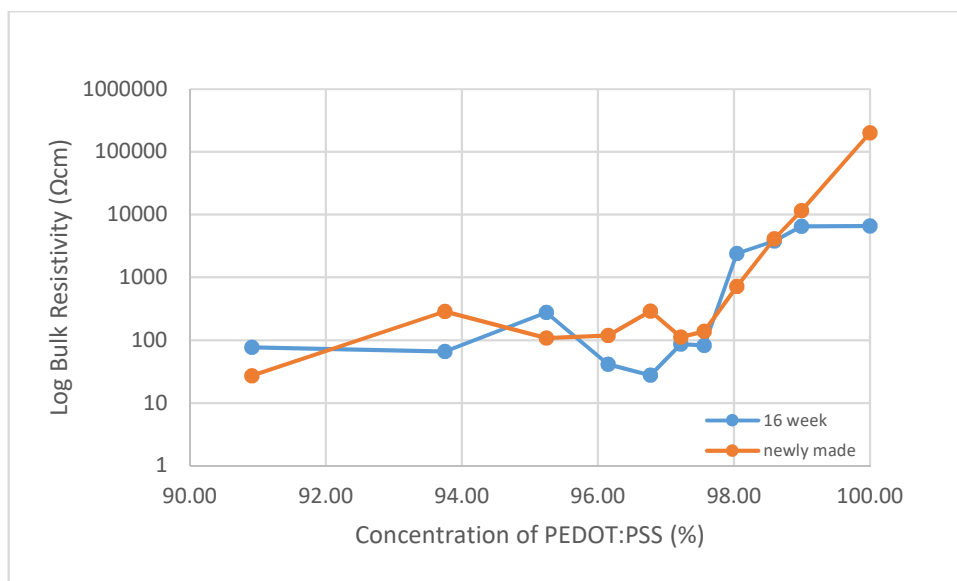


Figure 6.4: Bulk resistivity of the full set of Dipcoated shelf-life samples after 16 weeks of storage

Again, in Figure 6.5 the bulk resistivity rises with storage time. The 100 % PEDOT:PSS shows the least change but is less conductive. The 97 % and 99 % samples show similar in trends but the lowest resistivity is the 97 % enhanced sample. Both of the 97 % and 99 % samples are still more conductive than the starting material after 62 weeks of storage.

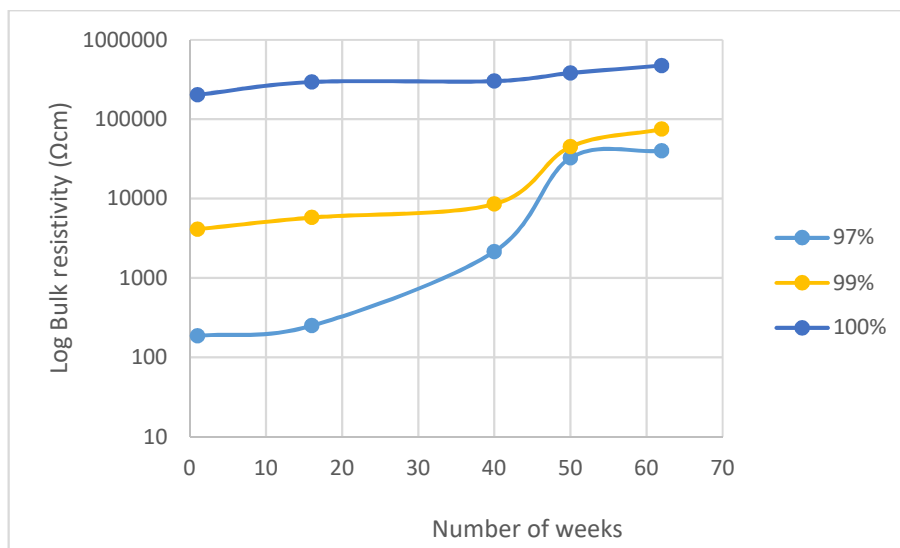


Figure 6.5: Bulk resistivity (Ωcm) of samples over 62 weeks

Generally samples of PEDOT:PSS whether doped or not, decayed as they aged. They were also more likely to delaminate and lose electrical conductivity. There could be a number of explanations for this; this could be due to some reaction between the TWEEN 80 surfactant and the PEDOT:PSS but this has not been investigated. This could be caused by water from the air being absorbed by the films. There was some possibility of ammonia, from air, in some of the IR spectra as described in Sections 5.5.2.3, 5.5.3, and 5.7, although this has not been definitely proved in this PhD project since the OH appears at the same place on the spectra. This was large and wide making it hard to verify if this was an ammonia peak or not. This could be worth investigating further, but is beyond the scope of this thesis.

Vitoratos (Evangelos, Sotirios *et al.*, 2012) investigated the degradation of conductivity of PEDOT:PSS with applied heat under air and helium. The difference between the conductivity decay was then measured and it was found that the samples measured under air decayed faster than those measured under helium. Since PEDOT:PSS is hygroscopic the films adsorb the water molecules in air which causes the PEDOT:PSS to degrade. Exactly how the PEDOT:PSS chains degrade is not established. Vitoratos established that the PEDOT:PSS lost conductivity faster in air. The graphs from the Keithley measurements show a different curve occurring at 40 V. The resistivity rises steadily with applied potential difference as shown in Section 5.4.3. Since applying a voltage to the samples could also raise the temperature of the sample Vitoratos's experiments may explain what is happening.

$$\text{Using: } V \times C = J \quad [6.1]$$

$$\text{And: } I \times s = C \quad [6.2]$$

Where: V = voltage, I = amperes, s = time which in all cases is taken as 1 second for these calculations, C = coulombs and J = Joules = heat energy

Using the results from dipcoated set 5 as a representative sample equation 6.1 was used to calculate the amount of heat, generated by the applied voltage, being applied to the samples. The results are shown in Figure 6.6.

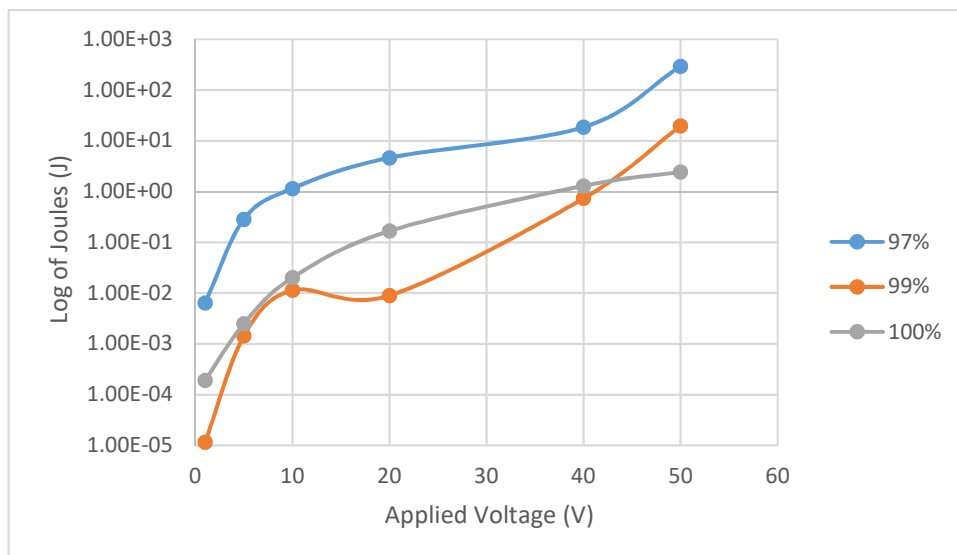


Figure 6.6: Heat energy generated (J) from the applied potential difference

In all cases as the applied potential difference rises, the resistivity rises and so also does the heat being applied to the samples so a similar effect may be occurring as was found by Vitoratos, where in air, the polymer conductivity degrades partly due to exposure to oxygen and water and also to increasing heat caused by applying the voltage. It could be that the heat causes more vibrations in the molecules and affects the additives. This could be causing disruption to the charge pathways in the polymer. Table 6.1 shows calculations of the heat generated:

Table 6.1: Heat energy generated (J) from the applied potential difference

PEDOT:PSS (%)	Voltage (V)	Amperes (I)	Coulombs (C)	Joules (J)
97	1	6.44×10^{-3}	6.44×10^{-3}	6.44×10^{-3}
97	5	1.14×10^{-2}	5.70×10^{-2}	2.85×10^{-1}
97	10	1.15×10^{-2}	1.15×10^{-1}	1.15×10^{-1}
97	20	1.16×10^{-2}	2.32×10^{-1}	4.64
97	40	1.17×10^{-2}	4.68×10^{-1}	1.87×10^{-1}
97	50	1.18×10^{-1}	5.90	2.95×10^{-2}
99	1	1.15×10^{-5}	1.15×10^{-5}	1.15×10^{-5}
99	5	5.72×10^{-5}	2.86×10^{-4}	1.43×10^{-3}
99	10	1.14×10^{-4}	1.14×10^{-3}	1.14×10^{-2}
99	20	2.24×10^{-5}	4.48×10^{-4}	8.96×10^{-3}
99	40	4.62×10^{-4}	1.85×10^{-2}	7.39×10^{-1}
99	50	7.85×10^{-3}	3.93×10^{-1}	1.96×10^{-1}
100	1	1.91×10^{-4}	1.91×10^{-4}	1.91×10^{-4}
100	5	1.00×10^{-4}	5.00×10^{-4}	2.50×10^{-3}
100	10	2.01×10^{-4}	2.01×10^{-3}	2.01×10^{-2}
100	20	4.20×10^{-4}	8.40×10^{-3}	1.68×10^{-1}
100	40	8.10×10^{-4}	3.24×10^{-2}	1.30
100	50	9.79×10^{-4}	4.90×10^{-2}	2.45

In conclusion, it would appear from these results that the best sample for conductivity after 62 weeks is the 97 % PEDOT:PSS despite the fact it seems to degrade the fastest and for any use in commercial applications the life of the PEDOT: PSS needs careful consideration until the nature of the electrical degradation can be elucidated further.

7.0 Conclusions

The overarching aim of this research project was to enhance the electrical conductivity of PEDOT:PSS with a view to eventually having an electrically conductive, bulk application polymer for use in mass production. These have been at least partially met by this work, though some questions still remain.

Since it is likely that surface measurements of resistivity show an interference from adsorbed species on the surface of the film and surface quality effects, bulk resistivity using the Jandel four-point-probe, was used to calculate the conductivity of the material. Table 7.1 shows the bulk resistivity enhancement achieved.

Table 7.1: Bulk Resistivity enhancement of the samples measured using a four-point-probe

PEDOT:PSS (%)	Additives (%)		Spraycoated and dipcoated Resistivity (Ωcm)	Spincoated Resistivity (Ωcm)
	TWEEN 80	MEK		
97.22	0.69	2.08	290	25
98.59	0.35	1.06	4130	724
100	0.00	0.00	207622	1494

From Table 7.1 the maximum enhancement achieved, when measuring bulk resistivity, using a four-point-probe, was for the spincoated films which had the lowest resistivity with the enhanced 97 % film being 25 Ωcm and the 100 % PEDOT:PSS film being 1494 Ωcm . Whilst this is not as conductive as copper whose resistivity is $1.68 \times 10^{-8} \Omega\text{m}$ (hyperphysics), this is an enhancement in comparison to 100 % PEDOT:PSS. The samples with modified substrates had very slightly higher resistivity, but with better conductivity than those made using other manufacturing methods. The largest improvement on resistivity from the starting material was for the dipcoated and spraycoated samples.

Although these had higher resistivity than the spincoated samples, the difference between the starting material and the 97 % enhanced samples was greater than the difference between the spincoated samples. The dipcoated and spraycoated samples both had similar results. The 97 % film resistivity was around 290 Ωcm and the 100 % PEDOT:PSS film had a resistivity of 207622 Ωcm . The largest enhancement from starting material to 97 % PEDOT:PSS was therefore the spraycoated and dipcoated samples.

The 97 % PEDOT:PSS mixture containing 97.22 % PEDOT:PSS with 0.69 % TWEEN 80 and 2.08 % MEK makes thin films that will withstand higher potentials up to 50 V and remains conductive with repeat application of potentials up to 50 V. Elschner (Elschner, Kirchmeyer *et al.*, 2011) states that PEDOT:PSS becomes irreparably damaged at an applied voltage of 1.4 V however, testing performed has proved that samples made with MEK and TWEEN 80 remain conductive when high voltages of up to 50 V is applied. The results are repeatable over 16 weeks. After this they begin to lose conductivity. It is not known how the films degrade. At 40 V each graph has a different shape to the lower voltage studies, indicating either a change in mechanism of charge carriers or that this is the point at which the polymer begins to degrade. However, if only lower voltages are applied the decay is slower than it is with higher voltages. Vitoratos (Vitoratos, Sakkopoulos *et al.*, 2009) studied degradation of PEDOT:PSS with heat under both air and helium. The experiments with helium showed slower degradation indicating that oxygen and the water molecules found in air increase the speed of degradation of PEDOT:PSS.

Since a higher applied voltage from the Keithley, would generate an increase in heat with respect to the lower applied potentials, this may increase the polymer degradation and this is further enhanced by the samples being both stored in air and measured in air.

The most stable of all samples is not the most conductive but is more conductive than the 100 % PEDOT:PSS starting material. The most stable sample was the 99 % PEDOT:PSS sample which is proposed as the most appropriate sample to take this work forward since it is very stable over time and when characterising resistivity.

The charge carriers generated within the 97 % and 98 % thin films are polarons with the molecule changing confirmation from aromatic to quinoid in order to allow the charge carriers to move. This equates with the findings of most other researchers although, probably due to the mixture of reagents being different to other researchers, the actual wavelength where polarons are detected was slightly different, but is still comparable to other findings, however, no other research group has used the additives studied here.

TWEEN 80 is similar to sorbitol in structure but most of the research community has concentrated on sorbitol not TWEEN 80. Only Nasybulin (Nasybulin, Wei *et al.*, 2012) did any experiments using TWEEN 80 and these were not to dope the polymer but instead to solubilise EDOT to polymerise into PEDOT. Nasybulin abandoned TWEEN 80 in favour of SDS. Nardes (Nardes, Kemerink *et al.*, 2008) states that sorbitol can enhance PEDOT's conductivity by up to three orders of magnitude. The conductivity of the samples shown in Table 7.2 is calculated from equation 3.6, Section 3.4.5 using the four-point probe results for bulk resistivity. As shown, the TWEEN 80 has also enhanced the conductivity of the 97 % samples with respect to the 100 % samples by three orders of magnitude when using spraycoating and dipcoating so this correlates well with Nardes findings on sorbitol enhancement. It also confirms that TWEEN 80 is a comparable dopant for PEDOT:PSS when mixed with MEK. However, TWEEN 80 and MEK only enhances the spincoated samples by two orders of magnitude from the starting material although spincoating gives greater conductivity.

Table 7.2 shows the conductivity enhancement of the samples calculated from the bulk resistivity measurements made using a four-point-probe.

Table 7.2: Conductivity enhancement of the samples from four-point-probe measurements.

Sample	Manufacturing method	Resistivity (Ωcm)	Conductivity (S cm^{-1})
97 %	Spraycoating/ Dipcoating	290	3.45×10^{-3}
99 %	Spraycoating/ Dipcoating	4130	2.42×10^{-4}
100 %	Spraycoating/ Dipcoating	207622	4.82×10^{-6}
97 %	Spincoating	25	4.00×10^{-2}
99 %	Spincoating	724	1.38×10^{-3}
100 %	Spincoating	1494	6.69×10^{-4}
Copper	Not applicable	168×10^{-8}	595×10^7

The influence of film thickness is complicated by differences in the possible orientation of the polymer due to different manufacturing methods used. Although the spincoated results were only enhanced in conductivity by two orders of magnitude, the actual conductivity is much higher than that of the thicker, spraycoated and dipcoated films, which were enhanced by three orders of magnitude from the starting material. Orientation, film thickness and film quality all influence the conductivity of the samples with:

spincoating > dipcoating > spraycoating

Adhesion of PEDOT to substrates, whether doped or 100 %, is very poor. This can be solved by applying a thin film of methyl cellulose or abrasion prior to the application of the PEDOT:PSS or mixture of PEDOT and additives. Methyl cellulose modification gave slightly higher resistivity films.

The spectra showing the aromatic form of PEDOT:PSS had higher resistivity than the samples in the quinoid form. The PEDOT molecule ionises which alters the conformation from aromatic and stable conformation to a higher energy quinoidal form this enables easy transfer of electrons. As the additive concentration increases the samples change. The higher the additives concentration Zone 1 (91-94 %) and

Zone 2 (95-98 %) samples are mainly in the quinoid form whereas the Zone 3 (99 %) samples are mainly aromatic with the exception of the starting material which is a mixture of both forms but predominantly quinoid.

Shelf-life would probably be improved if the samples were stored in an environment excluding oxygen and water since surface resistivity measurements are far higher resistivity than the bulk resistivity measurements which could be due to adsorbed species increasing resistivity of the films.

The samples were repeatedly exposed to high voltages and it was proved that this analogue of PEDOT:PSS when mixed with the additives TWEEN 80 and MEK does not show signs of degradation at higher potential difference despite other research stating it does. Degradation occurs over time with storage under air.

7.1 Contribution to Knowledge

The contribution to knowledge of this work is:

- Identifying that a mixture of additives (TWEEN 80, MEK), at certain concentrations enhances the conductivity of PEDOT:PSS with respect to the 100 % PEDOT:PSS alone with a bulk resistivity enhancement of three orders of magnitude for thicker films and two orders of magnitude for thinner spincoated films. The same mixture also improves film forming.
- This work has addressed the adhesion problems of PEDOT:PSS to PET which is reported to be a problem for most research groups. Methyl cellulose when spincoated onto the substrate and then dried allows good adhesion of PEDOT:PSS in both the doped mixtures and the 100 % dispersion starting material.

- The effect of high voltage on PEDOT has not until now been studied. Not only does PEDOT:PSS with TWEEN 80 and MEK withstand high voltage but it can be applied repeatedly over a period of several months.
- Shelf life studies have shown PEDOT:PSS, with the additives used for this project, degrades over time if stored under air but even after 62 weeks the enhanced samples were both more conductive than 100 % PEDOT:PSS.
- There is a difference in conductivity when measuring bulk resistivity and surface resistivity which is probably caused by adsorbed species on the surface of the film which raises the resistivity of the material.

This research has identified further investigation opportunities which would be recommended in order to progress the knowledge gained in this project into a bulk commercial application.

7.2 Further Research Opportunities

Future research opportunities are required in order to solve the remaining problems.

There are still several questions.

- 1) Which sample is the best? It may depend entirely on the application. It could be better using the stable, longest shelf life 99 % PEDOT:PSS sample rather than more conductivity enhanced samples, since these degrade faster.
- 2) Further characterisation of the exact composition of each annealed sample may help to explain why, when using UV, some samples have similar resistivity, but only two of the five, Zone 2 samples (97.22 % and 97.56 % PEDOT:PSS) show what was believed to be polarons.

- 3) For bulk processing it would be interesting to elucidate the relationship between thickness, polymer orientation, film quality and film surface and study the importance of each factor in subsequent properties.

Other areas of interest include:

- The annealing step should remove the MEK. However, it could be that there are traces remaining or that the MEK has reacted in some way with the other reagents in the mixture. This could influence conductivity enhancement. This may also be explained by further investigation using thermal degradation studies to try to understand what is happening with what appears to be a plasticising of the samples. Zhou (Zhou, Anjum *et al.*, 2014) found that water hydrogen bonds to PSS at room temperature and that PEDOT may become more conductive as the polymer is heated which removes bound water. Further work using DSC may explain differences in the water content between the samples and if there are any changes with increasing TWEEN 80 concentration. The lowering of the glass transition temperature with increasing surfactant suggests there may be a blending taking place between PEDOT:PSS and TWEEN 80 where some samples at some concentrations are immiscible and others are miscible which would explain differences in the conductivity between different samples. This could possibly be confirmed using a hot stage microscopy.
- Since agglomeration was a major problem, further research into prevention of agglomeration would further the chances of bulk application using the optimised (95-98 %) Zone 2 samples.
- Annealing under an inert gas rather than air may give a good idea of how oxygen or water affects the samples and if this makes any difference what-

so-ever to resistivity. Storage of the samples under an inert gas might extend shelf life. It is possible that the formation of PSS.NH_4^+ complex occurs within the samples which causes de-doping, but further investigation is required to prove this.

- All the conductive (95-98 %) Zone 2 samples showed a carbonyl peak whereas the higher resistivity samples had no carbonyl. As the concentration of surfactant decreases the carbonyl peak in IR in the samples moves from 1729 to 1733 cm^{-1} . PEDOT should not have a carbonyl and no references were found to explain this although it is possible this is caused by over-oxidation (Barsch and Beck, 1996). The problem with this explanation is it should have reduced conductivity but measurements have shown that samples having a carbonyl have increased conductivity. Therefore this is an unknown peak. It is possible the MEK may have interacted to form some kind of changes to the PEDOT molecules but this needs to be followed up with further analysis to discover what is causing the carbonyl. No spectroscopic analysis was performed on the aged samples so this may be worth investigating further to determine if there are structural changes when the samples are aged.
- Further analysis could prove whether or not ammonia is present. Both Raman and IR indicated that it is likely that ammonia, from air and water, could be adsorbing to the films which will increase degradation.
- Rather than buying a commercial product it would be interesting to use electrochemistry to synthesise PEDOT. Previous reported literature indicates that the most conductive forms of PEDOT and PEDOT:PSS are made in this way. If this electrochemically generated form of PEDOT:PSS was then doped with the TWEEN 80/MEK additives, it may be far more conductive.

- There were other different combinations of additives trialled which may enhance this analogue of PEDOT. In particular good results were obtained with ethanol and TWEEN 80 and with Ethanol/MEK and TWEEN 80 that were comparable with those investigated here with MEK.
- Finally, PEDOT has thermoelectric properties which have not been investigated in this project and has been reported to be of use to generate thermopower devices (Massonnet, Carella *et al.*, 2014) and it would be very interesting to attempt to use the enhanced, 95-98 % PEDOT:PSS, samples in this way. Zhou (Zhou, Anjum *et al.*, 2014) believed that PEDOT becomes more conductive when it is thermally activated which according to Zhou is due to the bound water being driven off. It would be interesting to explore further how heat applications may improve conductivity.

REFERENCES

Abdulla, H. S; and Abbo, A. I. (2012). Optical and electrical properties of thin films of polyaniline and polypyrrole. *Int J Electrochem Sci* 7 pp.10666-10678.

Adhesives.org and Sealants.org [Accessed 03/12/2016].

Agarwal, M; Lvov, Y. and Varahramyan, K. (2006). Conductive wood microfibres for smart paper through layer-by-layer nanocoating. *Nanotechnology* 17(21) p.5319.

Alicona.com, <http://www.alicon.com> [Accessed 23/02/2016].

Alemu, D; Wei, H; Ho, K; Chu, C. (2012). Highly conductive PEDOT: PSS electrode by simple film treatment with methanol for ITO-free polymer solar cells. *Energy & environmental science* 5(11) pp.9662-9671.

Anon (a). *Image of sorbitol* [online]. Available at: <http://www3.hhu.de/biodidaktik/zucker/sugar/sorbit.html> [Accessed 06/12/2016].

Anon (b). *Image of ethylene glycol* [online]. Available at: https://www.google.co.uk/imgres?imgurl=http://0.tqn.com/d/chemistry/1/0/G/p/ethylene-glycol.jpg&imgrefurl=http://chemistry.about.com/od/factsstructures/ig/Chemical-Structures---M/MEG---Monoethylene-Glycol.htm&h=218&w=640&tbnid=1hBZL4dTnEqVJM:&vet=1&tbnh=76&tbnw=223&docid=g1TG3hWq7t-__M&itg=1&client=firefox-b-ab&usq=__YXMpy5Aidg89uzJp5vkRkd-qmSY=&sa=X&ved=0ahUKEwjK9PSNw9_QAhWBkiwKHRkqDTMQ_B0IMzAB [Accessed 06/12/2016].

Anon (c). Development of thermoplastic conducting polymers; Chapter 11 ,Preparation and properties of PEDOT poly(3,4-ethylene dioxythiophene, pp. 133-134, http://shodhganga.inflibnet.ac.in/bitstream/10603/3499/1/11/11_chapter%205.pdf [Accessed 04/12/2016].

Arias-Pardilla, J; Gimenez-Gomez, P. A; de la Pena, A; Segura, J. L. Otero, T. F. (2012). Synthesis, electropolymerization and characterization of a cross-linked PEDOT derivative. *Journal of Materials Chemistry* 22(11) pp.4944-4952.

Ashery, A.; Said, G.; Arafa, W. A.; Gaballah, A. E. H.; Farag, A. A. M. (2016). Structural and optical characteristics of PEDOT/n-Si heterojunction diode. *Synthetic Metals* 214 pp.92-99.

Barsch, U. and Beck, F. (1996). Anodic overoxidation of polythiophenes in wet acetonitrile electrolytes. *Electrochimica acta* 41(11) pp.1761-1771.

Biolinscientific manual THEORY NOTE 4: Surface free energy - theory and calculations. Biolin Scientific.

Blythe, A. (1984). Electrical resistivity measurements of polymer materials. *Polymer testing* 4(2) pp.195-209.

Bredas, J.L; Themans, B; Andre, J.M; Chance, R.R; Silbey, R. (1984). The role of mobile organic radicals and ions (solitons, polarons and bipolarons) in the transport properties of doped conjugated polymers. *Synthetic Metals* 9 pp.265-274.

Bredas, J. L. and Street, G. B. (1985). Polarons, bipolarons, and solitons in conducting polymers. *Accounts of Chemical Research* 18(10) pp.309-315.

British Standard BS EN 828:2013 (2013). Adhesives - Wettability - Determination by measurement of contact angle and surface free energy of solid surface. The British Standards Institution.

Brédas, J. L., Wudl, F. and Heeger, A. J. (1987). Polarons and bipolarons in doped polythiophene: A theoretical investigation. *Solid State Communications* 63(7) pp.577-580.

Bubnova, O; Khan, Z.U; Wang, H; Braun, S; Evans, D. R.; Fabretto, M; Hojati-Talemi, P; Dagnelund, D; Arlin, J; Geerts, Y.H.; Desbief, S; Breiby, D.W; Andreasen, J.W; Lazzaroni, R; Chen, Weimin M; Zozoulenko, I; Fahlman, M; Murphy, P. J; Berggren, M; Crispin, X. (2014). Semi-metallic polymers. *Nature Materials* 13(2) pp.190-194.

Chang, C; Liao, J; Hung, M; Chen, S. (2007). Interface formation between poly (9, 9-dioctylfluorene) and poly (3, 4-ethylenedioxythiophene): poly (styrenesulfonic acid). *Applied physics letters* 90(6) p.063506.

Chen, X. and Inganäs, O. (1996). Three-step redox in polythiophenes: Evidence from electrochemistry at an ultramicroelectrode. *Journal of Physical Chemistry*® 100(37) pp.15202-15206.

Cho, C; Hwang, W; Eun, K; Choa, S; Na, S; Kim, H. (2011). Mechanical flexibility of transparent PEDOT: PSS electrodes prepared by gravure printing for flexible organic solar cells. *Solar Energy Materials and Solar Cells* 95(12) pp.3269-3275.

Choi, J. S., Cho, K. Y; and Yim, J.H. (2010). Micro-patterning of vapor-phase polymerized poly (3, 4-ethylenedioxythiophene)(PEDOT) using ink-jet printing/soft lithography. *European Polymer Journal* 46(3) pp.389-396.

Cirpan, A; Argun, A. A.; Grenier, C. R. G.; Reeves, B. D.; Reynolds, J. R.. (2003). Electrochromic devices based on soluble and processable dioxithiophene polymers. *Journal of Materials Chemistry* 13(10) pp.2422-2428.

Cristovan, F. H; Nascimento, C. M; Bell, M.J.V; Laureto, E; Duarte, J. L; Dias, I.F.L; Cruz, W. O; Marletta, A. (2006). Synthesis and optical characterization of poly (styrene sulfonate) films doped with Nd (III). *Chemical physics* 326(2) pp.514-520.

- DeLongchamp, D. and Hammond, P. T. (2001). Layer-by-Layer Assembly of PEDOT/Polyaniline Electrochromic Devices. *Advanced Materials* 13(19) pp.1455-1459.
- DeLongchamp, D. M; Vogt, B.D; Brooks, C.M; Kano, K; Obrzut, J; Richter, C.A; Kirillov, O.A; Lin, E.K. (2005). Influence of a Water Rinse on the Structure and Properties of Poly (3, 4-ethylene dioxythiophene): Poly (styrene sulfonate) Films. *Langmuir* 21(24) pp.11480-11483.
- Denneulin, Aurore; Bras, Julien; Carcone, Fiona; Neuman, Charles; Blayo, Anne. (2011). Impact of ink formulation on carbon nanotube network organization within inkjet printed conductive films. *Carbon* 49(8) pp.2603-2614.
- Dimic-Misic, K., P. A. C. Gane and J. Paltakari (2013). Micro- and Nanofibrillated Cellulose as a Rheology Modifier Additive in CMC-Containing Pigment-Coating Formulations. *Industrial & Engineering Chemistry Research* 52(45) pp.16066-16083.
- Dupont, Stephanie R.; Voroshazi, Eszter; Heremans, Paul; Dauskardt, Reinhold H.I. (2013). Adhesion properties of inverted polymer solarcells: Processing and film structure parameters. *Organic Electronics* 14(5) pp.1262-1270.
- Ebnesajjad, S. and Landrock A. H. (2015). Chapter 2 - Surface Tension and Its Measurement. *Adhesives Technology Handbook (Third Edition)*. Boston, William Andrew Publishing. p.19-34.
- Elschner, A; Kirchmeyer, S; Lovenich, W; Merker, U; Reuter, K.; *PEDOT: Principles and Applications of an Intrinsically Conductive Polymer*. United States of America: CRCPress, Taylor and Francis Group, 6000 Broken Sound Parkway NW, Suite 300, Boca Raton, FL 33487-2742.
- Encinas, N., Abenojar J. and Martínez, M. A.(2012). Development of improved polypropylene adhesive bonding by abrasion and atmospheric plasma surface modifications. *International Journal of Adhesion and Adhesives* 33 pp.1-6.
- Evangelos, Vitoratos; Sotirios, Sakkopoulos; Nikolaos, Paliatsas; Konstantinos, Emmanouil Choulis, S.A. (2012). Conductivity degradation study of PEDOT: PSS films under heat treatment in helium and atmospheric air. *Open Journal of Organic Polymer Materials* 2012.
- Fan, B., Mei, X. and Ouyang, J. (2008). Significant conductivity enhancement of conductive poly (3, 4-ethylenedioxythiophene): Poly (styrenesulfonate) films by adding anionic surfactants into polymer solution. *Macromolecules* 41(16) pp.5971-5973.
- Fehse, K; Meerheim, R; Walzer, K; Leo, K; Lövenich, W; Elschner, A. (2008). Lifetime of organic light emitting diodes on polymer anodes. *Applied Physics Letters* 93(8) p.312.

- Feng, Wei; Li, Y; Wu, J; Noda, H; Fujii, A; Ozaki, M; Yoshino, K. (2007). Improved electrical and optical properties of Poly (3, 4-ethylenedioxythiophene) via ordered microstructure. *Journal of Physics: Condensed Matter* 19(18) p.186220.
- Fichou, D; Horowitz, G; Xu, B; Garnier, F. (1990). Stoichiometric control of the successive generation of the radical cation and dication of extended α -conjugated oligothiophenes: a quantitative model for doped polythiophene. *Synthetic Metals* 39(2) pp.243-259.
- Friedel, B; Brenner, T. J. K; McNeill, C.R; Steiner, U; Greenham, N.C. (2011). Influence of solution heating on the properties of PEDOT:PSS colloidal solutions and impact on the device performance of polymer solar cells. *Organic Electronics* 12 pp.1736-1745.
- Friedel, B; Keivanidis, P.E; Brenner, T.J.K; Abrusci, A; McNeill, C.R; Friend, R.H; Greenham, N.C. (2009). Effects of layer thickness and annealing of PEDOT: PSS layers in organic photodetectors. *Macromolecules* 42(17) pp.6741-6747.
- Furukawa, Y. and Tasumi M. (1991). Vibrational Spectroscopy of Intact and Doped Conjugated Polymers and Their Models. *Modern Polymer Spectroscopy* pp.207-237.
- Gao, Y, Liu C.G. and Jiang Y.S. (2002). Electronic structure of thiophene oligomer dications: An alternative interpretation from the spin-unrestricted DFT study. *Journal of Physical Chemistry A* 106(21) pp.5380-5384.
- Gerwig, R; Fuchsberger, K; Schroepel, B; Link, G.S; Heusel, G; Kraushaar, U; Schuhmann, W; Stett, A; Stelzle, M. (2012). PEDOT–CNT composite microelectrodes for recording and electrostimulation applications: fabrication, morphology, and electrical properties. *Frontiers in neuroengineering* 5 p.8.
- Geskin, V. M. and Brédas J. L. (2003). Polaron pair versus bipolaron on oligothiophene chains: a theoretical study of the singlet and triplet states. *ChemPhysChem* 4(5) pp.498-505.
- Greczynski, G; Kugler, TH; Keil, M; Osikowicz, W; Fahlman, M; Salaneck, W. R. (2001). Photoelectron spectroscopy of thin films of PEDOT–PSS conjugated polymer blend: a mini-review and some new results. *Journal of Electron Spectroscopy and Related Phenomena* 121(1–3) pp.1-17.
- Greczynski, G., Kugler, T. and Salaneck, W. R. (1999). Characterization of the PEDOT-PSS system by means of X-ray and ultraviolet photoelectron spectroscopy. *Thin Solid Films* 354(1–2) pp.129-135.
- Han, M. G. and Foulger, S. H. (2004). Crystalline Colloidal Arrays Composed of Poly (3, 4-ethylenedioxythiophene)-Coated Polystyrene Particles with a Stop Band in the Visible Regime. *Advanced Materials* 16(3) pp.231-234.

Harima, Y; Eguchi, T; Yamashita, K; Kojima, K; Shiotani, M. (1999). An in situ ESR study on poly (3-methylthiophene): charge transport due to polarons and bipolarons before the evolution of metallic conduction. *Synthetic metals* 105(2) pp.121-128.

Horiba.com Raman Academy Tutorial Pages [online]. Available at: <http://www.horiba.com/uk/scientific/products/raman-spectroscopy/raman-academy/raman-tutorial/raman-scattering/> [Accessed 21/07/2016].

Horiba.com. Raman bands.pdf [online]. Available at: <http://www.horiba.com/fileadmin/uploads/Scientific/Documents/Raman/bands.pdf> [Accessed 16/01/2017].

<http://www.sigmaaldrich.com> [Accessed 16/09/2017].

Horowitz, G. A. and Delannoy P. (1999). Chapter 5; Charge Transport in Semiconducting Oligothiophenes. Fichou, D. ed., *Handbook of oligo-and polythiophenes*. John Wiley & Sons.

Hrehorova, E, Pekarovicova, A. and Fleming, P. D. (2006). Gravure printability of conducting polymer inks. NIP & Digital Fabrication Conference, Society for Imaging Science and Technology.

Huang, J; Miller, P.F; Wilson, J.S; de Mello, A.J; de Mello, J.C; Bradley, D.D.C. (2005). Investigation of the effects of doping and post-deposition treatments on the conductivity, morphology, and work function of poly (3, 4-ethylenedioxythiophene)/poly (styrene sulfonate) films. *Advanced Functional Materials* 15(2) pp.290-296.

Hyperphysics. *Resistivity and Temperature Coefficient at 20 C* [online]. Available at: <http://hyperphysics.phy-astr.gsu.edu/hbase/Tables/rstiv.html> [Accessed 05/04/2017].

Jandel Engineering. <http://www.jandel.co.uk/info/faq.html> [online] [Accessed 27/01/2017].

Jönsson, S. K. M; Birgersson, J; Crispin, X; Greczynski, G; Osikowicz, W; Denier van der Gon, A. W; Salaneck, W. R; Fahlman, M.(2003). The effects of solvents on the morphology and sheet resistance in poly (3, 4-ethylenedioxythiophene)–polystyrenesulfonic acid (PEDOT–PSS) films. *Synthetic Metals* 139(1) pp.1-10.

Kalagi, S. S. and Patil, P. S. (2016). Secondary electrochemical doping level effects on polaron and bipolaron bands evolution and interband transition energy from absorbance spectra of PEDOT: PSS thin films. *Synthetic Metals* 220 pp.661-666.

Kang, H. S; Lee, J. K; Lee, J. W; Joo, J; Ko, J. M; Kim, M. S; Lee, J. Y. (2005). Humidity-dependent characteristics of thin film poly(3,4-ethylenedioxythiophene) field-effect transistor. *Synthetic Metals* 155(1) pp.176-179.

Kang, M; Kim, M; Kim, J; Guo, L. J. (2008). Organic solar cells using nanoimprinted transparent metal electrodes. *Advanced Materials* 20(23) pp.4408-4413.

- Kang, T.J; Kim, J.Y; Kim, K.J; Lee, C; Rhee, S.B. (1995). Photoluminescence properties of various polythiophene derivatives. *Synthetic Metals* 69(1–3) pp.377-378.
- Kim, E.G. and Brédas, J.L. (2008). Electronic evolution of poly (3, 4-ethylenedioxythiophene)(PEDOT): From the isolated chain to the pristine and heavily doped crystals. *Journal of the American Chemical Society* 130(50) pp.16880-16889.
- Kim, J. Y; Jung, J. H; Lee, D. E; Joo, J. (2002). Enhancement of electrical conductivity of poly(3,4-ethylenedioxythiophene)/poly(4-styrenesulfonate) by a change of solvents. *Synthetic Metals* 126(2–3) pp.311-316.
- Kim, T; Kim, J; Kim, Y; Lee, T; Kim, W; Suh, K.S. (2009). Preparation and characterization of poly(3,4-ethylenedioxythiophene) (PEDOT) using partially sulfonated poly(styrene-butadiene-styrene) triblock copolymer as a polyelectrolyte. *Current Applied Physics* 9(1) pp.120-125.
- Kim, T.Y; Kim, J.E; Suh, K.S. (2006). Effects of alcoholic solvents on the conductivity of tosylate-doped poly(3,4-ethylenedioxythiophene) (PEDOT-OTs). *Polymer International* 55(1) pp.80-86.
- Kim, Y; Sachse, C; Machala, M.L; May, C; Müller-Meskamp, L; Leo, K. (2011). Highly conductive PEDOT: PSS electrode with optimized solvent and thermal post-treatment for ITO-free organic solar cells. *Advanced Functional Materials* 21(6) pp.1076-1081.
- Kline, R. J, McGehee, M. D. and Toney, M. F. (2006). Highly oriented crystals at the buried interface in polythiophene thin-film transistors. *Nature Materials* 5(3) pp.222.
- Koidis, C; Logothetidis, S; Kapnopoulos, C; Karagiannidis, P. G; Laskarakis, A; Hastas, N. A. (2011). Substrate treatment and drying conditions effect on the properties of roll-to-roll gravure printed PEDOT:PSS thin films. *Materials Science and Engineering: B* 176(19) pp.1556-1561.
- Kopola, P; Aernouts, T; Guillerez, S; Jin, H; Tuomikoski, M; Maaninen, A; Hast, J. (2010). High efficient plastic solar cells fabricated with a high-throughput gravure printing method. *Solar Energy Materials and Solar Cells* 94(10) pp.1673-1680.
- Kopola, P; Tuomikoski, M; Suhonen, R; Maaninen, A. (2009). Gravure printed organic light emitting diodes for lighting applications. *Thin Solid Films* 517(19) pp.5757-5762.
- Kossmehl, G. and Engelmann, G. (1999). Chapter 10 Application of Electrically Conductive Polythiophenes. Fichou, D. ed. *Handbook of oligo-and polythiophenes*. John Wiley & Sons.
- Krebs, F. C. (2009). Polymer solar cell modules prepared using roll-to-roll methods: knife-over-edge coating, slot-die coating and screen printing. *Solar Energy Materials and Solar Cells* 93(4) pp.465-475.
- Krebs, F.C; Jørgensen, M; Norrman, K; Hagemann, O; Alstrup, J; Nielsen, T.D;

- Fyenbo, J; Larsen, K; Kristensen, J. (2009). A complete process for production of flexible large area polymer solar cells entirely using screen printing—First public demonstration. *Solar Energy Materials and Solar Cells* 93(4) pp.422-441.
- Kroon, R; Mengistie, D.A; Kiefer, D; Hynynen, J; Ryan, J.D; Yu, L; Müller, C. (2016). Thermoelectric plastics: from design to synthesis, processing and structure–property relationships. *Chemical Society Reviews* 45, pp.6147-6164.
- Kvarnström, C; Neugebauer, H; Blomquist, S; Ahonen, H. J; Kankare, J; Ivaska, A.. (1999). In situ spectroelectrochemical characterization of poly(3,4-ethylenedioxythiophene). *Electrochimica Acta* 44(16) pp.2739-2750.
- Lang, U; Müller, E; Naujoks, N; Dual, J. (2009). Microscopical Investigations of PEDOT:PSS Thin Films. *Advanced Functional Materials* 19(8) p.1215.
- Li, Z; Meng, W; Tong, J; Zhao, C; Qin, F; Jiang, F; Xiong, S; Zeng, S; Xu, L; Hu, B; Zhou, Y. (2015). A nonionic surfactant simultaneously enhancing wetting property and electrical conductivity of PEDOT:PSS for vacuum-free organic solar cells. *Solar Energy Materials and Solar Cells* 137 pp.311-318.
- Li, Z, Qin, F; Liu, T; Ge, R; Meng, W; Tong, J; Xiong, S; Zhou, Y. (2015). Optical properties and conductivity of PEDOT:PSS films treated by polyethylenimine solution for organic solar cells. *Organic Electronics* 21(0) pp.144-148.
- Liu, C; Xu, J; Lu, B; Yue, R; Kong, F. (2012). Simultaneous Increases in Electrical Conductivity and Seebeck Coefficient of PEDOT:PSS Films by Adding Ionic Liquids into a Polymer Solution. *Journal of Electronic Materials* 41(4) pp.639-645.
- Liu, Y. D., J. E. Kim and H. J. Choi (2011). Core-Shell Structured Monodisperse Poly (3, 4-Ethylenedioxythiophene)/Poly (Styrenesulfonic Acid) Coated Polystyrene Microspheres and Their Electrorheological Response. *Macromolecular rapid communications* 32(12) pp.881-886.
- Luo, J; Billep, D; Waechtler, T; Otto, T; Toader, M; Gordan, O; Sheremet, E; Martin, J; Hietschold, M; Zahn, D.R.T; Gessner, T. (2013). Enhancement of the thermoelectric properties of PEDOT:PSS thin films by post-treatment. *Journal of Materials Chemistry A* 1(26) pp.7576-7583.
- Massonnet, N; Carella, A; Jaudouin, O; Rannou, P; Laval, G; Celle, C; Simonato, J. (2014). Improvement of the Seebeck coefficient of PEDOT: PSS by chemical reduction combined with a novel method for its transfer using free-standing thin films. *Journal of Materials Chemistry C* 2(7) pp.1278-1283.
- Meng, H; Perepichka, D.F; Bendikov, M; Wudl, F; Pan, G.Z; Yu, W; Dong, W; Brown, S. (2003). Solid-state synthesis of a conducting polythiophene via an unprecedented heterocyclic coupling reaction. *Journal of the American Chemical Society* 125(49) pp.15151-15162.
- Mengistie, D.A; Chen, C; Boopathi, K.M; Pranoto, F.W; Li, L; Chu, C. (2014).

- Enhanced thermoelectric performance of PEDOT: PSS flexible bulky papers by treatment with secondary dopants. *ACS applied materials & interfaces* 7(1) pp.94-100.
- Middleton, B. (2012). Injection moulding electroluminescent devices. PhD Thesis, University of Warwick.
- Morsy, F. A. (2005). Dielectric properties of coated paper and the effect of various soluble thickeners. *Polymer-Plastics Technology and Engineering* 44(3) pp.351-362.
- Nabid, M.R; Asadi, S; Shamsianpour, M; Sedghi, R; Osati, S; Safari, N. (2010). Oxidative polymerization of 3, 4-ethylenedioxythiophene using transition-metal tetrasulfonated phthalocyanine. *Reactive and Functional Polymers* 70(1) pp.75-80.
- Namkoong, G; Younes, E.M; Abdel-Fattah, T.M; El-Maghraby, E. M; Elsayed, A.H; Abo Elazm, A. H. (2015). Aging process of PEDOT:PSS dispersion and robust recovery of aged PEDOT:PSS as a hole transport layer for organic solar cells. *Organic Electronics* 25 pp.237-244.
- Nardes, A. M; Kemerink, M; de Kok, M. M; Vinken, E; Maturova, K; Janssen, R. A. J. (2008). Conductivity, work function, and environmental stability of PEDOT : PSS thin films treated with sorbitol. *Organic Electronics* 9(5) pp.727-734.
- Nasybulin, E; Wei, S; Kymissis, I; Levon, K. (2012). Effect of solubilizing agent on properties of poly(3,4-ethylenedioxythiophene) (PEDOT) electrodeposited from aqueous solution. *Electrochimica Acta* 78(0) pp.638-643.
- Ouyang, J. (2013a). Secondary doping” methods to significantly enhance the conductivity of PEDOT:PSS for its application as transparent electrode of optoelectronic devices. *Displays* 34(5) pp.423-436.
- Ouyang, J. (2013b). Solution-processed pedot:pss films with conductivities as indium tin oxide through a treatment with mild and weak organic acids. *ACS Applied Materials and Interfaces* 5(24) pp.13082-13088.
- Ouyang, J; Guo, T; Yang, Y; Higuchi, H; Yoshioka, M; Nagatsuka, T. (2002). High-performance, flexible polymer light-emitting diodes fabricated by a continuous polymer coating process. *Advanced Materials* 14(12) p.915.
- Ouyang, J; Xu, Q; Chu, C; Yang, Y; Li, G; Shinar, J. (2004). On the mechanism of conductivity enhancement in poly(3,4-ethylenedioxythiophene):poly(styrene sulfonate) film through solvent treatment. *Polymer* 45(25) pp.8443-8450.
- Palumbiny, C. M; Heller, C; Schaffer, C. J; Korstgens, V; Santoro, G; Roth, S. V; Muller-Buschbaum, P. (2014). Molecular Reorientation and Structural Changes in Cosolvent-Treated Highly Conductive PEDOT:PSS Electrodes for Flexible Indium Tin Oxide-Free Organic Electronics. *Journal of Physical Chemistry C* 118(25) pp.13598-13606.

- Park, T; Park, C; Kim, B; Shin, H; Kim, E. (2013). Flexible PEDOT electrodes with large thermoelectric power factors to generate electricity by the touch of fingertips. *Energy & Environmental Science* 6(3) pp.788-792.
- Pei, Q; Zuccarello, G; Ahlskog, M; Inganäs, O. (1994). Electrochromic and highly stable poly(3,4-ethylenedioxythiophene) switches between opaque blue-black and transparent sky blue. *Polymer* 35(7) pp.1347-1351.
- Pettersson, L. A. A, Ghosh, S. and Inganäs, O. (2002). Optical anisotropy in thin films of poly (3,4-ethylenedioxythiophene)-poly(4-styrenesulfonate). *Organic Electronics* 3(3–4) pp.143-148.
- Pham, L.Q; Sohn, J. H; Kim, C. W; Park, J.H; Kang, H.S; Lee, B.C; Kang, Y. S. (2012). Copper nanoparticles incorporated with conducting polymer: Effects of copper concentration and surfactants on the stability and conductivity. *Journal of Colloid And Interface Science* 365 pp.103-109.
- Prieto, C. and Calvo, L. (2013) Performance of the Biocompatible Surfactant Tween 80, for the Formation of Microemulsions Suitable for New Pharmaceutical Processing. *Journal of Applied Chemistry* [online]. Available at: <http://www.hindawi.com/journals/jac/2013/930356/abs/> [Accessed 22/09/14].
- Purdue University. *Vibrational modes of ammonia* [online]. Available at: <http://www.chem.purdue.edu/gchelp/vibs/nh3.html> [Accessed 09/01/2017].
- Rasmussen, P. S. C. (2011). *Designing Organic Semiconducting Materials: The Promise of Flexible Electronics* [online]. Available at: <http://www.azom.com/article.aspx?ArticleID=5591>. [Accessed 11/08/16].
- Royal Society of Chemistry. *Introduction to IR spectroscopy* [online]. Available at: http://www.rsc.org/learn-chemistry/wiki/Introduction_to_IR_spectroscopy [Accessed 09/01/2017].
- Sakamoto, S; Okumura, M; Zhao, Z; Furukawa, Y. (2005). Raman spectral changes of PEDOT–PSS in polymer light-emitting diodes upon operation. *Chemical Physics Letters* 412(4–6) pp.395-398.
- Sandoval, A. P; Suárez-Herrera, M. F; and Feliu, J. M. (2015). IR and electrochemical synthesis and characterization of thin films of PEDOT grown on platinum single crystal electrodes in [EMMIM] Tf₂N ionic liquid. *Beilstein journal of organic chemistry* 11(1) pp.348-357.
- Senghor, M., Berson, S. and Manceau, M. (2013). Forming of optoelectronic devices, particularly of inverted-type opv cells. Google Patents.
- Setti, L; Fraleoni-Morgera, A; Ballarin, B; Filippini, A; Frascaro, D; Piana, C. (2005). An amperometric glucose biosensor prototype fabricated by thermal inkjet printing. *Biosensors and Bioelectronics* 20(10) pp.2019-2026.

Shaheen, S.E; Radspinner, R; Peyghambarian, N; Jabbour, G.E. (2001). Fabrication of bulk heterojunction plastic solar cells by screen printing. *Applied Physics Letters* 79(18) pp.2996-2998.

Shimadzu Scientific Instruments. *Can you tell me why the baseline is curved?* [online]. Available at: <http://www.shimadzu.com/an/ftir/support/faq/5.html> [Accessed 28/04/2016].

Shodhganga, Chapter 5, Preparation and properties of PEDOT, http://shodhganga.inflibnet.ac.in/bitstream/10603/3499/11/11_chapter%205.pdf POL Y (3, 4-ETHYLENE DIOXYTHIOPHENE).

Skoog, D; West, D.M; and Holler, F.J. (1992). *Fundamentals of Analytical Chemistry* 6th ed. Saunders College Publishing:pp.514-583.

Skotheim, J and Reynolds, T. A; (2006). *Conjugated polymers: theory, synthesis, properties, and characterization*: CRC press.

Snaith, H.J; Kenrick, H; Chiesa, M; Friend, R.H.(2005). Morphological and electronic consequences of modifications to the polymer anode 'PEDOT:PSS'. *Polymer* 46(8) pp.2573-2578.

Snook, G. A; Peng, C; Fray, D.J; Chen, G. Z.(2007). Achieving high electrode specific capacitance with materials of low mass specific capacitance: Potentiostatically grown thick micro-nanoporous PEDOT films. *Electrochemistry Communications* 9(1) pp.83-88.

Soo Kim, Y; Bin Oh, S; Hyeok Park, J; Suk Cho, M; Lee, Y. (2010). Highly conductive PEDOT/silicate hybrid anode for ITO-free polymer solar cells. *Solar Energy Materials and Solar Cells* 94(3) pp.471-477.

Street, R. A. (2006). Conducting polymers: The benefit of order. *Nature Materials* 5(3) p.171.

Sukchol, K; Thongyai, S; Praserttham, P; Sotzing, G.A. (2013). Effects of the addition of anionic surfactant during template polymerization of conducting polymers containing pedot with sulfonated poly (imide) and poly (styrene sulfonate) as templates for nano-thin film applications. *Synthetic Metals* 179 pp.10-17.

Sun, B; Zhao, Y; Wu, J; Yang, Q; Xu, G. (1998). Crystal structure and FT-IR study of cesium 4-methylbenzenesulfonate. *Journal of molecular structure* 471(1) pp.63-66.

Tkalya, E.E; Ghislandi, M; de With, G; Koning, C.E (2012). The use of surfactants for dispersing carbon nanotubes and graphene to make conductive nanocomposites. *Current Opinion in Colloid & Interface Science* 17(4) pp.225-232.

Tran-Van, F; Garreau, S; Louarn, G; Froyer, G; Chevrot, C. (2001). Fully undoped and soluble oligo(3,4-ethylenedioxythiophene)s: spectroscopic study and electrochemical characterization. *Journal of Materials Chemistry* 11(5) pp.1378-1382.

U.S Department of Energy. *11-BM Frequently Asked Questions*, [online]. Available at: <http://11bm.xray.aps.anl.gov/faq.html#Q11> [Accessed 17/02/17].

University of Berkley. <http://four-point-probes.com/four-point-probe-manual/> [online]. Available at: <http://four-point-probes.com/four-point-probe-manual/> [Accessed 27/01/2017]

University of Toledo. (2011). *Sheet Resistance: Measurement and Significance* [online]. Available at: http://astro1.panet.utoledo.edu/~relling2/teach/archives/4580.6280.2011/20111025_lecture_4.2_phys4580.6280.pdf [Accessed 30/01/2017]

Vitoratos, E. Sakkopoulos, S. Dalas, E. Paliatsas, N. Karageorgopoulos, D. Petraki, F. Kennou, S. (2009). Thermal degradation mechanisms of PEDOT:PSS. *Organic Electronics* 10(1) pp.61-66.

Vosgueritchian, M; Lipomi, D. J; and Bao, Z. (2012). Highly conductive and transparent PEDOT: PSS films with a fluorosurfactant for stretchable and flexible transparent electrodes. *Advanced functional materials* 22(2) pp.421-428.

Wakizaka, D; Fushimi, T; Ohkita, H; Ito, S. (2004). Hole transport in conducting ultrathin films of PEDOT/PSS prepared by layer-by-layer deposition technique. *Polymer* 45(25) pp.8561-8565.

Wohlfart, E; Fernández-Blázquez, J.P; Arzt, E; del Campo, A. (2011). Nanofibrillar Patterns on PET: The Influence of Plasma Parameters in Surface Morphology. *Plasma Processes & Polymers* 8(9) p.876.

Xia, Y; Sun, K; and Ouyang, J. (2012a). Solution-processed metallic conducting polymer films as transparent electrode of optoelectronic devices. *Advanced Materials* 24(18) pp.2436-2440.

Xia, Y. J; Sun, K; and Ouyang, J. Y. (2012b). Highly conductive poly(3,4-ethylenedioxythiophene):poly(styrene sulfonate) films treated with an amphiphilic fluoro compound as the transparent electrode of polymer solar cells. *Energy & Environmental Science* 5(1) pp.5325-5332.

Xuan, Y; Sandberg, M; Berggren, M; Crispin, X. (2012). An all-polymer-air PEDOT battery. *Organic electronics* 13(4) 632-637.

Yoshioka, Y; and Jabbour, G. E. (2006). Inkjet Printing of Oxidants for Patterning of Nanometer-Thick Conducting Polymer Electrodes. *Advanced Materials* 18(10) pp.1307-1312.

Zhou, J; Anjum, D. H; Chen, L; Xu, X; Ventura, I.A; Jiang, L; Lubineau, G. (2014). The temperature-dependent microstructure of PEDOT/PSS films: insights from morphological, mechanical and electrical analyses. *Journal of Materials Chemistry C* 2(46) pp.9903-9910.

- Zhou, Y; Yuan, Y; Lian, J; Zhang, J; Pang, H; Cao, L; Zhou, X. (2006). Mild oxygen plasma treated PEDOT:PSS as anode buffer layer for vacuum deposited organic light-emitting diodes. *Chemical Physics Letters* 427(4–6) pp.394-398.
- Zhu, Z; Liu, C; Shi, H; Jiang, Q; Xu, J; Xiong, J; Liu, E; Jiang, F. (2015). An effective approach to enhanced thermoelectric properties of PEDOT:PSS films by a des post-treatment. *Journal of Polymer Science, Part B: Polymer Physics* 53(12) pp.885-892.
- Zotti, G; Zecchin, S; Schiavon, G; Louwet, F; Groenendaal, L; Crispin, X; Osikowicz, W; Salaneck, W; Fahlman, M.(2003). Electrochemical and XPS studies toward the role of monomeric and polymeric sulfonate counterions in the synthesis, composition, and properties of poly(3,4-ethylenedioxythiophene). *Macromolecules* 36(9) pp.3337-3344.
- Zykwinska, A; Domagala, W; Czardybon, A; Pilawa, B; Lapkowski, M. (2003). In situ EPR spectroelectrochemical studies of paramagnetic centres in poly(3,4-ethylenedioxythiophene) (PEDOT) and poly(3,4-butylenedioxythiophene) (PBuDOT) films. *Chemical Physics* 292(1) pp.31-45.